-RESEARCH THESIS-

CHARACTERISATION OF ATMOSPHERIC PARTICULATE MATTER FROM OPENCAST COAL MINING ACTIVITIES AND ADJACENT COMMUNITIES

by

Lerato Khumalo
14213151

Submitted in fulfilment of the requirements for the degree

PhD in Chemical Technology

in the

FACULTY OF ENGINEERING, BUILT ENVIRONMENT AND INFORMATION TECHNOLOGY

at the

UNIVERSITY OF PRETORIA

Study leader:

Dr G Kornelius

Date of submission
August 2020

Department of Chemical Engineering

Declaration Regarding Plagiarism

I (full names & surname):	Lerato Khumalo
Student number:	14213151

Declare the following:

1. I understand what plagiarism entails and am aware of the University's policy in this regard.
2. I declare that this assignment is my own, original work. Where someone else's work was used (whether from a printed source, the Internet or any other source) due acknowledgement was given and reference was made according to departmental requirements.
3. I did not copy and paste any information directly from an electronic source (e.g., a web page, electronic journal article or CD ROM) into this document.
4. I did not make use of another student's previous work and submitted it as my own.
5. I did not allow and will not allow anyone to copy my work with the intention of presenting it as his/her own work.

Signature

Date

ACKNOWLEDGEMENTS

I wish to express my appreciation to the following persons and organisations without whom I would not have been able to complete this PhD research study. Special thanks to my supervisor Dr Gerrit Kornelius at the University of Pretoria for his guidance, insight and knowledge into the subject matter which steered me through this research. The following persons are also highly acknowledged for their technical assistance and contributions during the study, Dr Andre Botha (University of Pretoria), Dr Eudri Venter (University of Pretoria), Dr Grant Hall (University of Pretoria), Dr Pieter Van Zyl (North West University), Jan-Stefan Swartz (North West University), Dr Nicola Wagner (University of Johannesburg), Dr Mbuso Mlambo (University of Pretoria) and Dr Liza Coetsee-Hugo (University of Free State). I would also like to thank the institutions in which they are based for providing the facilities for the study. I also wish to express my appreciation to Airshed Planning Professionals for providing monitoring equipment and mostly, to Exxaro Resources for supporting and funding the study.

I would also like to thank management and personnel of the opencast coal mines included in this study for their cooperation and for allowing me to undertake the study in their operations. To the residents of Delpark, Clewer and Marapong, thank you for your cooperation and for allowing me into your homes for monitoring and discussion purposes during the study. Special thanks to Jacob Nkabinde from Victor Khanye Local Municipality for his assistance in engaging the community members and site selection for monitoring. I would also like to thank my colleagues for their unwavering support, especially Mongezi Veti and Rakesh Mooni. My biggest thanks to my family for all the support you have shown me through this research, especially my sister Matshidiso. To my husband Nqobile, thank you for your patience and all your support, without which I would have stopped these studies a long time ago. Many thanks to my boys Kyle and Shane.

TABLE OF CONTENTS

LIST OF FIGURES

LIST OF TABLES

ABSTRACT

Characterisation of Atmospheric Particulate Matter from Opencast Coal Mining Activities and Adjacent Communities

Fugitive coal dust emissions are a cause of concern from a government and public perspective, particularly so in communities living in proximity of the coal mines. Atmospheric dust contains various constituents and coal dust is only one of the constituents. However, the general perceptions or views have always been that a significant proportion of dust consists of fugitive coal dust which is respirable. Compounding these perceptions is that currently, there is a relative level of difficulty in presenting dust analysis information in a manner which identifies and characterises the coal component of dust.

The aim of this study is the characterisation of atmospheric PM from opencast coal mines and adjacent communities through the application of various microscopic, spectroscopic, thermogravimetric and thermal optical techniques to distinguish the carbon component originating from coal mining and from other sources such as biological and combustion sources in coal mining regions.

Atmospheric particulate matter (PM) of 10 micrometers (µm) or smaller collected from three opencast coal mines and adjacent communities in the Mpumalanga and Limpopo Provinces in South Africa using both active and passive sampling were used as a case study. The analytical techniques include Scanning Electron Microscopy (SEM) with Energy Dispersive X-ray Spectroscopy (EDS), reflectance microscopy (reflectance), optical microscopy, X-Ray Photoelectron Spectroscopy (XPS), Raman Spectroscopy (Raman), Thermogravimetric Analysis (TGA), Isotope Ratio Mass Spectrometry (IRMS) and thermal optical analysis.

Atmospheric PM sampled through passive samplers was analysed through SEM-EDS and optical microscopy, while the atmospheric PM samples from active monitoring (filtration) were analysed using Raman, reflectance, TGA, XPS, IRMS and thermal optical techniques Optical microscopy on the passive samples did enable the quantification of $PM_{10-2.5}$ concentrations for PM from the opencast coal mines and adjacent communities. At the magnifications used, accurate quantification of $PM_{2.5}$ is not possible. Useful information on the morphology and chemical composition of individual particles was obtained, but this was

not adequate for source apportionment, as the mineral composition in mines and in adjacent residential areas is often similar.

For the active monitoring campaign, PM_{10} daily average concentrations ranged from 59 µg/m³ to 90 ug/m³. The PM_{10} daily NAAQS was only exceeded at one of the residential stations viz. Clewer.

The differentiation between elemental carbon (EC) and brown/ organic carbon (OC) of the individual particles could not be achieved through SEM-EDS, nor through XPS, Raman, TGA, reflectance microscopy of bulk samples.

Thermal optical analysis allowed the quantification of the EC/OC fraction on actively collected bulk samples and indicated a clear distinction between the EC and OC contents as well as the OC/EC ratio from the mine and residential samples. The analysis of the stable carbon (C) and nitrogen (N) isotope ratios ($\delta^{13}C/\delta^{12}C$) and ($\delta^{15}N/\delta^{14}N$) of bulk samples showed that the values obtained for both ratios and the relationship between them could also distinguish between samples from the mines and the adjacent residential areas. Further development to refine the source apportionment based on a combination of these techniques is proposed, which will require further sampling and detailed analysis of potential carbonaceous sources.

1 INTRODUCTION

Air pollution, the presence of contaminants or pollutants in the atmosphere, is not a modern phenomenon and historical evidence attests to this (Akatsu, 2015; Hanlon, 2016). Air pollution and its negative impacts on health and the environment have been documented over the years, with more frequent references dating as far back as the Industrial Revolution (Bloss, 2014). Atmospheric PM has been a dominant factor in historical air pollution episodes, including the London smogs of the 1950s and the Donora Valley (Pennsylvania) and Meuse Valley (Belgium) episodes (Bloss, 2014).

Depending on their concentration, physical and chemical properties, air pollutants can result in injurious or negative impacts on human or animal health and the environment (Kantova *et al*., 2017). Once emitted into the atmosphere, air pollutants contribute to air quality degradation and depending on their atmospheric residence times, can continue to degrade air quality for long periods (Mishra *et al*., 2013). The long-term impacts of air pollutants due to long atmospheric residence times, high concentrations and transboundary movement, is evident in greenhouse gases and their contribution to global climate change over long periods (Kantova *et al*., 2017).

The residence times of air pollutants in the atmosphere is also highly dependent on their sizes (Jia & Jia, 2014). Gravitational effects result in the rapid removal of coarse particles from the atmosphere by sedimentation (residence time between minutes and hours). Pollutants or particles in the accumulation mode exhibit the highest residence time in the atmosphere (weeks) and these particles can be easily transported by wind for distances of up to thousands of kilometres from their sources (Perrino, 2010).

Globally, a significant number of regions face environmental crises due to severe air pollution and its negative impacts on health and the environment. There are various causes of air pollution and these include population growth, rapid urbanisation and migration, industrial developments and economic growth, transport related emissions due to unprecedented levels of vehicle numbers and other modes of transport and the increase in energy demand, production and consumption (Laskin *et al.*, 2012). The global population is currently estimated to be over 6 billion and is forecasted to increase to over 7 billion by 2020

and approximately 9 billion by 2050. The implications of population growth include increased demand for goods and services, pressure on natural resources, increase in energy demand, production and consumption (Laskin *et al.*, 2012). This scenario will most likely occur in developing countries, where it is estimated that 90% of future growth will occur. This growth will be concentrated in urban areas (Popescu & Ionel, 2010). These developments have culminated in the increase of anthropogenic air pollution emissions of unprecedented severity and extent (Mishra *et al.*, 2013).

South Africa is no exception where air quality degradation due to high air pollution levels in some regions is concerned. This is evidenced by the declaration of certain regions as air quality management priority areas. The declaration of these priority areas is largely dependent on whether ambient air quality standards are being exceeded or could be potentially exceeded in the area (Department of Environmental Affairs (DEA), 2011). The existence of any potential air quality threats is one of the criteria used in the declaration of priority areas. Three priority areas have declared in South Africa so far and these are the Highveld Priority Area, Waterberg-Bojanala Priority Area and the Vaal Triangle Priority Area (DEA, 2018). Anthropogenic sources of air pollution in these areas include industrial facilities, power generation, transport, agricultural activities and coal mining (DEA, 2011).

Coal mining activities, particularly open cast mining, result in fugitive coal dust emissions. Fugitive coal dust and its associated negative impacts on health and the environment, has been an issue of concern in many parts of the world, particularly in communities that live close to coal mining operations (Ghose, 2002). Various perceptions and views exist on coal dust and impacts among various stakeholders. These perceptions and views include that coal dust is the only constituent of dust, significant proportions of dust are due to coal mining and that all black dust particulates are inhalable and respiratory coal dust, which will eventually culminate in adverse health effects (Warren *et al.*, 2015). However, there are different constituents of black dust and these include black soils, mould, soot and rubber from tyres (Hatch *et al*., 2008).

There are often challenges related to proving or disproving these perceptions or views. However, comprehensive analyses of collected dust samples can be undertaken for the identification, characterisation and quantification of the coal dust constituent. It is through such analyses that some of the perceptions about coal dust can be dispelled or

authenticated, resulting in common understanding and acceptance among stakeholders (Hartmann, 2016). The positive outcomes of the analyses will be that where air pollution impacts due to coal dust have been identified and authenticated, credible implementation of effective mitigation measures to reduce the impacts can be initiated (Cohen *et al*., 2010).

Atmospheric composition studies have been undertaken in various parts of the world, with the main purposes including the identification, characterisation and quantification of ambient particulate matter. There are various reasons why such studies are undertaken and some of the underlying reasons include the fact that atmospheric PM may contribute to significant environmental and/ or air quality degradation, negative health impacts and transboundary pollution problems (Cohen *et al*., 2010). The mitigation of these impacts often requires comprehensive identification, characterisation and quantification studies to identify the sources of the particulate emissions or air pollutants (Ferreira *et al.*, 2013).

Particulates can either be derived or emitted from various sources which are normally differentiated as biogenic (natural) or anthropogenic (human) sources (Ferreira *et al*., 2013). However, anthropogenic activities contribute significantly to atmospheric pollution compared to the biogenic sources (Schwarz *et al*., 2008). The biogenic sources of particulate emissions include volcanoes, wildfires, sea salt sprayed into the atmosphere and windblown dust while the anthropogenic sources include agricultural activities, power generation and other fossil fuel combustion activities, transport-related emissions, construction activities, biomass burning, solid waste and industrial processes (Aneja *et al.*, 2012; Seinfield *et al*.,1998).

The components of atmospheric PM may include a significant amount of carbonaceous material generally differentiated between organic carbon (OC) and elemental carbon (EC) (Li *et al*., 2013) accounting for between 10% to 50% of atmospheric PM mass (Schwarz *et al*., 2008). Elemental carbon is generated predominantly from incomplete combustion while organic carbon consists of carbonaceous material emitted in particulate form and secondary organic carbon which is generated by atmospheric chemical and physical reactions (Seinfield *et al*., 1998).

Mining is one of the anthropogenic sources of particulate matter emissions. Although the generation of particulate matter is associated with all types of mining activities, coal mining

has been identified as one of the contributors to ambient particulate matter emissions, particularly open pit coal mining (Gautam *et al.*, 2012) through activities such as excavation, drilling and blasting, materials handling, wind erosion of stockpiles and open areas, vehicle entrainment of dust, processing plants, spontaneous combustion, crushing and screening (Chaulya, 2004).

Fugitive coal dust emissions are a cause of concern from a government and public perspective, particularly so in communities living in proximity of the coal mines (Warren *et al*, 2015). Atmospheric dust contains various constituents and coal dust is only one of the constituents (Kunzli & Tager, 2000). However, the general perceptions or views have always been that a significant proportion of dust consists of fugitive coal dust which is respirable (Hartmann *et al.,* 2016). Compounding these perceptions is that currently there is a relative level of difficulty in presenting dust analysis information in a manner which identifies and characterises the coal component of dust (Warren *et al.*, 2015).

Atmospheric PM of 10 µm or less (>2.5 µm) is also referred to as inhalable particulates and is of significant relevance with regards to human health effects (Albers *et al*., 2015; Kesavachandran *et al*., 2015; Kunzli & Tager, 2000). This inhalable particulate fraction of dust consists of particulates that can be breathed in and deposited into the nose or mouth (World Health Organisation (WHO), 2004). Atmospheric PM can also be defined as respirable (less than 2.5µm) and thoracic (below 10 µm) (Kim *et al*., 2015; Lipsky *et al.*, 2002). Respirable particulate matter is the fraction of inhaled atmospheric particulates which can penetrate further than the bronchioles into the gas exchange section of the lungs (Hartmann *et al*., 2016; WHO, 2004).

1.1 PROJECT RATIONALE

Research studies have indicated that atmospheric PM concentrations are increasing in the atmosphere, particularly carbonaceous aerosols derived from anthropogenic activities which include industrial and chemical processes, power generation plants, mining and biomass burning. Given the negative health and environmental impacts associated with atmospheric PM, its characterisation has increasingly become critical. Attention has been directed over the years to carbonaceous aerosols which constitute a significant proportion of atmospheric PM and exhibit complex formation processes, atmospheric chemical and physical

transformation, various sizes and negative impacts on health and environment (Gieré & Querol, 2010). In addition, challenges associated with air pollution and general environmental degradation are increasingly intertwined with sustainability considerations and affect livelihoods and social well-being of the impacted communities.

In South Africa, different sources of atmospheric PM exist, particularly in highly industrialised areas such as the Highveld Priority Area, parts of the Waterberg -Bojanala Priority Area and the Vaal-Triangle Airshed Priority Area (VTAPA). Sources of atmospheric PM in these priority areas include anthropogenic activities such as power generation, industrial processes, vehicle emissions and biomass burning (DEA, 2011). The characterisation of atmospheric PM and the identification of the different anthropogenic sources of atmospheric PM in such areas is crucial. This is especially the case given that exceedances of the National Ambient Air Quality Standard for PM_{10} have been recorded in these priority areas. Given that atmospheric PM contains a significant fraction of carbonaceous species, it is important to characterise and differentiate between the different forms of carbon in atmospheric PM samples for the purposes of source identification, source apportionment and application of mitigation measures and environmental and health management.

Given that coal mining has been identified as one of the contributors to atmospheric PM in South Africa, particularly in the Highveld region of Mpumalanga, it is important that air quality management measures take into consideration research information based on the characterisation of coal dust and other carbonaceous particulates, especially in communities located adjacent to coal mining operations. This is critical for the determination of its concentration (particulate mass), chemical composition, sources of emissions, compliance and health risks assessments and effective mitigation measures.

1.2 PROJECT AIM AND OBJECTIVES

The aim of the research study is the characterisation of atmospheric PM from opencast coal mines and adjacent communities through the application of various microscopic, spectroscopic, thermogravimetric and thermal optical techniques with the following objectives;

- To distinguish carbon from coal mining and carbon from other sources such as biological and combustion sources in coal mining regions, i.e characterisation of the carbonaceous component (EC and OC) of atmospheric PM;
- Contribution to knowledge on the characteristics of the carbonaceous component of atmospheric PM from coal mining regions and adjacent communities, including the identification of coal dust and non-coal dust particulates.

1.2.1 Knowledge Gap and Problem Statement

It is envisaged that the study will bridge some of the knowledge gaps associated with the origin of atmospheric PM found in communities located adjacent to coal mining operations. Currently, in coal mining regions, there are open discussions on the origin of atmospheric particulates found in these regions. However, there is no factual evidence that these particulates originate from coal mining activities since their composition is similar to that of particles emanating from other human activities within these regions.

1.2.2 Hypothesis

The hypothesis is that the properties of the carbon content of the particulates, along with their morphological characteristics, such as size and shape, will segregate atmospheric particulates from opencast coal mining and adjacent communities.

1.3 CONTRIBUTION TO SCIENCE

The research study investigated the application of eight different locally available techniques for the characterisation of atmospheric PM. Some of these had not previously been applied for the characterisation of the carbonaceous component of atmospheric PM samples, or to individual atmospheric particles, the collection of which was made possible by the application of passive monitoring techniques not previously applied in this sector. It concludes that no single technique is available to unambiguously identify particulates arising from coal mining and other human activities, but that a combination of thermal optical methods and IRMS, with corroboration from some of the other techniques such as SEM-EDS, will enable the identification and determination of the origin of atmospheric particulate PM found in coal mining regions. The application of these techniques enables the

contribution of coal mining activities to the atmospheric particulate load in coal mining areas to be quantified.

2 LITERATURE REVIEW

2.1 Introduction

In South Africa, coal is a significant source of primary energy and plays a pivotal role in powering the country's economy, including job creation. It is seen as one of the means of meeting the goals of the National Development Plan-2030 (Department of Energy (DoE), 2015), which include the elimination of poverty and reduction of inequality by 2030 (National Planning Commission (NPC), 2010) which require rapid economic growth.

Coal mining and other industrial activities such as power generation, primary metal production, petrochemical facilities and smelters contribute to air pollution and pose a threat to the environment (DEA, 2011). Environmental degradation poses health risks to communities adjacent to these industrial activities and negatively impacts on efforts to achieve sustainability and sustainable livelihoods. To deal with environmental degradation caused by industrial activities, South Africa has developed the National Environmental Management Act (NEMA) (Act 14 of 2009), which is the overarching and framework for various pieces of legislation that address the management of critical resources such as air quality, water and biodiversity (DEA, 2011).

Despite the development and implementation of this legislation, environmental pollution is still a huge challenge in the country, with growing public concern in regions were industrial activities are concentrated. Coal mining has been identified as one of the contributors to air pollution in regions that are dominated by this activity. These include the Highveld Priority Area, where there are growing concerns on the health and environmental impacts associated with air pollution due to coal mining and other industries. (DEA, 2011). As far as the problem of air pollution and coal mining is concerned, the public concerns have been guided by perceptions, facts and conflicts. Compounding the problem, has been the lack of detailed information on particulate matter, including coal dust. To date, few research studies have been conducted on the characterisation of coal dust and atmospheric PM in general.

This research study therefore focuses on the characterisation of atmospheric PM and coal dust, particularly PM_{10}, from coal mines and adjacent communities given that it is one of the most significant pollutants emitted from coal mining regions and has direct effects on human

health and the environment. This information could be of great interest to the public in general, communities adjacent to coal mining activities, health practitioners, government authorities, atmospheric chemists and the coal industry. The coal mining industry could further apply information on particulates and coal dust for the purposes of air quality management planning, occupational health and community health.

2.2 Atmospheric Particulate Matter

Atmospheric PM is a mixture of fine and coarse aerosols in solid and/or liquid form. The solid component of aerosols is often referred to as airborne particulates or dust (Chatterton *et al*., 2002; Gautam, 2012; Perrino, 2010;). Although reference is often made to solid particles being PM, atmospheric aerosols are very complex mixtures of particles from diverse natural and anthropogenic (human) sources, with considerable variations in size and physico-chemical properties (Laskin *et al.*, 2012). This is particularly evident in urban aerosols and is due to the diverse and numerous emission sources, photochemical reactions, high concentrations, transboundary pollution and regional impacts (Roy & Singh, 2014). Characteristic aerodynamic diameters or sizes of atmospheric PM can range from nanometers to tens of micrometres (µm) and these include fine atmospheric PM with aerodynamic diameters of 2.5 or less ($PM_{2.5}$), coarse atmospheric PM with aerodynamic diameters of 10 µm or less (PM_{10}) (Gautam *et al.*, 2012). Atmospheric PM between 10-30 µm and above are known as total suspended particulate matter (TSP) (Roy & Singh, 2014).

Various physico-chemical factors influence the dispersion of PM in the atmosphere. These include the nature of particles, their size, shape and density (Kantova *et al*., 2017). Atmospheric meteorological conditions such as wind speed, wind direction and atmospheric stability, also influence the dispersion of PM in the atmosphere (Gautam *et al.*, 2012). Fine atmospheric PM can be suspended in the atmosphere for longer periods of time and can be transported for long distances, which may result in transboundary air pollution (Menon *et al*., 2008).

Atmospheric PM is a significant air pollutant which is also a central component of the atmosphere, biological systems and biogeochemical cycles (Baltensperger, 2007; Bloss, 2014). Due to the critical role that atmospheric PM plays in air quality degradation, various

studies have been undertaken in different fields, including environmental and health sciences, on the physico-chemical properties of atmospheric PM, gas-particle chemical atmospheric reactions, environment-atmosphere interactions and the impact on human health and climate change (George & Abbat, 2010). In summary, atmospheric PM can be classified based on its source, size, mode of formation and effects (Figure 1) (Gautam *et al.,* 2016).

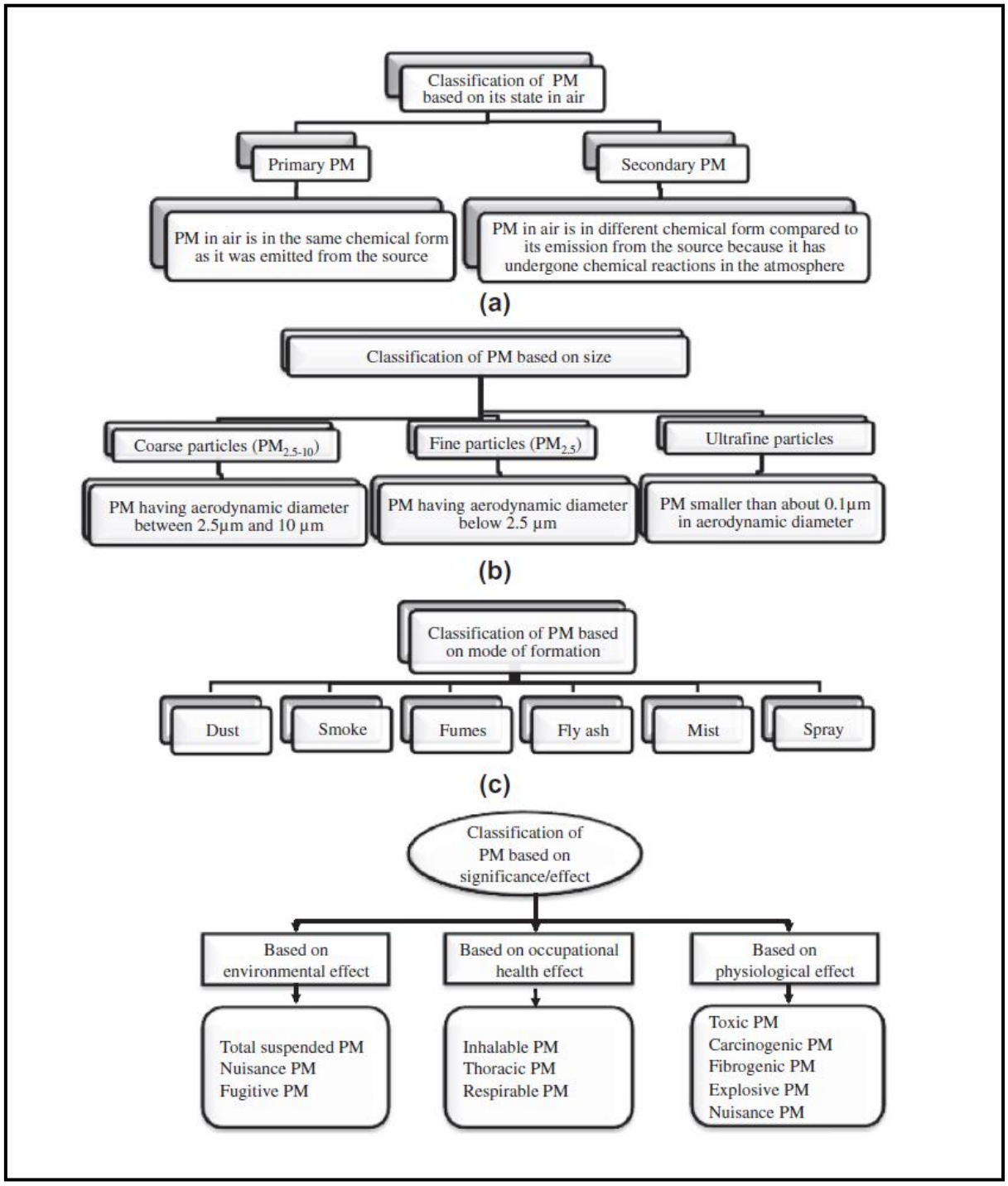

Figure 1: Classification of atmospheric PM (Gautam *et al.*, 2016).

2.3 SOURCES OF ATMOSPHERIC PARTICULATE MATTER

Sources of atmospheric PM are generally classified as natural and anthropogenic. Natural sources include volcanic emissions, wildfires, sea spray, wind erosion of open areas, while anthropogenic sources include industrial processes, fossil fuel burning, biomass burning, vehicle or transport related emissions (D'Almeida *et al.*, 1991). The direct emissions of particulates into the atmosphere results in primary particulates, while secondary particulates are formed due to the oxidation of gas-phase primary pollutants or from the condensation of semi-volatile species (Anderson *et al.*, 2012). The contribution of natural sources to particulate emissions is not overly significant and is not of major concern as they are part of the natural environment equilibrium (Popescu & Ionel, 2010). On the other hand, anthropogenic emissions contribute significantly to atmospheric pollution and are of major concern due to the increase in the number of anthropogenic sources of emissions and associated pollutant concentrations in the atmosphere, which are mainly driven by an increasing global population and energy demand (Bray *et al.*, 2017).

Fine particulate matter ($PM_{2.5}$) is mainly generated by combustion processes such as fossil fuel combustion for power generation purposes, vehicle or transport emissions and industrial processes such the smelting of ore and metals (D'Almeida *et al.*, 1991). It is also generated by sources such as biomass burning, open burning of waste, vehicle emissions and domestic fuel burning (Andrade *et al*., 1993). Domestic fuel burning of coal in South Africa is largely undertaken in Mpumalanga due to the abundance of coal and its relatively low price (Balmer, 2007; Naidoo *et al*., 2015). Coal is used for cooking and space heating, particularly in the winter months (Makonese *et al*., 2016). In the Limpopo Province, wood is the main domestic fuel used for space heating and cooking, although coal is used in areas where it is abundant. The combustion of these fuels is carried out using simple devices or coal stoves and *imbawula* (brazier) which are inefficient as they do not result in full combustion of the fuel (Makonese *et al*., 2016). This incomplete combustion results in the release of a mixture of pollutants such as fine and coarse atmospheric PM, gaseous chemical species such as SO_2 and PAHs (Balmer, 2007; Naidoo *et al*., 2015).

Coarse particulates are derived from various sources such as mining, construction, agricultural activities, soil dust and unpaved roads (Andrade *et al*., 1993; Chow *et al.*, 1992). Atmospheric PM contains significant amounts of carbonaceous components in the form of

brown /organic carbon (OC) and elemental carbon (EC) (D'Almeida *et al.*, 1991). Carbonaceous atmospheric PM is generally divided into three categories i.e OC, EC and carbonate carbon (CC) (Zhang *et al*., 2017). Carbonate carbon is much less common in the atmosphere and is usually attributed only to local sources (Karanasiou, 2015). Primary organic carbon consists of carbon that is directly released to the atmosphere as particulates (Klejnowski *et al*., 2017). Organic carbon can also be formed through the photolysis of gas-phase material, resulting in the formation of secondary organic aerosols (Karanasiou, 2015; Klejnowski *et al*., 2017). Elemental carbon is derived from incomplete combustion and its sources are predominantly anthropogenic (Contini *et al*., 2018; Karanasiou, 2015). However, there are challenges associated with techniques that are commonly applied for the purposes of determining OC and EC, which can only provide information on operationally defined quantities of BO or EC (Karanasiou, 2015).

Natural sources also contribute to fine PM emissions and these sources include volcanic emissions, biomass burning and windblown dust (Cohen, 2002). The sources of windblown dust include local and regional sources which contribute to atmospheric particulate loading (Al Ameri *et al*., 2019; Kohfeld & Harrison, 2001). Various regional sources and transportation mechanisms occur. Wind-blown dust in the form of atmospheric dust storms, is transported from various regions (Engelstaedter *et al*., 2006; Goudie & Middleton, 1992). Atmospheric dust storms are visible from space and images of dust storms clearly indicate evidence of their contribution to atmospheric dust loading (Kohfeld & Harrison, 2001; Tegen *et al.*, 2002). Large quantities of atmospheric dust originate from sparsely vegetated regions such as deserts (arid and semi-arid) (Figure 2) (Tegen *et al*., 2002). Deserts located in northern Africa such as the Sahara and deserts located in the Middle East produce most of the dust with a contribution of 70% to global annual dust emissions (Al Ameri *et al*., 2019; Engelstaedter *et al*., 2006). Other dust generating regions include Australia and Asia (Tegen *et al.,* 2002). Dust plays a critical role in the climate system, a role which is evident in its effects on cloud formation and atmospheric energy balance through absorption and scattering of solar energy (Goudie & Middleton, 1992; Kohfeld & Tegen, 2007). Atmospheric chemical transformation of dust occurs when dust particulate surfaces become coated with soluble nitrate and sulphate species (Albarakat & Lakshmi, 2019; Tegen *et al*., 2002). The extent or degree to which natural and anthropogenic soil dust influences the climate system and the distribution of dust storms from a global perspective have been continuous subjects of research. However, very few studies exist on the global distribution of dust storms (Tegen

et al., 2002). One such study was undertaken by Engelstaedter *et al* (2006) and the study focused on the use of climatological average of annual dust storm frequency (Figure 3). Simulated dust concentrations in South Africa range from 3 to 80 µg/m-³, with high concentrations in the north, north western and north eastern parts of the country. The Limpopo and Mpumalanga Provinces are within the areas of the country whose particulate loading is impacted by dust storms.

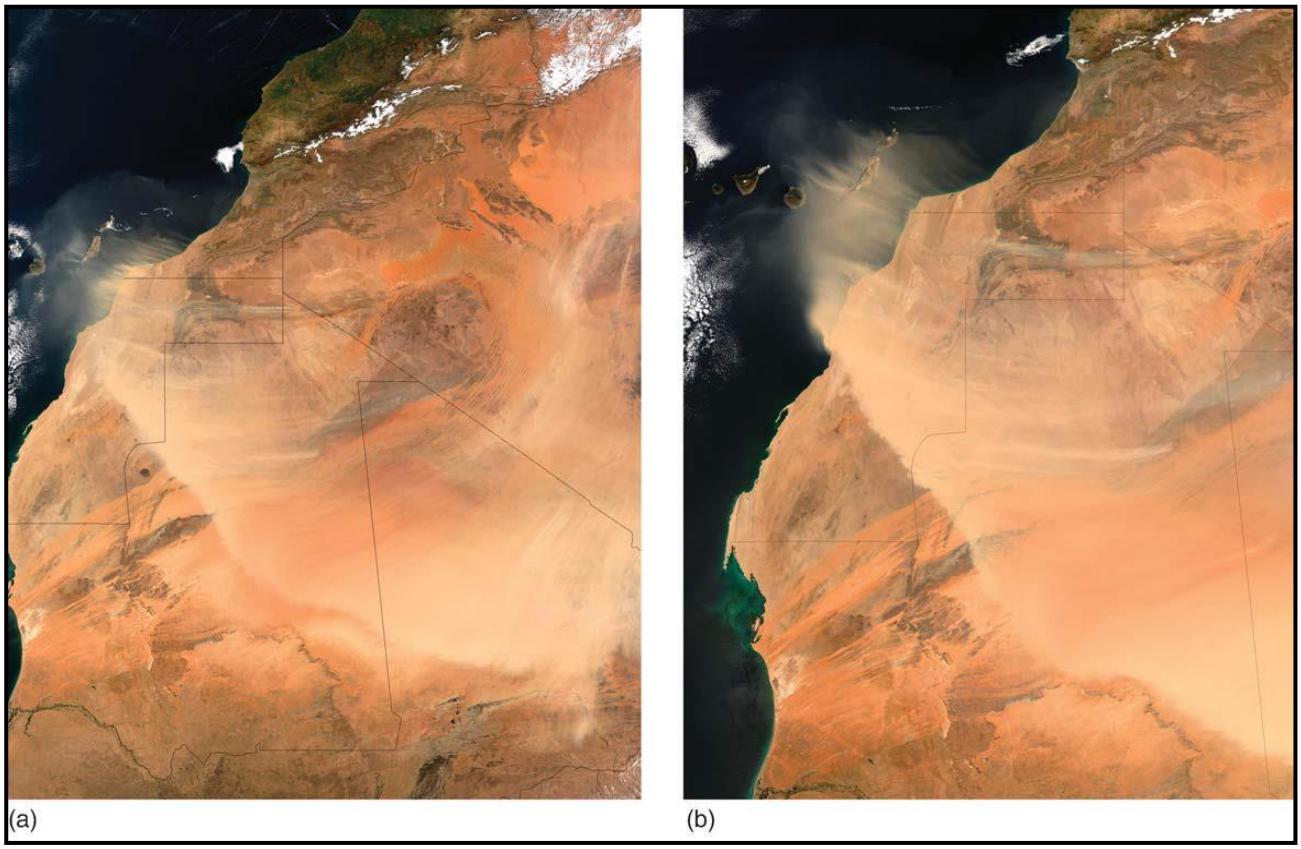

Figure 2: Sahara dust storm satellite images (March 2004) (a) Sahara dust storm across Mauritiana and Mali (morning) (b) Sahara dust storm across Mauritiana and Mali (afternoon) (Tegen *et al.*, 2002). Images acquired by the Moderate Resolution Imaging Spectroradiometer (MODIS) (NASA Visible Earth Observatory, 2006).

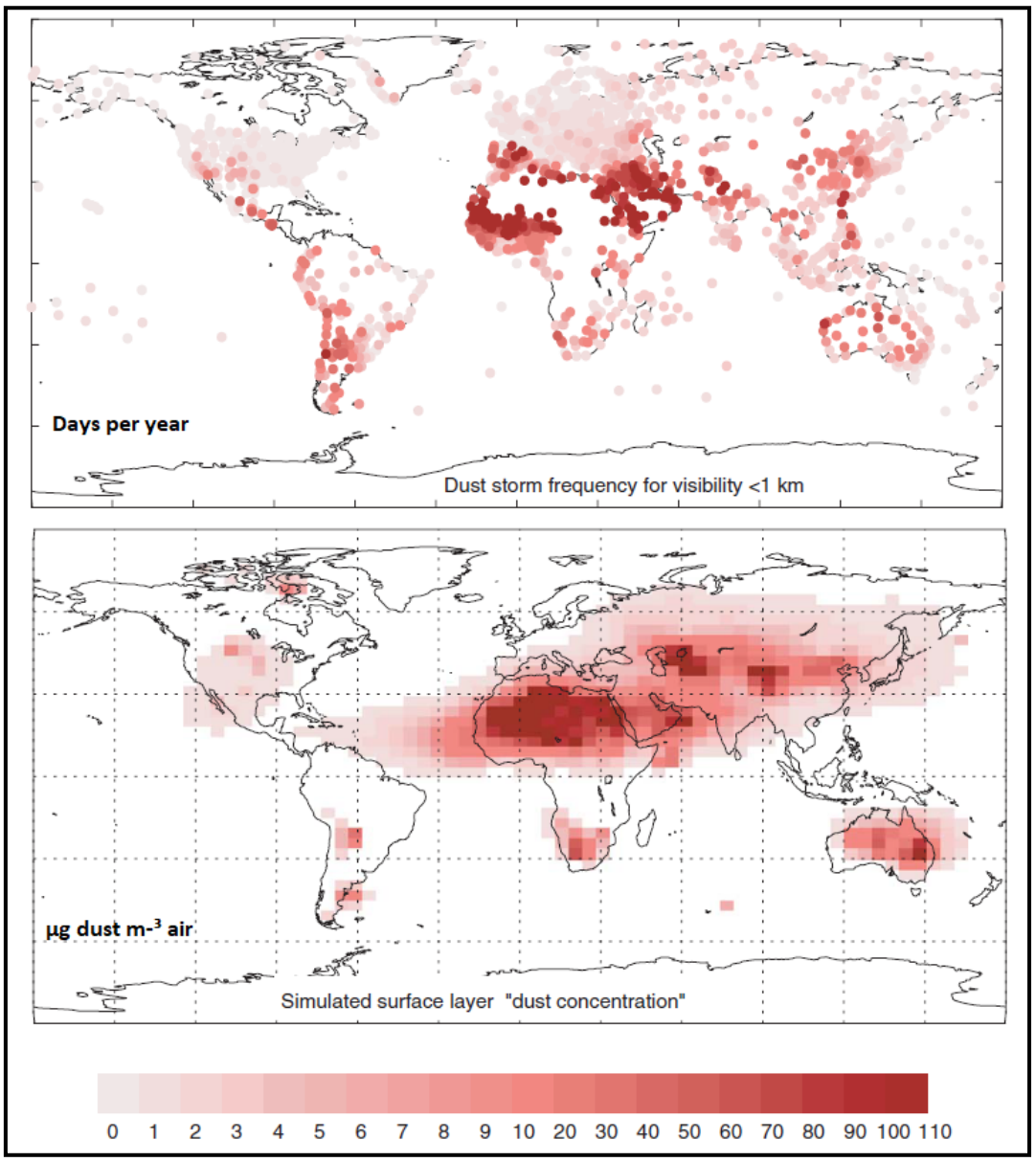

Figure 3: Frequency of annual dust storms (days per year) averaged from 1971- 1996 (Engelstaedter, *et al*., 2006) (Tegen *et al*., 2002).

2.3.1 Modes of Atmospheric Particulate Matter Formation

Atmospheric PM can be chemically transformed through complex and diverse reactions in the atmosphere (Cohen, 2010). The continuous evolvement of particulates in the atmosphere due to physical and chemical transformations results in 'atmospheric aging' (Gieré & Querol, 2010). The tropospheric and stratospheric chemical reactions are complex as photochemical reactions can occur (Tsiouri, *et al*., 2014), with the potential to produce radicals which have a high affinity to further react with other pollutants (Lagzi *et al.*, 2014). The generation process of atmospheric PM has a great influence on particle sizes. There are three different modes of particle formation (Tsiouri, *et al*., 2014). These include the

nucleation mode or ultrafine particle mode, accumulation mode and the coarse mode (Figure 4) (Gieré & Querol, 2010; Perrino, 2010). This trimodal size distribution is mainly observed in the lower atmosphere (Bloss, 2014). Particles generated through the nucleation mode have aerodynamic diameters of below 0.1 microns (µm) and are mainly formed by combustion processes and homogenous nucleation of precursor gases on the surface of pre-existing particles (John, 2001; Tsiouri, *et al*., 2014). Particles formed though the accumulation mode are in the range of 0.1- 1 µm and are formed due to the coagulation of particles in the nucleation mode and the condensation of gaseous species on the surface of pre-existing particles (Lagzi *et al.*, 2014). Mechanically generated primary particles are emitted in the coarse mode, are emitted from sources such as mining and erosion and have aerodynamic diameter of more than 1 µm (Kohfeld & Tegen, 2007; Perrino, 2010).

A comparison of the composition and sources of fine and coarse atmospheric PM is shown in Table 1 below.

Table 1: Composition and sources of fine and coarse atmospheric PM (Perrino, 2010).

	Fine Mode Particles	**Coarse Mode Particles**
Composed of:	Sulfate, SO^{2-}_4; Nitrate, NO^-_3; Ammonium, NH^+_4; Hydrogen ion, H^+; Elemental carbon, C; Organic Compounds; PAH; Metals, Pb, Cd, V, Ni, Cu, Zn; Particle-bound water; Biogenic organics.	Resuspended dusts, soil dust, street dust; Coal and oil fly ash; Metal oxides of Si, Al, Mg, Ti, Fe. $CaCO_3$, NaCl, sea salt; Pollen, mold spores, plant parts.
Sources:	Combustion of coal, oil, gasoline; Transformation products of NO_x, SO_2, and organics including biogenic organics, e.g., terpenes; High temperature processes; Smelters, steel mills, etc.	Resuspension of soil tracked onto roads and streets; Suspension from disturbed soils, e.g., farming, mining; Resuspension of industrial dusts; Construction, coal and oil combustion, ocean spray.
Lifetimes:	Days to weeks	Minutes to hours
Travel Distance:	100s to 1000s of kilometers.	1 to 10s of kilometers.

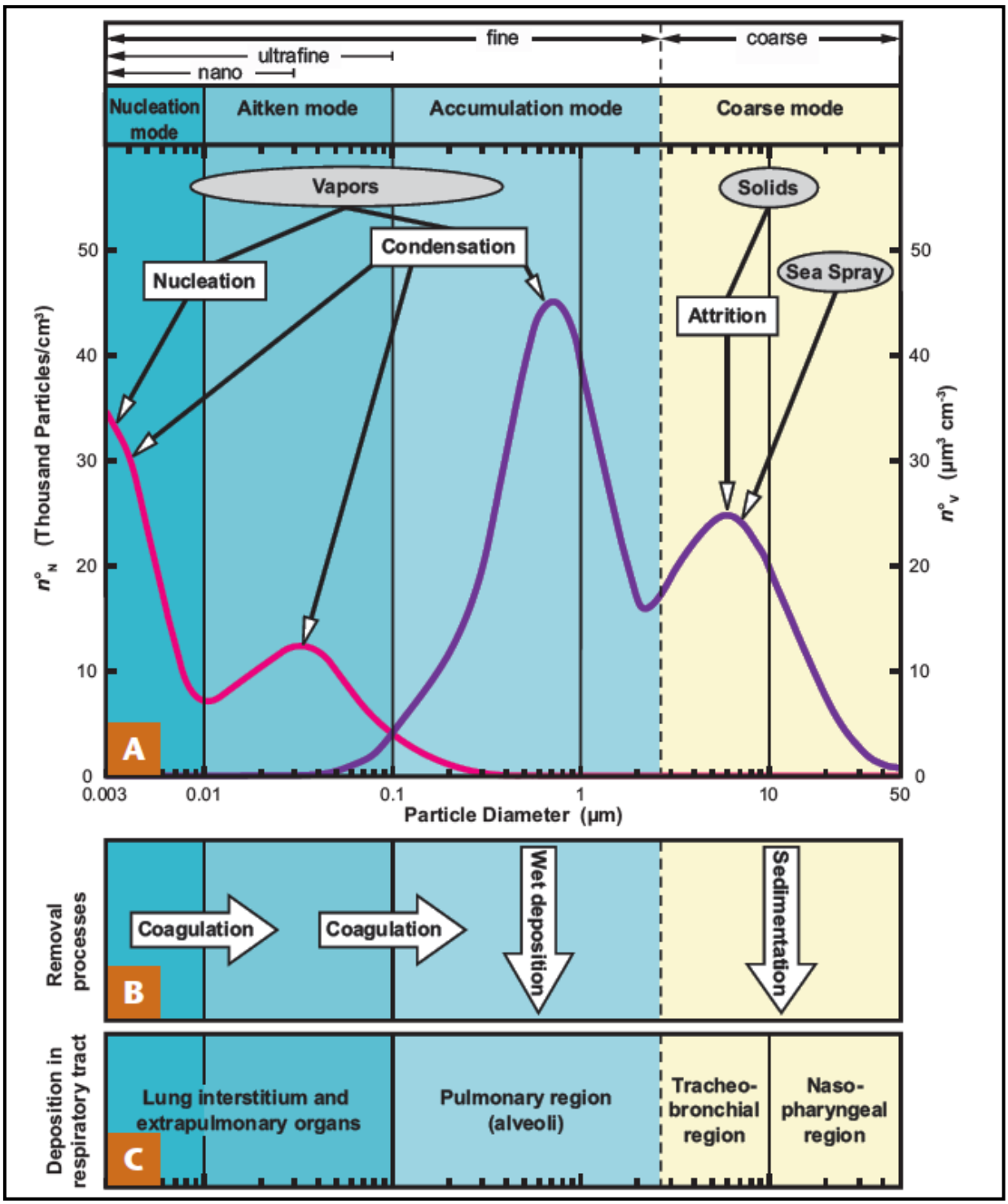

Figure 4: (A)Typical size distributions of the number (n_N, magenta line) and the volume (n_V, purple line) of atmospheric particles per cm³ of air (Gieré & Querol, 2010). Particles sources shown in grey ellipses; particle formation processes shown in white rectangles and associated arrows in A; particle removal processes in B. C shows respiratory tract areas where inhaled particulate matter is preferentially deposited.

2.3.2 Atmospheric Particulate Matter Shape and Form

Atmospheric PM is also characterised by different shapes which can be viewed microscopically (Gieré & Querol, 2010). The physical properties of atmospheric PM are key in their characterisation, identification of their sources, potential health risks and mitigation measures (Aneja *et al.*, 2012). With regards to the health risks, the shape and diameter of PM can be pivotal in determining issues related to inhalation, respiration and deposition of the PM in the respiratory system (Gieré & Querol, 2010). Information on the shapes and diameters of PM can be obtained through microscopic analysis of particulate samples with an electron microscope (Cavalli *et al*., 2016); examples are shown in Figure 5 below. The microscopy information can then be applied for the identification of potential sources and exposure estimation (Ebert *et al*., 2004; Ličbinský *et al*., 2010).

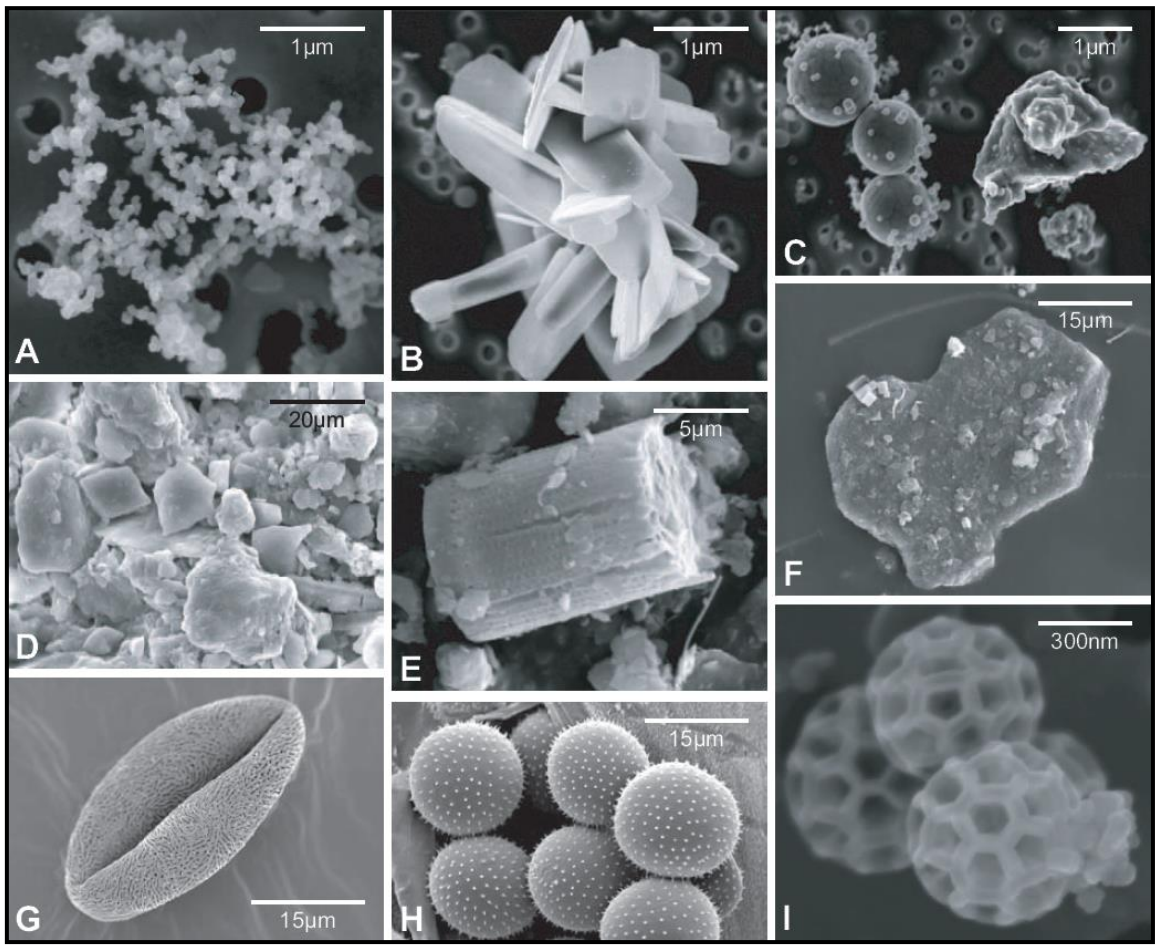

Figure 5: Scanning electron microscopy photomicrographs of various particulates (Gieré and Querol, 2010). (A) Soot particles (B) Calcium sulphate crystals derived from combustion (C) Plagioclase and magnetite spheres derived from combustion (D) Clay and calcite (E) Diatoms (F) Illite (G) Pollen (H) Spores (I) Brochosomes

2.3.3 Atmospheric Residence Time of Particulate Matter

The residence time of atmospheric aerosols is dependent on their physico-chemical properties and on altitude (Figure 6) (Jaenicke, 1980; Perrino, 2010). Smaller particles have very short atmospheric residence times (minutes to a day) due to efficient removal through coagulation with other particles (Lipsky *et al.,* 2002). Sedimentation, the rapid removal of particles from the atmosphere through gravitational effects, results in short residence times for coarse or large particles (Gatari *et al*., 2006). Longest residence times are associated with particles in the accumulation mode (average of 1 week to 10 days) (Pokorná, *et al*., 2012). This is because sedimentation (and Brownian diffusion to a lesser extent) are the methods of removal of these particles (Jaenicke, 1980). Instead, wet deposition is the predominant mechanism of removal of coarse particles in the atmosphere (John, 2001; Lagzi *et al*., 2014). The number, surface or volume of particles generally define their distribution in the atmosphere (Lagzi *et al*., 2014).

Fine particles are associated with residence times of days to weeks and this can result in local air pollution issues, which in turn, have the capability of being transformed to regional or global issues (Figure 7) (Cohen *et al*., 2004; Tegen & Kohfeld, 2006). This is because these particles can potentially result in transboundary air pollution in other regions or countries and have global climate change implications (Gatari *et al*., 2006).

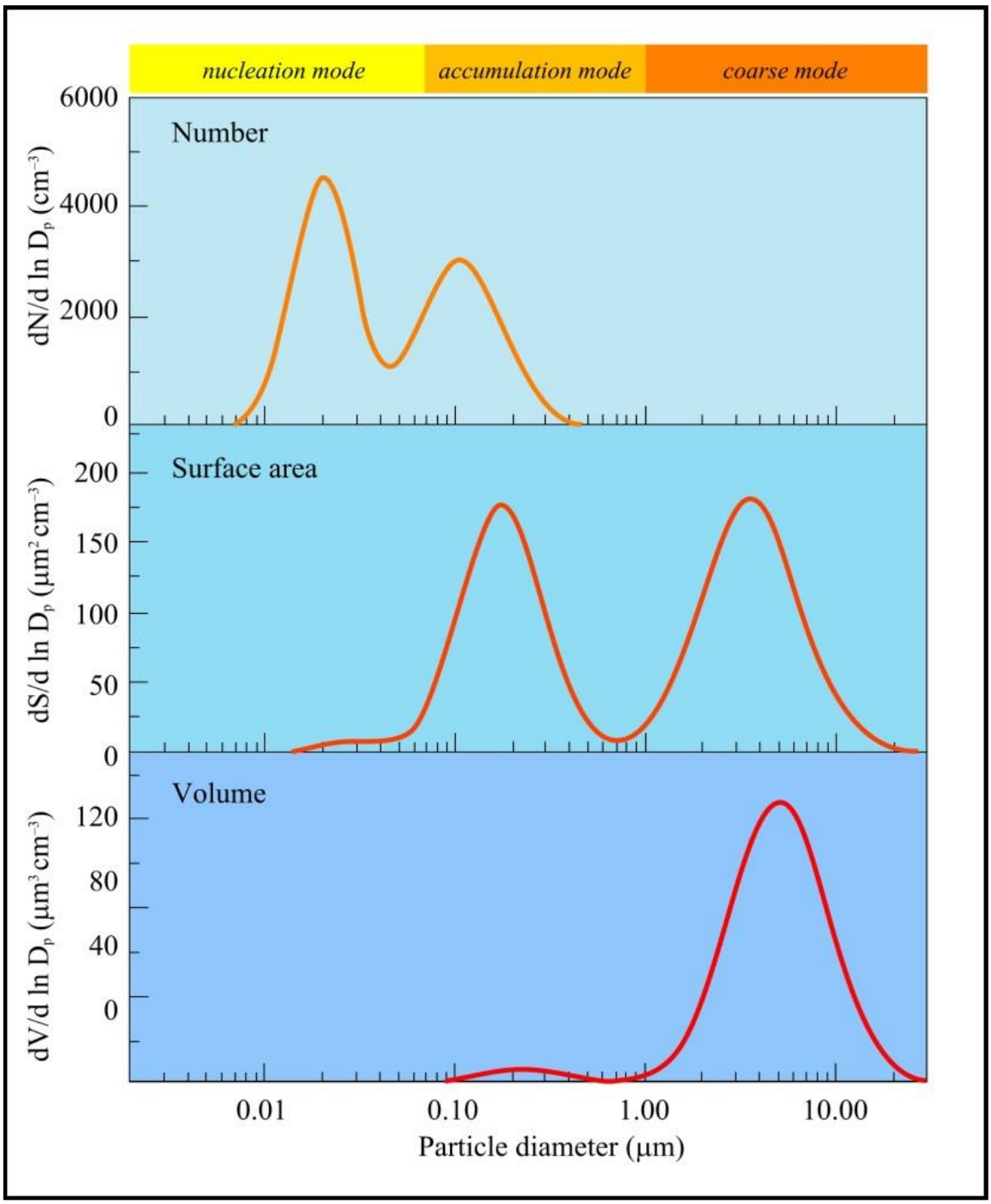

Figure 6: Number, surface and volume distributions of aerosol particles) (Lagzi *et al.*, 2014). (The areas below the curves correspond to the total aerosol number, surface and volume, respectively).

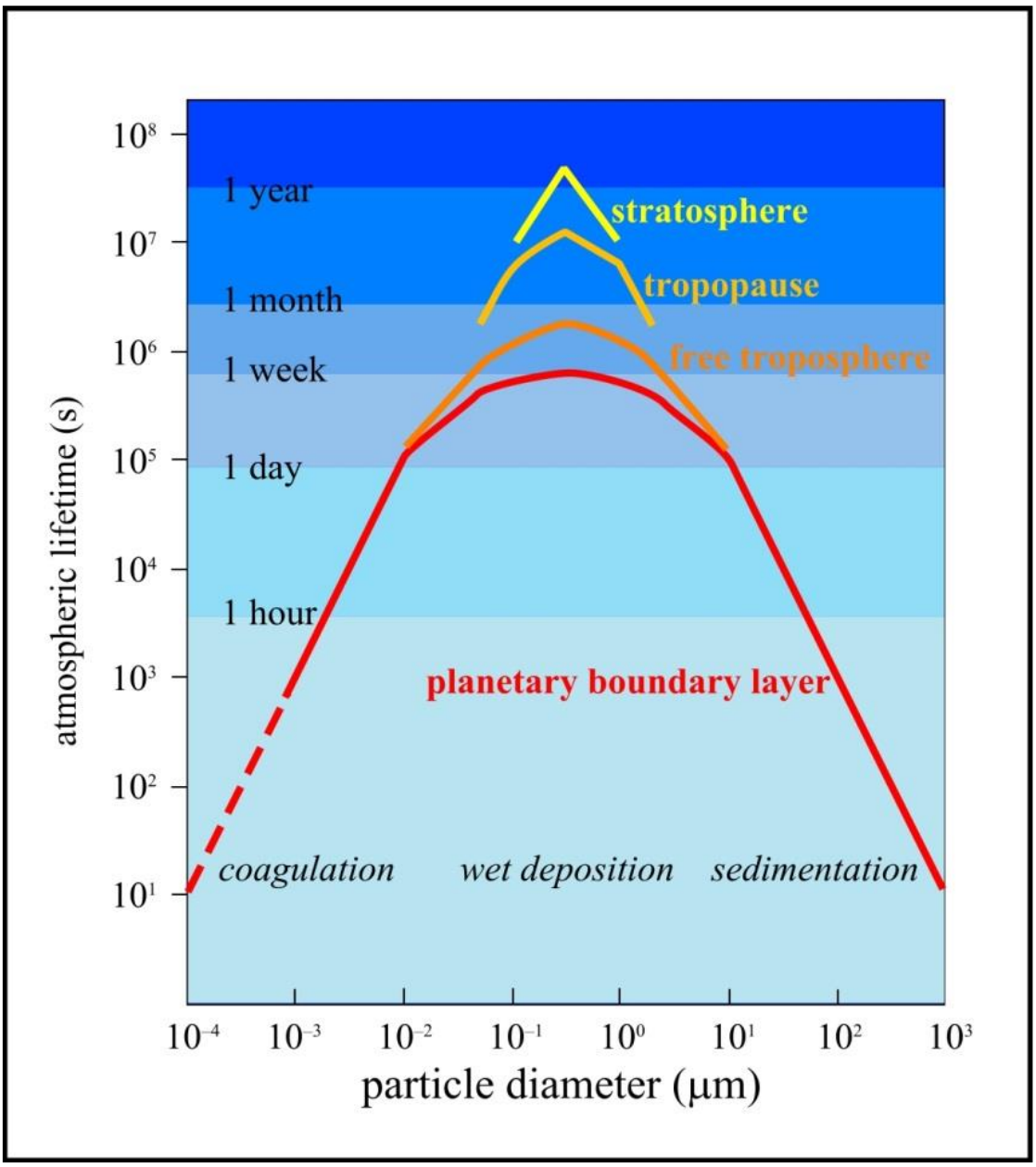

Figure 7: Atmospheric lifetime of different particle sizes at different levels of the atmosphere (Jaenicke, 1980).

2.3.4 Atmospheric Particulate Matter Health Impacts

Atmospheric PM is increasingly becoming a critical issue due to its impacts on human health, the environment and its associated financial and socio-economic burdens (Anderson *et al.*, 2012; Panyacosit *et al.*, 2000; Smith, 1993). Atmospheric PM of 10 μm or less is also referred to as inhalable particulate and is of significant relevance with regards to human health effects (Albers *et al*., 2015; Kesavachandran *et al*., 2015; Kunzli & Tager, 2000). Particulate matter can also be classified as respirable (less than 2.5μm) and thoracic (below 10μm) (Kim *et al*., 2015; Lipsky *et al.*, 2002). The typical curves that define inhalable,

thoracic and respirable PM are shown in Figure 8 (United Kingdom (UK) Department of the Environment ,1993).

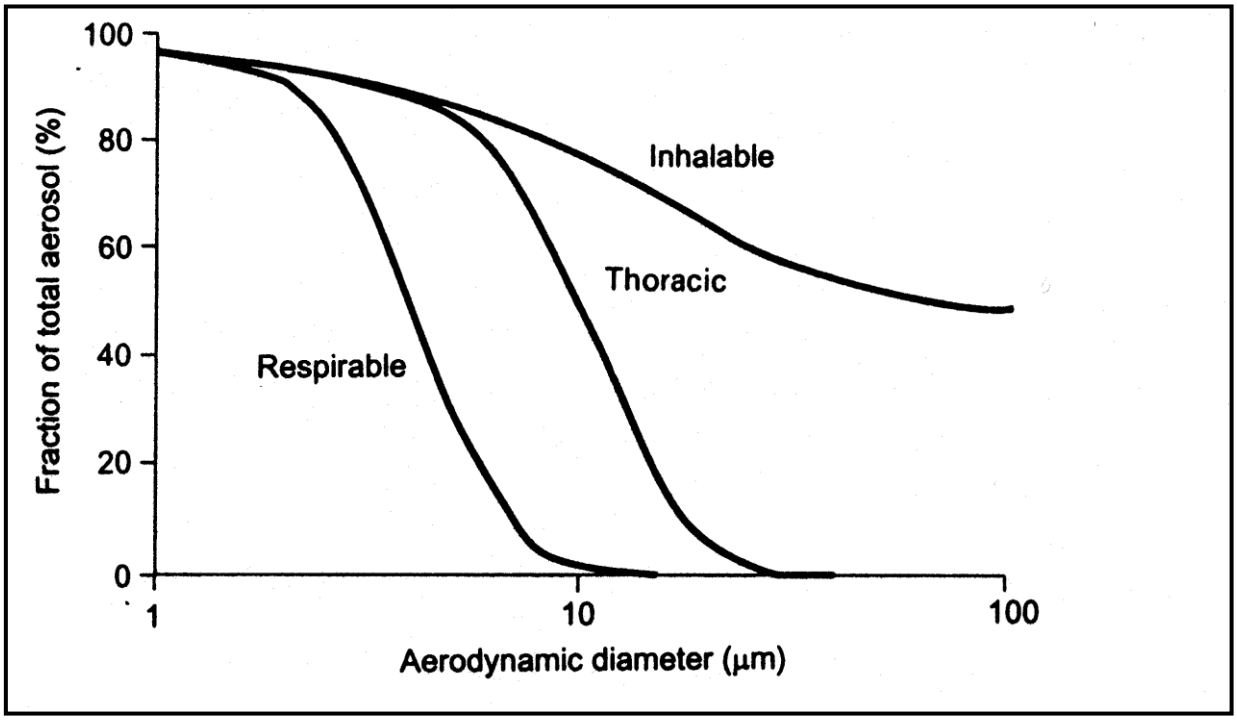

Figure 8: Typical curves for inhalable, thoracic and respirable particulate matter (The U.K. Department of the Environment ,1993).

The effects of atmospheric PM on health is dependent on particulate size, chemical composition and shape (Barraza, 2018). Particulate size is a determinant of the deposition areas of atmospheric PM in the respiratory system upon inhalation (Anderson *et al*., 2012). In the lungs, PM_{10} can penetrate the bronchi while $PM_{2.5}$ can enter the circulatory system (Dockery & Stone, 2007). In addition, there is significant evidence that indicates that fine PM of 2.5 µm or less, contributes significantly in the observed health impacts (Jimoda, 2012). This is due to the deposition of these particulates in the lower respiratory system, i.e bronchi walls, while the coarse particles are effectively removed from the respiratory system via the muco-ciliary elevator mechanism (Dockery & Stone, 2007; Kim *et al*., 2015). For particulates smaller than 0.1 µm, Brownian motion is the main mode of movement and deposition occurs in the bronchi (Spengler *et al*., 1990). Particulates of between 0.1 -1 µm are too large for Brownian motion and are not trapped in the trachea because of their size (Kesavachandran *et al*., 2015). Hence, deposition in the lungs is their final fate (Kim *et al.*, 2015).

Penetration of the respiratory tract by these particles reaches as far as the alveoli, which are located deep within the lungs (Figure 9) (Barraza, 2018; Stern *et al*., 1984). The penetration process is dependent on the particle diameter size (Table 2) (Spengler *et al.*, 1990; Stern *et al.*, 1984). Particulate deposition in various parts of the respiratory system is also dependent on size (Roy & Singh, 2014; Nagar *et al*., 2014; Panyacosit, 2000).

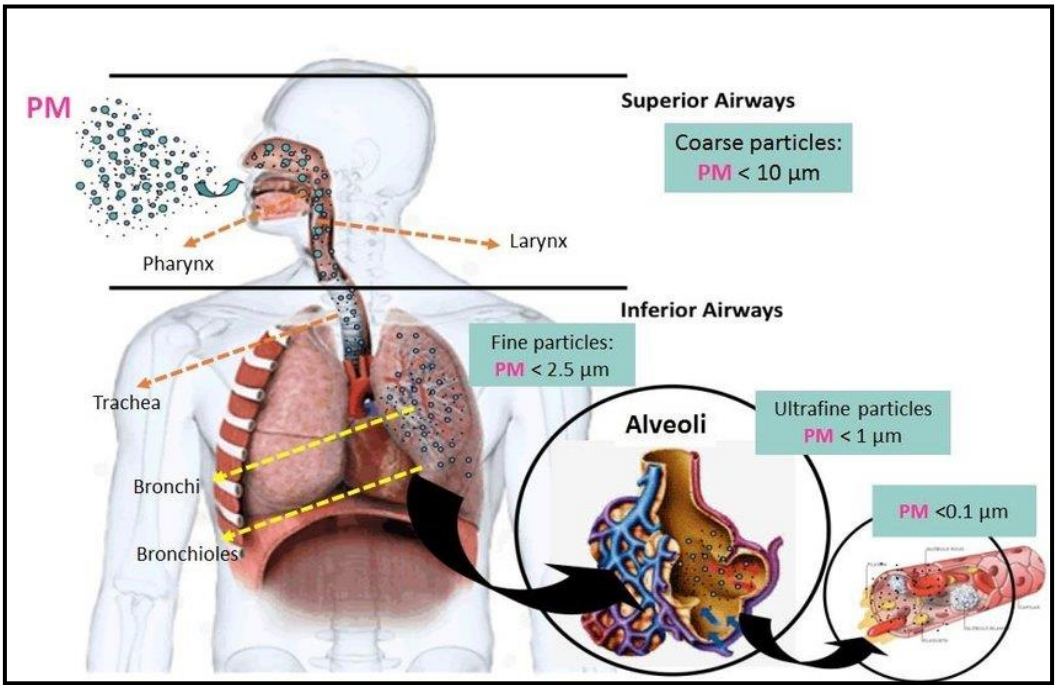

Figure 9: Respiratory tract and PM size classification (Barraza, 2018).

Table 2: Respiratory system penetration vs. particle size (Spengler *et al.,* 1990).

Particle size (range) (µm)	Penetration of Particles
11	and up particles do not penetrate
7-11	and up particles penetrate nasal passages
4.7-7	particles penetrate pharynx
3.3-4.7	particles penetrate trachea and primary bronchi
2.1-3.3	particles penetrate secondary bronchi
1.1-2.1	particles penetrate terminal bronchi
0.65-1.1	particles penetrate bronchioli
0.43-0.65	particles penetrate alveoli

Multiple epidemiological studies with varying populations, methodologies and regions have demonstrated a dose-dependent relationship between PM concentrations and observed human health impacts (Stern *et al.*, 1984; Johnston, 2000). Atmospheric PM contributes significantly to increase in the risk of respiratory diseases, cardiovascular diseases and mortality, especially in vulnerable groups such as newborns, the elderly, children and pregnant women (Anderson *et al*., 2012; Dockery *et al.*, 1994; Kim *et al.,* 2015; Li *et al*., 2015; Nagar *et al.*, 2014; Panyacosit *et al.*, 2000; WHO, 2006). In addition, epidemiological studies indicate that the removal of people exposed to a PM rich environment to one that is not, reduces the prevalence of respiratory and cardiovascular diseases (Kunzli & Tager, 2000; Panyacosit *et al.*, 2000).

Epidemiological studies also indicate that atmospheric PM continues to be the constituent of air pollution that is most reliably associated with health impacts (Kim *et al.*, 2015; Anderson *et al.*, 2012). In addition, there is adequate and consistent data that demonstrates the effect of PM on the cardiovascular system (Nagar *et al*., 2014; Ward & Sua´rez-Ruiz, 2008). It has also been demonstrated that populations that are subjected to long term exposure to PM emissions tend to exhibit significantly higher cardiovascular incident and mortality rate. The United States Environmental Protection Agency (USEPA) has developed a list of short and long-term impacts of PM based on various epidemiological studies undertaken in the United States (Table 3) (USEPA, 2009).

Atmospheric particulate matter characteristics are not the only factors that determine the nature and severity of human health impacts (Mannucci & Franchin, 2017). The human and environment components are also critical as they dictate the frequency and type of the observed health impacts (Smith, 1993). The physical characteristics of the person exposed to atmospheric PM pollution, breathing mode, rates and volume are among the determinants of health impacts (Lim *et al*., 2012). The local conditions such as weather, topography, seasons, particulate sources, particulate concentrations are also important determinants of health impacts (WHO, 2016). These components determine exposure rate and effectiveness, i.e particulate matter concentration that is breathed in and the received dosage (Dockery *et al.*, 1994; Smith, 1993).

According to a Global Burden of Disease Study 2010 study findings by Lim *et al*., (2012), ambient PM pollution accounted for an average of 3.1 million deaths and 3.1% of global

disability-adjusted life years (DALYs) and household air pollution for 3·5 million deaths and 4·5% of global DALYs in 2010 The global proportion of ischaemic heart disease disability-adjusted life-years attributable to ambient particulate matter is 22% and 18% for household air pollution from solid fuels (Table 4).

The burdens associated with atmospheric PM i.e, human, environmental and socio-economic, are largely felt in the developing countries, particularly in low income areas (Mannucci & Franchin, 2017; WHO, 2016). According to the WHO, more than 80% of urban dwellers are exposed to air quality levels which exceed the WHO 24 hour (daily) and annual limits (Table 5, Table 6 and Figure 10). The decline in urban air quality has resulted in increases of chronic and acute respiratory diseases, cardiovascular diseases, lung cancer and risk of stroke (WHO, 2016).

Table 3: Consequences, deposition and sources of PM_{10} and $PM_{2.5}$ inhalation (USEPA, 2009).

PM inhalation	Sources	Deposition %	Organ affected directly	How affected	Organ affected indirectly
PM_{10}, coarse particles	Include crushing or grinding operations, and dust stirred up by vehicles traveling on roads.	60% in upper respiratory tract; 20% bronchial tube	Lungs	Inflammation, oxidative stress, accelerated progression and exacerbation of COPD, increased respiratory symptoms, effected pulmonary reflexes reduced lung function	Heart, blood, systemic inflammation oxidative stress
$PM_{2.5}$, fine particles	Include all types of combustion, including motor vehicles, power plants, residential wood burning, forest fires, agricultural burning, and some industrial processes.	4% in upper respiratory tract; 7% bronchial tube; 10% fine pulmonary airways; 50% pulmonary alveolus	Heart	Altered cardiac autonomic function, increased dysrhythmic susceptibility, altered cardiac repolarization, increased myocardial ischemia	Vasculature
			Blood	Altered rheology, increased coagulability, translocated particles, peripheral thrombosis, reduced oxygen saturation	Brain, systemic inflammation oxidative stress
			Systemic inflammation oxidative stress	Increased CRP, proinflammatory mediators, leukocyte and platelet activation	Heart, blood, vasculature
			Vasculature	Atherosclerosis, accelerated progression of and destabilization of plaques, endothelial dysfunction, vasoconstriction and Hypertension	Heart, brain
			Brain	Increased cerebrovascular ischemia	Vasculature, blood

Table 4: Proportion of ischaemic heart disease disability-adjusted life-years attributable to individual risk factors, worldwide, 2010 (Lim *et al*., 2012).

	Disability-adjusted life-years (%)
Physiological risk factors	
High blood pressure	53%
High total cholesterol	29%
High body-mass index	23%
High fasting plasma glucose	16%
Alcohol use	33%
Tobacco smoking, including second-hand smoke	31%
Dietary risk factors and physical inactivity	
Diet low in nuts and seeds	40%
Physical inactivity and low physical activity	31%
Diet low in fruits	30%
Diet low in seafood omega-3 fatty acids	22%
Diet low in whole grains	17%
Diet high in sodium	17%
Diet high in processed meat	13%
Diet low in vegetables	12%
Diet low in fibre	11%
Diet low in polyunsaturated fatty acids	9%
Diet high in trans fatty acids	9%
Diet high in sugar-sweetened beverages	2%
Air pollution	
Ambient particulate matter pollution	22%
Household air pollution from solid fuels	18%
Other environmental risks	
Lead exposure	4%

Table 5: WHO Air Quality Guidelines and Interim Targets for Particulate Matter (24 hour Mean Concentrations) (WHO, 2006).

WHO air quality guidelines and interim targets for particulate matter: 24-hour concentrations[a]

	PM_{10} ($\mu g/m^3$)	$PM_{2.5}$ ($\mu g/m^3$)	Basis for the selected level
Interim target-1 (IT-1)	150	75	Based on published risk coefficients from multi-centre studies and meta-analyses (about 5% increase of short-term mortality over the AQG value).
Interim target-2 (IT-2)	100	50	Based on published risk coefficients from multi-centre studies and meta-analyses (about 2.5% increase of short-term mortality over the AQG value).
Interim target-3 (IT-3)*	75	37.5	Based on published risk coefficients from multi-centre studies and meta-analyses (about 1.2% increase in short-term mortality over the AQG value).
Air quality guideline (AQG)	**50**	**25**	Based on relationship between 24-hour and annual PM levels.

Table 6: WHO Air Quality Guidelines and Interim Targets for Particulate Matter (Annual Mean Concentrations) (WHO, 2006).

WHOair quality guidelines and interim targets for particulate matter: annual mean concentrations[a]

	PM_{10} ($\mu g/m^3$)	$PM_{2.5}$ ($\mu g/m^3$)	Basis for the selected level
Iinterim target-1 (IT-1)	70	35	These levels are associated with about a 15% higher long-term mortality risk relative to the AQG level.
Interim target-2 (IT-2)	50	25	In addition to other health benefits, these levels lower the risk of premature mortality by approximately 6% [2–11%] relative to theIT-1 level.
Interim target-3 (IT-3)	30	15	In addition to other health benefits, these levels reduce the mortality risk by approximately 6% [2-11%] relative to the -IT-2 level.
Air quality guideline (AQG)	**20**	**10**	These are the lowest levels at which total, cardiopulmonary and lung cancer mortality have been shown to increase with more than 95% confidence in response to long-term exposure to $PM_{2.5}$

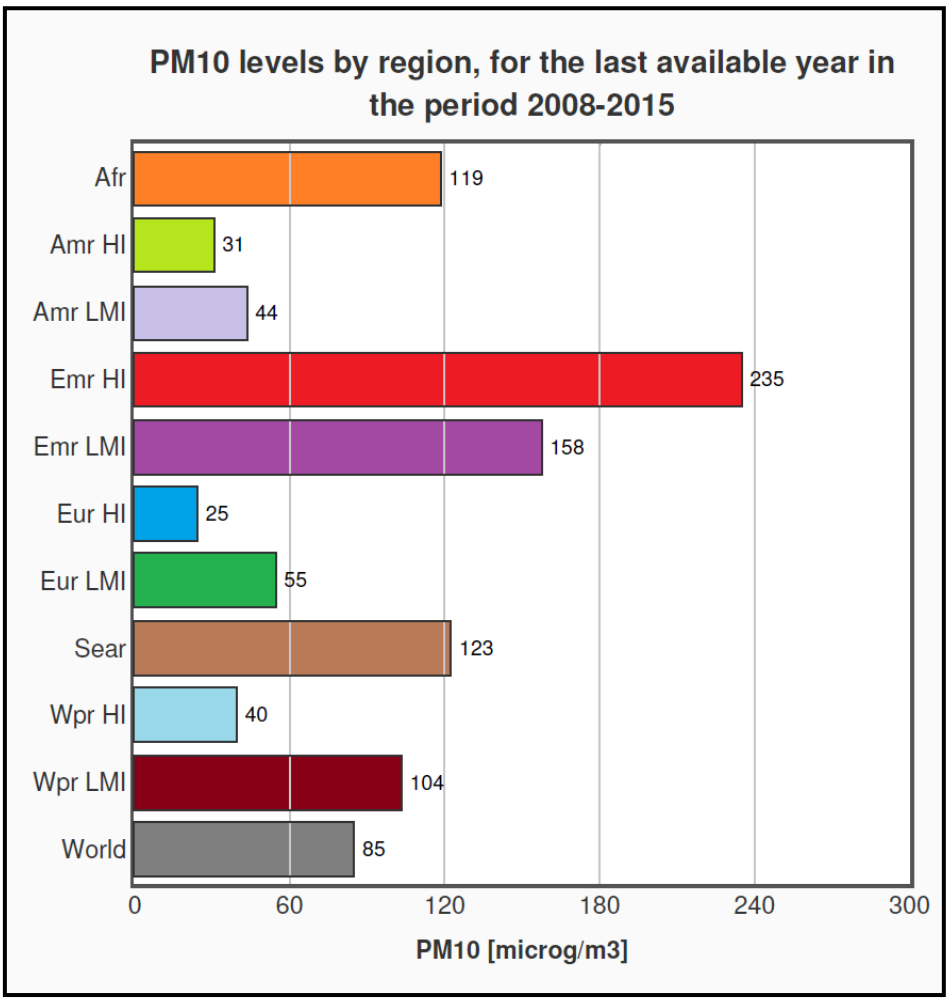

Figure 10: PM_{10} levels by region (WHO, 2016) (AFR: Africa; AMR: America; EMR: Eastern Mediterranean; EUR: Europe; SEAR: South-East Asia; WPR: Western Pacific; LMCI: Low- and middle-income countries; HIC: High-income countries.

Given, this background and the fact that PM_{10} levels in most African countries exceed the WHO PM_{10} daily or 24-hour mean guideline of 50 µg/m^3, intensified air quality management measures, research studies on PM_{10} and $PM_{2.5}$ health and environmental impacts should be undertaken (WHO, 2016). However, the assessment of the potential environmental and health effects of atmospheric PM in ambient air requires detailed chemical, physical and morphological characterisation of the particulates, which is the purpose of this research study.

2.3.5 Other Impacts of Atmospheric Particulate Matter

Atmospheric particulate matter influences climate through the absorption and scattering of solar radiation (Cohen, 2010; Lipsky *et al.*, 2002). Particulates can also act as condensation nuclei in the atmosphere and therefore play an important role in cloud formation processes

(Perrino, 2010). They also play an important role in atmospheric chemistry by enabling the occurrence of heterogenous reactions (Capes *et al.*, 2009). This influence on solar radiation has significant consequences on the radiation budget and climate. Fossil fuel soot, biomass burning, sulphate aerosols and black carbon contribute to particulate radiative forcing properties (Penner *et al*., 1993).

The US National Aeronautics and Space Administration (NASA) indicated that about 8000 kilotonnes of black carbon are emitted globally per annum and that developing countries are responsible for 77% of these emissions through sources such as open burning of waste, biomass burning, diesel engines which are old and domestic cookstoves (Figure 11) (NASA, 2013). This data is based on long simulation campaigns by NASA's Goddard Earth Observing System Model, Version 5 (GEOS-5), a system of models which uses aerosol processes' data obtained from Goddard Global Ozone Chemistry Aerosol Radiation and Transport (GOCART) model (Colarco *et al*., 2010; Putman & da Silva, 2013). Aerosol processes modelled by the GOCART models include tropospheric mixing, emissions, deposition and chemistry of key aerosols such as black carbon, dust and sulphates found in the troposphere (NASA, 2013; Forster, 2007). Given the complexities associated with black carbon and atmospheric interactions, models improve the ability of understanding black carbon, atmospheric processes, climate change and the possible mitigation measures and strategies (Colarco *et al*., 2010; Forster, 2007).

The atmospheric oxidation of air pollutants such as sulphur dioxide (SO_2), carbon dioxide (CO_2) and nitrogen oxides (NO_x) results in the formation of sulphates, carbonates and nitrates, respectively (Adams *et al*., 1999). These substances can be removed from the atmosphere through wet and dry deposition, leading to the formation of acids which can impact soils and vegetation through acidification and eutrophication (Lipsky *et al.*, 2002; Szmigielski, 2012). Buildings and other man-made surfaces can also be impacted by acidification, resulting in financial impacts related to repairing and restoring infrastructure (Hamilton & Mansfield, 1993). Eutrophication is a global concern, as nutrient enriched water bodies promote the growth of aquatic plants, resulting in deoxygenation of water and oxygen deficiency which kills aquatic organisms (Adams *et al.,* 1999).

Other impacts of atmospheric PM include reduction in visibility due absorption and scattering of light in the atmosphere (Capes *et al.*, 2009).

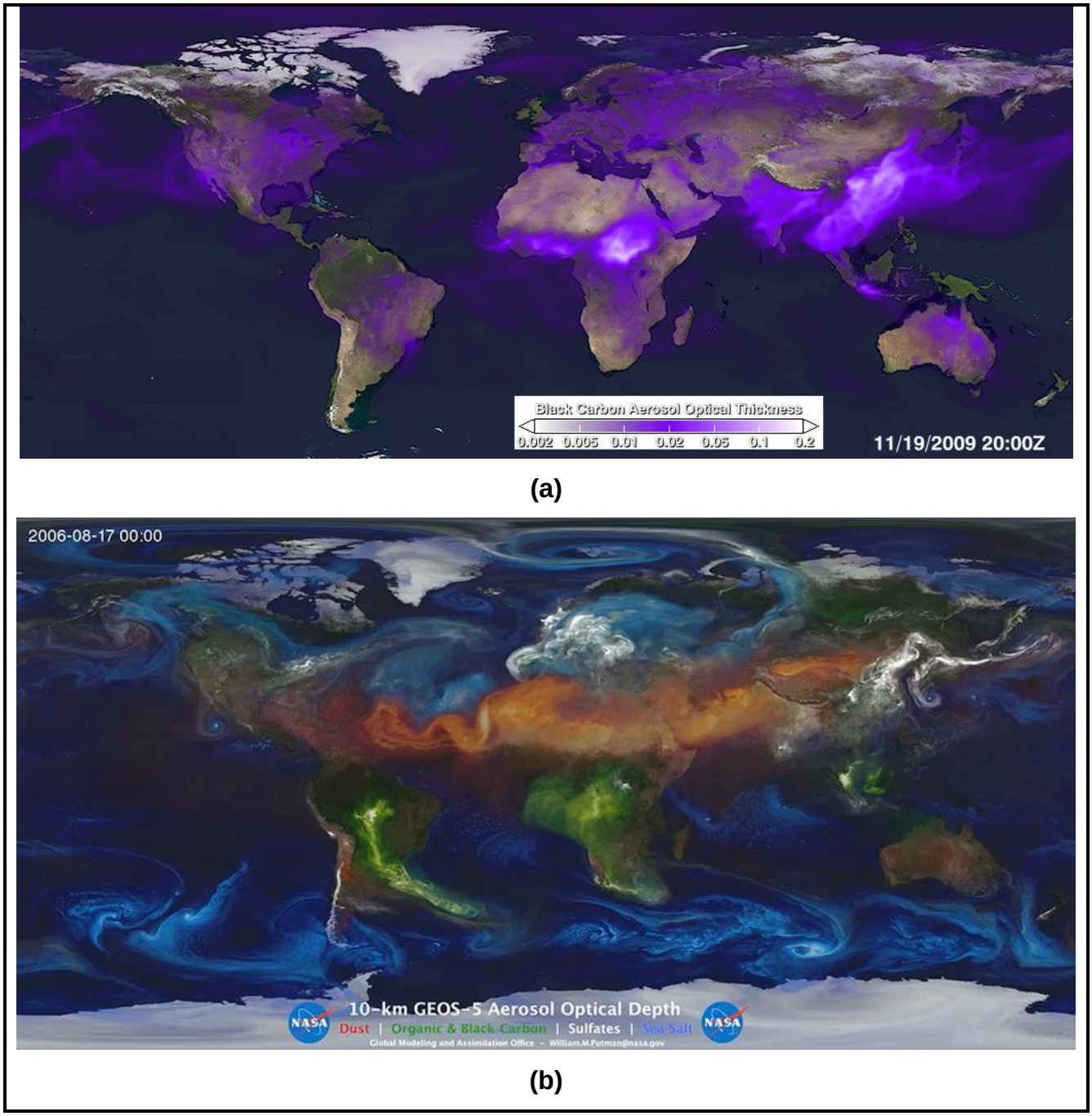

Figure 11: Black carbon aerosol optical thickness and aerosol optical thickness of dust (NASA, 2013) (a) Black carbon aerosol optical thickness (b) Aerosol optical thickness of dust (red-orange), black and organic carbon (green), sea salt (blue) and sulphates (white), from a 10 km resolution GEOS-5 "nature run" using the GOCART model.

2.4 COAL MINING

2.4.1 Coal Mining and Energy Supply

Globally, coal mining has been identified as one of the anthropogenic sources of atmospheric PM (Patra *et al.*, 2016). Concerns about air pollution from coal mining, particularly coal dust, have been traced as far back as the Industrial Revolution which took place from the 18th to 19th century (Hanlon, 2016). These concerns still exist in the modern era and the dilemma is that large amounts of coal are currently being mined globally to meet the ever- growing demand for energy (Ghose & Majee, 2007; Lei *et al*., 2014). This growing demand for energy is in turn fueled by other factors such as economic growth and population growth (Gautam *et al*., 2016). This scenario has led to on-going debates about the ever contesting environmental and economic development issues (Ward & Sua´rez-Ruiz, 2008).

Coal is a fossil fuel that has historically been used for a variety of domestic and industrial purposes (Ghose & Majee, 2007). The versatility of coal has also been evident in its essential role in the global energy mix as one of the main fuels for power generation purposes (Ward & Sua´rez-Ruiz, 2008). In some parts of the world, particularly in developing countries such as China, India and South Africa, coal use continues to increase as coal is considered as a critical element in powering these economies (Lei *et al*., 2014; International Energy Agency, 2016). This is because energy is an enabler of development and accessibility to a reliable and affordable source of energy is critical in today's modern world (World Coal Association, 2018).

For billions of people around the world, coal continues to be a major source of energy and it is the second-largest source of primary energy, providing more than 27% of total energy demand, while petroleum which is rated first, provides 33% of the total energy demand (International Energy Agency, 2017; Kim *et al*., 2015). 21% of the total energy demand is supplied by natural gas. In total, fossil fuels supply 81% of the world's primary energy demand. The energy supply from other sources include 10% from biomass, 6% from nuclear and 2% from hydro. Renewable energy supplies less than 2% of global energy requirements (International Energy Agency, 2017).

It is envisaged that with the current levels of development, affluence, population growth and urbanisation, future energy demand will exceed supply and that fossil fuels will continue to be the dominant source of energy for some economies in the coming decades (Kim *et al*.,

2015; World Coal Association, 2018). A comparison of prices of fossil fuels indicates that coal is generally cheaper, more abundant and the most competitive economically, compared to oil and natural gas (International Energy Agency, 2016). This low-cost advantage of coal has resulted in both developed and developed countries using coal for the large-scale provision of cheaper electricity (Ward & Sua´rez-Ruiz, 2008). From an infrastructure point of view, coal's uses include cement manufacturing and steel production (metallurgical coal). Steel is used in many applications and is one of the most important industrial construction materials for i.e. bridges, buildings and pipelines (International Energy Agency, 2016). Coal can be converted into liquid fuels while several by-products can be produced from coal. These include solvents, dyes and plastics (World Coal Association, 2018).

The total world coal production and consumption figures from 1971 to 2016 are shown in Figure 12 and Figure 13 respectively. According to the International Energy Agency, historically there has been a steady increase in coal production, with a decline only from 2014 to 458 megatonnes (Mt) in 2016. This decline was attributed to factors which include quotas for mine operating timeframes in China due to the high air pollution levels, especially for particulate matter, in that country (International Energy Agency, 2016). Environmental and health concerns and changes in the political climate have also resulted in a negative reputational image for the coal industry (Ward & Sua´rez-Ruiz, 2008). The contribution of the coal sector to climate change as a result of direct and indirect greenhouse gas emissions, mainly from power generation, has resulted in further scrutiny of the industry (Ward & Sua´rez-Ruiz, 2008). In 2007, the International Energy Agency stated that in 2004, among the fossil fuels, coal became the most significant source of anthropogenic carbon dioxide (CO_2) emissions, overtaking oil and natural gas emissions sources (International Energy Agency, 2007).

The expected energy demand forecast to 2050 in South Arica is shown in Figure 14. The Department of Energy is forecasting an increase in energy demand going forward and this has implications in terms of the country's energy mix (Department of Energy, 2019).

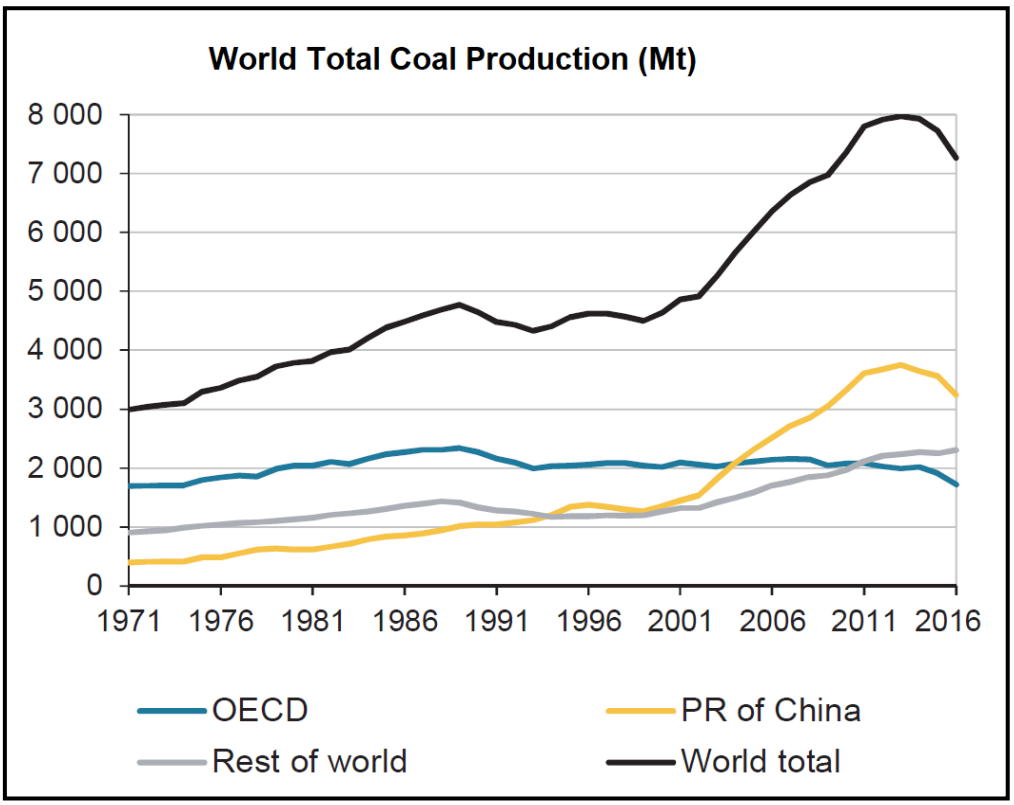

Figure 12: World Total Coal Production from 1971 to 2016 (International Energy Agency, 2017).

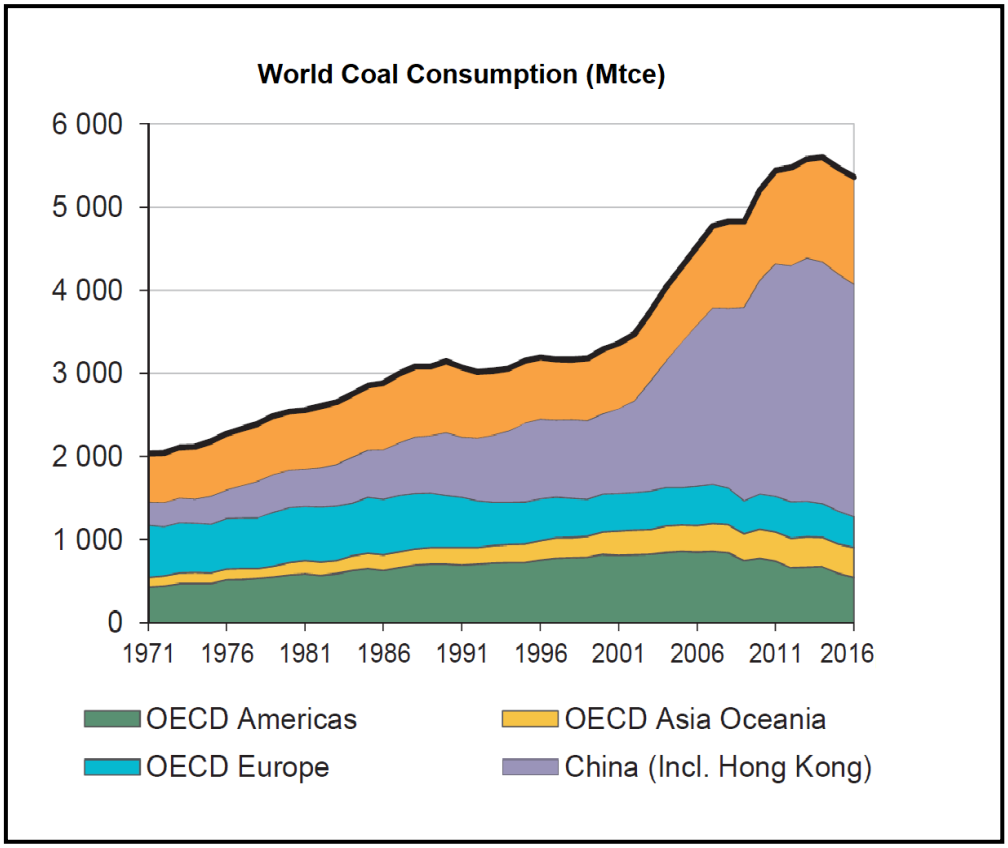

Figure 13: World Coal Consumption from 1971 to 2016 (International Energy Agency, 2017).

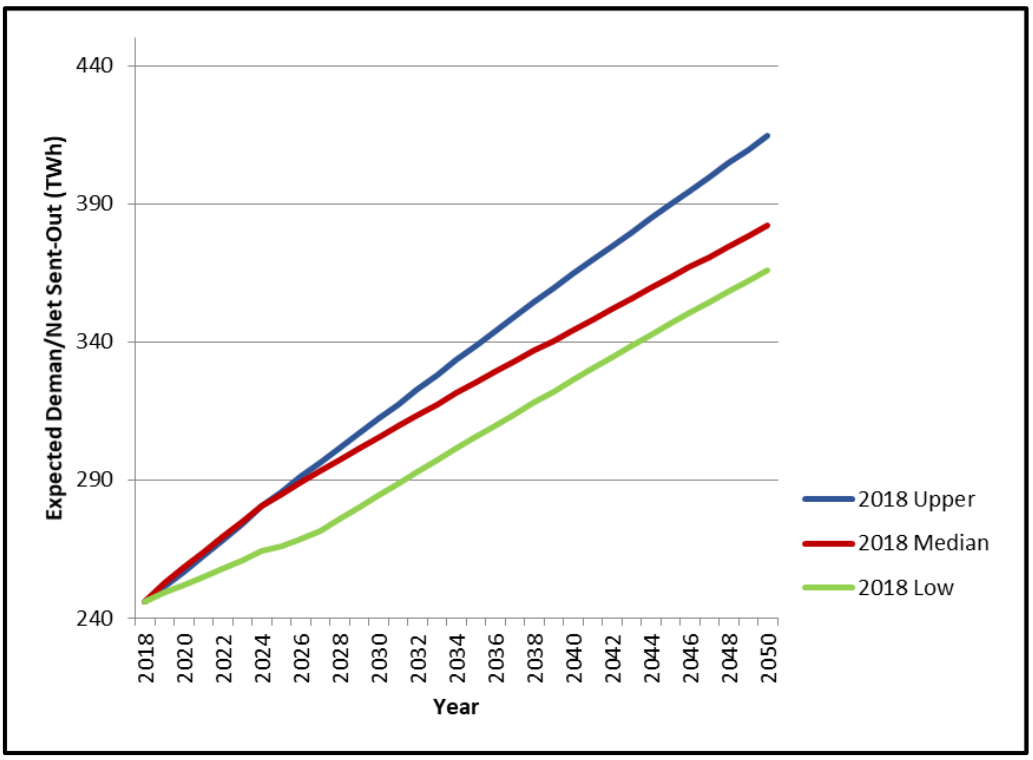

Figure 14: Expected electricity demand forecast for South Africa to the year 2050 (Department of Energy, 2019)

Climate change is one of the most significant global threats to sustainability and humanity (Edwards, 2003; United Nations Environment Programme (UNEP), 2018; WHO, 2003; WorldWatch Institute, 2018). Climate change has potential impacts for water security, energy security, agricultural productivity, biodiversity, infrastructure, financial flows and economies, rising temperatures, droughts, floods, changing migration patterns, global security and health (Durant *et al.,* 2011; Muenstermann, 2012; WorldWatch Institute, 2018).) The climate change pathways and impacts on health are shown in Figure 15 (WHO, 2003). Climate change will also undermine global efforts of achieving the United Nations Sustainability Goals (SDGs) and efforts to reduce poverty (United Nations Environment Programme, (UNEP) 2018).

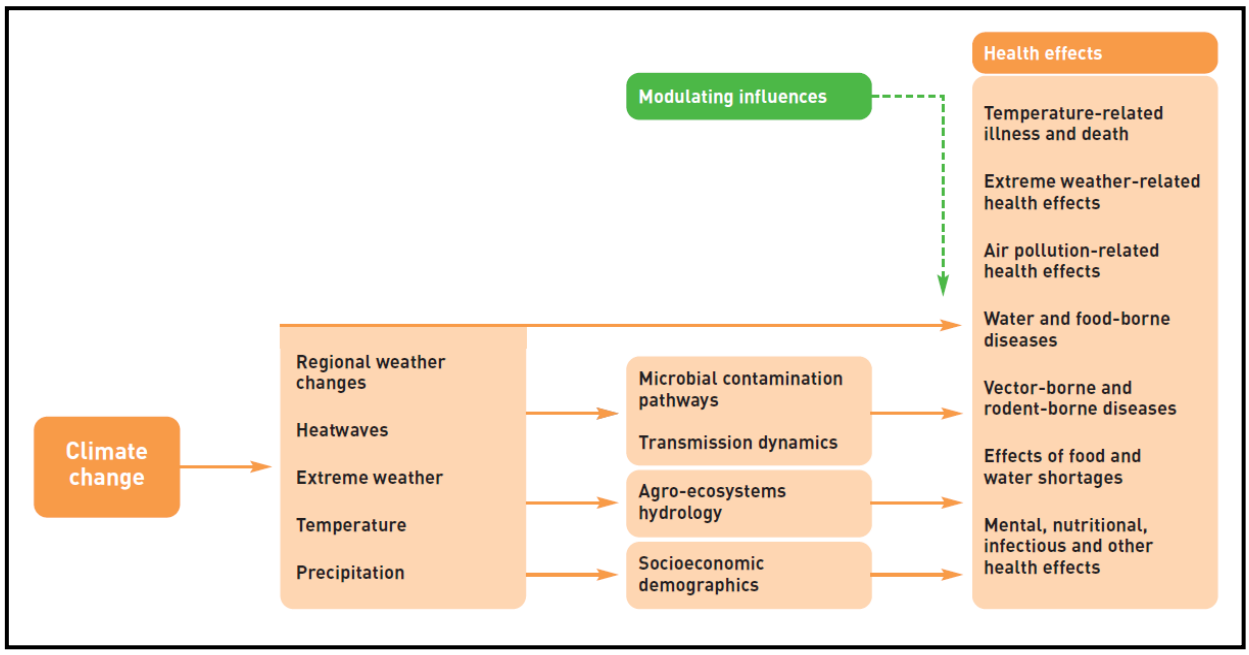

Figure 15: Climate change pathways and effects on human health (WHO, 2003).

Global efforts have been directed towards mitigation, adaptation to ensure resilience to the negative impacts of climate change, and transitions to low carbon economies (Wei *et al.*, 2016). The mitigation measures include decarbonisation of economies through reviews of the energy mix, implementation of sustainable energy policies, market incentives, renewable energy programmes and market-based cap and trade systems for carbon emissions (Durant *et al*., 2011).

Energy efficiency is widely recognised as a key mitigation option for the reduction of greenhouse gas emissions and for the transition of countries to low carbon economies (Wei *et al.*, 2016). Although there has been a significant uptake of renewable energy technologies such as wind and solar photovoltaic energy (PV), there has been slow uptake of key technologies for energy and carbon emission savings such as carbon capture and storage (CCS) (International Energy Agency, 2017).

However, the entry into force of the Paris Agreement in 2016, was a huge international milestone for global efforts to tackle climate change and the deployment of renewable energy technologies (Weis *et al.*, 2016). The Paris Agreement is an agreement within the United Nations Framework Convention on Climate Change (UNFCCC) which addresses climate change mitigation, adaptation and finance (UNEP, 2018). One of the main objectives of the agreement is to keep global warming levels well below 2 degrees Celsius (2°C),

preferably limiting the warming to 1.5 degrees Celsius(1.5°C). Individual countries are expected to table mitigation measures or nationally determined contributions (NDCs) which will be reviewed at least every five years (United Nations, 2015).

South Africa is a party to the Paris Agreement and the SA government, through the national Department of Environmental Affairs, has initiated various policies and instruments aimed at climate change mitigation and adaptation (DEA, 2018). The policies and instruments aimed at greenhouse gas emitting industries and other stakeholders, include carbon budgets, carbon tax, greenhouse gas reporting, Pollution Prevention Plans for greenhouse gas emissions, carbon offsets and the draft National Climate Change Bill (DEA, 2018).

However, the impacts of the various global climate policies have been widely debated with views that economic development in developing countries will be highly impacted by these policies as most of these countries are dependent on fossil fuels such as coal to power their economies and social development (Ahuja & Tatsutani, 2009; Shukla, 2019). It is further argued that these countries do not have the financial and technological means to transition to low carbon technologies and economies (Smit & Pilifosova, 2003). The rate of technological transfer and financial assistance by developed countries to the developing countries for the purposed of climate change mitigation and adaptation has been deemed to be very low (International Energy Agency, 2016).

Climate change also presents different risks and opportunities to many industries, particularly fossil fuel-based industries such as coal mining (Task Force on Climate Related Financial Disclosures (TCFD) 2017a, 2017b; Forster, 2007; Shukla, 2019). The TCFD was formed by the Financial Stability Board (FSB) in December 2015 to address climate change impacts on businesses and the global financial system through disclosure (TCFD, 2017a). The risks to businesses which have been documented by the TCFD include the following;

- Reputational risks associated with the failure to deliver on the expectations of investors and other key stakeholders;
- Physical risks such as flooding and other extreme weather events which can potentially destroy infrastructure, disrupt operations and supply chains, negative impacts on workforce health and well-being;

- Financial risks associated with the disruption of operations, physical damage of infrastructure and high insurance costs;
- Regulatory risk due to increasingly stringent climate policies and regulations;
- Market risk due to a shift in consumer behaviour, decline in product demand due to product preference shifts (Figure 16) (TCFD, 2017a,b; Tyagi, 2018).

However, there are also opportunities for organisations or industries that can be potentially impacted by climate change. These opportunities include new markets for new products and technologies, resource efficiency and new energy sources (TCFD, 2017a).

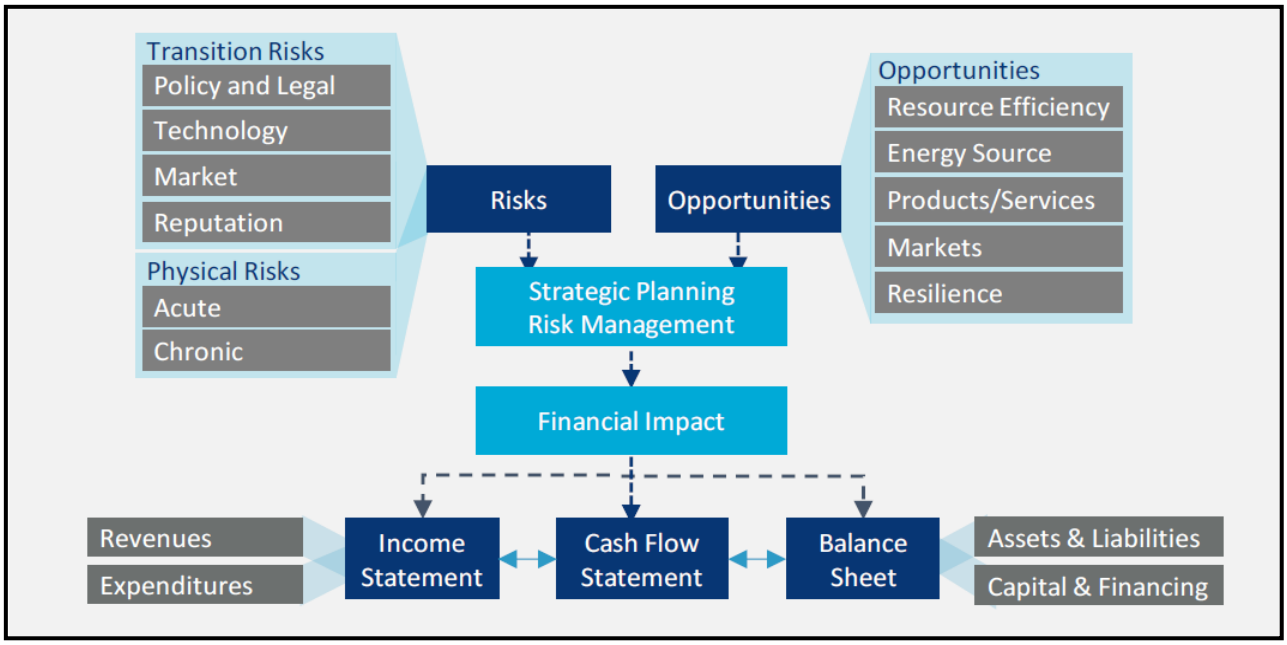

Figure 16: Organisational climate related risks and opportunities.

Whether coal will remain a fuel of choice in future will depend on the design and implementation of policy measures that are meant to drive low carbon emissions energy technologies, energy efficiency, the use or deployment of more efficient coal combustion technologies and key technologies such as carbon capture and storage (Lei *et al*, 2014; International Energy Agency, 2016). The International Energy Agency modelled various scenarios in their World Energy Outlook (WEO) series (Figure 17). These scenarios take into consideration current climate policies, new policies and the 450 Scenario which adopts a target setting approach or a specified outcome to spur action for the achievement of targets in the energy sector (International Energy Agency, 2016). This is considered key for the

limitation of long-term global temperature increases to 2°C. This scenario also provides key steps for the energy sector to achieve its goals or targets (TCFD, 2017a).

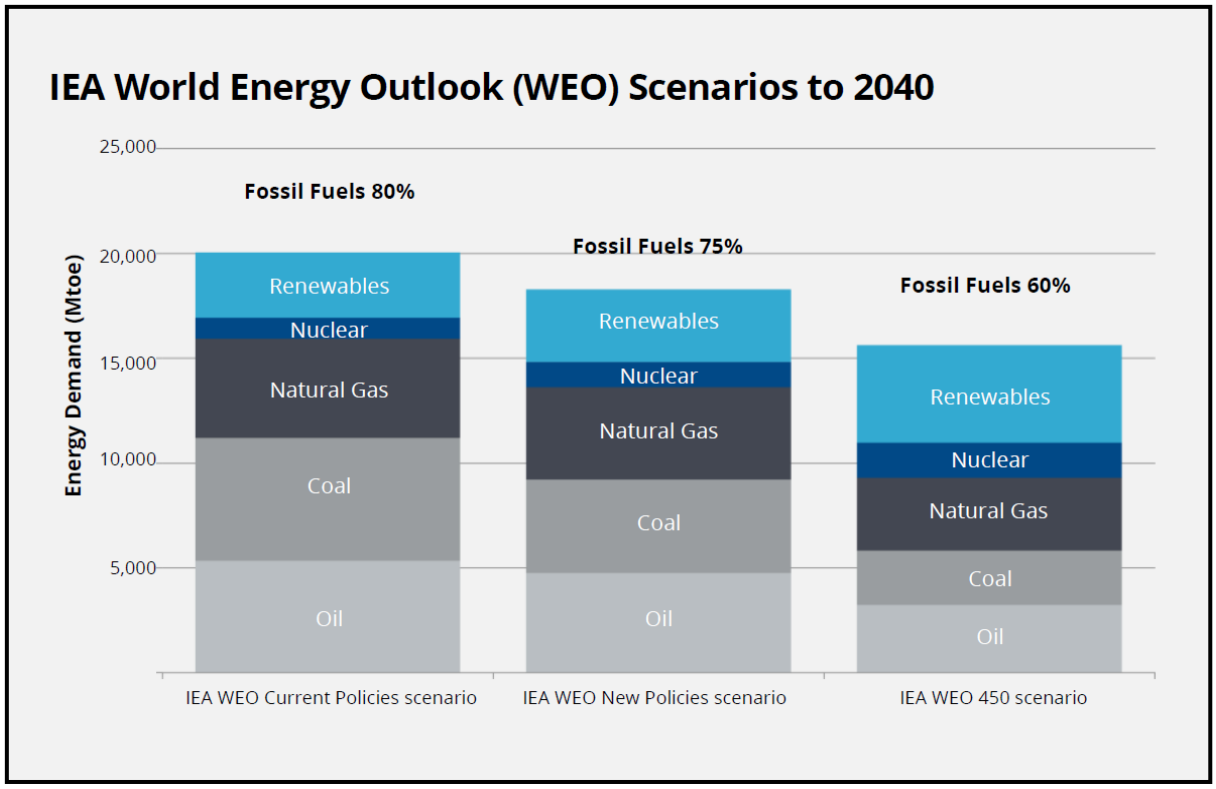

Figure 17: International Energy Agency World Energy Outlook Scenarios to 2040 (International Energy Agency, 2016).

In the South African context, the 2019 Integrated Resource Plan (IRP) includes modelling and analysis of various scenarios and their potential impacts on the energy mix of the country going forward (Department of Energy, 2019). The scenario analysis process was undertaken in line with minimising impacts on the environment, minimising cost of supply and ensuring security of supply (Department of Energy, 2019). The results indicate the reduction of coal as the major source of energy going forward and this is a clear indication of South Africa's intent to transition to a low carbon economy through the energy sector (Figure 18 to 20 below) (Department of Energy, 2019).

However, the positive outcomes thus far include increased research and development on clean coal technologies, implementation of these technologies and a renewed interest to keep the coal industry on a sustainable path (Ward and Sua´rez-Ruiz, 2008).

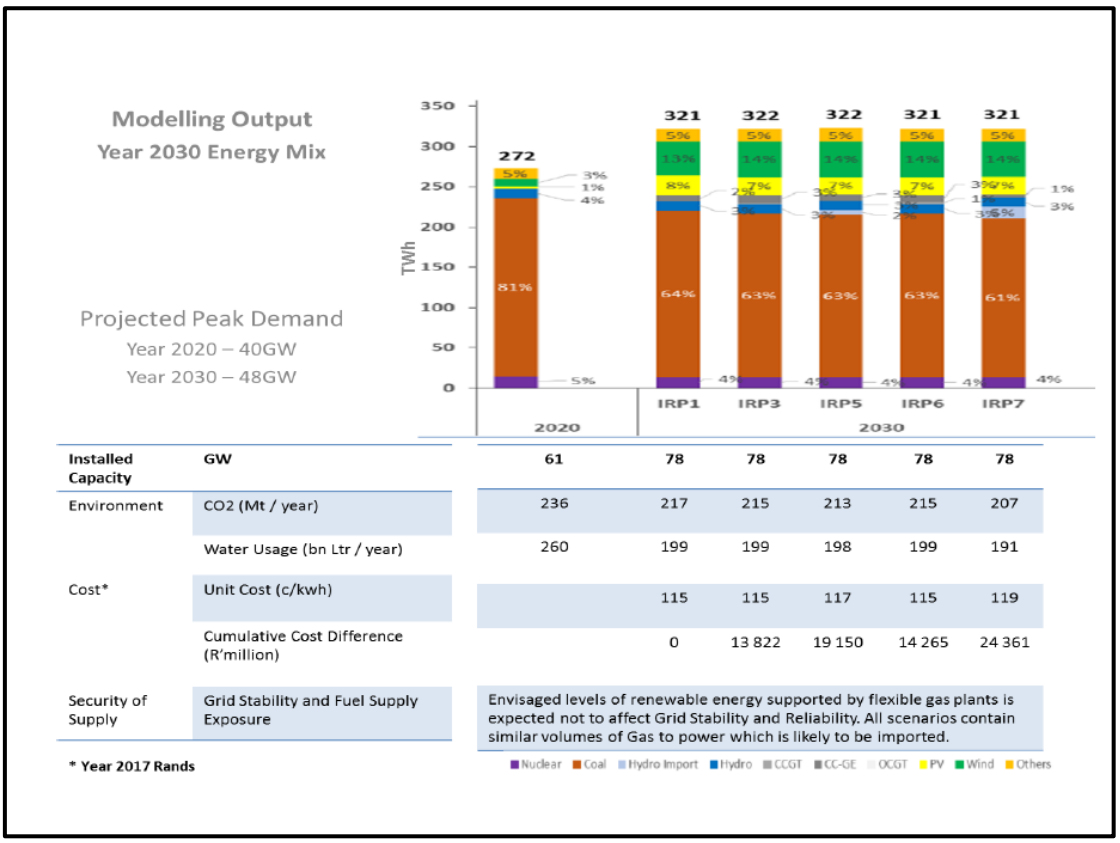

Installed Capacity	GW	61	78	78	78	78	78
Environment	CO2 (Mt / year)	236	217	215	213	215	207
	Water Usage (bn Ltr / year)	260	199	199	198	199	191
Cost*	Unit Cost (c/kwh)		115	115	117	115	119
	Cumulative Cost Difference (R'million)		0	13 822	19 150	14 265	24 361
Security of Supply	Grid Stability and Fuel Supply Exposure	Envisaged levels of renewable energy supported by flexible gas plants is expected not to affect Grid Stability and Reliability. All scenarios contain similar volumes of Gas to power which is likely to be imported.					

* Year 2017 Rands

Figure 18: Scenario analysis outputs for the period ending 2030 (Department of Energy, 2019).

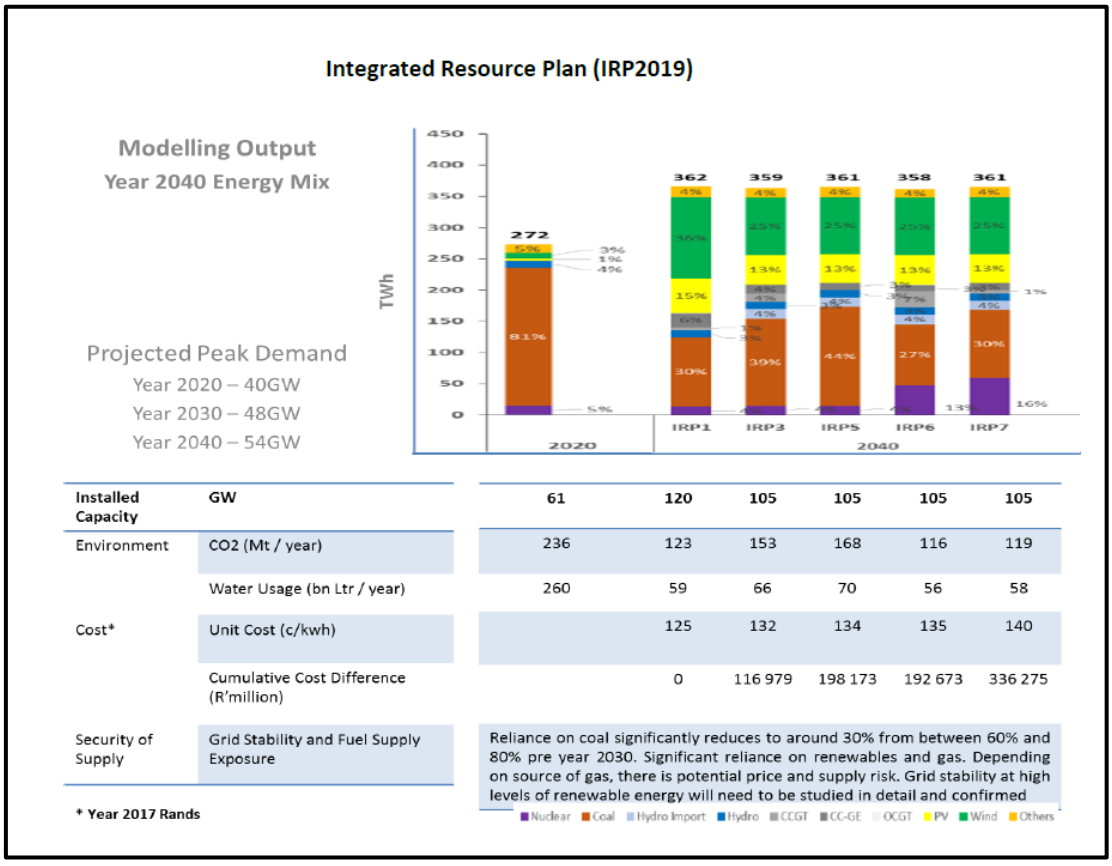

Installed Capacity	GW	61	120	105	105	105	105
Environment	CO2 (Mt / year)	236	123	153	168	116	119
	Water Usage (bn Ltr / year)	260	59	66	70	56	58
Cost*	Unit Cost (c/kwh)		125	132	134	135	140
	Cumulative Cost Difference (R'million)		0	116 979	198 173	192 673	336 275
Security of Supply	Grid Stability and Fuel Supply Exposure	Reliance on coal significantly reduces to around 30% from between 60% and 80% pre year 2030. Significant reliance on renewables and gas. Depending on source of gas, there is potential price and supply risk. Grid stability at high levels of renewable energy will need to be studied in detail and confirmed					

* Year 2017 Rands

Figure 19: Scenario analysis outputs for the period 2031-2040 (Department of Energy, 2019).

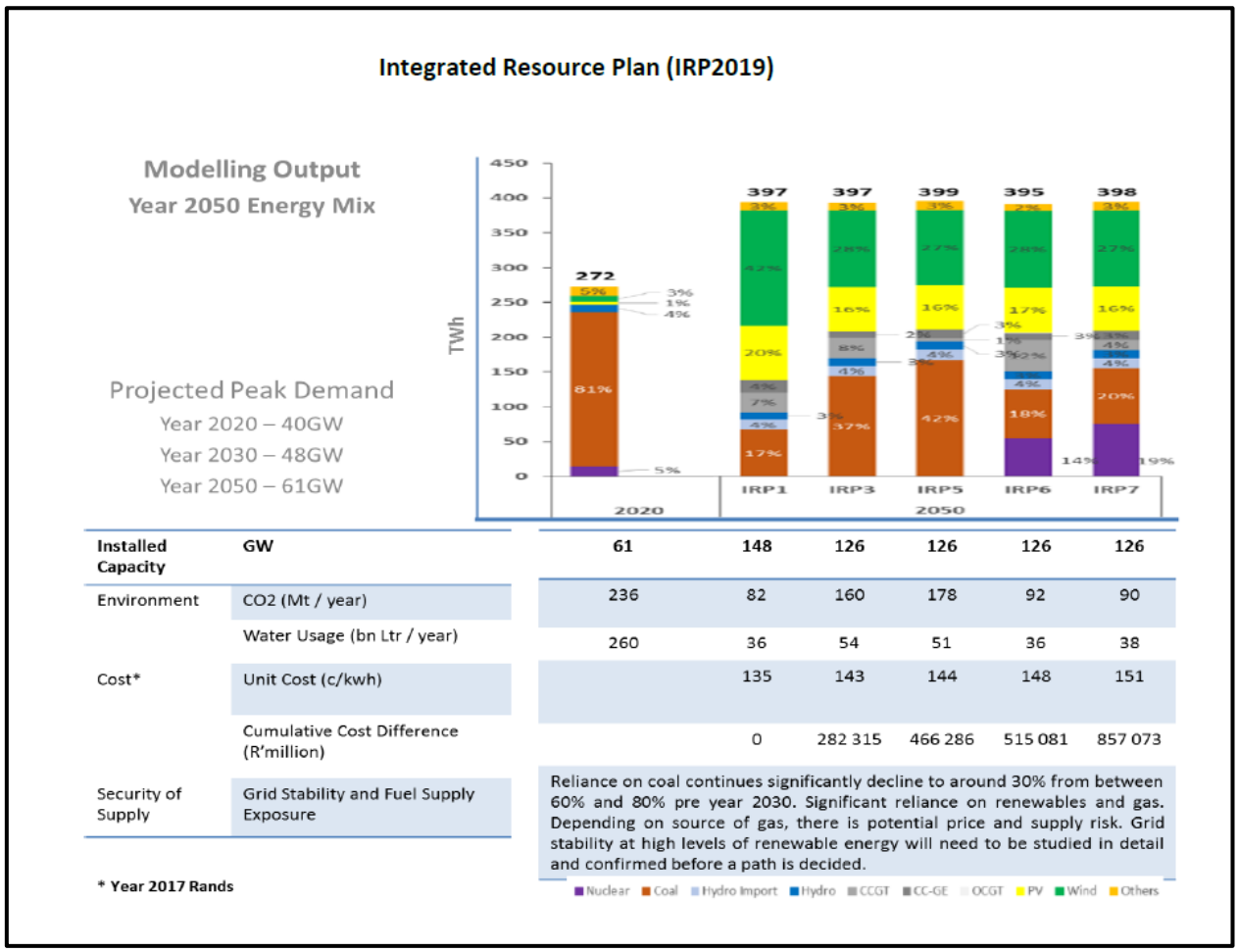

Figure 20: Scenario analysis outputs for the period 2041-2050 (Department of Energy, 2019).

2.4.2 Coal Mining in South Africa

In South Africa, coal is largely used for power generation in the energy supply sector (Eskom, 2018). About 77% of South Africa's primary energy needs are provided by coal (Eskom, 2018). This scenario is unlikely to change significantly over the next decade due to lack of suitable alternatives or insufficient power generated from other sources such as renewables (Department of Energy, 2019; Eskom, 2018).

An average of 224 million tonnes of marketable coal is produced annually in South Africa (Minerals Council of South Africa, 2018). This results in South Africa being the 5th largest coal producing country in the world (Department of Energy, 2019; Minerals Council of South Africa, 2018). South Africa is also the third largest coal exporting country globally as 25% of coal production is exported internationally. The primary export port in South Africa is the Richards Bay Coal Terminal (RBCT) (Minerals Council South Africa, 2018). The remainder of South Africa's coal production is used for electricity generation, the production of liquid

fuels, metallurgical and other industrial production, and domestic use. The country's coal reserves are estimated at 53 billion tonnes (Minerals Council South Africa, 2018). Given the current production rates, estimates indicate that there could potentially be approximately 200 years of coal supply (Department of Energy, 2018). In South Africa, it is likely that coal will remain the significant energy source in the foreseeable future, despite forecasts which indicate that renewables, natural gas and nuclear energy will increasingly contribute to the primary energy supply. This is attributed to the abundance of coal at low cost (Jeffrey, 2005).

In South Africa, coal is found in 19 coalfields located mainly in Mpumalanga, Limpopo, KwaZulu-Natal and the Free State (Figure 21 below) (Prevost, 2004). The main coal mining areas in Mpumalanga are presently in Emalahleni (previously known as Witbank), Middelburg, Ermelo and Standerton-Secunda (Jeffrey, 2005). In the Free State, the main coal mining areas are around Sasolburg-Vereeniging. In the Limpopo Province, large collieries are found near Lephalale (Jeffrey, 2005). The location of coal mines which are currently operational and in closure in South Africa are shown in Figure 22 (Minerals Council South Africa, 2018. Coal production is shifting gradually from the Emalahleni coal field due to end of life of mine (LOM) of some of the coal mines (Ngwenyama *et al*, 2017; Jeffrey, 2005; Minerals Council South Africa, 2018). Significant exploration work geared toward the development of the Waterberg coal field and other areas in the Limpopo Province is currently underway (Minerals Council South Africa, 2018).

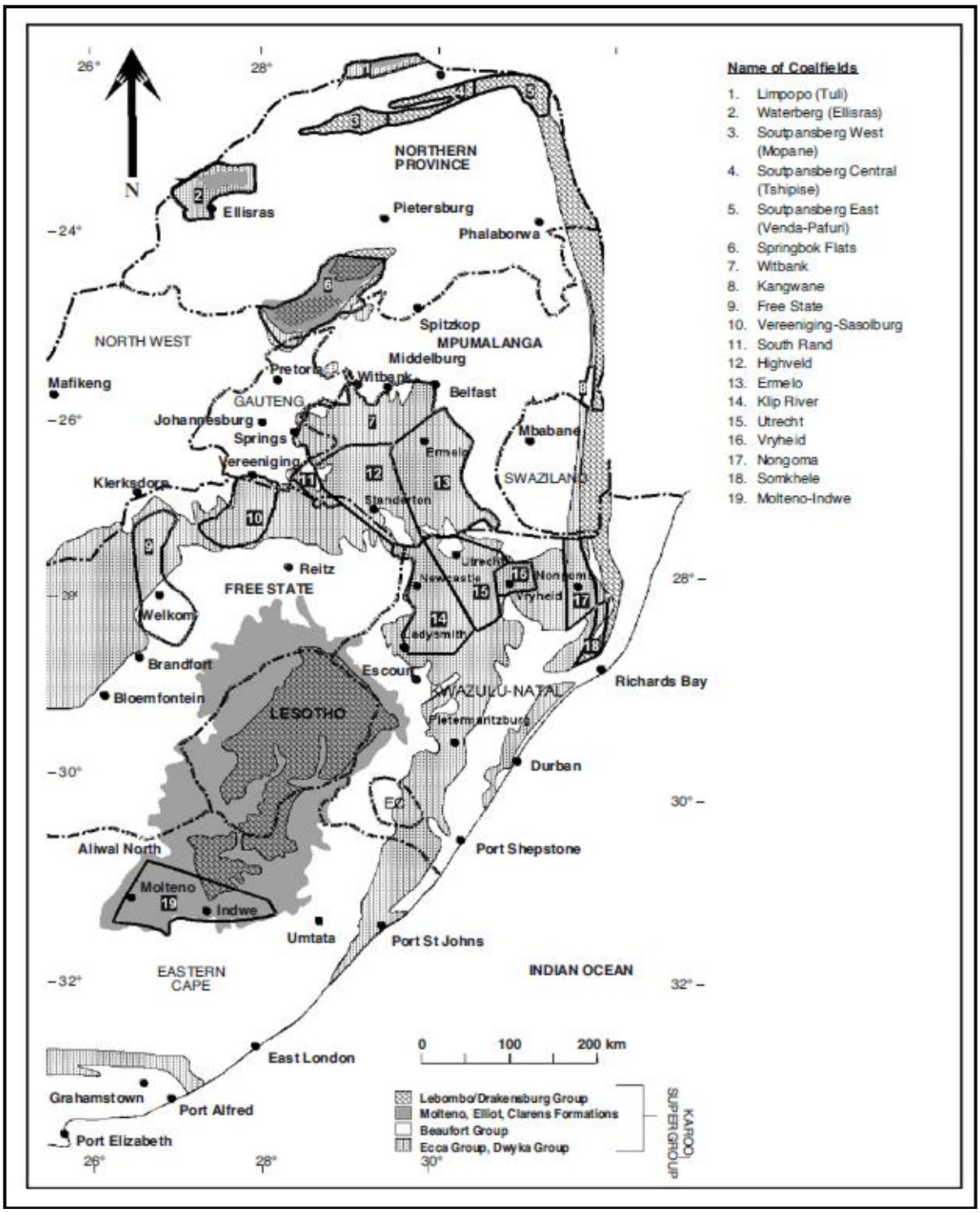

Figure 21: Coalfields in South Africa (Prevost, 2004).

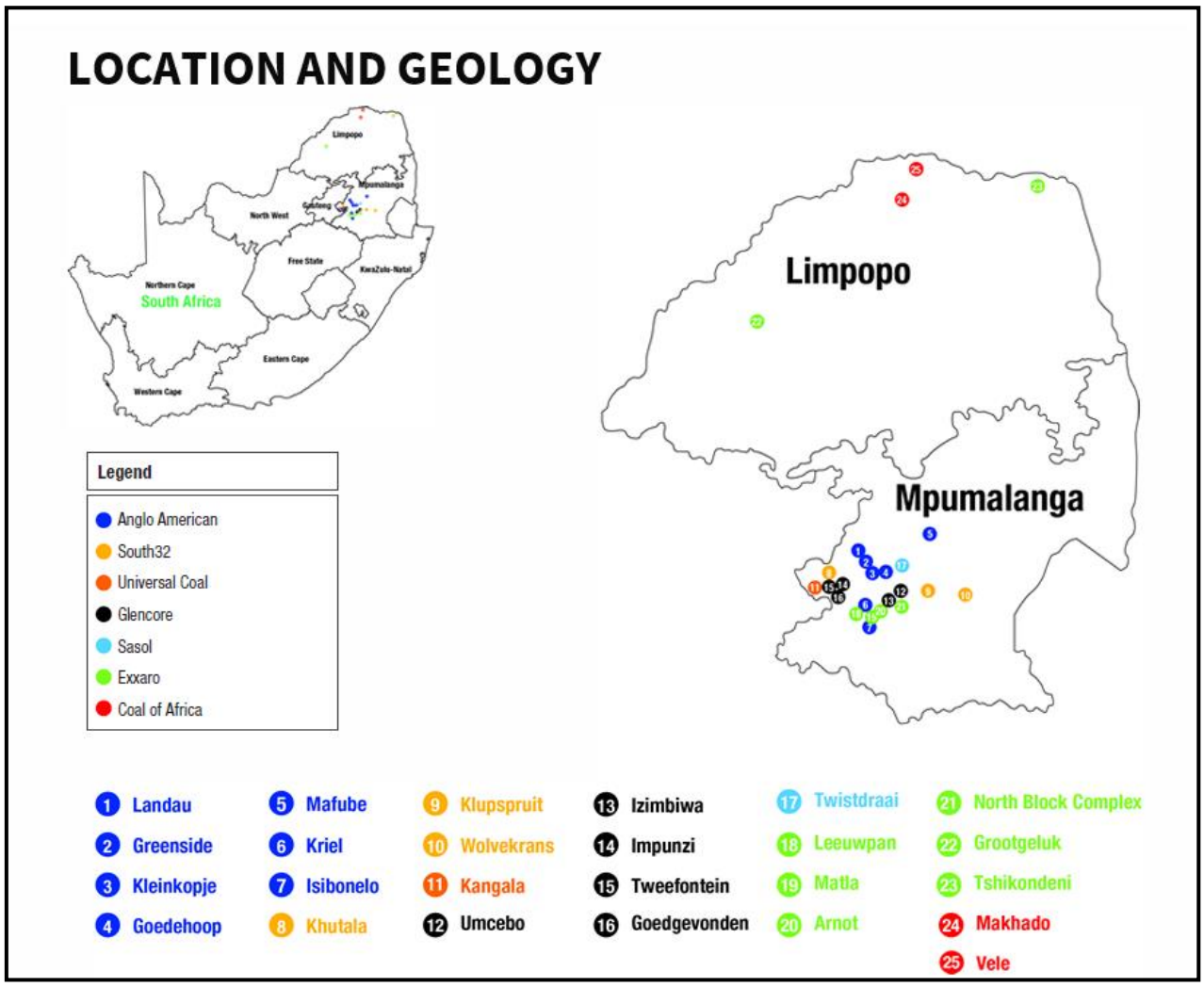

Figure 22: Major coal mines in South Africa (Minerals Council South Africa, 2018).

2.4.3 Coal Mining Methods

Although coal is normally associated with socio-economic progress and powering of economies, there has been increasing concern globally on the contribution of the coal mining industry to air pollution, climate change and health impacts (Huertas *et al.*, 2012; Ward & Sua´rez-Ruiz, 2008). Coal mining is associated with emissions of criteria pollutants such as PM, SO_2, nitrous oxides (NO_x), and GHG emissions in the form of CO_2 and CH_4 (Trivedi *et al.*, 2010). In addition, coal dust emissions contain various sizes of atmospheric PM i.e coarse and fine PM. Coal mining is associated with the emission of coarse PM due to the mechanical nature of mining processes (Kantova *et al.*, 2017).

The extraction of coal is usually undertaken using the opencast or surface coal mining methodology, underground mining or a combination of both (Dougall & Mmola, 2015;

Speight, 2012). The mining methodology is based on the geology and depth of the coal seam, with opencast mining being deployed when the coal seam is close to the surface and underground mining for deeper coal seams (Ghose, 2002; Speight, 2015). The advantages of opencast coal mining include the economic removal of coal as a high proportion of in-situ coal (up to 90%) is recovered for use (Dougall & Mmola, 2015; Huertas *et al.*, 2012). This includes the recovery of coal from seams that present challenges related to thickness which would not normally be recovered during underground mining (Ramani & Evans, 2017). Opencast mining methods generally provide coal at lower overall costs compared to underground mining and avoid potential safety hazards associated with underground mining (Huertas *et al.*, 2012). These safety hazards include coal dust explosions, gas outbursts due to methane and other gases and roof falls (National Research Council (NRC), 2007; Ward & Sua´rez-Ruiz, 2008).

Underground coal mining in South Africa generally deploys the room and pillar method or pillar support method which involves the extraction of coal around vertical pillars which are left intact for roof support (Figure 23) (Lloyd, 2002; Speight, 2012). After the cessation of mining activities, these pillars might collapse, resulting in subsidence (United States Energy Information Administration (EIA, 1978). Long wall mining is not commonly used in South Africa. This method involves the extraction of all coal in the seam, with the roof permitted to collapse behind the mined-out area (Lloyd, 2002).

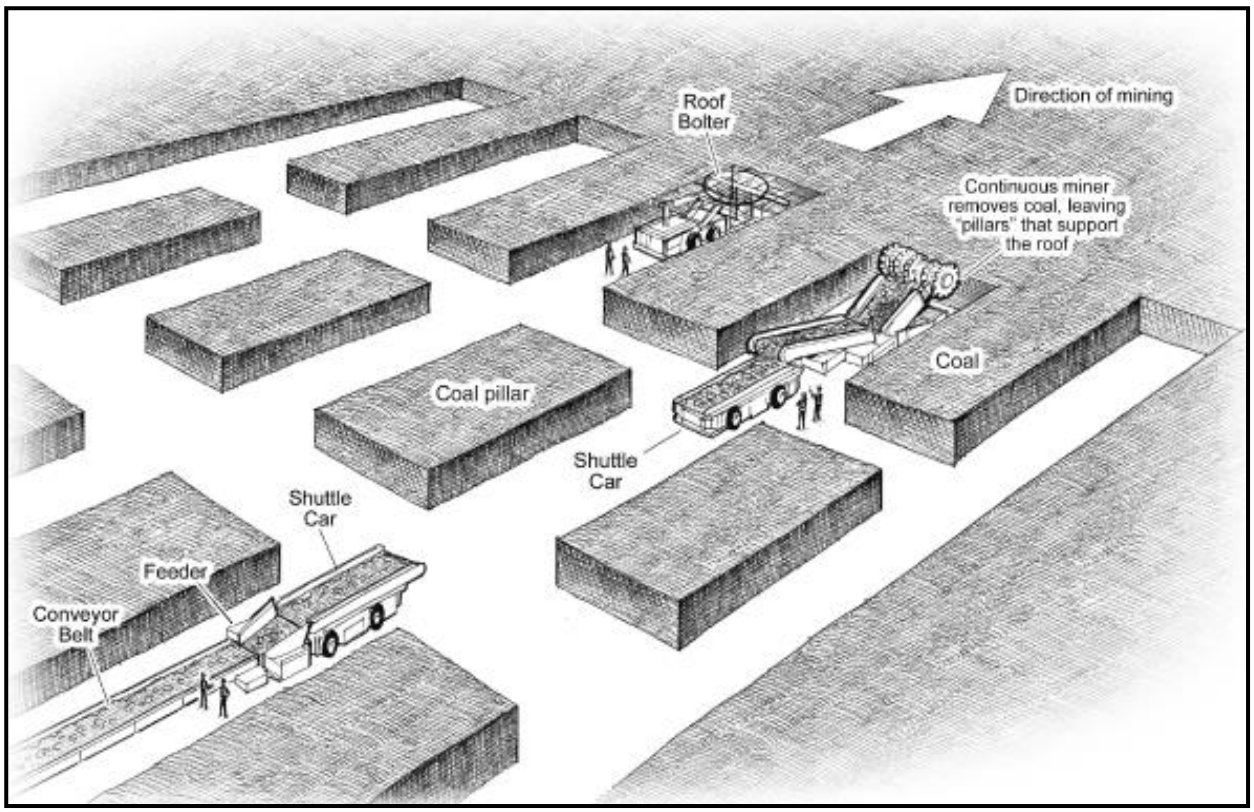

Figure 23: Room and pillar underground mining (United States Energy Information Administration (EIA, 1978).

2.4.4 Coal Mining and Atmospheric Particulate Emissions

The contribution of opencast coal mining to air pollution and environmental degradation is higher than that of underground mining (Munnik *et al*., 2010; Banerjee, 2006). This is because opencast mining includes a significant number of mining related activities that are primary sources of fugitive dust emissions (Patra *et al.*, 2016; Sahu *et al*., 2018). These activities include excavation, overburden removal; drilling and blasting, crushing and screening, vehicle entrainment on unpaved roads, materials handling and stockpiling, loading and hauling, transportation of material, wind erosion of open areas and storage piles (Kumar *et al.*, 2016; Lal & Tripathy, 2012) (Figure 24). In most of the opencast and underground coal mines, the removal of impurities from the mined material or run of mine (ROM) is undertaken through the beneficiation process for the provision of coal of a consistent quality to customers (Sahu *et al*., 2018; Speight, 2015). This process can also contribute to atmospheric PM emissions through materials handling (Huertas, 2002).

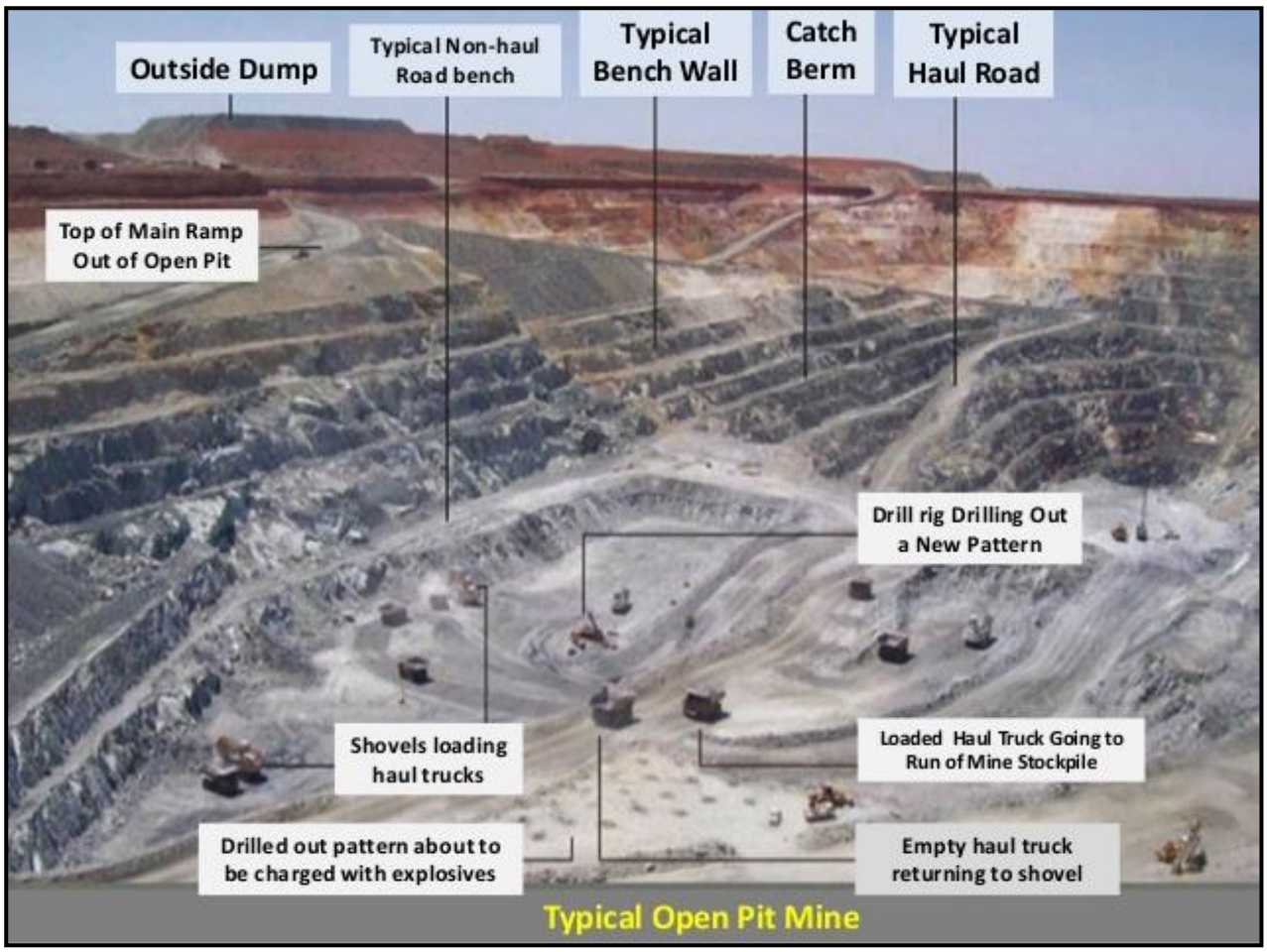

Figure 24: Opencast and underground mining related activities.

A significant number of opencast mining related activities are mechanical in nature and result in the formation of coarse mode particles which are emitted as part of fugitive dust (Banerjee, 2006). In the South African context, dust emissions from unpaved haul roads in mining areas are normally identified as significant sources of fugitive dust emissions (DEA, 2011). One air quality study that was undertaken in an coal opencast mine by Amponsah-Dacosta (1997), reported that over 93% of total mine emissions were due to dust generated from unpaved mine haul roads (Figure 25).

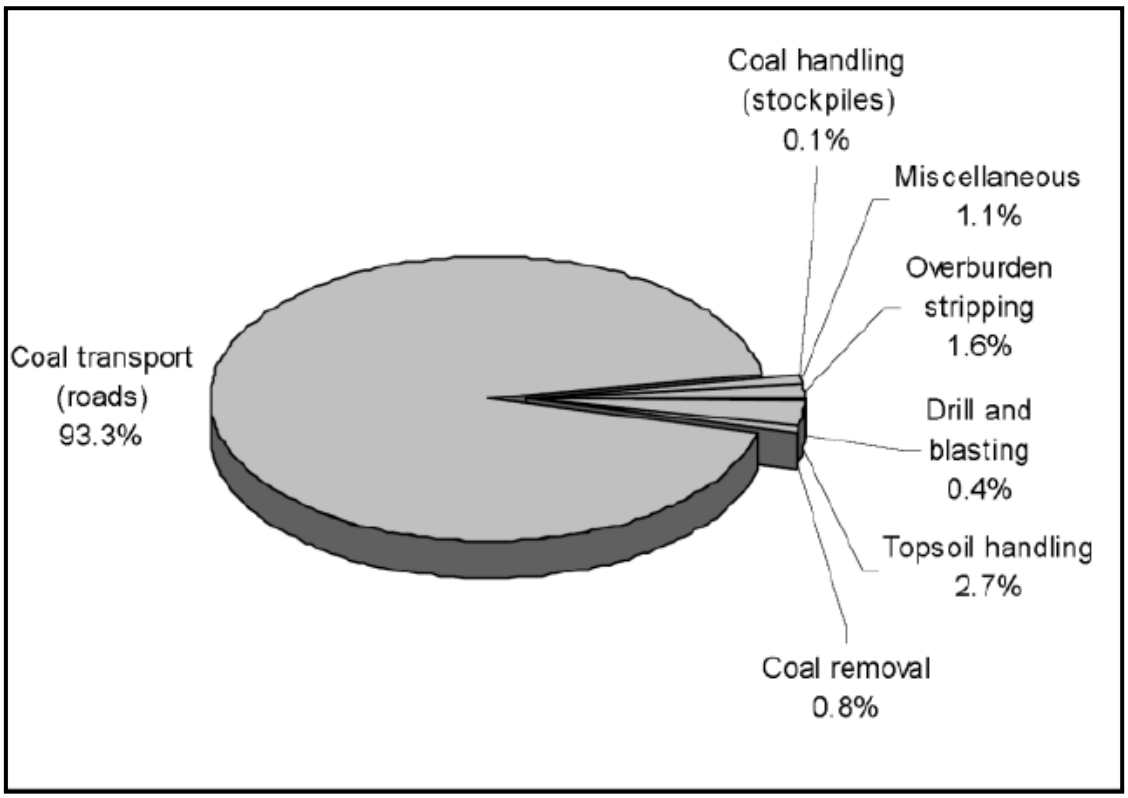

Figure 25: Source contribution to total dust emissions from a typical South African open pit mine (Visser and Thompson, 2003).

However, the dust emissions from unpaved roads may vary due to factors such as the amount of vehicle traffic and silt loading on the unpaved road surface (Cowherd and Englehart, 1985). Vehicle traffic on unpaved haul roads of mechanised opencast mines can contribute up to 80% to fugitive dust emissions (Cowherd & Englehart, 1985). However, other mining related activities also contribute to gaseous pollutant and particulate emissions (Chaulya, 2005; Trivedi *et al.*, 2010). These activities include vehicle emissions which result in the generation of SO_2, NO_x, diesel particulate matter, CO_2 and carbon monoxide (CO), volatile organic compounds (VOCs) and ozone (O_3) (Trivedi *et al.*, 2010; USEPA, 2002).

Spontaneous combustion and its associated risks are well known in the coal mining industry and have been a source of major concern from all aspects, including environmental aspects (Denis *et al*., 2007; Pone *et al*., 2007). Factors such as increased production rates and very high stripping ratios will result in the increase of volumes of discard material (Genc & Cook, 2015). Spontaneous combustion in coal mines contributes to atmospheric PM emissions (Denis *et al.*, 2007; Pone *et al*., 2007; Singh, 2013). Other air pollutants emitted due to spontaneous combustion include greenhouse gases (GHGs) such as CO_2, CH_4 and criteria pollutants such as SO_2, NO_x, CO, polyaromatic hydrocarbon (PAHs) and VOCs (Carras *et*

al., 2005; Ozdogan *et al.*, 2018). The Intergovernmental Panel on Climate Change (IPCC), has identified spontaneous combustion as a potential significant source of GHG emissions (Denis *et al.*, 2007; Myhre *et al.*, 2013). However, the lack of a globally acceptable method for estimating greenhouse gas emissions has been a barrier in the inclusion of spontaneous combustion in GHG emission inventories (Carras *et al.*, 2005).

2.4.5 Atmospheric PM in coal-mining areas in South Africa.

In various parts of the country, high concentrations of atmospheric PM still occur, especially in highly industrialised areas and residential areas where domestic fuel burning also contributes to high atmospheric PM concentrations (DEA, 2011). Exceedances of the PM National Ambient Air Quality Standards (NAAQS) (Table 7) which were promulgated under the National Environmental Management: Air Quality Act (NEMAQA) of 2004, occur in priority areas and elsewhere (DEA, 2011).

Air quality management priority areas are declared in South Africa based on exceedances or potential to exceed the NAAQS for various criteria pollutants such as PM_{10}, $PM_{2.5}$, SO_2, NO_x and O_3 (DEA, 2011). Three priority areas have been declared in South Africa by the Department of Environmental Affairs and these are the Highveld Priority Area (HPA), declared in 2007, Vaal Triangle Airshed Priority Area (VTAPA), declared in 2006 and Waterberg-Bojanala Priority Areas (WBPA), declared in 2012 (Figure 26) (DEA, 2018b).

Table 7: South African National Ambient Air Quality Standards for PM_{10} and $PM_{2.5}$ (DEA, 2011)

Averaging period	Concentration	Frequency of Exceedance	Compliance Date
PM_{10}			
24 hours	75	4	Current
1 year	40		Current
$PM_{2.5}$			
24 hours	40	4	1 Jan 2016 to Dec 2029
1 year	20		1 Jan 2016 to Dec 2029
$PM_{2.5}$			
24 hours	25	4	1 Jan 2030
1 year	15		1 Jan 2030

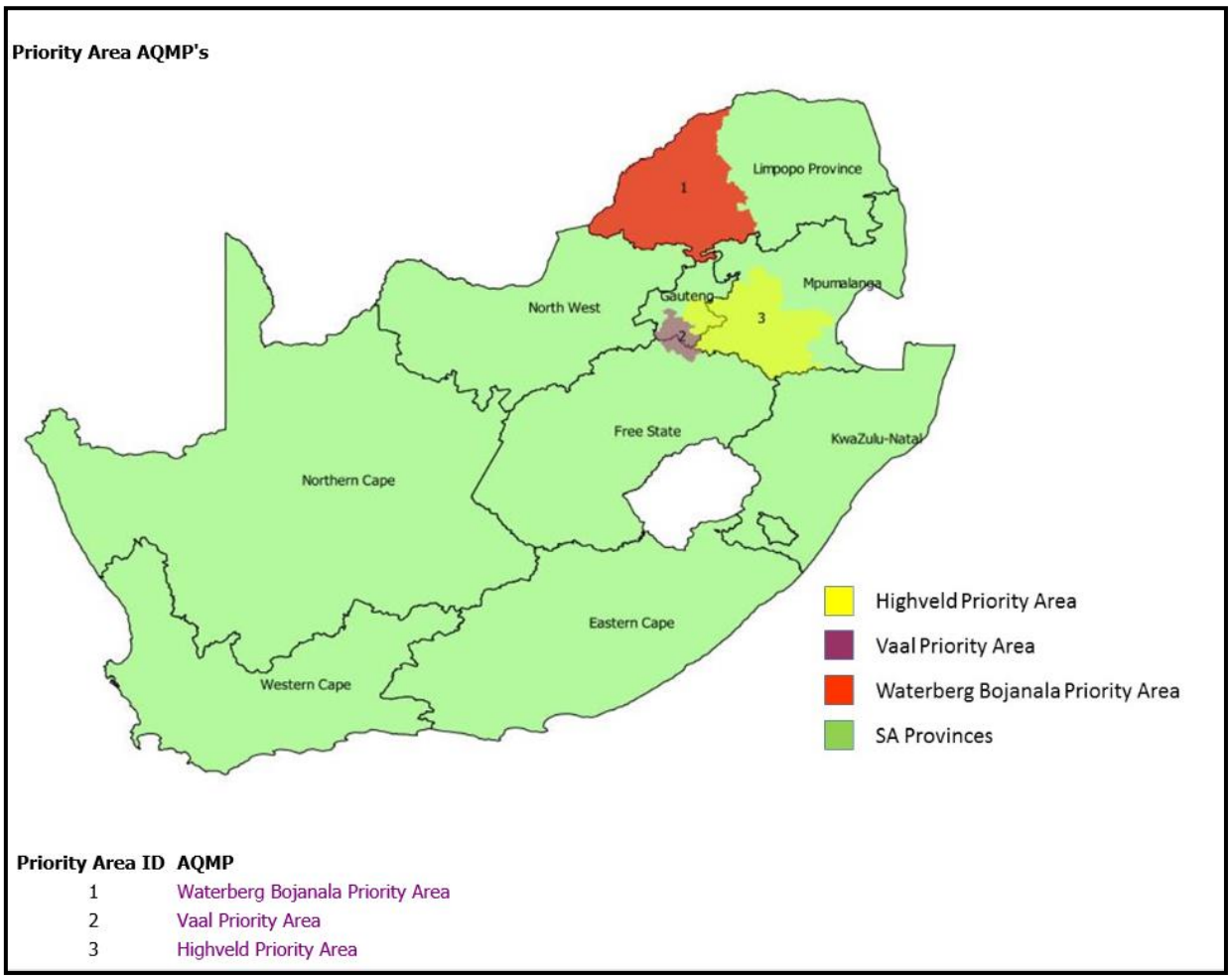

Figure 26: Air Quality Management Priority Areas in South Africa (DEA, 2018b).

Atmospheric PM emissions have been a source of concern in South Africa, particularly in the Highveld Priority Area (HPA) in the Mpumalanga Province, where elevated PM_{10} "hot spots" have been identified (Figure 27 and Figure 28) (DEA, 2011; DEA, 2017). Opencast mining contributes to PM emissions and the contribution of mining to annual atmospheric PM concentrations in the HPA due to unpaved haul roads is shown in Figure 29 (DEA, 2011). This contribution is evident in the local municipalities of Emalahleni and Steve Tshwete, where opencast coal mining is highly prevalent and concentrated (DEA 2011). However, other potentially significant mining sources of fugitive dust such as discard dumps were excluded during the emissions inventorying and dispersion modelling phases of the HPA air quality management study. The criticism against this approach has been centred on the under-estimation of coal mining particulate emissions in the HPA and the potential negative impacts for emission reduction initiatives and air quality management in the region.

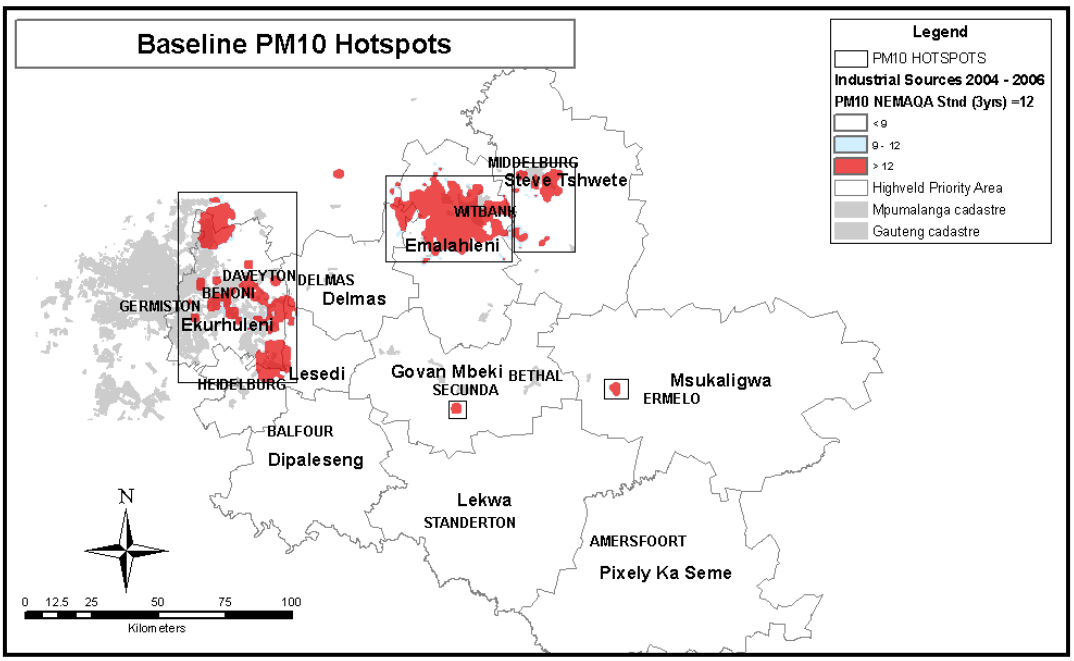

Figure 27: Modelled frequency of exceedance of daily (24 hours) PM10 standards in 'Hot Spot' areas in the Highveld Priority Area (DEA, 2011).

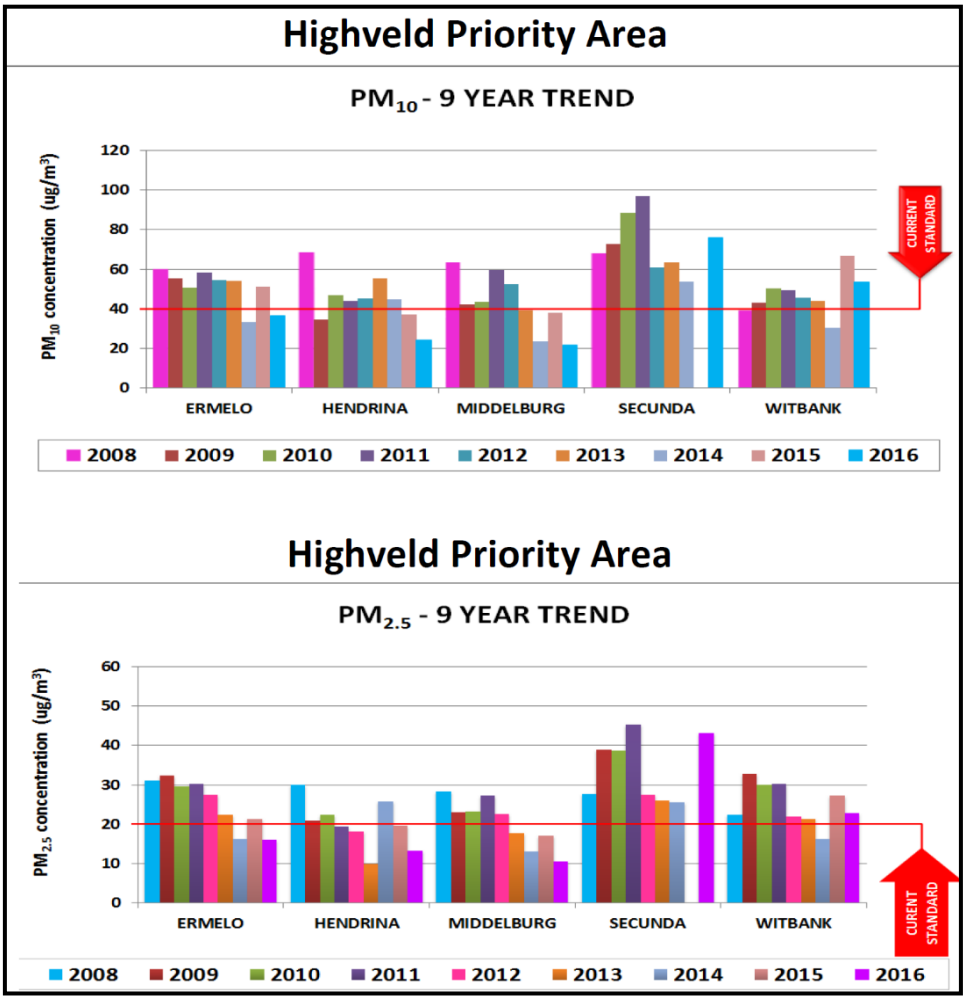

Figure 28: Particulate matter concentrations recorded from the five DEA monitoring stations in the HPA (DEA, 2016b).

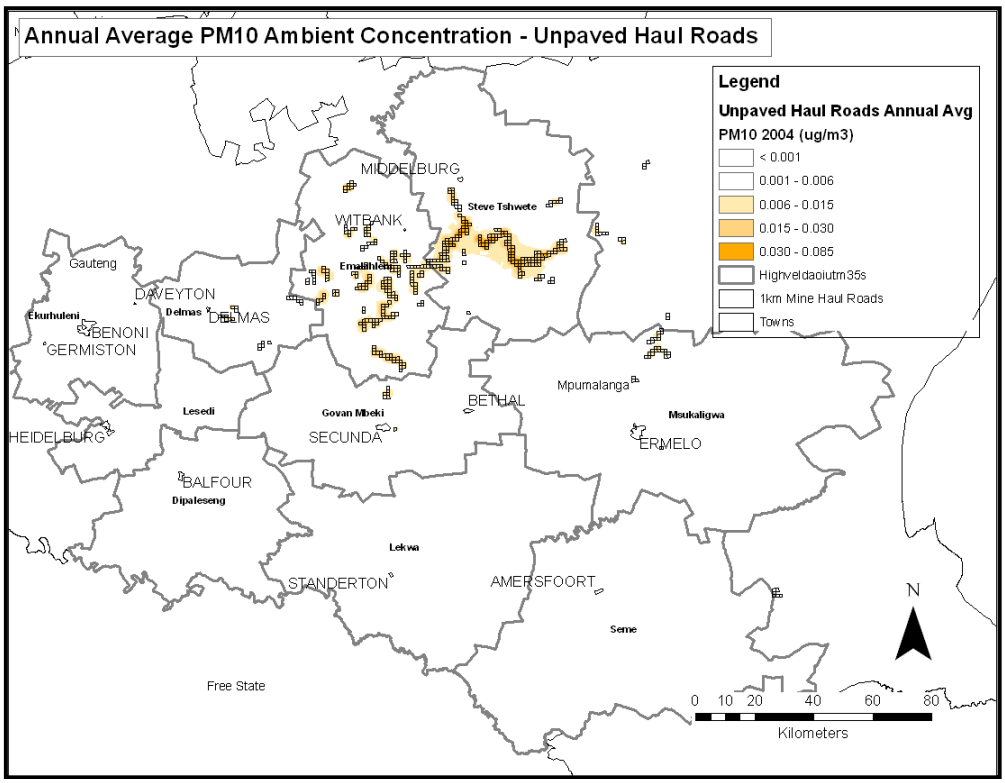

Figure 29: Contribution of opencast coal mining to annual PM_{10} concentrations in the HPA (DEA, 2011).

In the WBPA, potential exceedances and current exceedances of the NAAQS for atmospheric PM and other criteria air pollutants, have also been a cause of concern (Figure 30). The sources of emissions include industrial activities, coal mining, brickworks, power generation and domestic fuel burning (DEA, 2018a).

2.4.6 Coal Mining Atmospheric Particulate Emissions and Health Impacts

The impacts of coal mining on human health and the environment have long been a source of concern, with some researchers indicating that these concerns may date as far back as 3,000 years ago, in an era when coal was first used as a fuel in China, and the Industrial Revolution in the 17th century (Mamureklit, 2010; Rai, 2015). The impacts of air pollution from mining activities are not only restricted to the mining area boundary or premises, but also to the surrounding communities or sensitive receptor areas (Pless-Mulloli *et al*., 2000; Reddy & Ruj, 2003).

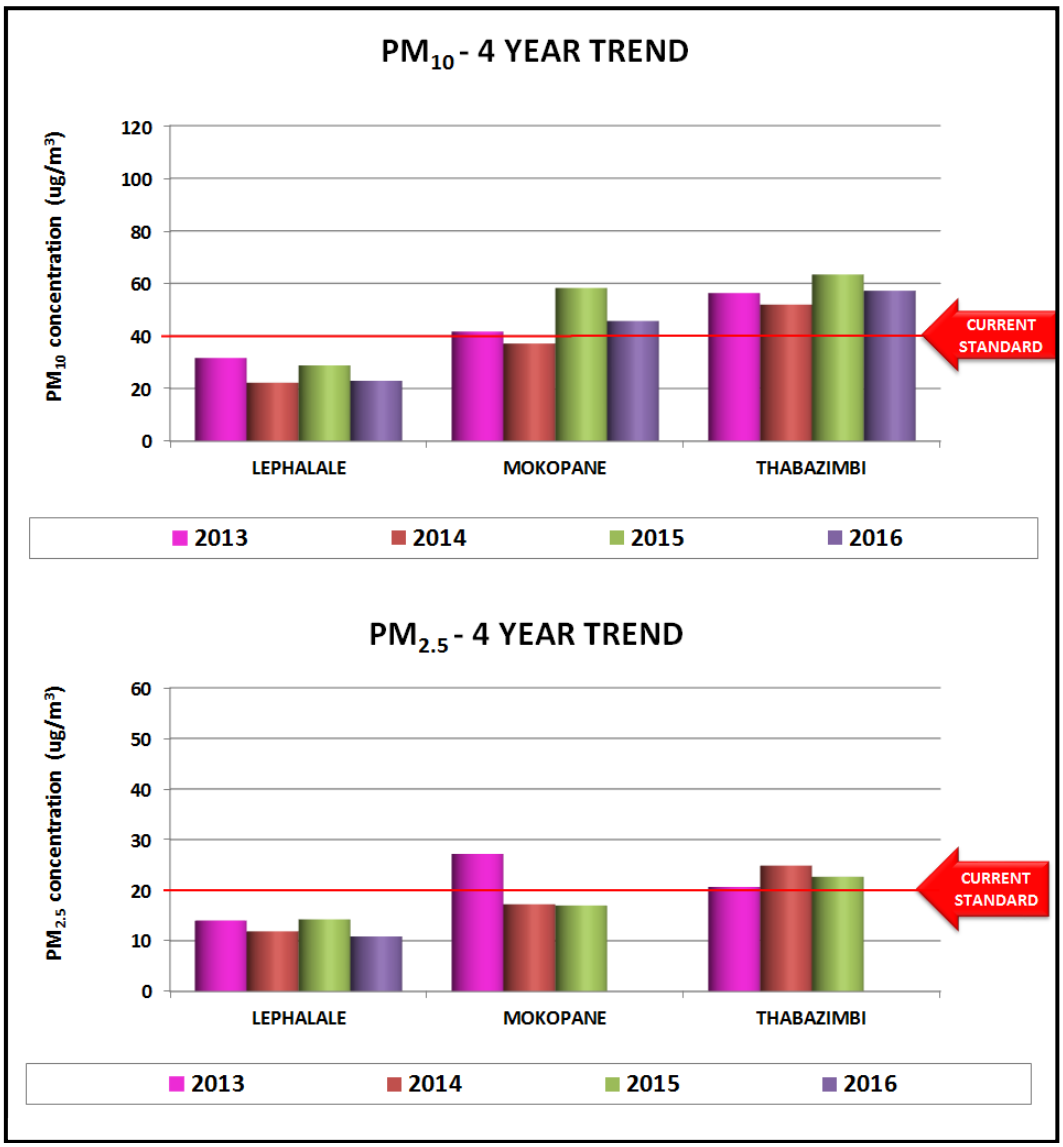

Figure 30: Particulate matter concentrations recorded from the three DEA monitoring stations in the WBPA (DEA, 2018a).

In South Africa, as in other countries, opencast coal mining activities are generally located close to communities (Munnik *et al*., 2010; Pretty & Odeku, 2017). Many communities in the HPA are located close to opencast mines and this has resulted in major concerns regarding the existing and potential health impacts of mining to these communities (DEA, 2011).

Atmospheric PM generated during coal mining activities is emitted to the atmosphere and surrounding areas and air quality degradation due to mining is a problem experienced globally (Pandey *et al.,* 2014). Several air quality studies have reported increased levels of atmospheric PM in proximity to opencast mines (Appleton *et al.,* 2006; Patra *et al.*, 2006). In some cases, despite the application of mitigation measures such as wet and chemical suppression and adherence to legislation for the reduction of coal dust or atmospheric

particulate emissions, coal dust continues to be a problem in some communities located in proximity to the mining operations (Jones *et al*., 2002; Merefield *et al*., 1995).

Atmospheric PM from coal mining includes coarse and fine particles (Kumar *et al*., 2011). A significant number of studies are available on particle size analysis of atmospheric PM emitted from coal mining operations (Dockery & Pope, 1994). These studies report that atmospheric PM from coal mines is a mixture of particle sizes (Greeley & Iversen, 1985; Panyacosit, 2000). Particles between 10-30 µm and above are known as total suspended particulate matter (TSP) and generally settle gravitationally close to the source of emission (Greeley & Iversen, 1985; Mannucci & Franchini, 2017; Singh, 1998; Tsiouri *et al*., 2015). Total suspended PM is not of major concern from a health point of view as these particles become trapped in the nostrils or are swallowed (Makua & Odeku, 2017). Inhalable particles include particle sizes of 10 µm or less, while respirable particles (2.5 µm) can penetrate deeper into the lungs, resulting in negative health impacts (Huertas, *et al*., 2012; Kumar *et al*., 2011; Munawer, 2018). It is for this reason that PM_{10} from coal mining activities which includes $PM_{2.5}$ and PM_1, is generally associated with negative impacts on human health (Munawer, 2018).

It has been shown that atmospheric PM results in short and long-term impacts on human health (Rai, 2015; Munawer, 2018), specifically with regards to respiratory effects, cardiovascular diseases and mortality (Panyacosit, 2000*;* USEPA, 2009). Specifically, the human body has been shown to be unable to remove coal dust which has been deposited progressively over the years. This results in fibrosis, inflammation and necrosis (Davis & Mundalamo, 2010).

In South Africa, a health risk study undertaken on behalf of the Fund for Research into Industrial Development, Growth and Equity (FRIDGE), reported that Emalahleni in the Mpumalanga Province, was one of the areas with a large population potentially at risk from ambient concentrations of PM_{10} and SO_2 (DEA, 2011). During the study, inference on health risk and exposure of populations in the HPA was made based on the location of hot spots relative to human populations (Figure 31) (DEA, 2011). In the Mpumalanga Highveld, hospital admissions were reported to be over 8 600 cases annually (Scorgie *et al.*, 2002). It is likely that some of the admissions were related to respiratory diseases associated with atmospheric air pollution (Scorgie *et al.*, 2002).

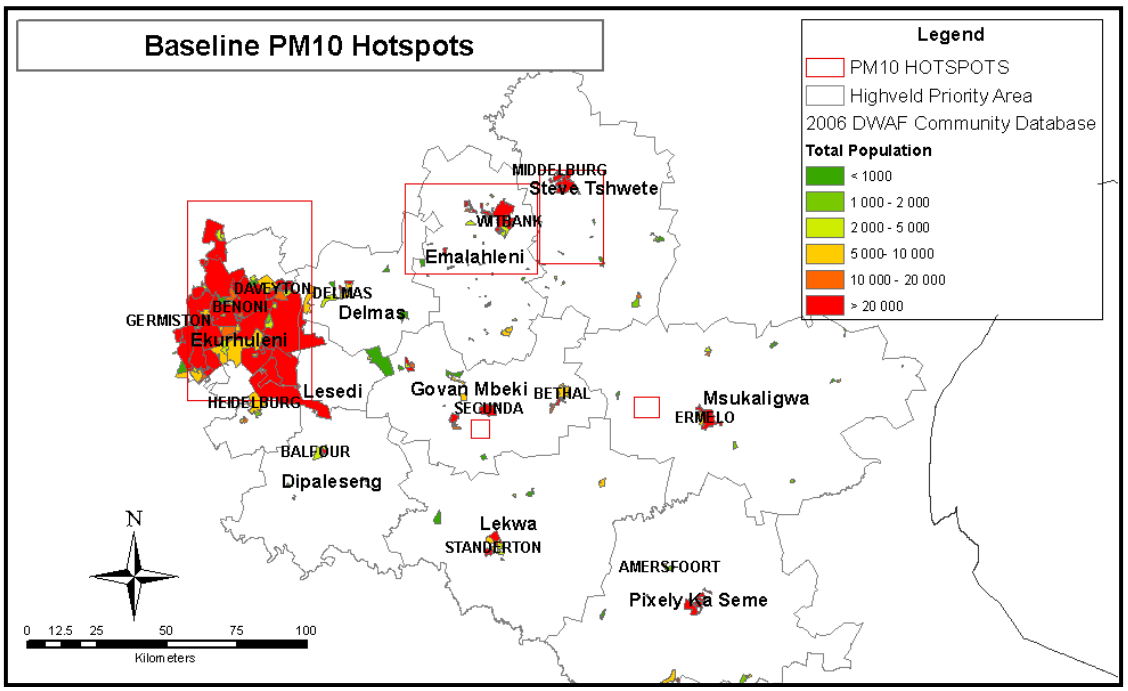

Figure 31: Location of PM_{10} 'Hot Spots' relative to human population (DEA, 2011).

A study undertaken by Norman *et al* (2007) indicated that in South African urban areas, 3.7% of total mortality from cardiopulmonary disease in adults aged 30 years and older was caused by air pollution. The study also indicated that 5.1% of mortality due to tracheal cancers, bronchus and lung in adults was due to air pollution. With regards to acute respiratory infections in children under 5 years of age, air pollution caused 1.1% of mortality (Table 8) (Norman *et al.*, 2007).

Table 8: Burden of disease relating to mortality outcomes from outdoor air pollution (Norman *et al.*, 2007).

Related health outcomes	Attributable deaths (in individuals)	Attributable years of life lost (in years)
Lung cancer (adults 30+years)	350	3 604
Cardiopulmonary disease (adults 30+years)	4 222	36 423
Asthma	237	2 644
Acute respiratory infections (children 0-4 years)	65	2 193
Lower respiratory infections	64	21 44
Upper respiratory infections	1	45
Total	4 637	42 219
% of total burden	0.9	0.4

The burden of disease is normally higher in developing countries and this is also the case with air quality deterioration (Mannucci & Franchini, 2017; Rai, 2015). However, the debate on the ever-contested issues of environmental degradation versus economic and social development is a complicated and on-going one (Kaygusuz, 2012). This is particularly the case in developing countries, where economic development through industrial growth, job creation (due to high unemployment rates) and poverty alleviation are critical focus areas for most governments (Rai, 2015). The challenge is that this creates an imbalance in addressing environmental, health and economic growth issues, which are individually delicate issues (Panyacosit, 2000). However, the application of sustainability principles, which foster the consideration of economic, social and environmental issues might provide a win-win situation for all.

2.4.7 Coal Dust

Coal dust is generally emitted by various sources in a coal mine and is part of atmospheric PM emissions (Ghose, 2002). Sources of coal dust include crushing and screening, coal stockpiles, drilling and blasting of coal, materials handling and coal transportation by trucks and trains (Ghose & Majee, 2000, Queensland Rail Management, 2008). Coal dust may contain heavy metals such as selenium, mercury, cadmium, antimony, lead, nickel and arsenic, whose toxicity levels vary (Finkelman *et al.,* 2002).

Coal dust emissions have historically been a source of concern, mainly due to occupational health impacts for mine workers (silicosis and coal worker's pneumocosis), health impacts on surrounding communities and environmental impacts (Petavratzi *et al*., 2005; Sellaro *et al*., 2015). Coal dust also presents other potential hazards such as coal dust explosions (Petavratzi *et al.,* 2005).

In addition to carbonaceous material, of coal mining dust is composed of minerals such as quartz (silicone dioxide- SiO_2), dolomite $(CaMg)(CO_3)_2$ which is a carbonate material, kaolinite $(Al_2Si_2O_5(OH)_4)$ which is a silicate, illite $(K, H_3O)(Al,Mg,Fe)_2(Si,Al)_4O_{10}[(OH)_2,(H_2O)]$ and calcite ($CaCO_3$) which is a carbonate mineral (Jones *et al*, 2000; Potgieter-Vermaak *et al.*, 2011). Many of the impurities present in dust, particularly coal dust, are due to the afore-mentioned minerals (Potgieter-Vermaak *et al.*, 2011). Therefore, the amount of carbon in coal and not its mineral composition generally determines its purity (Jones *et al*., 2002).

Generally, opencast coal mines are associated with a large proportion of impurities during the early stages of mining compared to underground coal mines (Huertas *et al.*, 2000; Jones *et al.*, 2000). This is due to topsoil and overburden which are initially removed for access to the coal seam (Pokorna, 2016). This results in a large proportion of non-coal particles in dust from opencast mines. However, as mining progresses and the coal seam is reached, coal dust which has a high proportion of carbon is produced and this contains less mineral matter (Jones *et al.,* 2000).

When coal is pulverised, its mineral components maybe liberated from the coal particulates, producing relatively pure mineral particles. The mineral grains in pulverised coal can be described as “included” or “excluded” (Liu *et al*., 2007). Included mineral grains are associated with or contained within a carbonaceous particle. Excluded mineral grains do not have any carbonaceous material associated with them (Liu *et al*., 2007).

Given the negative impacts of coal dust on health and the environment, the identification, characterisation and quantification of coal dust PM becomes critical for the full comprehension of all potential health impacts, mitigation of environmental impacts and reduction of health impacts among coal workers and the public in general, particularly communities living adjacent to coal mines (Ferreira *et al.*, 2013). However, very little literature exists on the characterisation of coal dust and information on particle size distribution and classification of coal dust particles as inhalable or respirable is inadequate for the full comprehension of coal dust and its associated health and environmental impacts (Wallace *et al.,* 1990). In addition, it is always assumed that the morphological, physical and chemical characteristics of dust from different coal mines are similar in the assessment of exposure to dust. This is a major shortcoming in most research studies (Wentzel, 2015).

Air quality management techniques such as emissions inventorying and dispersion modelling are generally used for the quantification of atmospheric PM emissions and prediction of coal mining impacts to adjacent communities. However, these techniques also do not involve the analysis of coal dust PM for the purposes of identifying and characterising atmospheric PM from coal mining activities (USEPA, 2018).

2.5 ATMOSPHERIC PARTICULATE MATTER CHARACTERISATION

Recently, there have been major advances with regards to instrumentation and analysis techniques for the purposes of identifying, characterising and quantifying coal dust or atmospheric PM (Baeten & Dardenne, 2002). These analysis techniques include microscopy and spectroscopic techniques such as SEM, EDS, transmission electron microscopy (TEM), reflectance microscopy, XPS, Raman and image analysis techniques, TGA, IRMS and thermal optical analysis (Adams, 1994; Cacuccio *et al.*, 2002; Li *et al*., 2005).

Spectroscopy is an important field of science which is used for the characterisation of matter. It involves the study of the interaction of electromagnetic radiation with matter (Helmenstine, 2018; Smith, 2016; Ahmed *et al*., 2017). Spectroscopic techniques or methods can be differentiated based on phenomena such as absorption, scattering, emission and fluorescence samples (Bumbrah & Sharma, 2016). There are a multitude of current and potential uses of spectroscopy (Olson, 2018; Smith, 2016). Modifications of spectroscopic techniques have been undertaken since their inception, with modifications mainly undertaken for improvement of analytical performance and adaptation to different and new applications (Baeten & Dardenne, 2002).

Recent advancements in numerous fields of study, particularly in the biology, material science, environmental science, drugs, chemistry, health science and nanotechnology fields have spurred continuous development in spectroscopic techniques (Olson, 2018). For example, researchers have developed micro infrared sensors (2 cm^2 chips) for the detection of material concentrations using spectroscopic technology, eradicating the need for benchtop analysis (Smith, 2016). The global increasing demand for food has led to research on the use of spectroscopy to increase or optimise plant productivity (Baeten & Dardenne, 2002). The argument of these researchers is that spectroscopy can be adopted for the analysis of plants and soil mineral content.

2.5.1 Scanning Electron Microscopy and Energy Dispersive Spectroscopy (SEM-EDS)

SEM-EDS has been applied in atmospheric research studies for the characterisation of atmospheric PM for a number of years (Genga *et al.*, 2013; Singh *et al*., 2014). It has been applied to the determination of the morphological characteristics of particles and the

simultaneous analysis of physical and chemical composition (elemental composition) of atmospheric PM (Adams, 1994; Casuccio *et al*., 2004; Grassi *et al*., 2004). This type of analysis is critical in extracting all available information in samples, especially for atmospheric PM analysis, where morphological information is inadequate without chemical characterisation for the determination of elemental composition (Ličbinský *et al*., 2010).

The SEM technique has several advantages over conventional light microscopes. These include high resolution which ranges from 1-20 nanometres (nm) (Swapp, 2018), three dimensional images which can be assessed for morphological, compositional and topographical information, wide range of magnification, greater depth of field and high resolving power (in the submicron level) which enables better analysis of atmospheric PM, particularly PM_{10} (Adams, 1994; Ergeton, 2005). The SEM technique involves the use of a focused electron beam over a surface to create an image (Goldstein *et al*., 2003). The electrons in the beam interact with the sample, producing secondary electrons, X-rays, backscattered electrons and various signals that can be used to obtain information about the surface topography and composition (Egerton, 2005; Reimer, 1998; Sellaro *et al*., 2015). The whole process results in the production of images which are in turn displayed on a computer screen which is part of the SEM equipment (Figure 32) (Nanoscience.com, 2018).

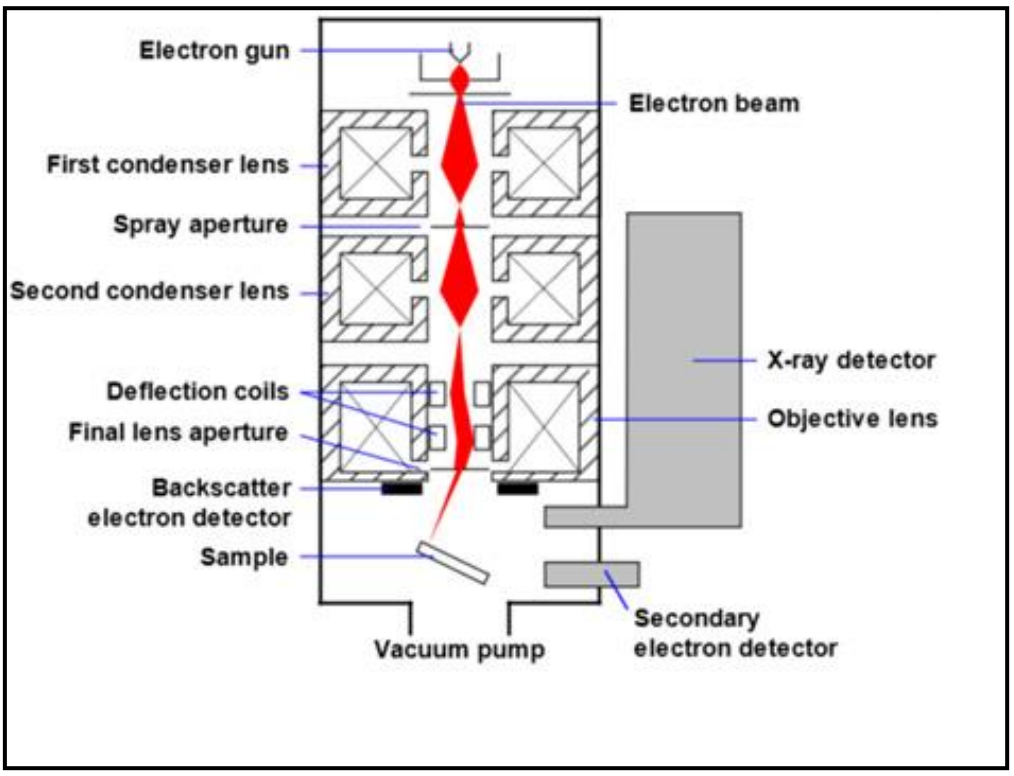

Figure 32: Scanning electron microscopy (Nanoscience.com, 2018).

Different scanning electron microscopy micrographs images of coal dust particulates are shown in Figures 33 to 36 below.

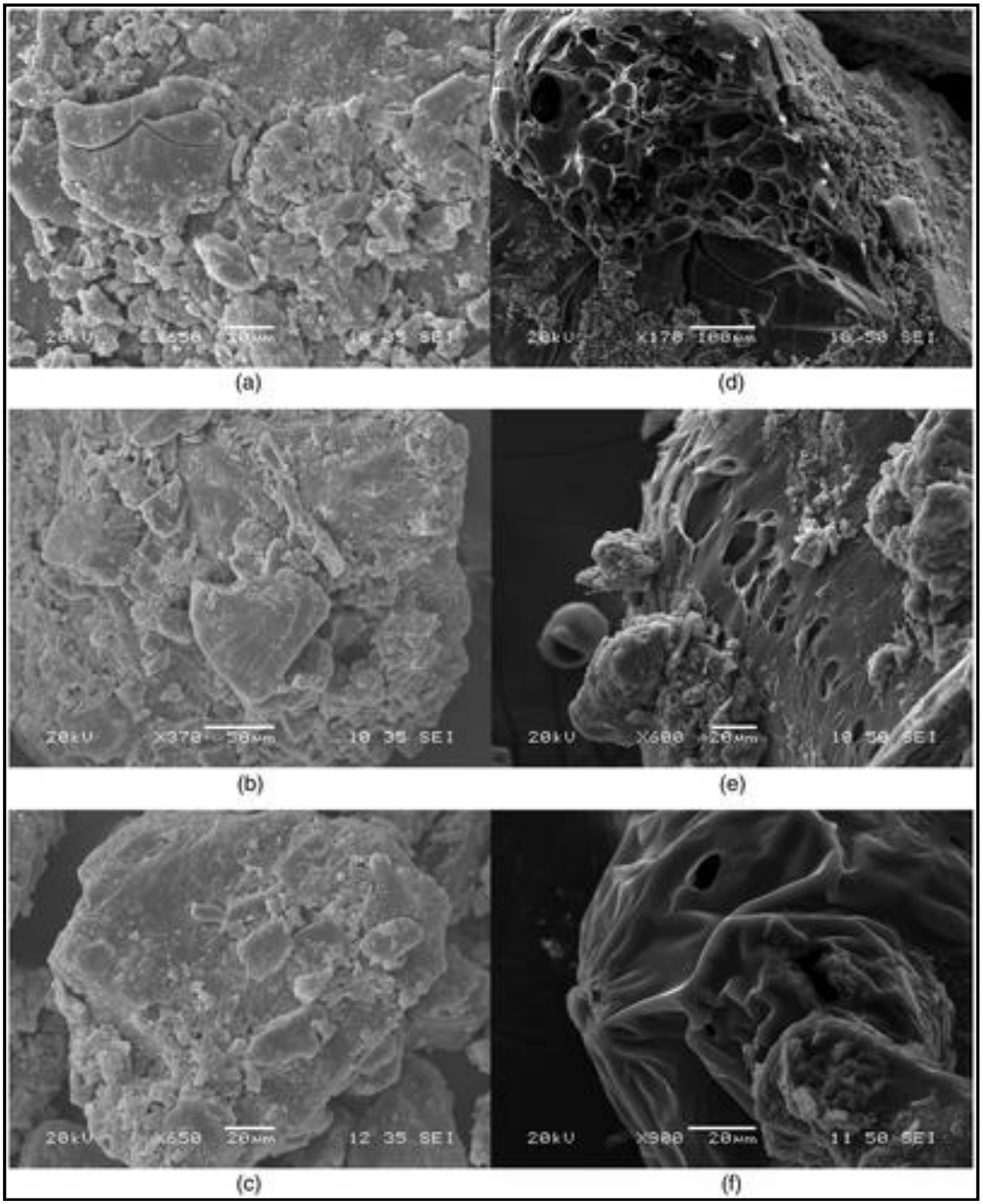

Figure 33: Coal dust particulates before combustion (a, b, c) and after combustion (d, e, f) (Rajasegar & Kyritsis, 2015).

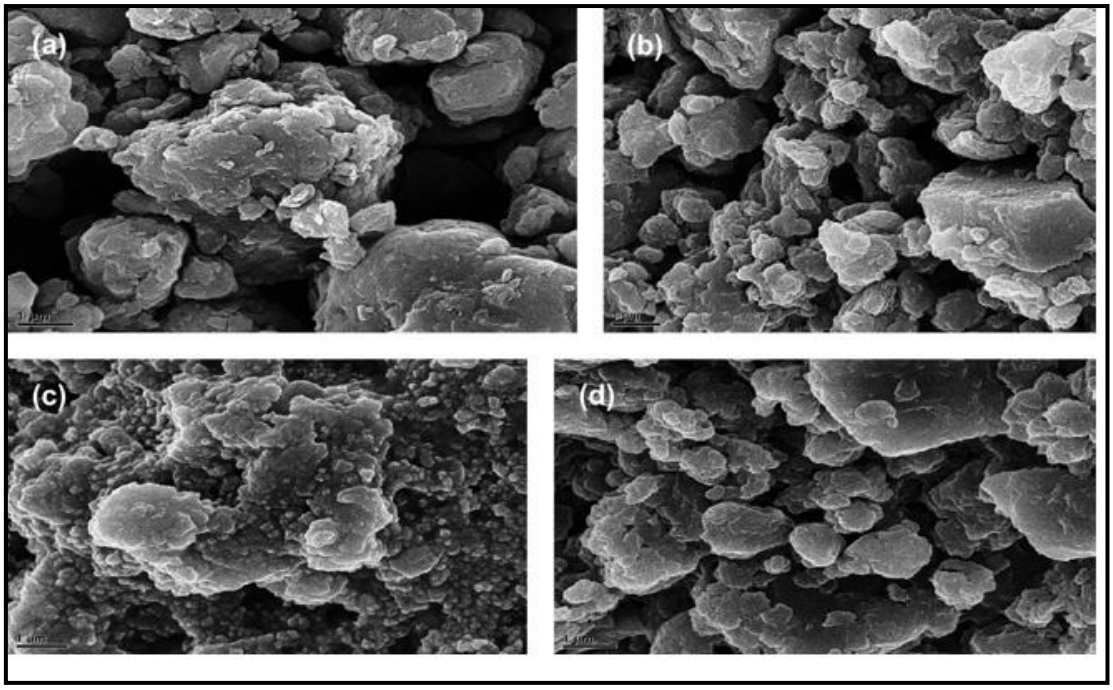

Figure 34: Coal atmospheric PM (Mujuru *et al.*, 2009).

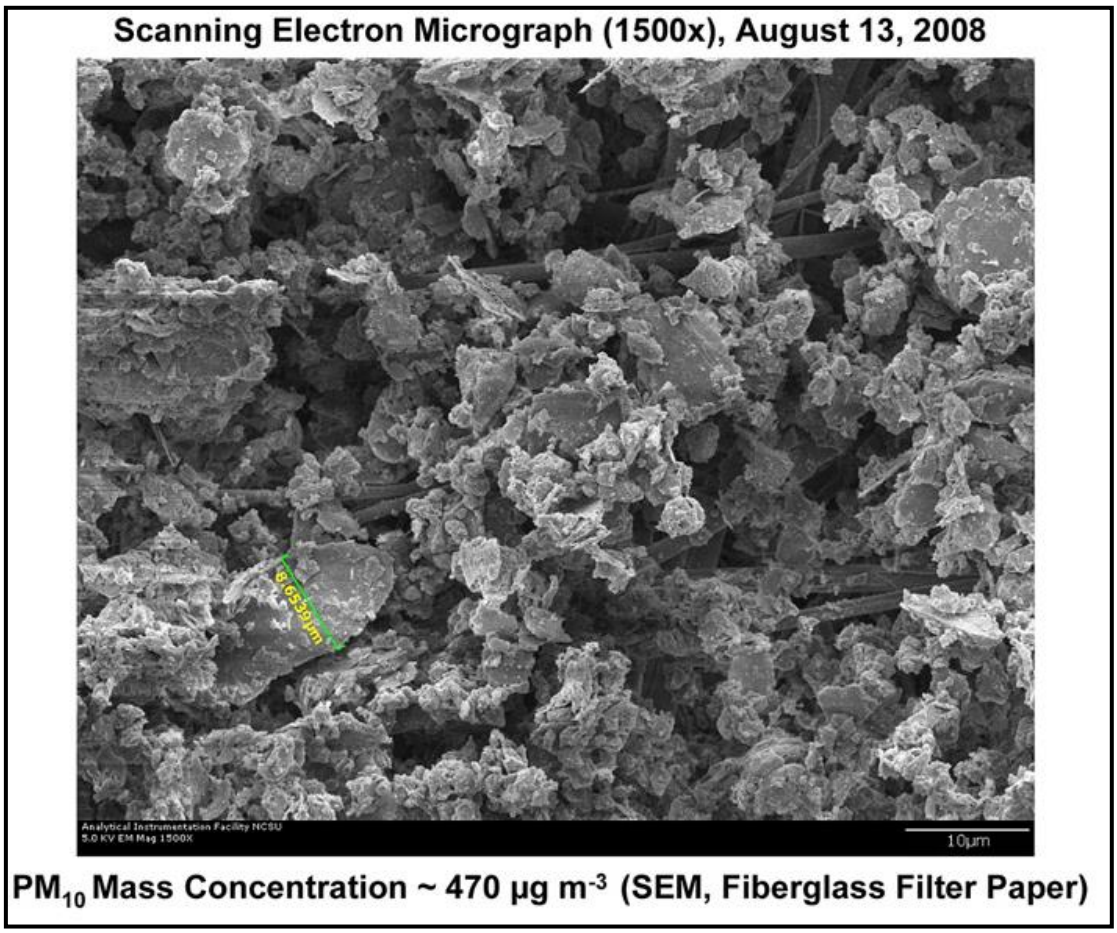

Figure 35: Coal atmospheric PM (Aneja, 2012).

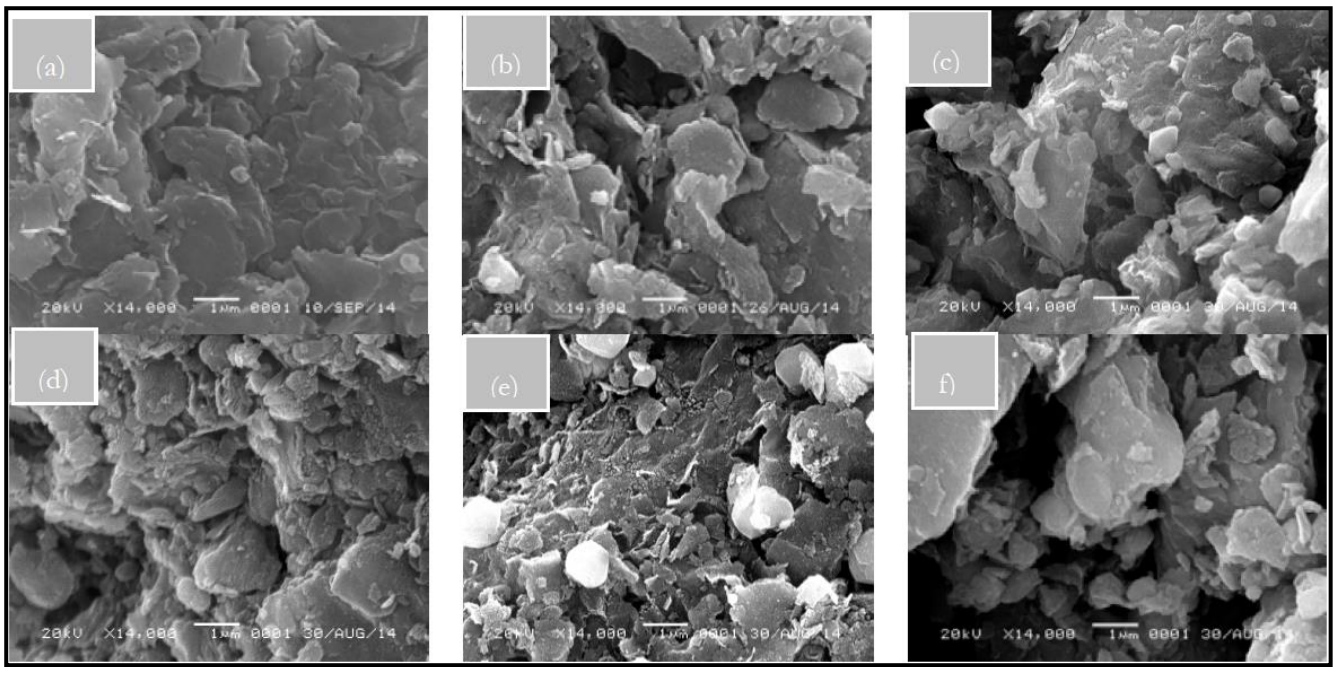

Figure 36: The morphology of coal tailings before activation, activated carbon and Fe-intercalated graphite. (a) before activation, (b) after activation at 500°C, (c) 1% Fe T 800°C, (d) 1% Fe T 900°C, (e) 2% Fe T at 800°C, (f) 2% Fe T 900°C (Gustian *et al*., 2015).

Elemental composition identification can be undertaken using EDS integrated or combined with SEM (Kgabi, 2010). The powerful feature of EDS is the submicron identification of elemental composition of a sample which is investigated on the SEM (Ferreira, 2013; Grassi *et al*., 2004). Generally, the elemental analysis of atmospheric PM samples presents analysis challenges due to the usually small sample sizes (Ramirez-Leal *et al*., 2009). These minute samples contain a wide range of information on elements and sometimes compounds, at different concentration levels (Casuccio *et al*., 2002; Genga *et al*., 2013).

EDS is widely applied for the investigation of materials, particularly morphological and textural properties, interactions between particles, growth of crystals and the formation of alloys (Reddy *et al.*, 2000). EDS includes the plotting of X-ray frequencies for each energy level of an atom in the sample (Adams, 1994). The plotted peaks in EDS represent highest frequencies of X-rays at corresponding energy levels (Genga *et al*., 2013). The peaks depicted in the spectrum are unique for each element present in the sample and are directly related to the elemental concentration in the sample (Adams, 1994).

However, the powerful combination of SEM-EDS for atmospheric PM characterisation also has its limitations (Reddy *et al.*, 2000). These include the fact that only solid samples can

be analysed through SEM-EDS and only sample sizes that fit into the microscope chamber can be assessed (Swapp, 2018). The horizontal dimensions of samples are usually limited to the order of 10cm while vertical dimensions have more limitations and sample sizes generally cannot exceed 40 mm (Ramirez-Leal *et al*., 2009). In addition, the high vacuum operating conditions of most instruments require sample stability at 10^{-5}-10^{-6} torr (Clarke, 2002). However, some samples outgas at low pressures, particularly organic materials and wet samples, and require usage of low vacuum SEMs (Clarke, 2002). Many SEMs are operated using solid state EDS detectors (Ramirez-Leal *et al*., 2009). Despite these detectors being fast and user friendly, poor or low energy resolution and low sensitivity to elements which are found in small concentrations in the sample are some of the shortcomings, especially when compared to wavelength dispersive X-ray detectors (Kgabi, 2010). In addition, for high vacuum analysis of samples, the application of electrically conductive coating must be undertaken to samples that are electrically insulating to ensure high resolution images (Swapp, 2018). Another shortcoming is that EDS analysis on small atmospheric particulates can be subject to interference from the sample background, i.e complete penetration of primary electrons through the sample occurs (Sellaro *et al*., 2015).

2.5.2 Reflectance Microscopy (Reflectance)

Coal exhibits optical properties which become evident after preparation of coal samples (Speight, 2015) so that coal can be examined by optical microscopy techniques such as reflectance microscopy (Xie, 2015). Recently, reflected light microscopy has been combined with other techniques such as image analysis for the analysis of samples for the identification and differentiation of coal from other particulates in the sample (Warren *et al*., 2015).

The reflectance of coal is generally determined by the degree of reflection of a beam of polarised or incident light from a polished coal surface (Averitt,1975). The procedure of making the polished block of coal includes crushing the coal sample and screening it to remove fine particulates (Speight, 2015; Xie, 2015). A binder is used to form a briquette, which is polished successively using fine abrasives, with the objective of producing a smooth surface which can be examined under an optical microscope for the determination of reflectance using polarised light which is directed vertically at the sample (Xie, 2015).

For reflectance microscopy purposes, the brightness of the polished surface is critical. Different coals have different reflective capacities. The reflectivity, R, of coal is calculated as follows:

$$R = \frac{I_r}{I_i} \times 100\,\%,$$

where I_r is the reflected light intensity and I_i is the incident light intensity. Reflectivity is an important property of opaque minerals and is also an important indicator of the coalification degree (Figure 37) (Averitt, 1975; Kie, 2015;). Reflectance values obtained through air being higher than those obtained using oil as a medium (Prusty, 2015) (Figure 38 and Figure 39).

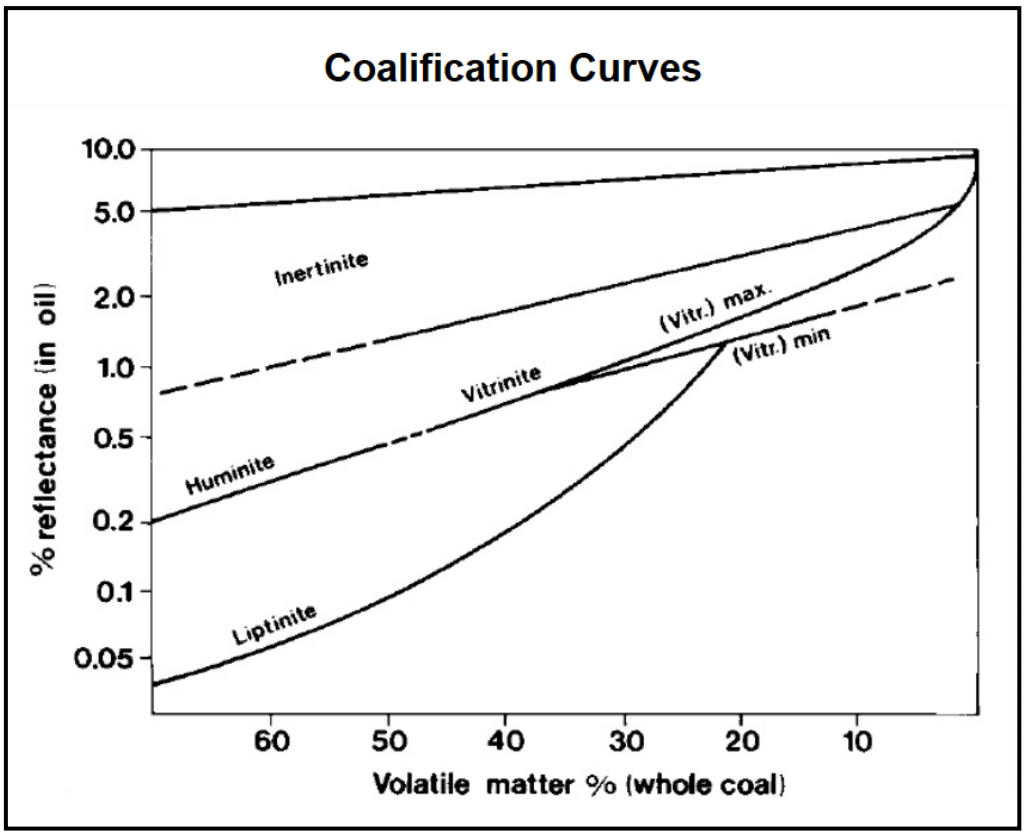

Figure 37: Coalification curves and reflectance values for coal (Averitt, 1975).

The reflectance is largely determined by coal macerals (Davis, 1978). Macerals are the microscopically identifiable organic constituents of coal, while the inorganic fraction is mainly mineral matter, known as ash after combustion (Davis *et al.*, 1991). There are three coal maceral groups, vitrinite, liptinite and inertinite. Vitrinite is the most abundant coal maceral and is formed from woody parts of plants, cellulose and lignin (Chaudhuri, 2016). The stems

Reflectance Data Obtained in Air and In Oil

	Maximum Reflectance, Approximate (%)	
Carbon Content of Coal (%)	Air	Oil
60	0.4	6
90	1.0	8
96	6.5	17

Figure 38: Coal reflectance data for air and oil mediums (Stach *et al.*, 1982).

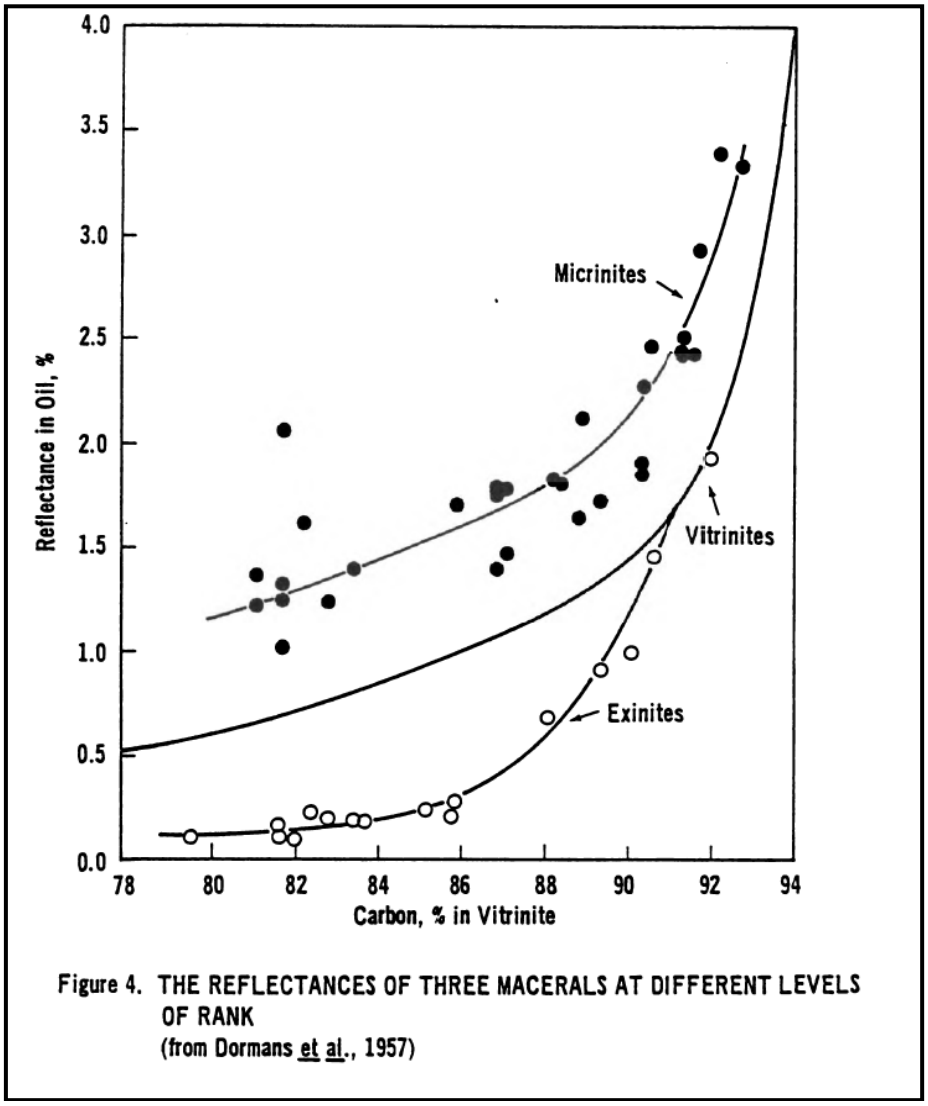

Figure 4. THE REFLECTANCES OF THREE MACERALS AT DIFFERENT LEVELS OF RANK
(from Dormans et al., 1957)

Figure 39: Reflectance values of coal macerals at different rank levels (Stach *et al*., 1982).

and roots of these plants are reinforced with wood and the outer layer of these plants is generally covered by bark (Chaudhuri, 2016). Liptinite is formed from pollen, spores, resins

and other material and is associated with the emission of volatiles and methane (Unsworth & Gough, 1989). Inertinite is the third maceral and is formed from plant trunks, cell walls and has a high carbon content (Figures 40 to 42) (Prusty, 2015; Spackman, 1958). The reflectance of vitrinite is commonly determined in most studies because it is the predominant maceral in many coals with a homogenous appearance under the microscope and large particles that enable easy measurement (Davis, 1978; Prusty ,2015).

Automated image analysis can be used to measure reflectance distribution of different macerals within a coal sample (Unsworth & Gough, 1989; Vleeskens *et al.,*1985). The main advantage of this approach is that it eliminates subjective interpretation, which mostly occurs when reflectance measurements are done manually (Davis, 1978). The automated image analysis approach, however, requires the eradication of reflectance measurements due to the mounting medium as this can coincide with that of coal components which exhibit low reflectance (Unsworth & Gough, 1989).

A literature review on techniques that are applied for the characterisation and quantification of coal dust indicates that currently, no standard technique exists for these purposes. The non-existence of such a technique is not limited to the characterisation of coal dust, but also includes the lack of sample preparation techniques which will enable comprehensive characterisation. As stated by the Coal Terminal Action Group in 2013, the problem is further compounded by the lack of petrographers who can undertake coal dust/particulate characterisation on a commercial basis.

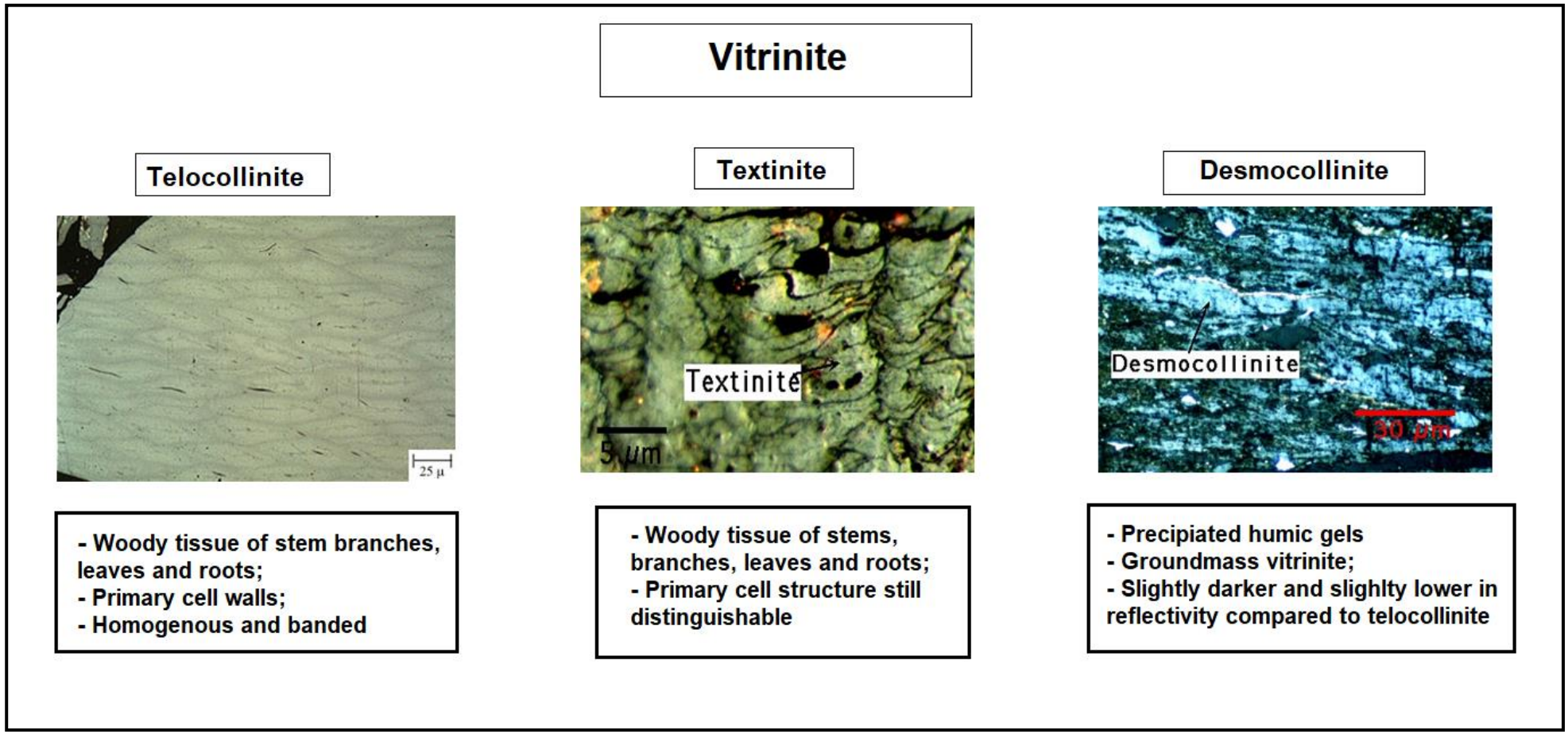

Figure 40: Coal genesis and characterisation- vitrinite (Prusty, 2015).

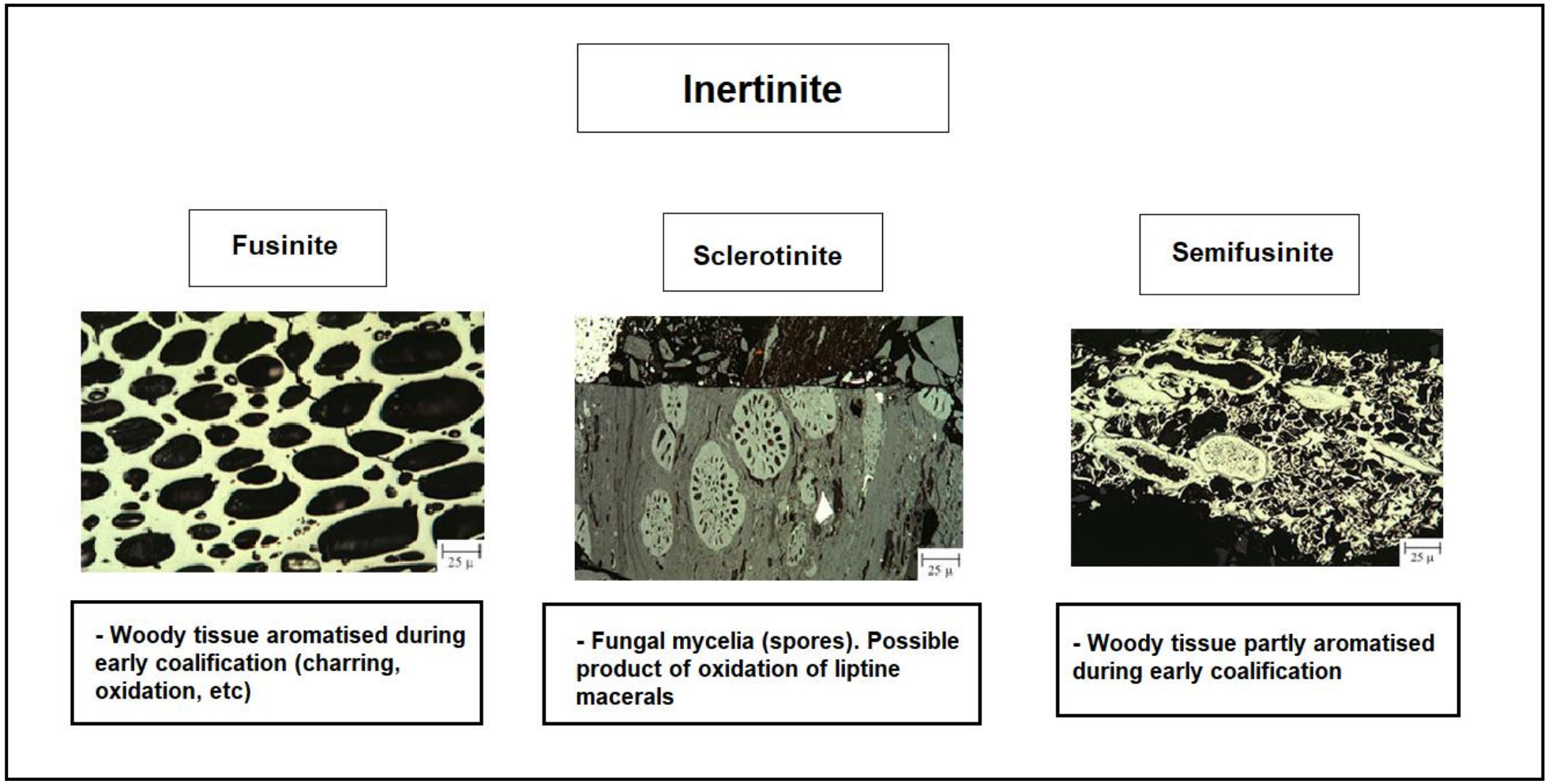

Figure 41: **Coal genesis and characterisation- inertinite (Prusty, 2015).**

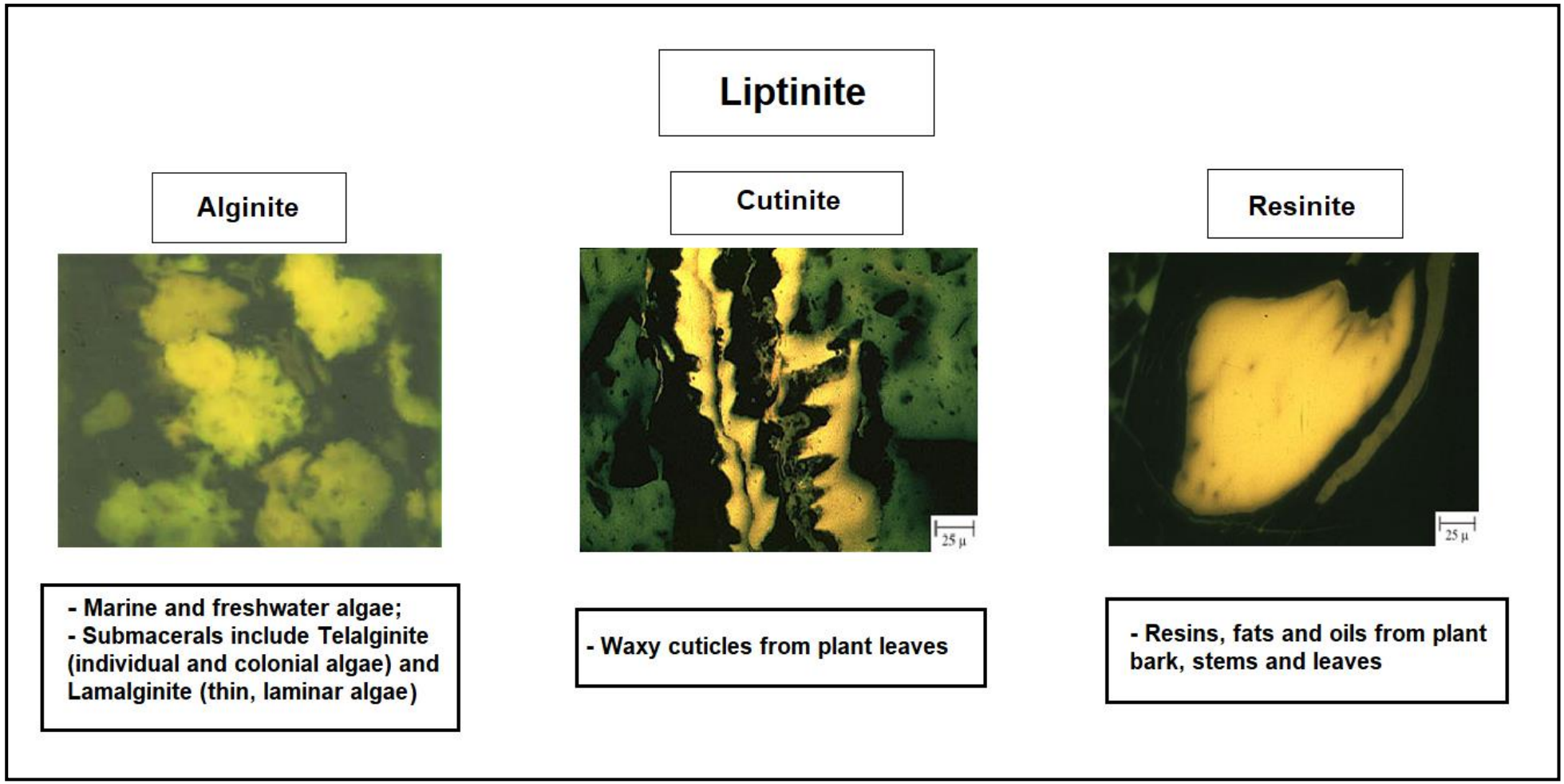

Figure 42: Coal genesis and characterisation- liptinite (Prusty, 2015).

Research studies have however been undertaken to fill this gap. One such study was undertaken by the Commonwealth Scientific and Industrial Research Organisation (CSIRO), an Australian research body. CSIRO initially developed a Coal Grain Analysis (CGA) system, which is a semi-automated imaging technique which collects and mosaics multiple images at high resolution to provide detail on urban dust particles (Warren *et al*., 2015). This process is undertaken using reflected light optical microscopy (air lens) to provide visual, qualitative and quantitative data on the size and composition detail of particles greater than 1 µm in a dust sample (O'Brien *et al*., 2017). Reflected light microscopy then provides colour images at high resolution and these images are processed by the CGA image processing software to create fingerprints or reflectance histograms of the individual particles in the mosaic image of the sample (Figure 43) (O'Brien *et al*., 2017). CSIRO then developed a semi-automated Optical Dust Marker (ODM) software (a supervised learning algorithm based on approximately 40 different types of particulate found in urban dust samples, with the reflectance fingerprint for each type acting as a reference) which utilises each individual particle's property, i.e colour reflectance fingerprint, for the classification of that particle (Figure 44) (O'Brien *et al*., 2017; Warren *et al*., 2015). Currently, Optical Dust Marker can be used for the differentiation between coal and non-coal particles and can be used for the identification of coal, quartz, iron, particulates from organic sources, dark minerals, combustion chars and pyrite/ bright materials (O'Brien *et al*., 2017; Warren *et al*., 2015).

Given the recent developments in the field of microscopy and techniques for dust analysis, it is envisaged that more analytic techniques that provide comprehensive information on dust particulates will be developed and will result in information that is acceptable to all stakeholders.

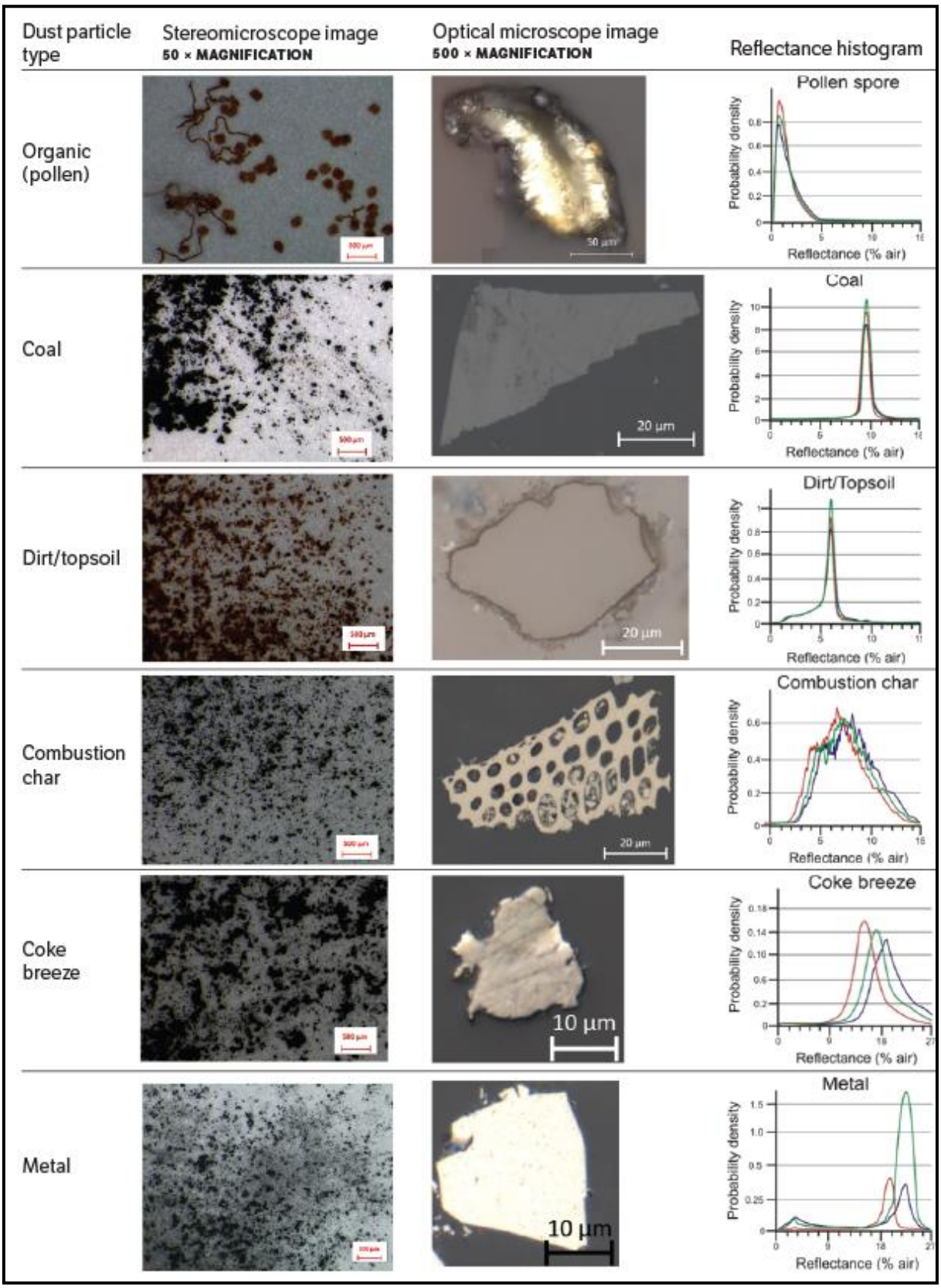

Figure 43: Stereomicroscope and optical photomicrographs of various dust particulates in the CSIRO's reference library (O'brien *et al.*, 2017).

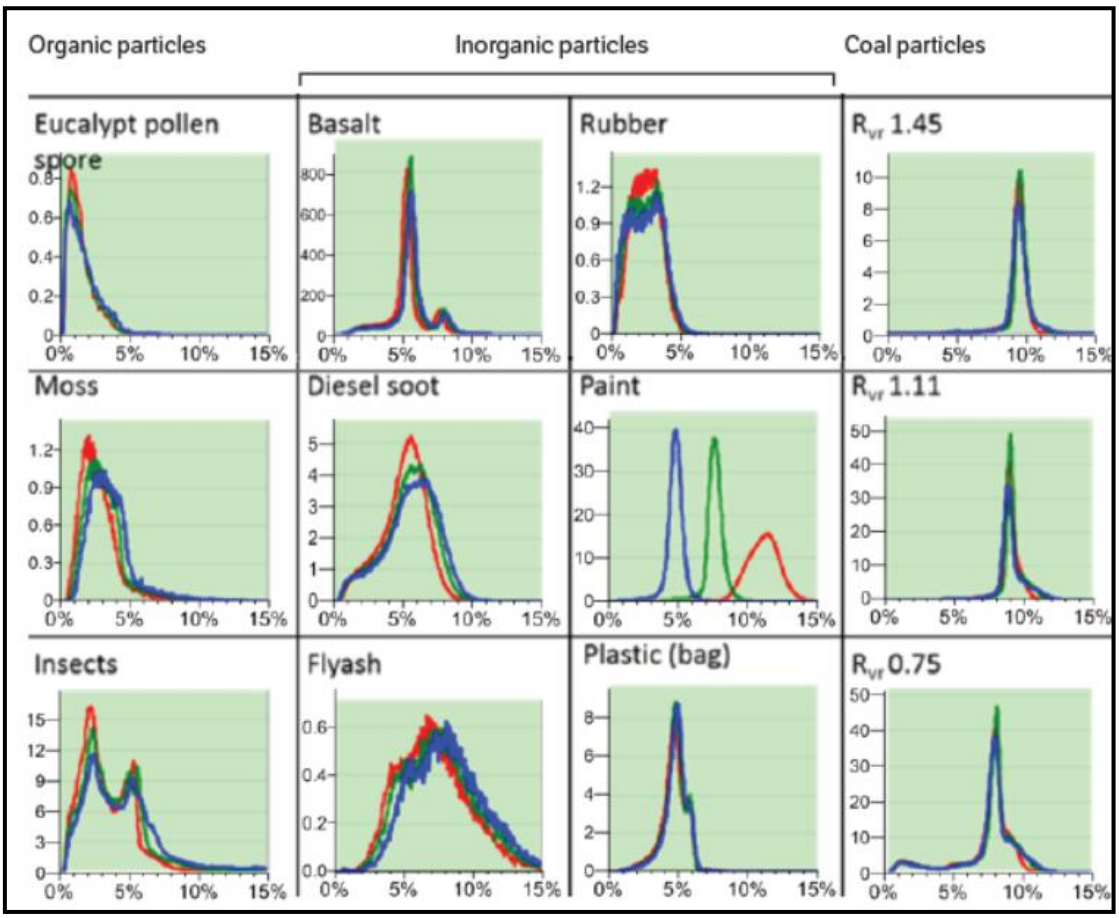

Figure 44: Fingerprints or reflectograms for various types of urban dust material (*O'Brien et al.*, 2017).

2.5.3 Optical (Light) Microscope

Optical or light microscopy is suitable for the analysis of particles in the size range of 0.8 µm to 150 µm, with a resolution of around 0.2 µm dependent on the wavelength of the light source (Allen, 2003). The formula for the theoretical limit of resolution of an optical microscope is expressed by the fundamental formula:

$$d_L = \frac{f^{\lambda}}{NA}$$

where d_L is the limit of resolution, whereby particulates in closer proximity than this appear as a single particle, λ is the wavelength of the illuminant, the numerical aperture of the objective NA= µsinθ where μ is the refractive index of the immersion medium, θ is the angular aperture of the objective and □ is a factor of about 0.6 to allow for the inefficiency of the system (Allen, 2003).

For particles which are smaller than the resolution limit, their appearance is changed to diffuse circles followed by the broadening of the image, resulting in oversizing (Weisenburger & Sandoghdar, 2015). Image broadening observed during the analysis of the atmospheric particulates results in the distortion of some of the particulate sizes (Allen, 2003).

2.5.4 X-ray Photoelectron Spectroscopy (XPS)

XPS is a powerful analysis technique for the determination of elemental composition and chemical state information from the surface of a solid sample (Materials Evaluation and Engineering, 2018; Song & Peng, 2009). It has been widely used for the analysis of the surface composition, chemical composition and state of atmospheric PM (Hutton & Williams, 2000; Lazzeri *et al*., 2003). The technique uses a monochromatic energy source to release incident X-rays on the sample (Figure 45) (Coetsee-Hugo, 2016; Song & Peng, 2009). Upon X-ray interaction with the sample, core level electrons are released from the sample's atoms (Briggs & Seah, 1990). The core electrons release photoenergy and this energy is a function of the atom's binding energy and is characteristic of the element from which it was emitted (Materials Evaluation and Engineering, 2018). The primary data for XPS is energy emitted by the photoelectrons. An electron energy analyser is used for the detection of photoelectrons emitted from the sample and the result is a spectrum which shows the surface composition of the sample (Adams, 1994). XPS is a non-destructive technique which can detect most elements except hydrogen (H) and helium (He). It provides chemical bonding information and has elemental sensitivity in the parts per 1000 range, (Andrade, 1985b; Hutton and Williams, 2000; Siegbahn, 1982). However, XPS has its shortcomings. These include the following;

- Low resolution which is in the range of approximately 0.1-1 eV;
- Slow- at least half an hour to 8 hours sometimes required per sample;
- Sample charging;
- High vacuum which is in the range of 10^{-8} to 10^{-11} torr;
- Energy referencing can be a problem (Andrade, 1985b).

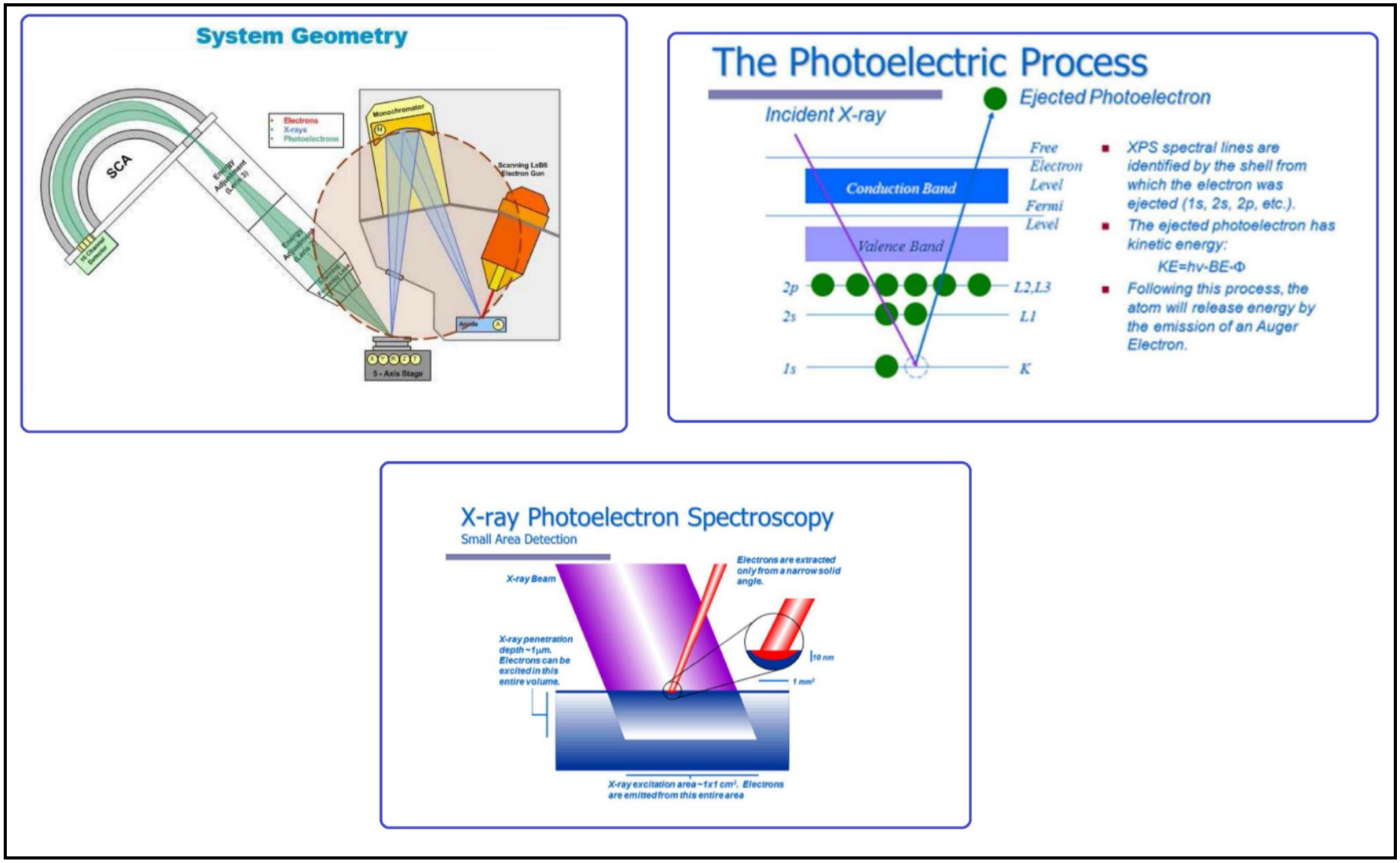

Figure 45: X-ray Photoelectron Spectroscopy: System Geometry (Coetsee-Hugo, 2016).

2.5.5 Raman Spectroscopy (Raman)

Raman spectroscopy is a technique which is applied to acquire information on the vibrations of molecules and crystal structures (Agarwal & Atalla, 1995; Nanophoton, 2018). The technique is based on the inelastic scattering of monochromatic light, which is generally derived from a laser source and is used to irradiate the sample (Bumbrah & Sharma, 2016). Upon interaction with the sample, the photons in the monochromatic light are absorbed and re-emitted with a change in their frequency (Lord, 1965; Princeton Instruments, 2018). The frequency of the re-emitted photons can be higher or lower than the frequency of the original monochromatic frequency and this change is referred to as the Raman effect or shift (Bumbrah & Sharma, 2016). This provides useful information on stress of molecules, molecular vibration, crystallinity, molecular rotation, orientation and other transitions in molecules which occur under low frequencies (Nanophoton, 2018). It must however be noted that Raman scattering is a very small percentage of scattering and is extremely weak (only one in 106-108 photons scatters (Le Pevelen & Tranter, 2017). The scattering of light by matter is largely an elastic process which is known as Rayleigh scattering and this process does not result in photon energy changes (Figure 46) (Bumbrah & Sharma, 2016; Le Pevelen & Tranter, 2017; Nanophoton, 2018). Raman spectroscopy is a powerful technique for structural investigation of carbon-based materials due to its sensitivity to the crystalline structures and molecular structures in amorphous matter (Le Pevelen & Tranter, 2017). The D and G peaks are the main features in Raman spectra of polyaromatic carbonaceous materials as highlighted in the work of Tuinstra & Koenig in 1970 (Buzgar *et al*., 2009; Ferralis, 2010). The bond stretching of all pairs of sp2 sites in hexagonal aromatic rings corresponds to the G peak. The D peak corresponds to the breathing modes of sp2 sites in rings and defects lead to the activation of the D peak (Le Pevelen & Tranter, 2017). There is a significant amount of experimental data which is available in literature with regards to the Raman spectra of carbonaceous materials. However, the focus of most of these research studies is on the Raman peak shapes and relative intensities and not on absolute intensities (Bumbrah & Sharma, 2016; Ferralis, 2010).

Some of the advantages of Raman spectroscopy include;

- High sensitivity to molecular vibration frequencies and chemical bonds
- Can be used for quantitative and qualitative analysis;
- Non-destructive technique;

- Requires no sample preparation;
- Analysis and measurement of organic and inorganic substances;
- Image analysis can be undertaken using a laser beam or scanning motorized stage;
- Fast analysis of samples (typically between 10 milliseconds to 1 second sample exposure) (Buzgar *et al*., 2009; Bumbrah & Sharma, 2016).
- Raman is the only technique than can identify the purity and physical state of elements such as carbon and sulphur (Lindon *et al*., 2016).

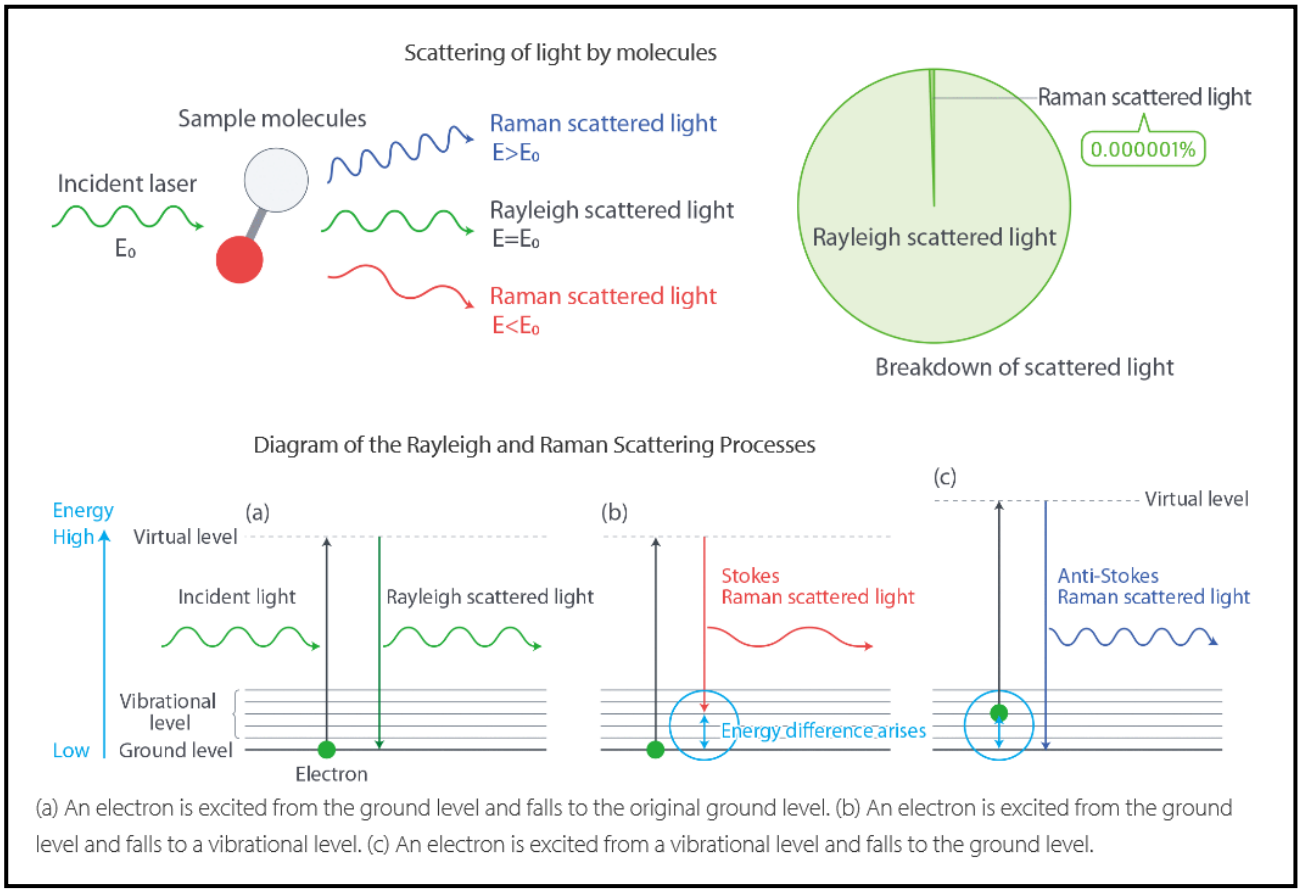

Figure 46: Scattering of light by molecules and the Rayleigh and Raman Scattering processes (Nanophoton, 2018).

However, the limitations of Raman Spectroscopy include the following;

- The Raman shift or effect is generally weak and this affects the detection limits of the technique. Highly sensitive and optimised instruments should therefore be used.
- Alloys or metals cannot be analysed using Raman Spectroscopy;
- Impurities that have fluoresced from the sample can interfere or cover the Raman spectrum (Princeton Instruments, 2018).

Raman Spectroscopy has been utilised for the characterisation of carbonaceous material, particularly coal and coal derived products in many studies (Potgieter-Vermaak *et al*., 2011). In most of these studies, the Raman spectrum of the graphite (G band- 1580- 1600 cm^{-1}) and defect bands (D band- 1340-1380 cm^{-1}) are used for the determination of coal structure, ranks and crystalline size of graphite (Manoj & Kunjomana, 2010 and Guedes *et al*., 2010).

2.5.6 Thermogravimetric Analysis (TGA)

Thermogravimetric analysis is a thermal analysis technique utilised in the measurement of the amount and rate of change in a material's weight as a function of temperature or time in a controlled environment or atmosphere (Wróblewski & Ceran, 2016). The controlled environment can be oxidizing, where oxygen is used during the analysis, or can be neutral where nitrogen or an inert gas such as argon is used (Johnson, 2010). The resultant mass variation is due to the chemical and physical changes in the sample that are driven by temperature and the controlled environment (ACTTR Technology, 2015). The change in sample weight is generally plotted as a function of time on a thermogram and interpretation of this information results in the understanding of chemical changes of the heated sample (Coats & Redfern, 1963; TA instruments, 2006).

In some samples, different degradation mechanisms may exist in the inert and oxidative environments (Johnson, 2010). Thus, the number of degradation steps and the temperatures at which the steps occur can be studied in different environments (Wróblewski & Ceran, 2016). The TGA measurements are mainly used for determining material composition and the prediction of thermal stability (Li, *et al*., 2005). It can be used as a complementary technique to microscopy for the identification of material or substances (Kwon & Vastola, 1995). The identification and measurement of vapours generated by the heating process can be undertaken through the coupling of TGA and mass spectroscopy (TGA-MS), TGA and Infrared Spectrometry (TG-IR) during TGA-TG-IR analysis and TGA with Gas Chromatography and Mass Spectrometry (TGA-GC/MS) (ACTTR Technology, 2015; Mohomed, 2016). In the latter, the gases are transferred to the GC for the purposes of material separation and peak identification using MS (Johnson, 2010). The TGA-GC/MS is a powerful combination due to its ability to detect very low levels of materials in complex mixtures (Johnson, 2010).

In the context of coal, TGA has been used for analysing coal and coal systems and to conduct proximate analysis for the determination of ash content (mineral fraction of coal or non-combustible portion of coal) (Li *et al.,* 2005). TGA has also been used for the purposes of rank classification of coal samples (Wróblewski & Ceran, 2016). The combustion of coal generally involves the combination of two significant processes i.e devolatilisation or pyrolysis due to thermal stress and heterogenous combustion of char according to carbon-oxygen reactions (Li *et al.,* 2005; Silva Filho & Milioli, 2008). The ignition rate is a critical factor during coal combustion, with high heating rates resulting in the evolution and ignition of volatiles while devolatilisation will occur prior to ignition and combustion during low heating rates (Kwon & Vastola, 1995). Different types of coal can be distinguished through their burning profiles (Silva Filho & Milioli, 2008).

Investigations on the application of TGA in the analysis of coal dust samples have been undertaken during various research studies, especially on respirable coal dust samples (Ceran, 2018; Scaggs *et al*., 2015). This is due to the association of respirable coal dust with occupational lung diseases such as coal workers' pneumoconiosis and silicosis (Scaggs *et al*., 2015). During the analysis of coal dust samples, the coal constituents are assumed to be totally degradable and oxidisable (Figure 47) (Mayoral *et al*., 2001; Scaggs *et al.,* 2015). It is also assumed that the mineral constituents will not degrade or react (except inorganic sulphur which is converted to SO_2) and that the residue at the end of the TGA analysis is the total mineral mass. TGA of dust samples can be treated as analogous to proximate analysis of bulk coal samples (Scaggs *et al*., 2015).

The advantages of TGA include the following:

- Various materials can be analysed using TGA and these include composite material, glasses, polymers and metals. The temperature ranges from 25°C to 1200°C (Anderson Materials Evaluation, 2018).
- Relatively small samples of 2 to 50milligrammes (mg) can be assessed using TGA;
- Variation in the value of kinetic parameters become evident as a single sample can be analysed over a whole range of temperatures;
- It is a relatively simple, precise and speedy method for analysing materials (Johnson, 2010).

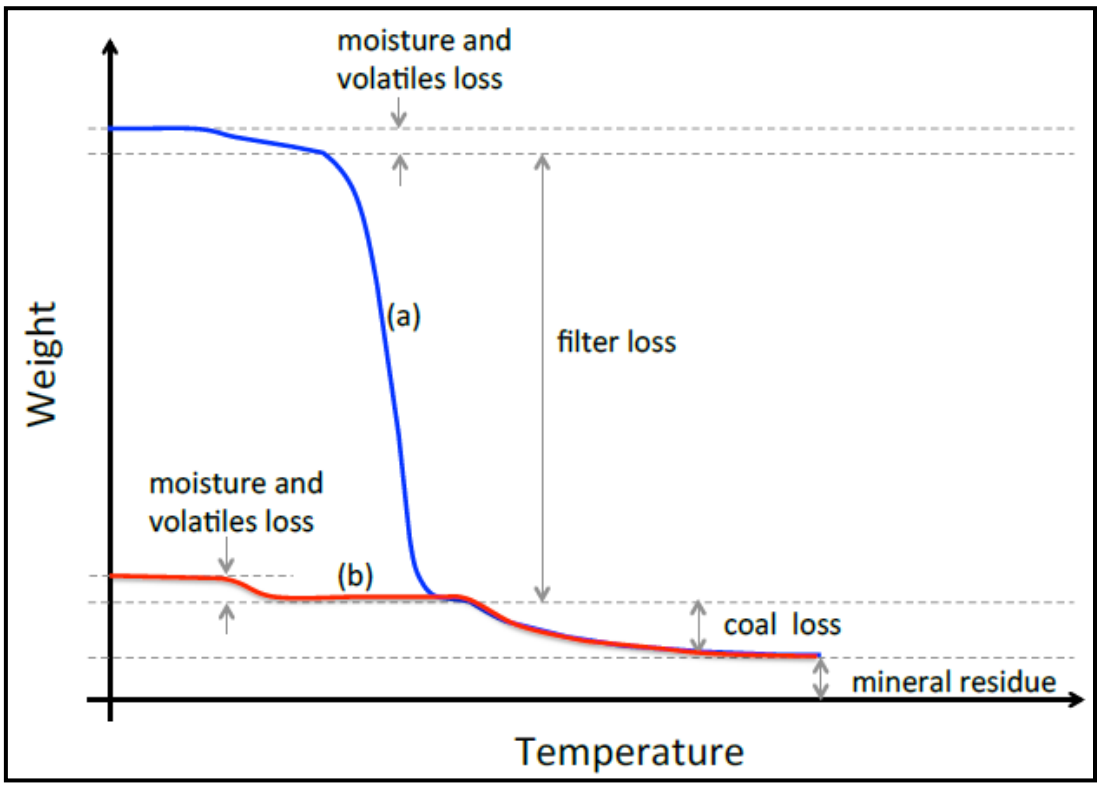

Figure 47: Hypothetical thermograms for (a) direct-on-filter, where total decomposition of the filter prior to coal oxidation is assumed and (b) dust only TGA of a respirable coal mine dust sample (Scaggs *et al*., 2015).

However, the limitations of TGA include the fact that substances or gases evolved during a specific weight loss event cannot be identified using this technique only (Scaggs *et al*., 2015). The identification process can only be undertaken when TGA is coupled with other techniques mentioned in the previous paragraph.

2.5.7 Isotope Ratio Mass Spectrometry (IRMS)

Isotope ratio mass spectrometry (IRMS) is a branch of mass spectrometry which involves the measurement of the abundance ratios of stable isotopes of elements (Dass, 2007). It is increasingly applied for the determination of information regarding the origin (geographic, biological and chemical) of substances in environmental science, forensics, agricultural science, geology, chemistry and planetary science based on the abundance of isotopes of elements found in the substance (Dass, 2007; Carter & Barwick, 2011; Savard *et al*., 2017; Muccio & Jackson, 2009). The technique enables the measurement of differences or variations (ratios) in the abundance of isotopes of light elements such as carbon (C) ($^{13}C/^{12}C$), hydrogen (H) ($^{2}H/^{1}H$), nitrogen (N) ($^{15}N/^{14}N$), sulphur (S) ($^{34}S/^{32}S$) and oxygen ($^{18}O/^{16}O$) (Dass, 2007; Marimon *et al.*, 2012). Carbon isotope analysis is a powerful tool for

source apportionment of organic substances (Walters *et al*., 2015). This is attributed to specific isotopic signatures linked to different anthropogenic and natural sources which include fossil fuels, marine sources and continental sources such as terrestrial plants (Ceburnis *et al.*, 2016). The isotopic composition of substances can vary due to biological, chemical and physical processes such as thermodynamic, equilibrium isotope and kinetic effects, which result in isotopic fractionation (de Groot, 2004; Muccio & Jackson, 2009). Isotope ratios are generally measured relative to an isotopic standard for the purposes of eliminating systematic errors and bias in the measurements (Muccio & Jackson, 2009). These standards include the National Institute of Standards and Technology (NIST-Washington DC, United States of America (USA) and the International Atomic Energy Agency (IAEA- Vienna, Austria), which supply various natural abundance standards (Berto *et al*., 2019). Isotope ratios of substances are generally measured relative to universal standards and are reported in the delta notation (δ) (Berto *et al*., 2019; Muccio & Jackson, 2009).

$$\delta=1000(R_{sample}-R_{standard})/R_{standard}$$

The R_{sample} value is the abundance ratio of the minor, heavier isotope of the element to the major, lighter isotope (Berto *et al*., 2019). Samples which establish the $R_{standard}$ values are usually selected because they represent a stable material which is highly enriched in the heavy (minor) isotopes (McSween *et al.,* 2003; Muccio and Jackson, 2009). Most analysed substances are depleted in the heavy-isotope relative to the standard and will therefore have negative δ values (Muccio & Jackson, 2009). A typical IRMS instrument consists of a system for sample introduction, electron ionisation source, collector detector array (mostly Faraday cup detection system), magnetic analyser and a data acquisition system which is computer controlled (Carter & Barwick, 2011; McSween *et al.,* 2003; Muccio & Jackson, 2009). The instrument configurations commonly applied for gas source IRMS include continuous flow IRMS (CF-IRMS) and dual inlet IRMS (DI-IRMS) (Pratt *et al.*, 2011). Sample introduction into the IRMS is generally undertaken through the application of techniques such as gas chromatograph (GC) (GC-IRMS) and elemental analysers (EA) (EA-IRMS) (Figure 48) (Muccio & Jackson, 2009; Pratt *et al.*, 2011).

2.5.7.1 Elemental Analysers (EA-IRMS)

Elemental analysers are commonly used for continuous flow systems and no prior separation of sample constituents is undertaken (Major *et al*., 2017). The bulk sample (liquid or solid) is normally weighed and placed in a silver or tin capsule which is introduced into a combustion furnace with high temperatures to form different oxides (Major *et al*., 2017; Pratt *et al.*, 2011). The analysis of C and N will typically include sample combustion in an O_2 atmosphere resulting in the formation of CO_2 and NO_x (Berto *et al*., 2019; Major *et al*., 2017). Water is removed from the analyte through a chemical trap (de Groot *et al*., 2004). The analyte is transported by a helium (He) gas stream into a reduction chamber where NO_x is converted into N_2 and the removal of excess O_2 is undertaken (de Groot *et al*., 2004). The N_2 and CO_2 are then separated in the gas chromatograph and the effluent from the EA is transferred to the IRMS (Figure 48) (de Groot *et al*., 2004; Muccio and Jackson, 2009). The next step is the introduction of evolved gases into the electron ionisation source which results in the formation of ionisation gas molecules (Pratt *et al.*, 2012). This process is followed by separation and ion detection in the mass spectrometer and finally by the evaluation of the raw data (Figure 49) (Muccio & Jackson, 2009).

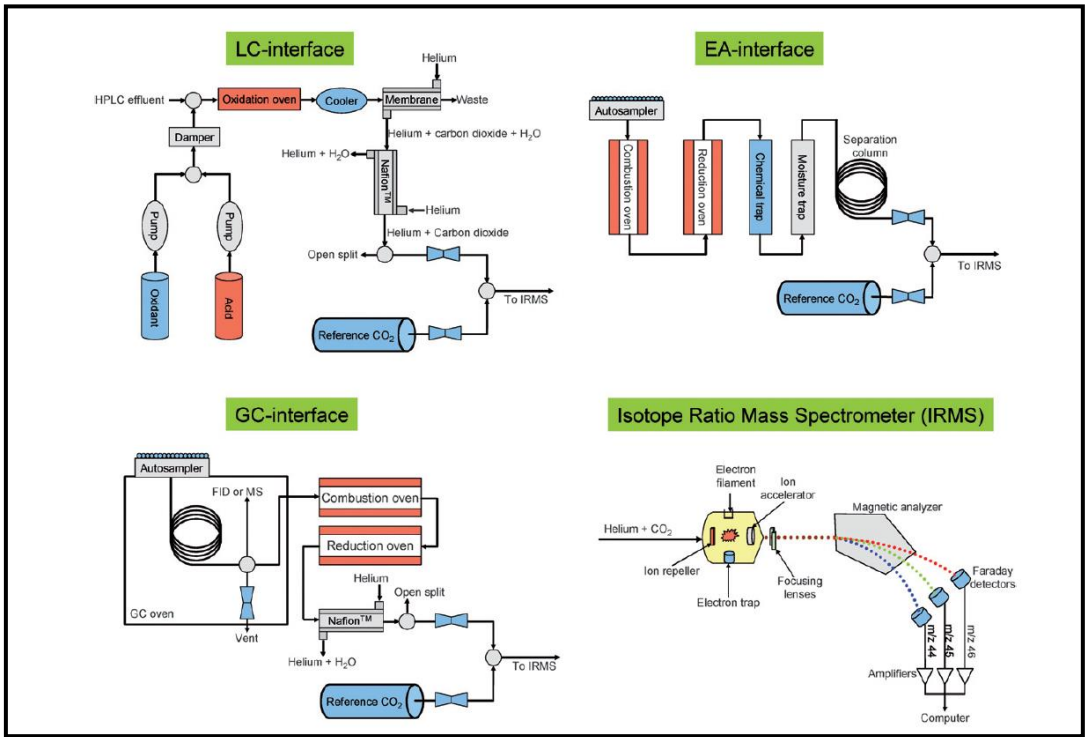

Figure 48: Schematic on the three most common techniques for sample introduction for carbon isotope measurements (LC- liquid chromatography, EA- elemental analyser and GC- gas chromatography (Muccio and Jackson, 2009).

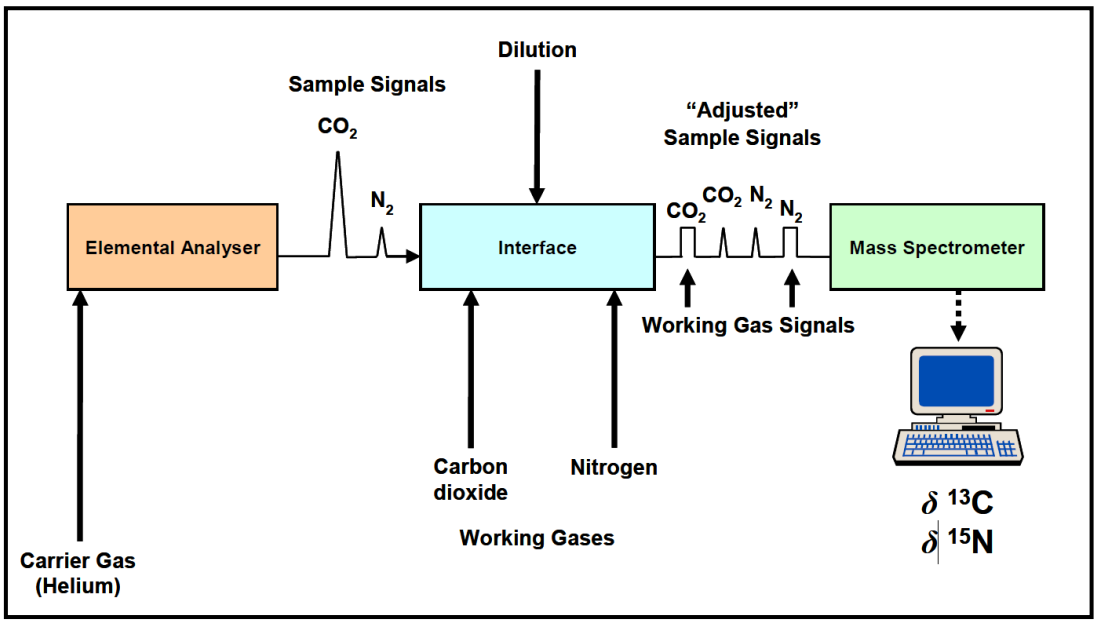

Figure 49: Simplified schematic process flow for the determination of $\delta^{13}C$ and $\delta^{15}N$ (Muccio and Jackson, 2009).

2.5.7.2 Application of IRMS in Air Pollution Studies

Atmospheric PM contains carbonaceous aerosols originating from diverse sources, particularly in highly industrialised regions such as the Highveld Priority Area in South Africa. IRMS can be used for carbon source apportionment. Carbon isotope fingerprint analysis is applied in the identification of fossil fuel sources which include diesel emissions from vehicles and coal (Zhang *et al.*, 2007). Carbon isotope ratios ($\delta^{13}C$) range from -19‰ to -35‰, indicating that the origin of fossil fuels can be identified, although some overlaps occur (Brodie *et al*., 2018; Cao et al., 2007; Dai *et al.*, 2015; Kunwar *et al.*, 2016; Masalaite *et al.*, 2012). Vehicle emissions are in the range of -25‰ to -28‰ (Dai *et al.*, 2015; Kunwar *et al.*, 2016; Masalaite *et al.*, 2012). Other sources of carbonaceous aerosols include biomass burning. Recent studies have indicated significant differences in the $\delta^{13}C$ of fossil and non-fossil fuel burning atmospheric PM with the values recorded as 24.5‰ for coal and 28‰ for liquid fossil fuel (Garbaras *et al.*, 2015; Górka *et al.*, 2009). These differences enable the identification and differentiation of specific atmospheric PM sources. Fossil fuel combustion and other anthropogenic activities are also sources of nitrogen compounds such as NO_x. Stable isotope nitrogen ratios can be used to differentiate these sources (^{14}N and ^{15}N) (Pavuluri *et al*., 2011; Walters *et al*., 2015).

2.5.8 Thermal Optical Techniques for Differentiating Brown/Organic Carbon and Elemental Carbon

The differentiation between OC and EC can also be achieved through other techniques which include modern light absorbing techniques (Figure 50) (Poschl, 2003). These techniques involve the use of a laser beam of a specific wavelength, through a particulate matter sample (Liousse *et al*., 1993). This can be undertaken on filter substrate or in air. Observations are made on the quantity of light absorbed by the particulates (Andreae & Gelencer, 2006). Generally, EC is measured over the green to infrared wavelengths because this type of carbon shows stronger absorption there (Andreae & Gelencer, 2006; Liousse *et al*., 1993).

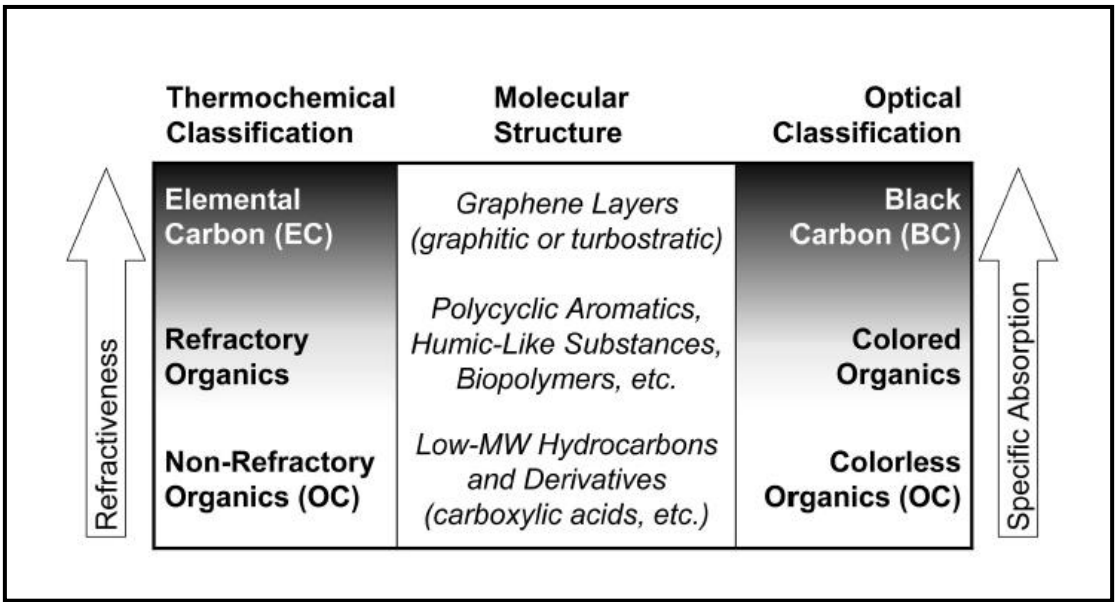

Figure 50: Classification and molecular structure of carbonaceous aerosol components (Poschl, 2003).

The absorption of light by EC is attributed to electrons within the graphite structure. Brown carbon or OC absorbs light closer to the UV range (Poschl, 2003). However, for the differentiation of OC and EC, instruments which measure light absorption by carbonaceous material over a range of the UV or visible spectrum are advisable (Liousse *et al*., 1993). The light absorption measurements for each category, i.e, EC or OC, can be converted to mass concentration through the application of conversion factors or mass absorption coefficients (Schimd *et al*., 2001). Estimates by Liousse *et al* (1993) indicate that the mass absorption efficiency of elemental carbon ranges from 2 to 20 m^2/g. Incident light wavelength has a major influence on particle light absorption (Liousse *et al*., 1993).

Other techniques, as described by Andreae & Gelencer (2006) also include thermal-optical techniques which distinguish between refractory and non-refractory carbonaceous components of atmospheric PM as EC and BC/OC (Figure 51) (Hemby *et al*., 2012).

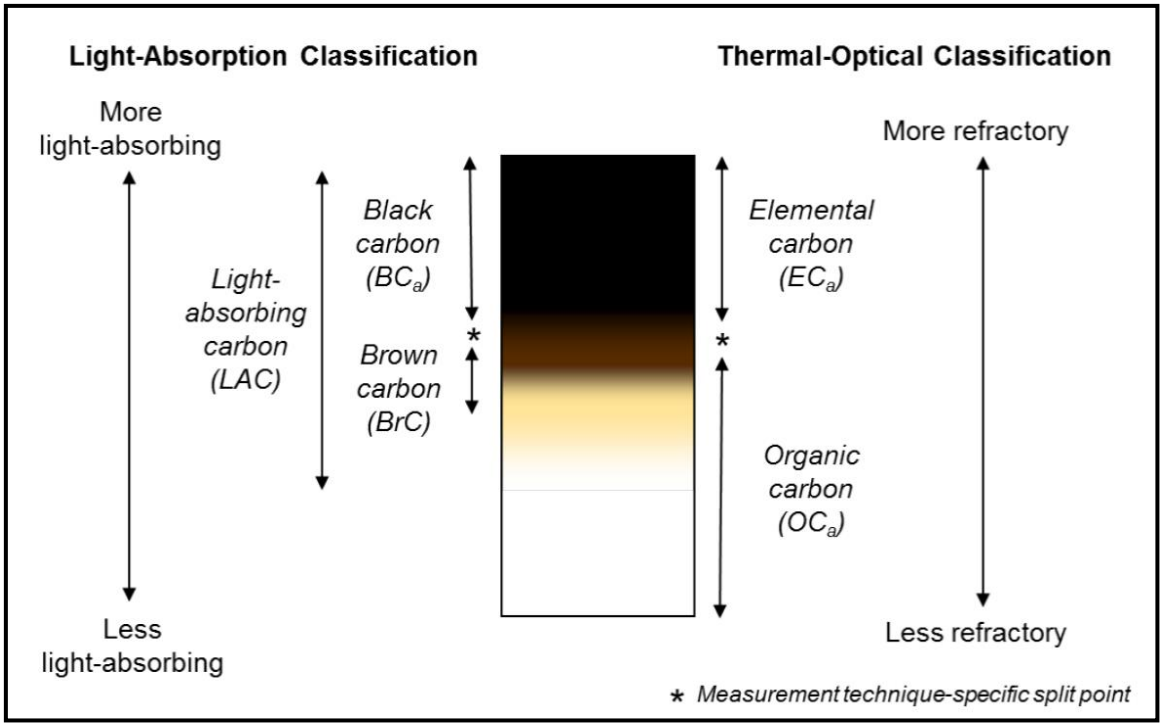

Figure 51: Measurement of the carbonaceous components of particles (Hemby *et al*., 2012).

Thermal optical techniques include the direct measurement of EC and OC through the application of thermal evolution methods (thermal/optical transmission (TOT) and/or thermal/optical reflectance (TOR) (Hemby *et al*., 2012; Schmid *et al*., 2001). These techniques employ different temperatures and atmospheric conditions during analysis for the evaporation, pyrolysis and combustion of carbon-containing material or compounds on a filter paper (usually quartz) (Chow *et al*., 1993; Desert Research Institute, 2019). They also enable the monitoring of the conversion of OC to EC and the quantification of the amount of carbon that is released from the filter at varying or different temperatures (Currie *et al*., 2002; Watson *et al.*, 2005). A number of these methods employ two different temperatures which define the carbon evolved below 580°C as OC and that which is evolved at temperatures above 650°C to 1100°C as EC (Birch & Cary, 1996; Turpin *et al*., 1990; Watson *et al*., 2005). In some of the methods, higher OC temperatures are applied in an atmosphere that is non-oxidizing, after which OC is assumed to have been removed from the sample (Chow *et al*., 1993; Watson *et al.*, 2005). Other techniques employ lower OC

temperatures in an oxidising atmosphere, with the assumption that the combustion rate of EC is lower under these conditions (Currie *et al*., 2002; Watson *et al.*, 2005). The CO_2 evolved from the process is then detected directly or reduced to CH_4 for sensitive detection (Desert Research Institute, 2019). The partitioning of EC and OC, therefore, occurs with the assumptions that the evolution of charred OC occurs before EC that was originally in the sample and that attenuation and transmittance is equal for charred OC and original OC (Yu *et al.*, 2002).

The most commonly applied thermal optical techniques for measuring OC and EC in atmospheric PM include those of the National Institute for Occupational Safety and Health (NIOSH) in the US (Chow *et al*., 1993), the US Interagency Monitoring of Protected Visual Environments (IMPROVE) (Birch & Cary, 1996) and the European Supersites for Atmospheric Aerosol Research (EUSAAR) (Cavalli *et al*., 2010). Although these protocols show good agreement in total carbon (TC) concentrations, they indicate differences in the concentrations of OC and EC and do not fully address or characterise interferences by carbonate (Cavalli *et al*., 2016).

For the NIOSH protocol, the thermal part of the process involves temperature increases from ambient to 580°C in a non-oxidising Helium (He) atmosphere (Desert Research Institute, 2019). The volatilisation of organic compounds (charring) from the filter occurs and EC remains unoxidized (Chow *et al*., 1993; Desert Research Institute, 2019). The addition of oxygen to helium at temperatures higher than 580°C results in the combustion of EC and the evolved gases enter the sample stream, where they pass through a bed of heated manganese dioxide (MnO_2), resulting in their oxidation to CO_2 (Currie *et al*., 2002). The evolved gases then pass through a heated nickel (Ni) catalyst, resulting in the reduction of CO_2 to CH_4 (Desert Research Institute, 2019). The quantification of methane is undertaken through a flame ionisation detector (FID) while the monitoring of reflected laser light is done continuously during the analysis cycle (Desert Research Institute, 2019). The degree of pyrolytic conversion from OC to EC is accounted for by the negative change in reflectance which takes place during OC analysis (Desert Research Institute, 2019). The introduction of O_2 results in an increase in reflectance due to the burning of light absorbing carbon off the filter (Currie *et al*., 2002). Therefore, EC is classified as carbon which attains the reflectance value it had at the beginning of the analysis cycle (Turpin *et al*., 1990; Watson *et al*., 2005).

This pyrolysis adjustment process is critical and can be as high as 25% of EC or OC (Chow *et al*., 1993; Desert Research Institute, 2019). A typical thermogram for thermal optical analysis of carbonaceous material is shown in Figure 52 below.

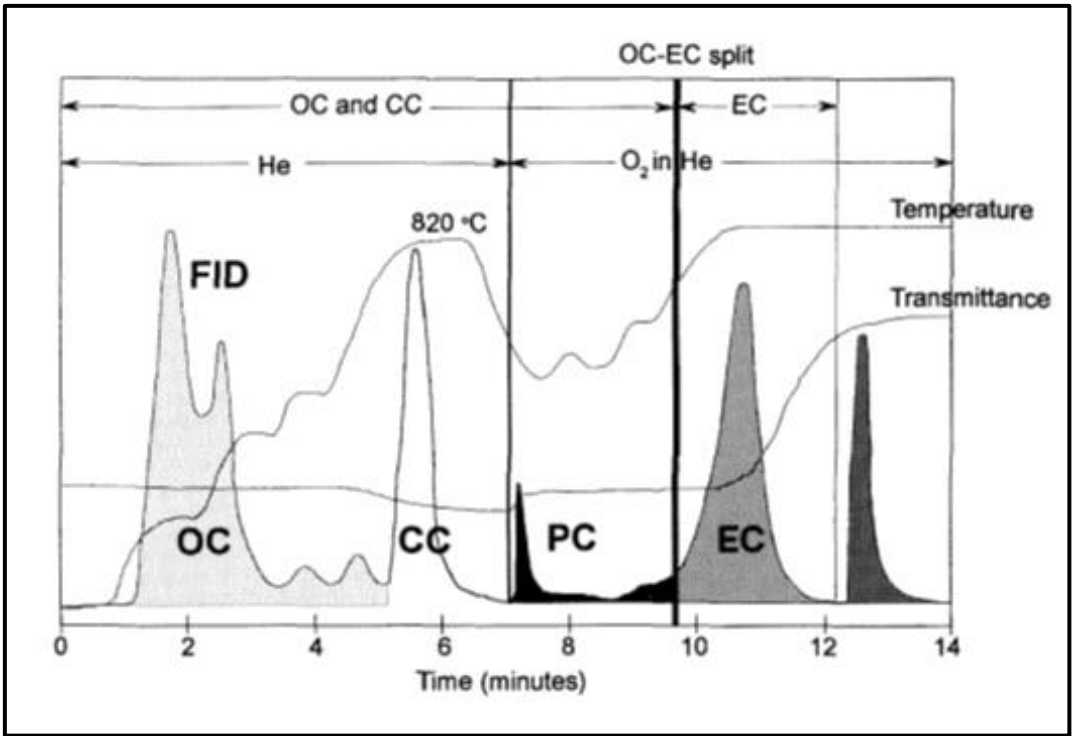

Figure 52: Thermogram for carbonaceous material (rock dust consisting of carbonate) and diesel exhaust (Birch & Cary, 1996).

There are critical factors which determine the successful application of thermal-optical techniques. For example, the rate of material evaporation is dependent on filter handling and storage between the sampling campaign and analysis (Hemby *et al*., 2012). Quartz fibre filters are generally used for thermal-optical carbon analysis and present a problem as they absorb some of the organic vapours (Poschl, 2003). In some cases, the misinterpretation of these gas vapours as OC or EC (if the organic carbon is charred) often occurs. For the prevention of the misinterpretation of charred organic substances as elemental carbon, laser correction measurements are employed (Chen *et al.*, 2004; Poschl, 2003). Many of the thermal-optical methods that have been applied for the purposes of estimating EC, OC and total carbon (TC), result in different concentrations for OC and EC. These concentrations are defined by the method rather than by an absolute standard (Watson *et al*., 2005). The methods differ with respect to factors such as catalysts employed for the oxidation and reduction processes, charring correction, analysis atmospheres, temperature ramping up

rates, methodologies for the detection of evolved carbon, carrier gas flow, optical pyrolysis monitoring, etc., (Chen *et al.*, 2004).

Complexities during the thermal optical characterisation of atmospheric PM may arise due to different compositions and structures of carbonaceous material from different sources (Chow & Watson, 2002). In addition, although CC is generally found in low quantities in some atmospheric PM samples, it is rarely compared to the EC content (Cao *et al*., 2004; Chow & Watson, 2002; Watson *et al*., 2005). Some components of OC may also absorb light in the visible spectrum and therefore can be classified as EC (Chow & Watson, 2002). There may be differences in the absorption and scattering properties of atmospheric PM particulates on the filter and atmosphere (Horvath, 1993), or changes in collected particles during extraction from the atmosphere onto the quartz filter (Watson *et al*., 2005). In addition, the rate of evaporation of the material is dependent on filter handling and storage between sampling and analysis (Horvath, 1993). Quartz fibre filters tend to absorb organic vapours which are then interpreted as OC or a portion of EC, depending on whether the OC has undergone charring or not (Watson *et al*., 2005).

2.6 ATMOSPHERIC PARTICULATE MATTER MONITORING

Given the health and environmental impacts of atmospheric PM, monitoring becomes crucial (Garland *et al*., 2017; Wu *et al*., 2017). Monitoring of atmospheric PM provides information which is useful for the determination of concentration levels (Wichmann, 2017). Most research studies on atmospheric PM have demonstrated the importance of separately monitoring the components of PM based on size i.e fine and coarse particulates (Wu *et al*., 2017). This is evident in studies undertaken in the fields of epidemiology, environment, chemistry and toxicology (Assael *et al*., 2010). Two methods are currently used for the measurement of atmospheric PM concentration and these are passive and active monitoring (Huertas *et al*., 2012).

2.6.1 Active Sampling

Active methods are the most common method of atmospheric PM monitoring due to reliability of the results and low uncertainty (Assael *et al*., 2010). The principle of active atmospheric PM monitoring is based on drawing a volume of air into the monitor using a

pump or suction and the measurement of atmospheric PM entrained in this volume of air (Snyder, 2013; Stern *et al*., 1994, Turpin *et al*., 1994). Other active methods of monitoring include beta attenuation monitoring (BAM), gravimetric, oscillating element and light scattering methods (Snyder, 2013; Stern *et al*., 1994; USEPA, 2009).

In South Africa, active ambient monitoring stations are largely owned by the Department of Environmental Affairs and most of these stations are in air quality management priority areas (Figure 53) (DEA, 2011; DEA, 2017; Garland *et al*., 2017).

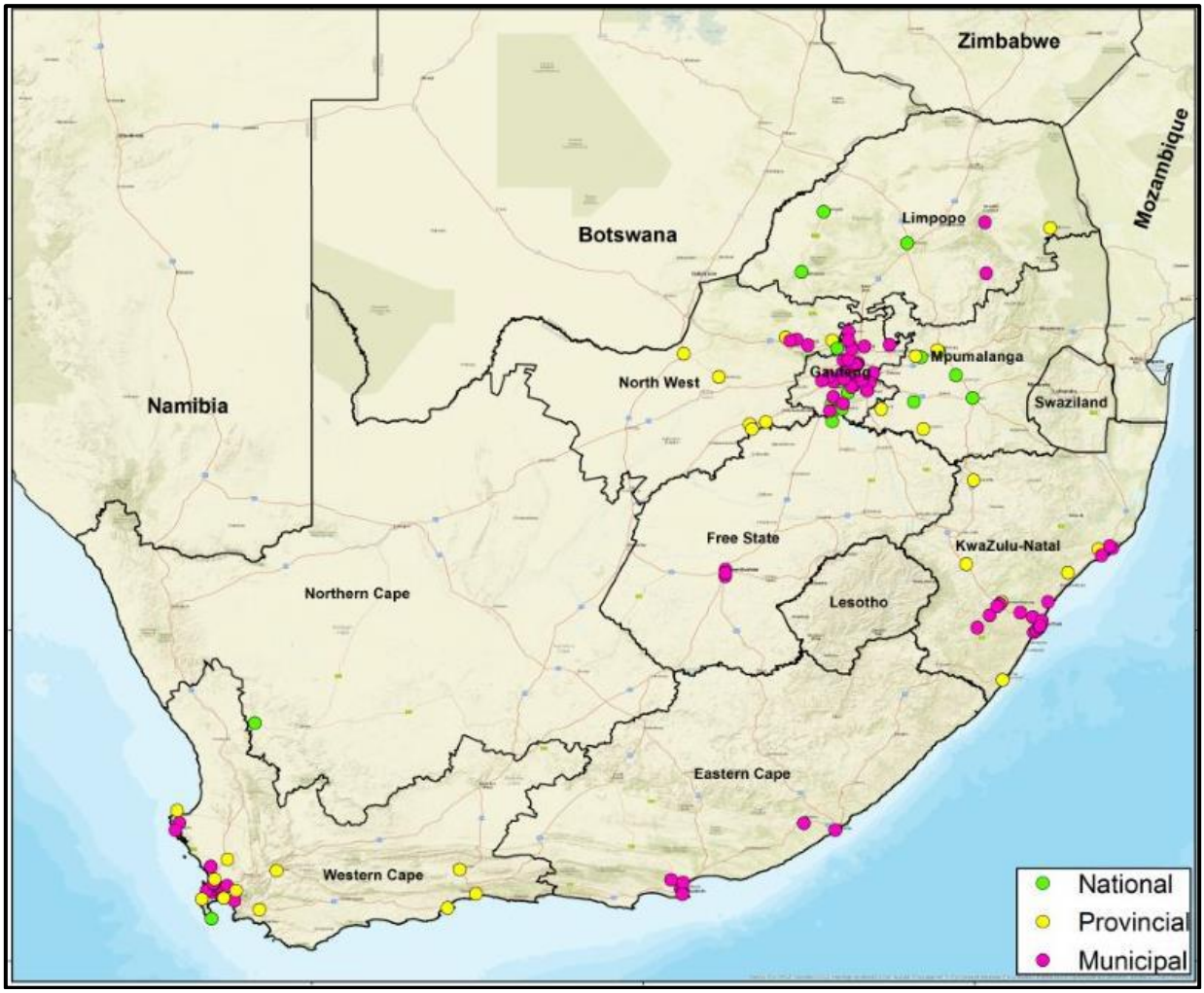

Figure 53: National Ambient Air Quality Monitoring Network (DEA, 2017).

The data obtained from these stations is useful for compliance and health risks assessments. The main problem is the limited number of ambient monitoring stations, especially for atmospheric PM, for the overall representation of the air quality problems across various parts of the country (Wichmann, 2017). This is a common occurrence in

developing countries due to various reasons. The reasons include more pressing socio-economic factors and lack of resources to purchase expensive active monitors used for real time detection of air pollutant mass concentrations (Engel-Cox *et al*., 2013; Huertas *et al*., 2012; Panyacosit, 2000). This is exacerbated by the fact that developing countries are currently experiencing high levels of air pollution due to developmental and economic pressures and are in dire need of ambient air quality monitoring to inform health risk assessments and environmental management decision making processes (Garland *et al*., 2017; Laskin *et al*., 2012). In addition, a limited number of samplers may not provide adequate exposure information for outlying regions (Liu *et al*., 1995). A sizeable number of samplers are normally required for the investigation of the relationship between outdoor and indoor pollution (Suh *et al*., 1992). If active monitors are used for such campaigns, then the costs will be exorbitant (Assael *et al*., 2009).

2.6.2 Passive Sampling

Passive samplers have been used for the purposes of air quality monitoring for long periods of years and this is due to lower costs associated with these samplers compared to active monitors (Brown, 1993; Brown *et al*., 1996). Various passive samplers have been designed over the years and these include a small passive sampler for particulate or aerosol sampling (Figure 54) (Wagner & Leith, 2001a). The passive sampler is exposed to the environment for periods ranging from hours to weeks, for the purposes of monitoring ambient aerosols, indoor air quality and occupational pollutants (Brown, 1993).

The sampler is easy to operate and after sampling has been completed, samples can be assessed using techniques such as SEM and automated image analysis (Wagner & Leith, 2001b). It is made either from aluminum or carbon, with the former being commonly used for size distribution analysis due to the high conductivity of aluminum (Brown *et al*., 1996). If the objective is to undertake an elemental analysis, then carbon-based samplers are the preferable option as they cause less interference with the elemental spectra if SEM-EDS is used (Figure 54) (Wagner & Leith, 2001b). Mesh caps or covers are put on the sampler during sampling and can be removed afterwards for sample analysis (Wagner & Leith, 2001b). The mesh cover restricts the deposition of large particles on the sampler's collection surface, but also restricts the collection of smaller particles which may diffuse or be intercepted (Wagner & Leith, 2001c) and must therefore be compensated for in calculating

concentration from the number of particles collected. The mesh used by these authors has holes of conical cross section and dimensions of a top diameter of 160 µm and a bottom diameter of 225 µm. The collection region of the sampler is 1.2 mm in depth and has a diameter of 6.8 mm and the mesh is 127 µm thick (Wagner & Leith, 2001b). Thin aluminum tape is placed at the base of the collection region of the sampler to minimise microscopic imperfections and interference. The deposition mechanisms for the particles into the sampler include gravitational settling, convective diffusion and inertia (Figure 55) (Wagner & Leith, 2001b).

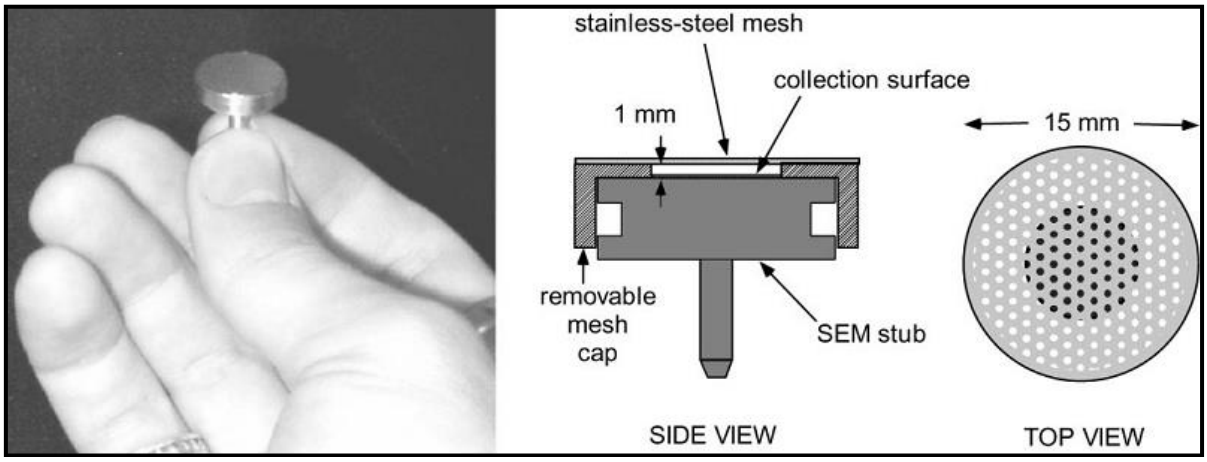

Figure 54: Passive sampler design (Wagner & Leith, 2001b).

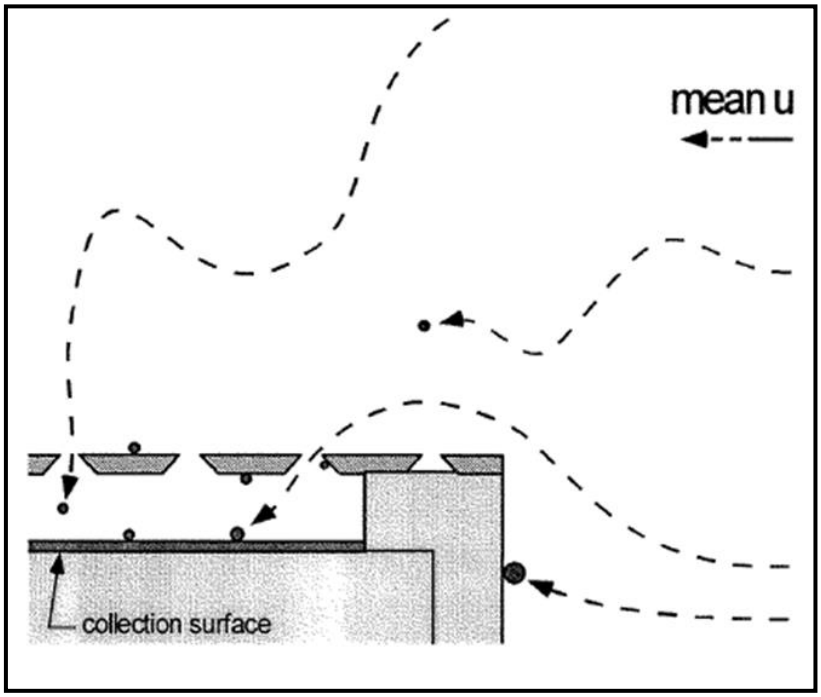

Figure 55: Schematic of deposition into passive sampler (with horizontal mean wind velocity, *u*) (Wagner & Leith, 2001b).

Locally developed (South Africa) passive samplers were manufactured by Mukota & Kornelius (2017) using a locally produced mesh with untapered holes with a diameter of 200 µm (Figure 56), and this was used in the present study.

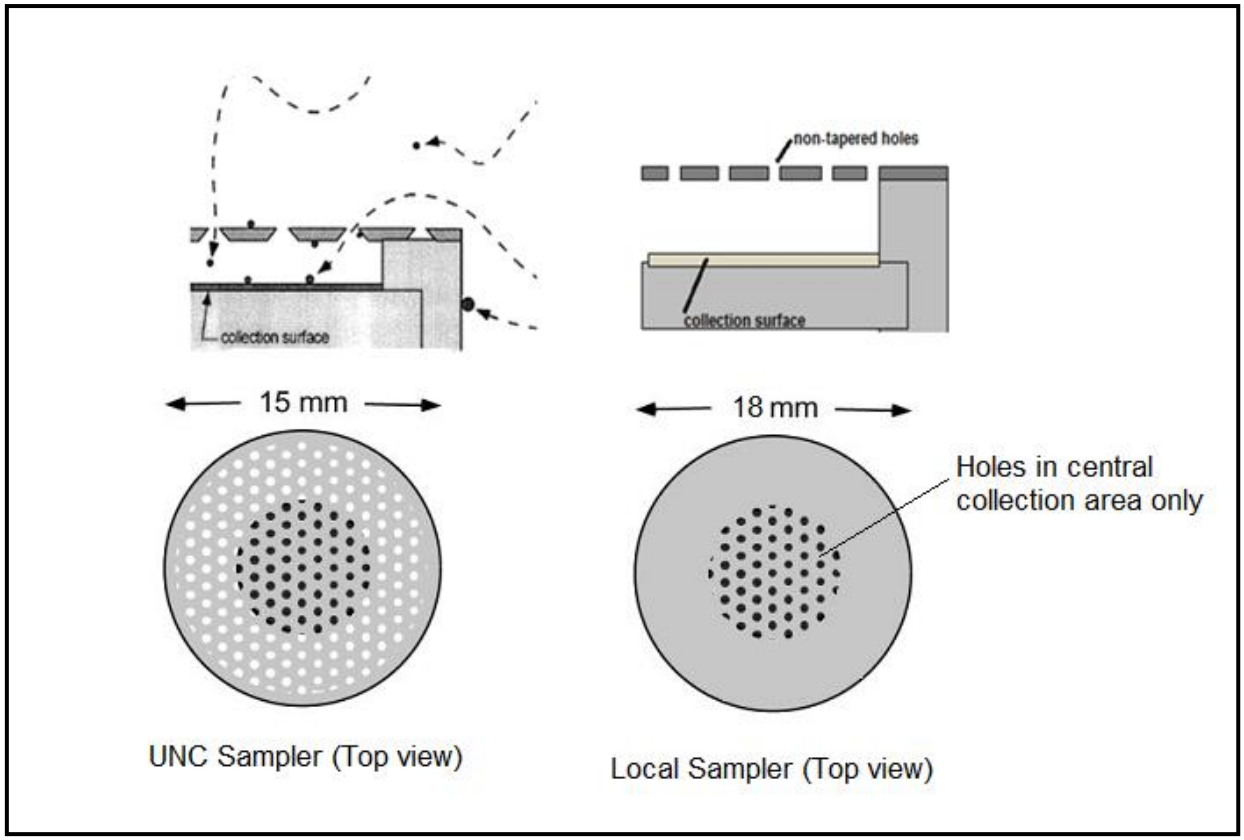

Figure 56: UNC passive sampler and locally developed SA sampler (Wagner & Leith, 2001; Mukota & Kornelius, 2017).

3 METHODOLOGY

3.1 Introduction

Particulate size and concentration are characteristics that have long been used for the characterisation of atmospheric PM. This has enabled the description of its multimodal nature i.e. coarse, fine and ultrafine particulates, which are emitted by various anthropogenic sources and natural sources (Ramirez-Leal *et al*., 2014). Developments in electron microscopy and other technical fields have enabled the comprehensive characterisation of individual particles. The electron microscopy and spectroscopic techniques that have been pivotal in the identification and characterisation of atmospheric PM include SEM-EDS, reflectance, optical microscopy, Raman, XPS and IRMS. Non-microscopic and non-spectroscopic techniques which have been applied for the characterisation of atmospheric PM include TGA and thermal optical analysis. These have also been employed in this study for the characterisation of atmospheric PM from opencast coal mines and adjacent communities.

3.1.1 Selection of Study Areas

The research study includes randomly selected PM 'hotspots areas' characterised by coal mining activities in the Highveld Priority Area and Waterberg-Bojanala Priority Area. 3 opencast coal mines and 3 community areas located adjacent to these mines were selected for the study. The residential areas selected in the Mpumalanga Province include Clewer near Emalahleni and Delpark in Delmas, both in proximity to coal mines. In Limpopo Province, the mining area near Lephalale and the adjacent residential area of Marapong were selected for the study (Figure 57). The selected areas in the Mpumalanga Province have a high concentration of coal mining activities, particularly in Emalahleni. During the selection of the study areas, existing and potential sources of emissions were considered as these would have an impact on the type, size and nature of atmospheric PM that will be sampled during the research study. The identified sources of emissions in both the Mpumalanga and Limpopo study areas include power generation activities and other industrial sources of emissions, domestic fuel burning and clay brick manufacturing. Other considerations for the study areas included security of monitoring equipment, accessibility and prevailing wind direction.

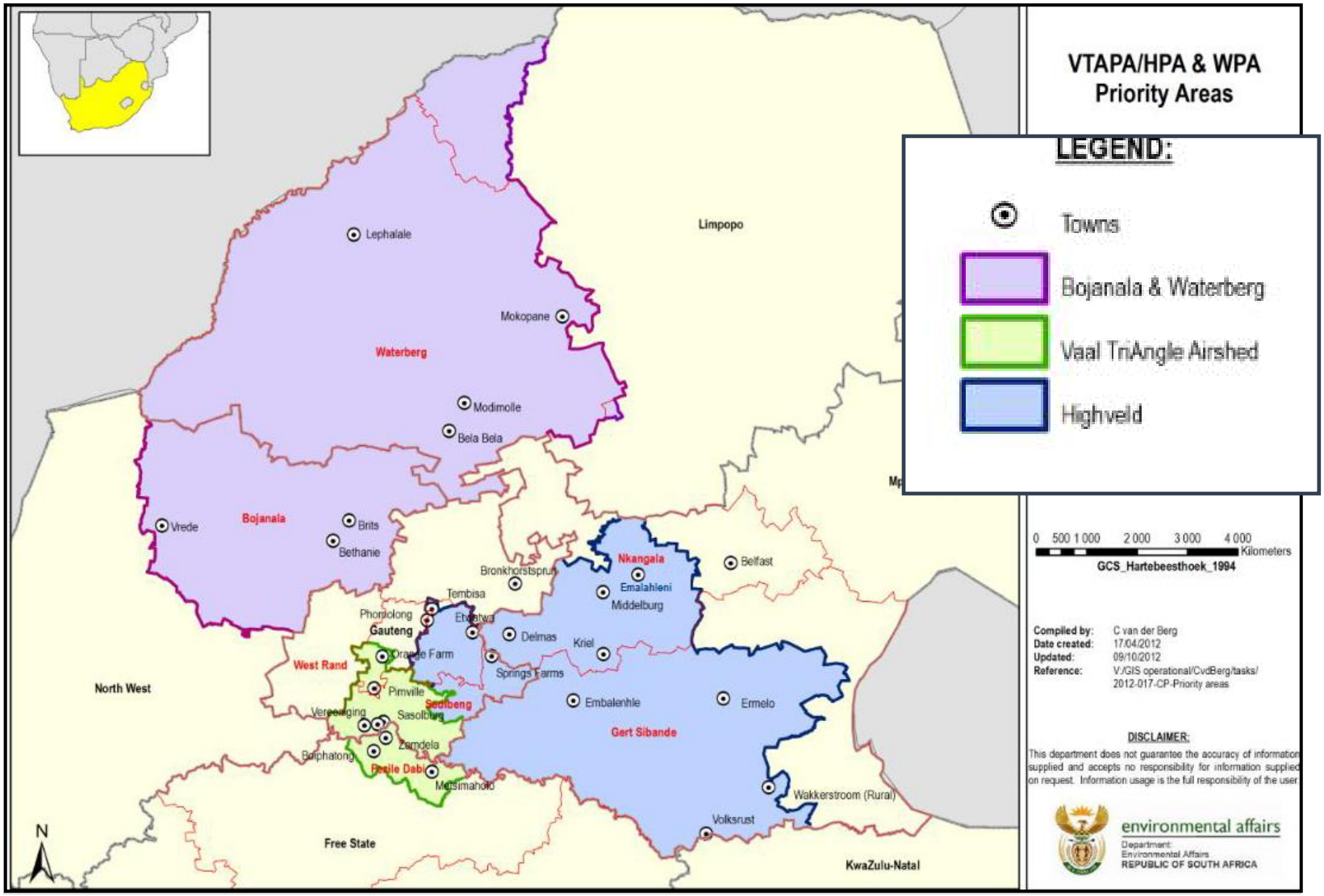

Figure 57: Location of Emalahleni, Delmas and Lephalale within the HPA and WBPA (DEA, 2017).

Meteorological data for the assessment of site dispersion potential and generation of wind roses was obtained from Windfinder for the South Africa Weather Services Stations located in Emalahleni and Lephalale for the period 2011- 2018. Meteorological data for 2011-2018 for Delmas was obtained from the Fifth-Generation Penn State/NCAR Mesoscale Model (MM5), a regional mesoscale model used for creating weather forecasts and climate projections, due to the lack of a weather station in the area during the time of study. The locations of some of the study areas and meteorological stations are shown in Table 9 below.

Table 9: GPS locations for the selected study areas

Study Area	GPS Coordinate of Study Area	
	Latitude	Longitude
Delpark (Delmas)	26° 8'28.84"S	28°41'36.75"E
Clewer (Emalahleni)	25°54'25.47"S	29° 8'10.56"E
Marapong (Lephalale)	23°39'23.03"S	27°37'44.34"E
Emalahleni Weather Services Station	25°49'59.45"S	29°11'25.50"E
Lephalale Weather Services Station	23°40'35.81"S	27°42'15.53"E
Delmas MM5 Data Point	26° 8'38.95"S	28°40'29.44"E

3.1.2 Study Area Description: Delmas

Delmas is a small town located in the Mpumalanga Province, South Africa. The town is well known for agricultural activities, particularly maize farming. Delmas is considered a PM 'hot spot' area due to poor ambient air quality and general exceedances of ambient PM_{10} NAAQS. Sources of emissions in Delmas include industries, agriculture, domestic fuel burning, coal mining activities, vehicle emissions and open burning of waste (Figure 58) (DEA, 2011). Sensitive receptor areas in the town of Delmas include Delpark residential area, which is located approximately 1.5 km to the north east of Delmas. Atmospheric PM monitoring was undertaken in this residential area.

The site dispersion potential of an area is generally governed by meteorological characteristics or mechanisms (Shenfield, 1970; Tyson & Preston-Whyte, 2002). These characteristics determine pollutant dispersion, atmospheric transformation and atmospheric

removal of pollutants. In addition, the wind field largely determines the vertical dispersion of pollutants. The dilution of pollutants, pollutant dispersion and mechanical turbulence are largely determined by wind speed in area (Shenfield, 1970). The wind field in Delmas for the period 2011 to 2018 is largely characterised by north, north westerly and easterly winds (Figure 58). The dispersion of the pollution plume is expected to occur in the westerly, south westerly and southerly direction. Opencast Coal Mine 2 in Mpumalanga is located approximately 6 km to the south east of the MM5 meteorological data point in Delmas, while the community of Delpark is located approximately 2 km north east of the MM5 data point.

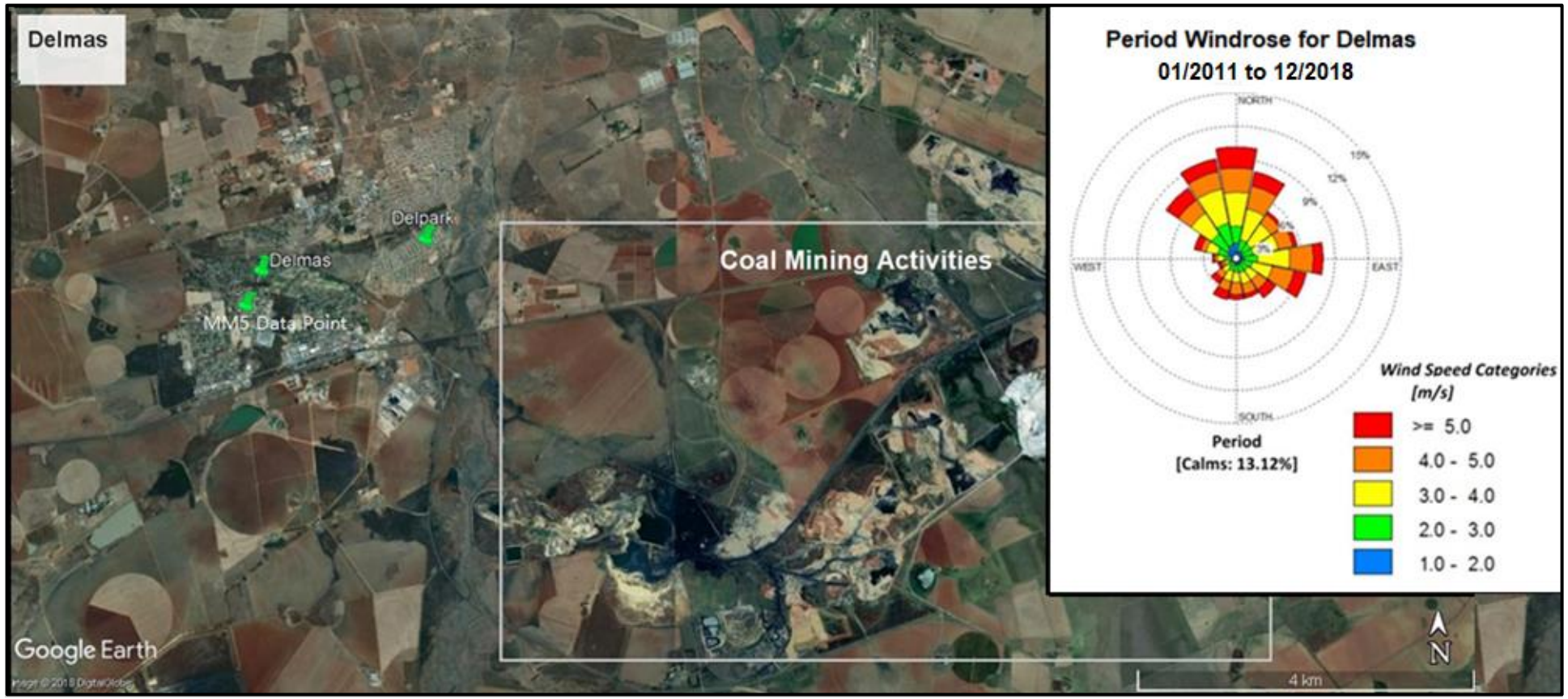

Figure 58: Location of Delpark relative to opencast coal mining activities in Delmas, Mpumalanga (Google Earth, 2018).

3.1.3 Study Area Description: Emalahleni

Emalahleni is a town located in the Highveld region of the Mpumalanga Province. The town is well known as the centre of coal mining, power generation and other industrial activities in South Africa (Figure 59). Air pollution problems have long plagued the town and the Highveld region, resulting in growing public concern. Emalahleni is considered an atmospheric PM hotspot area due to exceedances of National Ambient Air Quality Standards (NAAQS) for various criteria pollutants including atmospheric PM. Sources of emissions include domestic fuel burning, industrial sources such as primary and secondary metallurgical processes, power generation, coal mining, vehicle emissions and agricultural activities (DEA, 2011). The residential area of Clewer is located approximately 10 km to the south west of Emalahleni and is located adjacent to coal mining operations, a rail siding, agricultural activities and provincial roads (Figure 60).

The wind rose for Emalahleni for the period December 2011 to September 2018, based on Windfinder data for the Emalahleni Weather Station is shown in Figure 60. The community of Clewer is located approximately 10 km to the south west of the Emalahleni weather station while Opencast Coal Mine 3 in Mpumalanga is located approximately 8 km north east of the weather station. Predominant winds during this period were from the north, north west and west directions. Predominant winds generally determine the site dispersion potential and pollutant transportation to sensitive receptors and other areas. It is expected that the pollution plumes will travel towards the south, south easterly and easterly directions in the area.

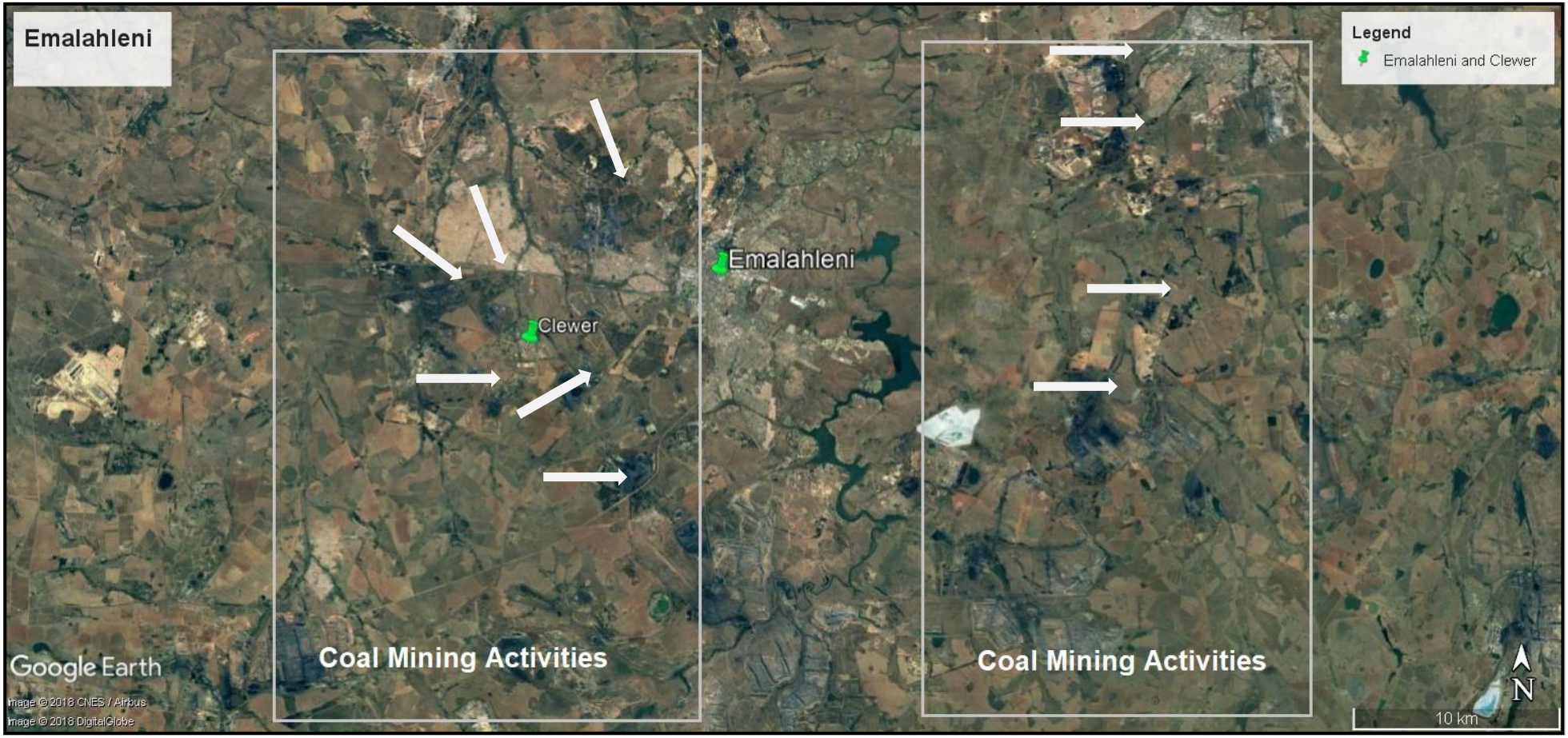

Figure 59: Location of Clewer relative to opencast coal mining activities in Emalahleni, Mpumalanga (Google Earth, 2018).

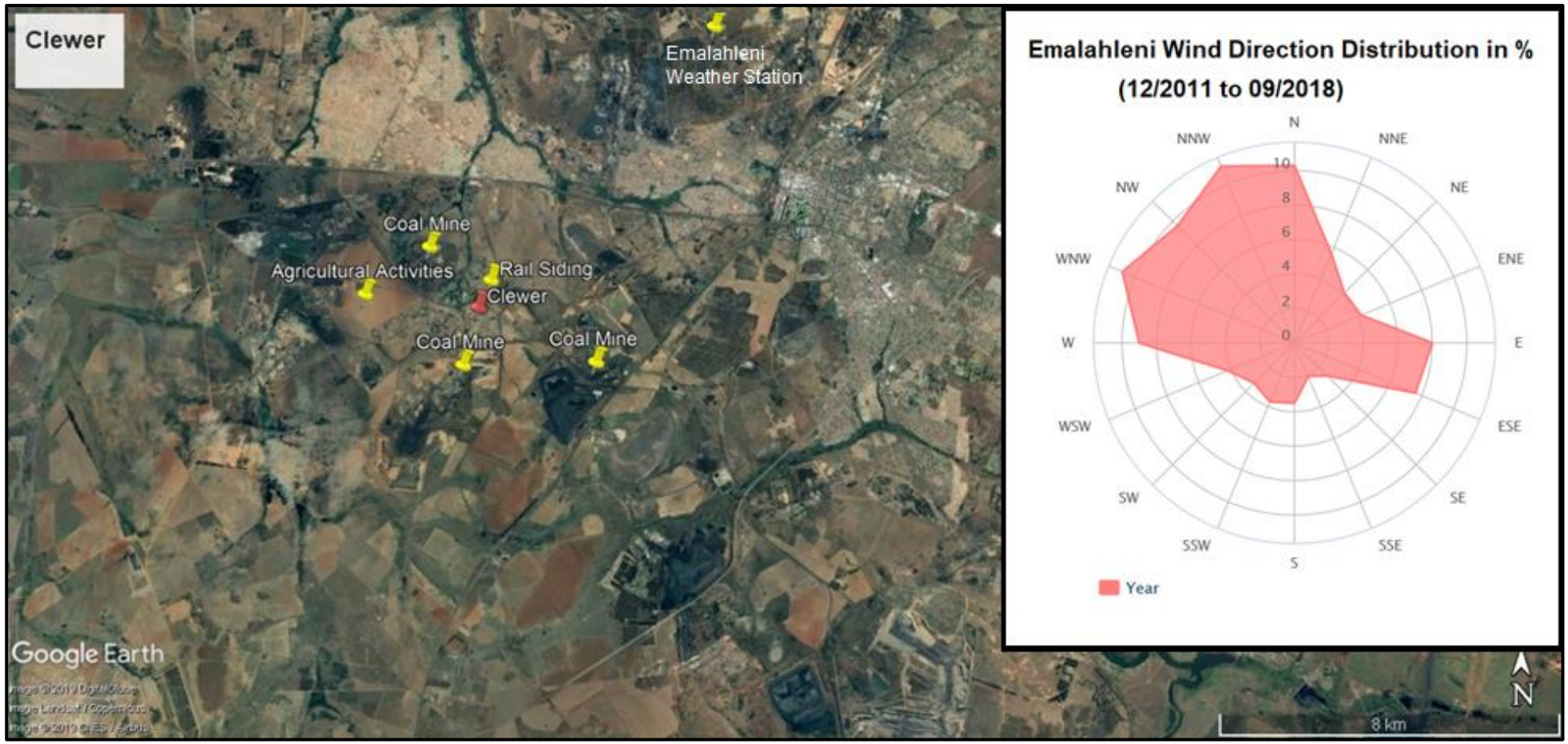

Figure 60: Location of opencast coal mines, coal siding and power station in relation to Clewer, Mpumalanga (Google Earth, 2018).

3.1.4 Study Area Description: Lephalale

Lephalale is a coal mining town located in the Limpopo Province and is located within the Waterberg-Bojanala Priority Area (Figure 61). The Waterberg Coalfield is the source of this coal, with reserve estimations at 55 gigatonnes (Gt), with a potential resource of 121 Gt (Snyman and Botha, 1993). Sources of air pollution in Lephalale include coal mining, power generation, brickworks, domestic fuel burning, vehicle emissions and agriculture. Exceedances of the NAAQS for criteria pollutants, including PM, have been recorded in the area. Marapong is a low-income residential area located approximately 12 km to the west of Lephalale (Figure 61). Passive monitoring of atmospheric PM was undertaken at this sensitive receptor area. The period wind rose for Lephalale for December 2011 to September 2018, obtained from Windfinder, is based on real observations from the Lephalale Weather Station (Figure 61). Marapong is located approximately 8 km north west of the weather station while Opencast Coal Mine 1 is located approximately 15 km to the north west of the weather station. North easterly winds are predominant in the region and the wind direction will result in pollution plumes to the south west of the sources.

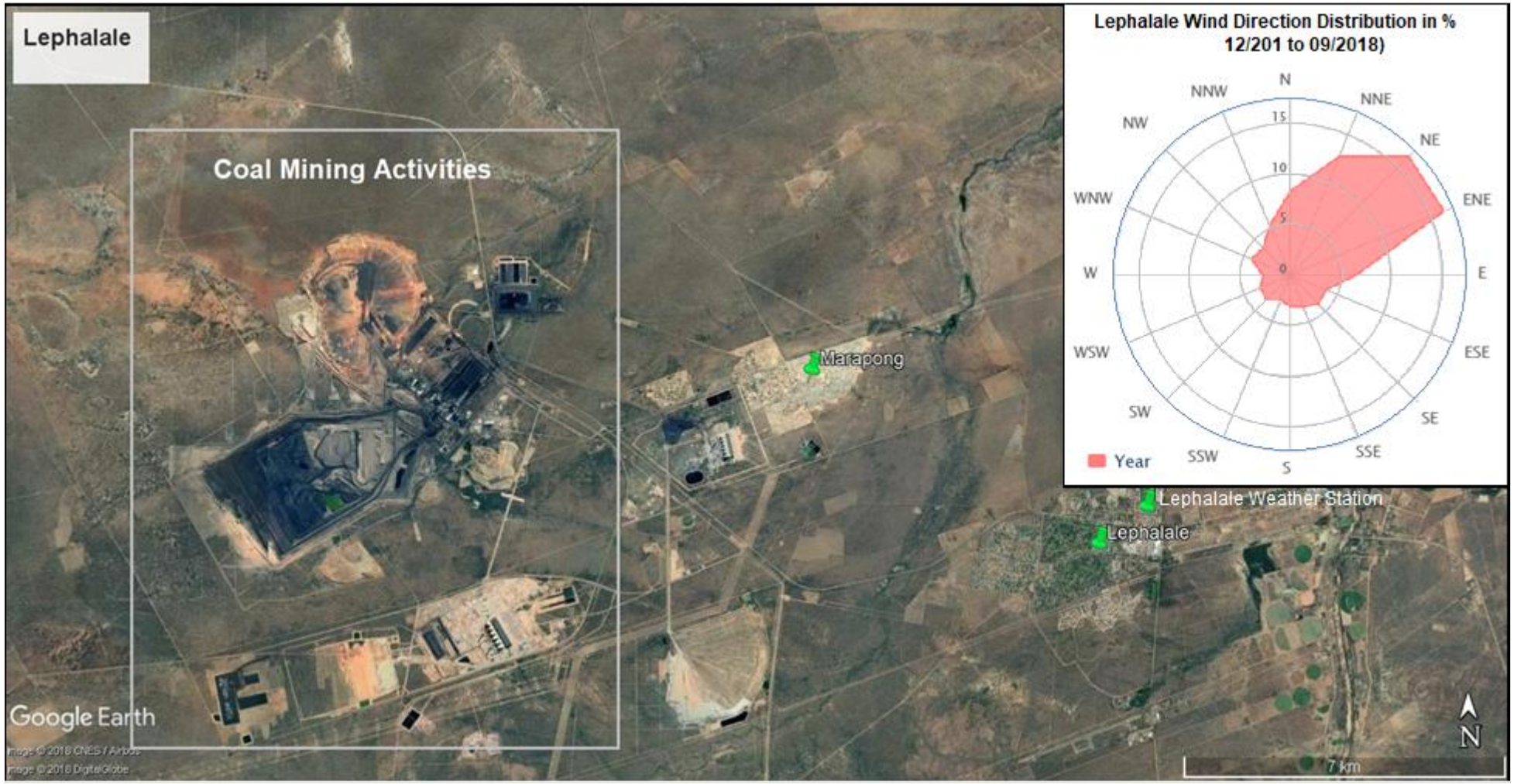

Figure 61: Location of Marapong and Lephalale in Limpopo (Google Earth, 2018) and period wind rose for Lephalale (Windfinder, 2018).

3.2 SAMPLING

Sampling technique selection is determined by the intended analysis method (Sielicki *et al.*, 2011). For example, for the purposes of sample analysis using TEM, a decontaminated, smooth, very thin (approximately 100 nm) and flat sample is required (Winey *et al*., 2014). Sample thickness is not critical in SEM as samples do not have to be thin, smooth and flat. This because the SEM has greater depth of focus hence image depth compared to TEM (Sielicki *et al.*, 2011).

3.2.1 Passive Sampling

Atmospheric PM sampling was performed during the months of May 2018 for 24 hours at each study area or location (3 different opencast coal mines and 3 communities). The sampling locations were selected following two criteria, i.e PM_{10} 'hot spot' areas and the presence of opencast coal mining activities and adjacent residential areas.

For the purposes of this research, locally produced outdoor passive samplers were deployed to the study areas, i.e, 3 opencast coal mines and 3 residential areas during the period of sampling. Four passive samplers were deployed per monitoring location to ensure the availability of adequate samples for analysis purposes. The passive samplers deployed for the research study were locally developed by Kornelius & Mukota (2017) based on the Wagner & Leith (2001) passive sampler design (Figure 56 and Figure 62). The calibration of this locally developed passive sampler was previously undertaken against the University of North Carolina passive aerosol sampler (UNC sampler) and active monitors, namely the Tapered Element Oscillating Microbalances (TEOMs) and Beta Attenuation Monitors (BAMs) (Mukota 2019). Sample imaging was carried out using an optical microscope and the collected images were analysed using Zeiss Axiovision® (proprietary software) and Image J (open-source software).

An outdoor shelter was used to protect the passive samplers from weather elements such as rain, as this would introduce experimental errors in the sampling and potentially impact on the accuracy of the study results. The exposure time for the passive samplers was limited to a period of 24 hours to avoid particulate loading and cluster formation due to over-exposure of passive samplers. In addition, for morphological and chemical analyses of particles using SEM-EDS, the best results are obtained when particles are separated from

each other (Genga *et al.*, 2013). After the 24-hour sampling period, the passive samplers were collected from the monitoring sites and placed in well labelled glass vials and transported to the laboratory for analysis (Figure 62). At the laboratory, the cover slips with the collected samples were carefully removed from the passive samplers using clean tweezers and were transferred onto clean, well labelled glass slides. The procedure involved taping each cover slip onto the glass slide with the exposure side facing the glass slide. The slides were then placed in containers to prevent contamination before optical and SEM-EDS analysis were undertaken.

Figure 62: Passive diffusive samplers (Kornelius & Mukota, 2017).

3.2.2 Active Sampling

3.2.2.1 Monitoring: Teflon Filters

The active sampling campaign for the research study was undertaken in December 2015 and May 2018. The campaign included the use of calibrated low volume MiniVol sampling pumps with automatic flow correction, fitted with impactors having a cut diameter of 10 µm (Airmetrics, Springfield, Oregon). No $PM_{2.5}$ was monitored during this campaign. The same opencast coal mines and residential areas selected for the passive sampling campaign were included in the active monitoring campaign.

Pre-weighed 47 mm diameter polytetrafluoroethylene (PTFE) filters transported in clean marked polystyrene Petri dishes were used for monitoring purposes and for assessment through the application of XPS, Raman, TGA and reflectance microscopy. Teflon filters were employed because filter mass changes are stated to be not significant for Teflon filters. A MiniVol sampler was placed at each of the selected opencast mines and residential areas (Figure 63).

Figure 63: MiniVol samplers used for PM_{10} monitoring at opencast coal mines and community areas.

The MiniVol samplers were set to 5 litres per minute (5l/min) at local conditions and programmed for a period of 24 hours at each monitoring site. Detail of the active sampling campaigns undertaken during the study is shown in Table 10. After completion of each 24-hour sampling period, each filter holder assembly unit was removed from the MiniVol sampler and placed in a well labelled, clean container with a lid for post sampling weighing. A second filter holder assembly unit with a clean filter was then inserted into the MiniVol for the purposes of collecting the next sample.

The start and end times of monitoring were recorded for the purposes of ensuring filter collection at exactly 24 hours.

In the laboratory, each Teflon filter was carefully removed from the filter holder assembly unit using clean tweezers and weighed using a calibrated 5 decimal electronic balance at room temperature for the determination of sample weight and PM_{10} concentration. Each weighed filter was then placed in a well labelled clean Petri dish using tweezers, in preparation for particulate matter sample analysis using XPS, Raman and TGA. Previously weighed blank Teflon filter papers were also re-weighed. Atmospheric PM concentration in the ambient air was calculated using the total mass of collected particulates in the PM_{10} range (adjusted for the change in blank mass), divided by the total volume of sampled air. The total volume of sampled air was determined from the sampling time (24 hours) and the volumetric flow. The PM_{10} concentrations of the samples were expressed in ($\mu g/m^3$). Average PM_{10} concentrations were calculated for each site based on the concentration results of the two filters from each site.

3.2.2.2 Monitoring: Quartz Fibre Filters

Atmospheric PM for stable carbon and nitrogen isotope analysis and thermal optical techniques for TC, EC and OC were collected through MiniVol samplers as described above in the selected opencast coal mines and adjacent communities' study areas, but using quartz fibre filters due to their suitability in OC/EC or thermal desorption analysis and stable carbon and nitrogen isotope analysis. Sampling numbers and dates are given in Table 10.

3.3 SAMPLE ANALYSIS

The type and date of monitoring for the active and passive sampling campaigns for the study are shown in Table 10 below.

Table 10: Active and passive diffusive sampling parameters

Location	Type and Date of Sampling							
	Active Sampling (Preliminary Active Sampling for XPS, TGA and Raman)	Date of Sampling	Passive Sampling	Date of sampling	Active Sampling Campaigns	Date of sampling	Active Sampling (Quartz Filters)	Date of sampling
Opencast Coal Mine 1 (Limpopo)	2	04/12/2015	4	11/05/2018	3	11/05/2018	3	14/06/2019
Opencast Coal Mine 2 (Mpumalanga)	2	08/12/2015	4	19/05/2018	3	19/05/2018	3	18/06/2019
Opencast Coal Mine 3 (Mpumalanga)	2	12/12/2015	4	21/05/2018	3	21/05/2018	3	23/06/2019
Delpark	2	08/12/2015	4	19/05/2018	2	19/05/2018	2	18/06/2019
Clewer	2	12/12/2015	4	21/05/2018	2	21/05/2018	2	23/06/2019
Marapong	2	04/12/2015	4	16/05/2018	2	16/05/2018	2	14/06/2019

3.3.1 Optical Microscopy

Particle size is an important determinant of physical, chemical and formation properties of particulates and has profound implications for particulate transport, transformation and, removal in the atmosphere (Vallius, 2005). Microscopy, particularly electron microscopy, is used for obtaining information on the morphology and size distribution of particulates. The importance of morphology as a potential contributor to toxicity can be related to the influence of morphology on both surface composition and particle transport properties (Mamani-Paco & Helble, 2007). For each mine and adjacent community, 2 glass slides with atmospheric PM samples were analysed using optical microscopy. A blank glass slide was also analysed for experimental control purpose. The samples were viewed through a light microscope, Zeiss Imager- A1m Microscope set up with Kohler Illumination and equipped with a digital camera AxioCam MRc5 (Carl Zeiss, Germany). The samples were viewed at 200X magnification with a ~6mm exposure diameter. Background subtraction and shading correction were undertaken on the optical microscope before sample analysis, with shading correction applied to correct for stray light and non-uniformity in the illumination system. Background subtraction and shading correction enable the quantification of intensities and improvement in image quality.

Photographs of the samples were taken using a specific Cartesian plane pattern enabling the capture of the entire surface. The light intensity, hue, saturation and background were kept constant for all photos by setting the measurement parameters, so enabling a uniform histogram. Digital images were saved and stored in a tiff format in corresponding folders using the AxioVision SE64 software (Carl Zeiss, Germany).

Quantification of the atmospheric PM concentrations was undertaken through imaging of each glass cover slip over an area of approximately 6mm in diameter. Particle sizing and counting was undertaken using the AxioVision SE64 software. All the images were taken at a constant or fixed hue saturation and light intensity. The images' threshold was then set to a value that avoids bias by either erosion or dilation after having converted it to a binary image. Automated counting using a custom macro followed. The macro output consisted of a list of projected area, image coordinates, and circularity for each particle detected in the images. Image edge effects were neglected because the area of the image was very large compared to the size of the particles of interest and because the imaging minimises double

capturing of any particles due to the pattern used. During atmospheric particulate analysis (using the Axio Vision software), parameters such as particle diameter (µm), particle area (µm) and perimeter (µm) were recorded for each particle. Results from the AxioVision particle analysis software were exported to an Excel spread sheet for further analysis. This data was used for atmospheric PM concentration calculations (µg/m^3).

To obtain the atmospheric particulate concentrations, the methods applied by Mukota (2019) were used.

3.3.2 Scanning Electron Microscopy Analysis and Energy Dispersive Spectroscopy (SEM-EDS)

The glass slides from the optical microscopy analysis were also used for SEM-EDS analysis as described in Section 3.3.1. Each glass slide was removed from its container with clean tweezers for the purposes of carbon coating. Carbon coating was undertaken to minimise specimen charging. The energy dispersive spectrometer used in this study has a background subtraction function for coating material to ensure that the EDS results do not include carbon used during the carbon coating process. After carbon coating, the samples were analysed under the SEM. Various magnifications of up to 30,000X were applied during the analysis given the different particulate sizes. For the purposes of SEM analysis, magnifications of 1,000X to 20,000X are generally set.

SEM and EDS analysis were not undertaken simultaneously due to the poor image quality obtained from EDS when used in conjunction with SEM. Poor image resolution presents a challenge during particle morphological analysis. Therefore, the applied procedure involved particle analysis and the capturing of high-resolution images using SEM, followed by elemental composition analysis using EDS for various individual and bulk particles.

A Zeiss Ultra PLUS FEG scanning electron microscope equipped with an Oxford X Max EDS (spectroscope) was used for sample analysis. In conjunction with the SEM-EDS hardware, an Oxford Instruments Aztec 3.0 SP1 image analysis software provided imaging and graphical spectra results. The Zeiss Ultra PLUS FEG SEM was operated under vacuum at an accelerating voltage of 15kV for the primary electrons, with an ideal resolution and a working distance of approximately 4 mm, which was observed to be optimal for this research study. A secondary detector was employed for the detection of secondary electrons from

the samples due to its capability of yielding a good quality image and depth of focus resulting in an image with a three-dimensional perspective (Casuccio *et al*., 2002; Casuccio *et al*., 2004).

The determination of the optimal primary electron accelerating voltage for the study was based on the consideration that in theory, the highest image resolution, is obtained through a highly energetic electron beam (Sellaro *et al*., 2002; Willis *et al.*, 2002). The implications for employing higher energy to the sample is that the generation of secondary electrons, which form the particle image, occurs over a much larger volume of the sample due to the high depth of penetration of the primary electron beam (Casuccio *et al*., 2002; Galvez *et al*., 2013). Consequently, lowering the energy of the primary electron beam results in surface detection of secondary electrons on the sample, leading to the enhancement of surface detail in the SEM image (Willis *et al.*, 2002).

Electron micrographs of individual and bulk atmospheric PM in the samples were taken at different magnifications depending on the sizes of the individual and bulk particulates. The same approach was followed for EDS, where elemental analyses of individual particles and bulk atmospheric particulate analysis was undertaken using spot and area analysis. The EDS system employed in the research study has a capability of detecting elements with an atomic number 6 (carbon) and greater. The analysis of the particulates using EDS was narrowed down to individual atmospheric particulates due to the highly variable chemical composition of bulk particulates. The percentage weight of each element present in the spectrum was identified for the individual particles. The individual atmospheric particulates, including coal dust particulates, were classified based on their EDS spectra, provides graphical representation of the elements associated with each particle. During the characterisation of the atmospheric particulates, observations were also made on the relationships between peak heights in the different spectra, to obtain information and indications of the elemental composition and other relevant information.

3.3.3 X-ray Photoelectron Spectroscopy (XPS)

XPS was employed in an attempt to determine the surface chemical compositions of the samples to differentiate between OC and EC from coal mining and other activities such as combustion related activities.

A total of 3 samples, 1 from an opencast coal mine, 1 from an adjacent community and a reference sample (blank filter cut) were analysed. One set (before and after sputtering) of XPS measurements was done for each sample. Small sections of Teflon filter samples of 6mm x 3mm were cut from each of the filters (Figure 64). The cut sections from each filter were taken from the filter area judged to have the highest deposit of atmospheric PM. The cut filters were placed on a sampler holder using clean tweezers and the sample holder was placed in the PHI 5000 Scanning ESCA Microprobe X-ray photoelectron spectrometer sample chamber (Figure 64). The surface compositions and the chemical states of elements in the filter samples were then determined. Carbon was the critical element in the analysis given the objective of differentiating between EC and OC.

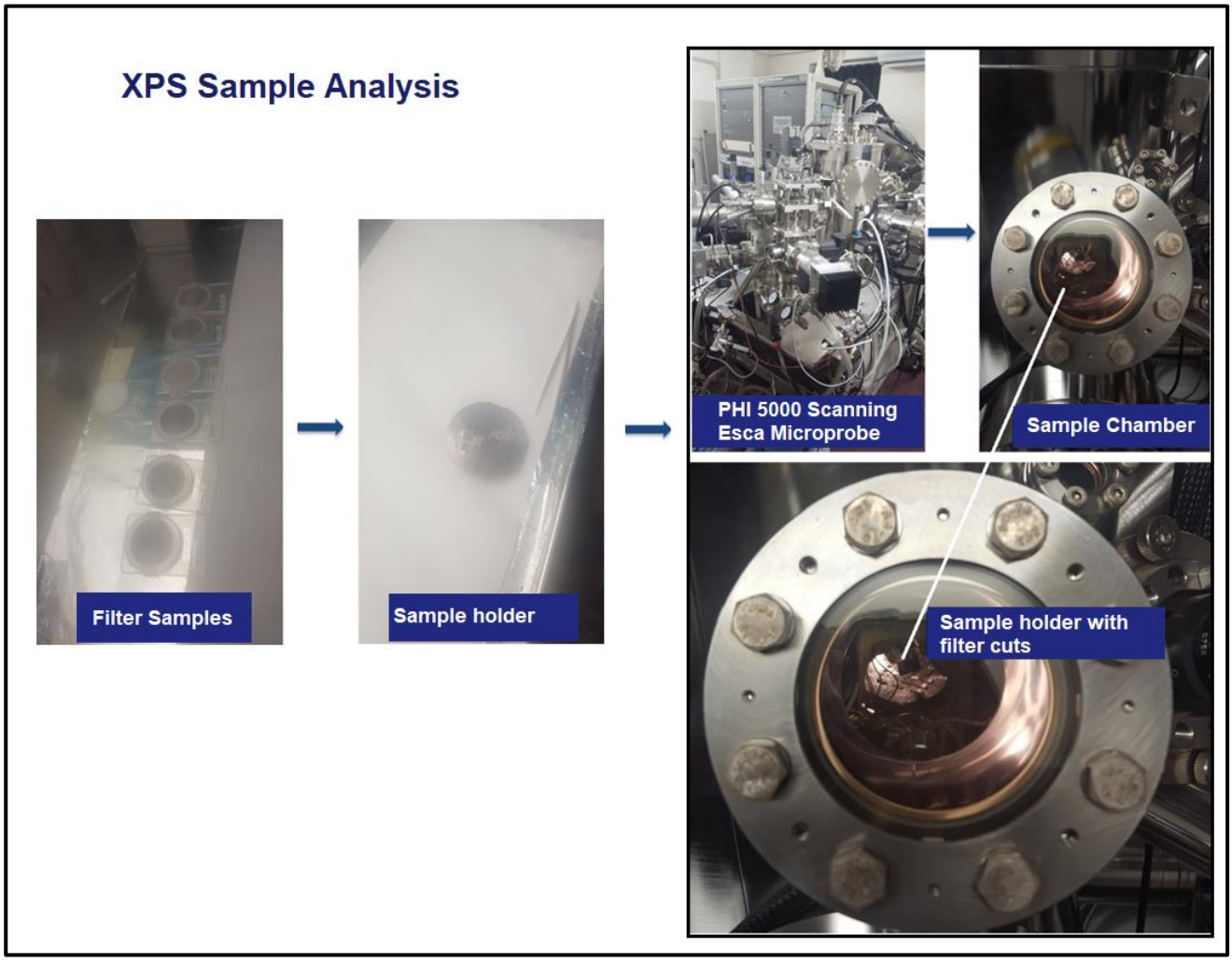

Figure 64: XPS sample analysis using the PHI 5000 Scanning ESCA Microprobe (University of Free State).

For the identification of the chemical state of the atomic species in the samples, high resolution spectra were collected. Survey spectra (binding energy peaks) of the atmospheric particulates were collected through a 100 µm diameter monochromatic Al Kα x-ray beam (hv = 1486.6eV) generated by a 25W, 15kV electron beam, 187eV Pass energy, 1 eV/step 100ms/step and UHV Base Pressure 2.8E-9 Torr. High resolution spectra for the atmospheric particulates were also collected through a 100µm diameter monochromatic Al Kα x-ray beam (hv= 1486.6eV) generated by a 25W, 15kV electron beam, at an energy resolution of 0.5eV. Sputter for the analysis was done using an Argon (Ar) ion gun at 2kV 2uA 1x1mm Raster and a sputter rate of about 4.5nm/min (see Table 11 below). Data relating to the assessed peaks, repeats and cycles is shown in Table 12 below.

Table 11: Parameters employed for XPS analysis

Characterisation	Al X-Ray Beam	Ar Ion Gun	Description
Survey	100µm 25W 15kW		187eV Pass energy, 1eV/ step 100ms/ step UHV Base Pressure 2.8E-9Torr
High Resolution	100µm 25W 15kW		0.5eV
Sputter		2kV 2uA	1x1mm Raster Sputter rate of about 4.5nm/min

Table 12: Cycles and repeats for XPS analysis

No. of samples analysed	Peak	Pass Energy (eV)	Cycles	Energy step (eV)	Time/ Step (ms)
3	C1S	23.5	10	0.1	100
3	O1S	23.5	10	0.1	100

The X-ray energy dispersion eliminates the Kα3,4, Kα5,6, and Kβ X-ray lines and the Al Bremsstrahlung radiation background and narrows the Al Kα1,2 line to approximately 0.26 eV Full Width at Half Maximum (FWHM). FWHM is a full width of a spectroscopic peak measured at a half of its maximum height. This narrow line allows core and valence band spectra to be acquired with high energy resolution of the photoemission peaks and without X-ray satellite-induced photoemission peak overlaps. The removal of X-ray and

Bremsstrahlung satellite radiation coupled with a narrow principle excitation line width results in significantly higher signal-to-background ratio data. The narrower X-ray line width also allows an electron energy analyzer to be observed with higher transmission, thereby reducing the observed damage rate in monochromator excited XPS spectra of X-ray sensitive sample. With the proper geometry configuration of X-ray source, crystal substrate and analysis target, the reflection beam yields a highly focused, monochromatic source of X-rays. Multipack Version 9 software can be utilised to analyse the spectra to identify the chemical compounds and their electronic states using Gaussian–Lorentz fits. A low energy Ar+ ion gun and low energy neutralizer electron gun is used to minimize charging on the surface.

3.3.4 Raman Spectroscopy (Raman)

Raman was attempted for the differentiation of EC and OC in the atmospheric PM samples. Raman analysis of a blank Teflon filter, 2 residential/community and 5 coal mining atmospheric PM samples (on Teflon Filters) were recorded using a T64000 Series II Triple Spectrometer system from HORIBA Scientific, Jobin Yvon Technology. The 514.3 nm laser line of a coherent Innova® 70C series Ar^+ laser (spot size ~ 2 µm) with a resolution of 2 cm^{-1} in the range of 1200 cm^{-1}–1800 cm^{-1} was used. This is because the spectral region between 1000 cm^{-1} and 1800 cm^{-1} contains the most detail on the structural information for carbonaceous materials. The objective of the Raman instrument focused on three spots of each sample. The area which showed the most intense peaks or bands was utilised in the study.

The undeconvoluted Raman spectra for all the opencast coal mines and communities' samples were obtained in a backscattering configuration with an Olympus microscope attached to the instrument (using an LD 50x objective). The laser power was set at 1.7 mW. An integrated triple spectrometer was used in the double subtractive mode to reject Rayleigh scattering and dispersed the light onto a liquid nitrogen cooled Symphony CCD detector.

3.3.5 Thermogravimetric Analysis (TGA)

A Hitachi STA7300 TGA-DTA equipped with alumina crucibles was used for the thermogravimetric analysis of 7 filter samples (5 from the opencast coal mines and 2 from the communities) for differentiating EC and OC in the atmospheric particulate samples.

A section of the filter paper or disc was cut to the height of the crucible (5 mm) and coiled inside the crucible. The cut section was taken from the filter area judged to have the most deposit. All filter samples were run once under instrument air (obtained from Afrox). Nitrogen runs were also undertaken once for each sample for the determination of any existing differences in the burn kinetics of the atmospheric PM samples with air or nitrogen. The samples were ramped from 30°C to 1000°C at a rate of 10°C/min under air flowing at a rate of 200 mL/min. Once the samples reached 1000°C, they were kept isothermal for 20 minutes before being cooled down.

Nominally, different carbon types (amorphous, glassy, graphitic) as well as the particle sizes of those carbon types can be distinguished by the differences in their burn kinetics in an air environment. Ideally, 10% O_2 in 90% N_2 should be used. However, for the purposes of this research, instrument air of 29% O_2 was used as the 10% mixture was not locally available.

“Ashing” of the entire sample filter was undertaken in the TGA instrument to understand the filter media behaviour during heating and to observe any potential interactions between the filter and the sample matrix. For TGA analysis using the direct-on-filter method, it is ideal for the decomposition of the filter media to occur at a different temperature range from the sample.

3.3.6 Reflectance Microscopy (Reflectance)

For the purposes of characterising the coal dust of atmospheric dust samples, sample preparation for reflectance microscopy involved the extraction of particulates obtained from randomly selected filters (Teflon filters) from the active sampling campaign. 3 opencast mining filters (one from each opencast coal mine) and 3 community filters (one from each of the adjacent communities) were used during sample preparation. Extraction of atmospheric PM from the filters was performed using alcohol (ethanol). The filters with the atmospheric particulate samples were submerged in two different containers with alcohol. The alcohol was then evaporated using a hand blow dryer for the purposes of collection of the atmospheric particulates that were dislodged from the Teflon filters. The collected atmospheric particulates were afterwards set in two polyester resin blocks, one for the coal mine samples and one for the community samples. The resin blocks had been previously

prepared using methods adapted from the South African National Standards for Coal Petrography SANS 7404-2:2009.

To ensure total transfer of the atmospheric particulates to the polyester resin block, the particulates were mixed with a small amount of polyester resin which was poured into a blank hole of a block (one block for the opencast coal mining samples and one for the community samples). These were cured for 24 hours to allow the resin to reach its gelation stage and to settle. To obtain smooth surfaces, the cured resin blocks were polished up to 5 times using a Saphir 550 polishing machine. A Zeiss AxioImager M2M reflected light microscope with oil immersion lenses of X50 and X100 was used to identify the particulates on the resin blocks. Images were taken using the Hilgers Diskus Fossil system attached to the microscope.

3.3.7 Isotope Ratio Mass Spectrometry (IRMS)

For stable isotope analysis ($\delta^{13}C$ and $\delta^{15}N$), quartz filters collected from the field during the active monitoring campaign were analysed. A total of 10 atmospheric PM samples from the opencast coal mines and adjacent communities were analysed (7 samples from the opencast coal mines and 3 from adjacent communities). Each sample was analysed once and the $\delta^{13}C$ and $\delta^{15}N$ ratios were recorded. The samples were combusted at 1020°C using an elemental analyser (EA) (Flash EA 1112 Series) coupled to a Delta V Plus stable light isotope ratio mass spectrometer (IRMS) via a ConFlo IV system (all equipment supplied by Thermo Fischer, Bremen, Germany), housed at the UP Stable Isotope Laboratory, Mammal Research Institute, University of Pretoria.

Two laboratory running standards (Merck Gel: $\delta^{13}C$ = -20.26‰, $\delta^{15}N$= 7.89‰, C%= 41.28, N%= 15.29) & (DL-Valine: $\delta^{13}C$ = -10.57‰, $\delta^{15}N$ = -6.15‰, C%= 55.50, N%= 11.86) and a blank sample were run after every 11 unknown samples.

Data corrections were done using the values obtained for the Merck Gel during each run. The standard deviations of the nitrogen and carbon values for the DL-Valine standard provided the ± error for $\delta^{15}N$ and $\delta^{13}C$ values for the samples.

The carbon and nitrogen ratios for all secondary (NIST) and lab running (Merck & DL-Valine) standards were all calibrated using the following primary standards;

- IAEA-CH-3 (Cellulose),
- IAEA-CH-6 (Sucrose),
- IAEA-CH-7 (Polyethylene foil),
- IAEA N-1 & IAEA N-2 (Ammonium sulphate),
- IAEA NO-3 (Potassium nitrate).

All the results were referenced to Vienna Pee-Dee Belemnite for carbon isotope values and to air for nitrogen isotope values. Results were expressed in delta notation using a per mille scale using the standard equation:

$$\delta X\ (‰) = [(R_{sample}\text{-}R_{standard})/R_{standard}\text{-}1]$$

where X= ^{15}N or ^{13}C and R represents $^{15}N/^{14}N$ or $^{13}C/^{12}C$ respectively.

3.3.8 Thermal Optical Characterisation of Brown/Organic Carbon and Elemental Carbon

The quartz filters collected from the field during the active monitoring campaign were analysed using a thermal/optical carbon analyser (Sunset Laboratory Inc's Lab OC-EC Aerosol Analyser). A total of 10 samples from the opencast coal mines and communities were analysed (7 atmospheric PM samples from the opencast coal mines and 3 atmospheric PM samples from adjacent communities). Each sample was analysed once as this is standard procedure when performing OC/EC analysis.

The filters were pre-fired in air (700°C for one hour) for the removal of residual carbon contaminants and to take advantage of the low detection limits of the technique. The instrument and analysis process followed during this investigation is shown in Figure 65. Punch aliquots of 1.5cm² of the filter deposits were used for the analysis. Each aliquot was heated in a sample oven in four increasing temperatures of 140°C (OC1), 280°C (OC2), 480°C (OC3) and 580°C (OC4) in a non-oxidizing helium (He) atmosphere for the removal of all organic carbon (OC) on the filter.

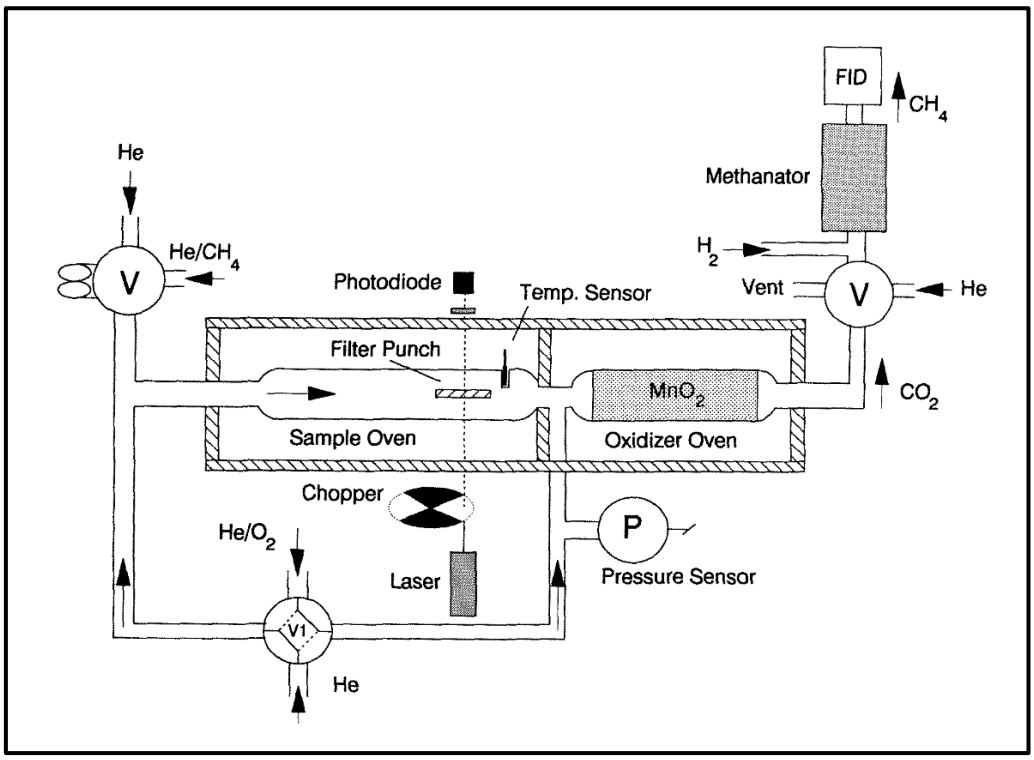

Figure 65: Schematic of thermal-optical instrumentation (Birch & Cary, 1996).

The first phase is defined by the pyrolytic conversion of some OC to elemental carbon (EC). The carbon that evaporated at each temperature was catalytically oxidized by MnO_2 into CO_2 in the oxidiser oven. The CO_2 entrained in the He gas flow, was converted to CH_4 in the methanator oven. The detection and quantification of methane was undertaken through a flame ionisation detector while the pyrolitic conversion was continuously monitored by measuring the transmission of a He-Ne laser through the quartz filter. The darkness of the filter was also continuously monitored throughout all stages of the analysis. Ramping up to the next temperature or atmosphere was undertaken when the flame ionization detector's response returned to baseline or a constant value (subject to the condition of the time spent in any segment (OC1, OC2, etc).

The sample oven was then cooled to 525°C and the pure helium eluent was switched to a 2% O_2/98% He mixture. Peaks were integrated at 580°C (EC1), 740°C (EC2), and 840°C (EC3). The sample oven temperature was then stepped up to 850°C (EC4). During this phase, both the original EC and EC produced through the pyrolysis of OC during the first phase were oxidized to CO_2 due to the presence of oxygen in the eluent. The CO_2 was then converted to CH_4 and detected by the flame ionisation detector. The darkness of the filter was also continuously monitored throughout all stages of the analysis by reflectance of 633

nm of light from a He-Ne laser. During this phase, original and pyrolized black carbon were combusted and the increases in the reflectance were observed. The amount of carbon that was measured after the addition of oxygen until the reflectance achieved its original value was reported as optically detected pyrolized carbon (PC).

After the oxidation of all the carbon from each sample, a known volume and concentration of methane was injected into the sample oven, resulting in each sample being calibrated to a known quantity of carbon. Based on the FID response and laser transmission data, the quantities of OC and EC were calculated for each sample and thermograms were displayed graphically. The concentration of OC and EC on each filter punch aliquot was calculated by multiplying reported values by the sample deposit area. The concentrations were reported in $\mu g/cm^2$ of deposit area. This approach assumed a homogenous filter deposit. The precision of this technique (Sunset Laboratory method of OC/EC analysis), measured as a relative standard deviation, typically falls into the 4-6% range for samples that are in the afore-mentioned OC and EC concentration ranges. This relative standard deviation range is applicable to the OC/EC speciation values as well as to the TC.

4 RESULTS

4.1 INTRODUCTION

The results from the application of microscopic, spectroscopic, TGA and thermal optical techniques for the characterisation of atmospheric PM are presented in this section.

4.2 Characterisation of Atmospheric Particulate Matter Through SEM-EDS

SEM-EDS analysis was employed for the characterisation and semi-quantitative analysis (EDS) of atmospheric PM samples from opencast coal mining operations and adjacent communities. The morphological, dimensional and elemental composition of bulk and individual atmospheric particulates are analysed in this section.

4.2.1 Opencast Coal Mining Atmospheric Particulate Matter Samples: SEM

Sample electron micrographs of bulk atmospheric particulates collected from the opencast coal mines in Limpopo and Mpumalanga are shown in Figures 66 to 69, while the individual atmospheric particulates are shown in Figures 70 to 72. These can mostly be identified from their morphology. Particle dimensions range from 1 µm to 50 µm, with the larger dimensions being attributed to solid irregular and linear atmospheric particulates (coarse particulates). Particle sizes of the coal particulates vary from 2.5-30 µm, being differentiated by their characteristic sharp, serrated edges, layered appearance (Figure 70 and Figure 71) and the lack of smooth spherical shapes which are characteristic of combustion-derived particulates (Figure 73). Particulates with smaller dimensions (>1 µm to 2.5 µm) are also observed in all the atmospheric particulate samples. These atmospheric particulates include fine chain agglomerates which consist of spherical particles of much less than 1 µm in dimension. These atmospheric particulates are identified as diesel particulate matter (DPM associated) with vehicle emissions (Figure 69 and Figure 73) due to the large-scale usage of heavy vehicles, machinery and other internal combustion-driven mining equipment which is intrinsic to opencast coal mining (Section 2.4.4). The detection of DPM in the mining samples is a result of the placement of passive samplers close to unpaved and paved roads (roadside) and open pit mining areas during the study sampling campaign.

Unaggregated and non-spherical PM with particle sizes of 2.5 µm or less are also observed (Figure 72). These atmospheric particulates are identified as mineral material re-suspended material from the coal mine roads (unpaved and paved). Fly ash particulates are also identified due to their typical cenosphere morphology (Figure 73) given the existence of power stations to the opencast coal mines selected for the study in both Mpumalanga and Limpopo. However, the percentage of identified fly ash particulates was less than 5% for all the opencast atmospheric PM samples.

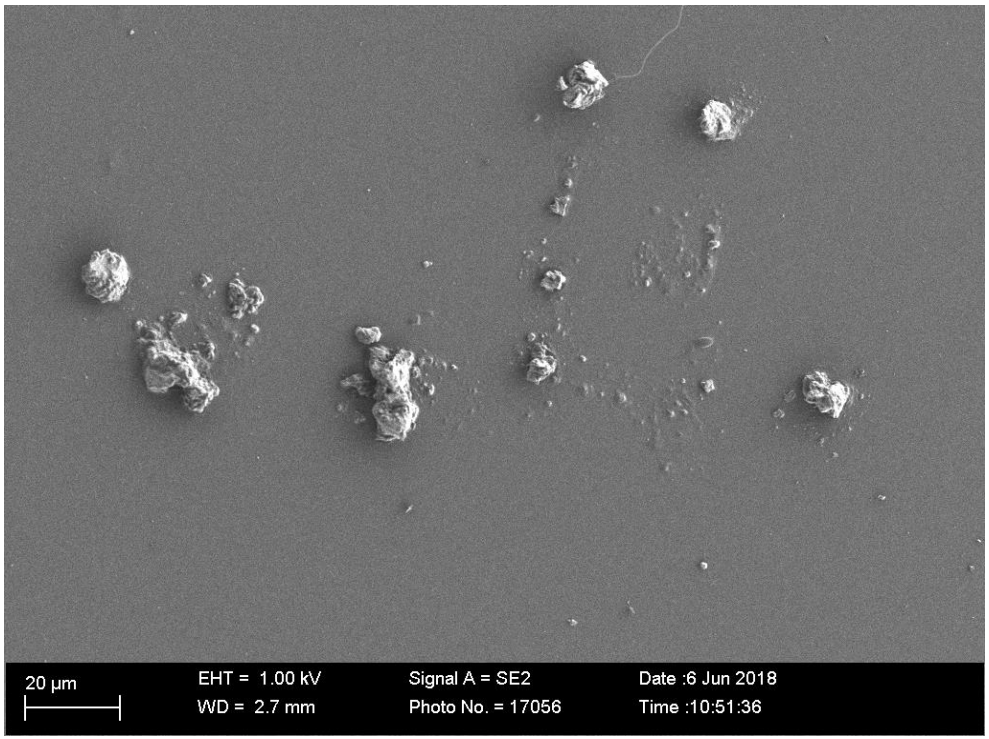

Geological material

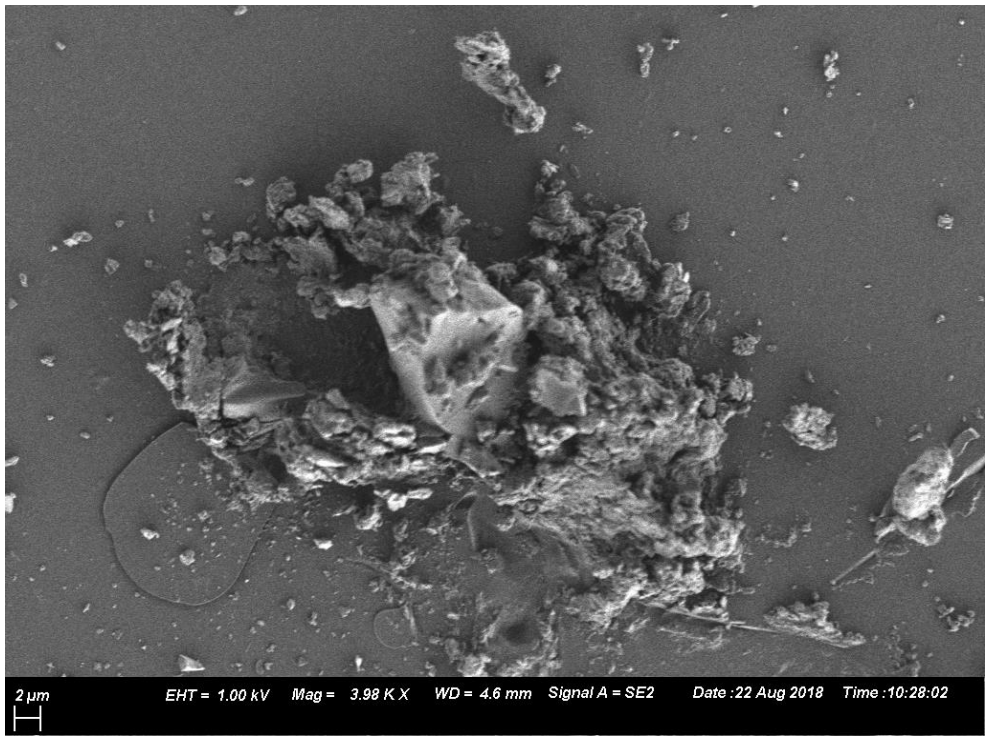

Coal dust- elemental carbon and geological material

Figure 66: Electron micrographs for bulk atmospheric PM samples (geological material and coal dust) from opencast coal mines (Limpopo and Mpumalanga).

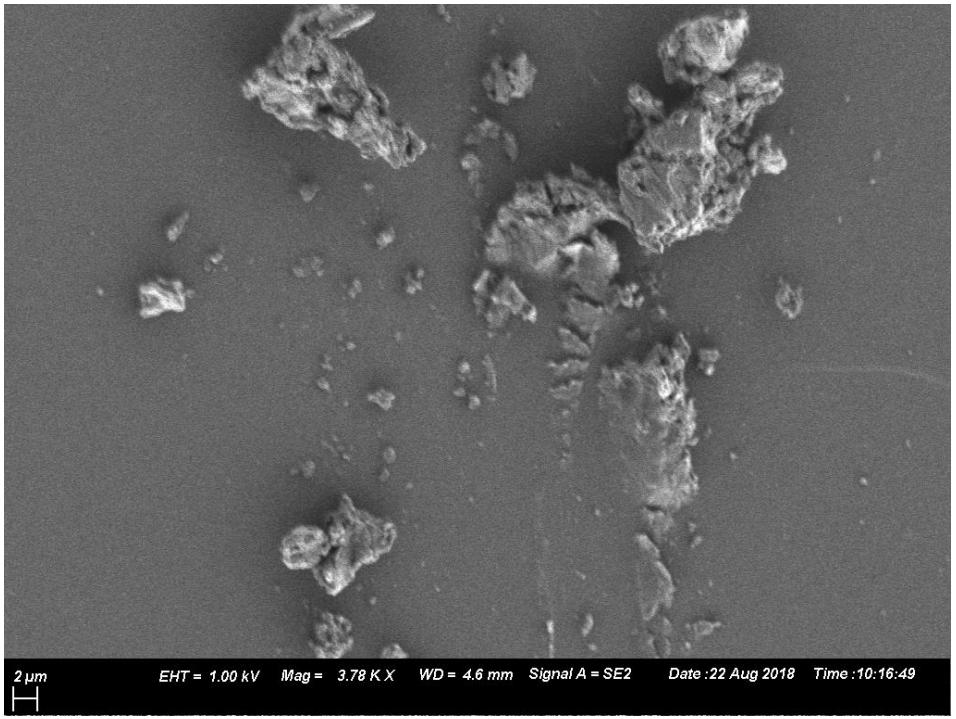

Coal dust- elemental carbon and geological material

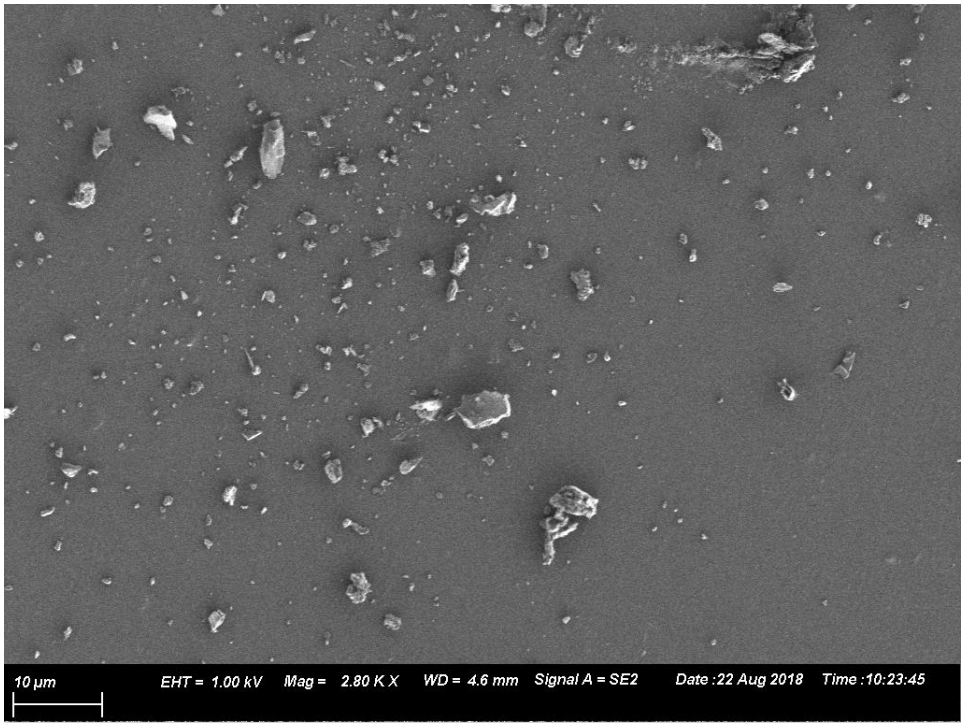

Coal dust- elemental carbon and geological material

Figure 67: Electron micrographs for bulk atmospheric PM samples (coal dust and geological material) from opencast coal mines (Limpopo and Mpumalanga).

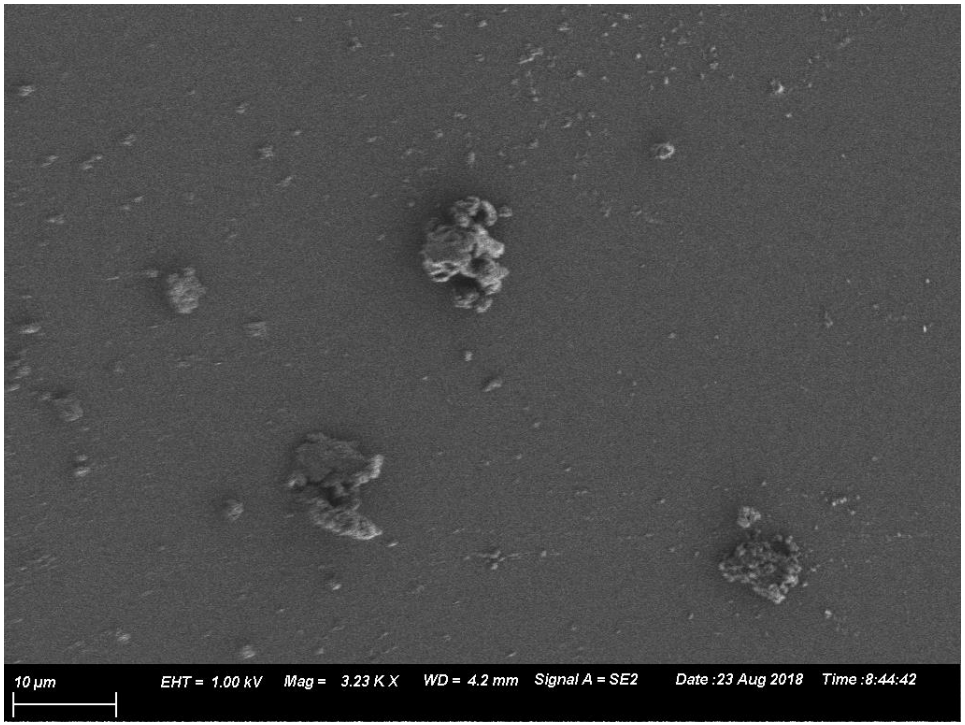

Coal dust

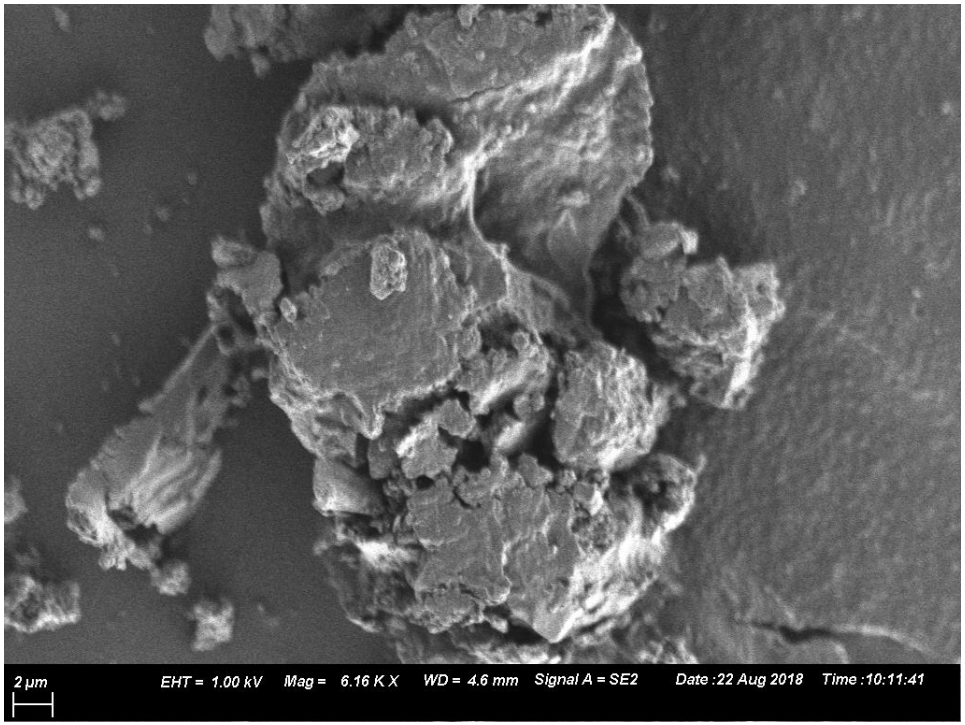

Coal dust

Figure 68: Electron micrographs for bulk atmospheric PM (coal dust) from opencast coal mines (Limpopo and Mpumalanga).

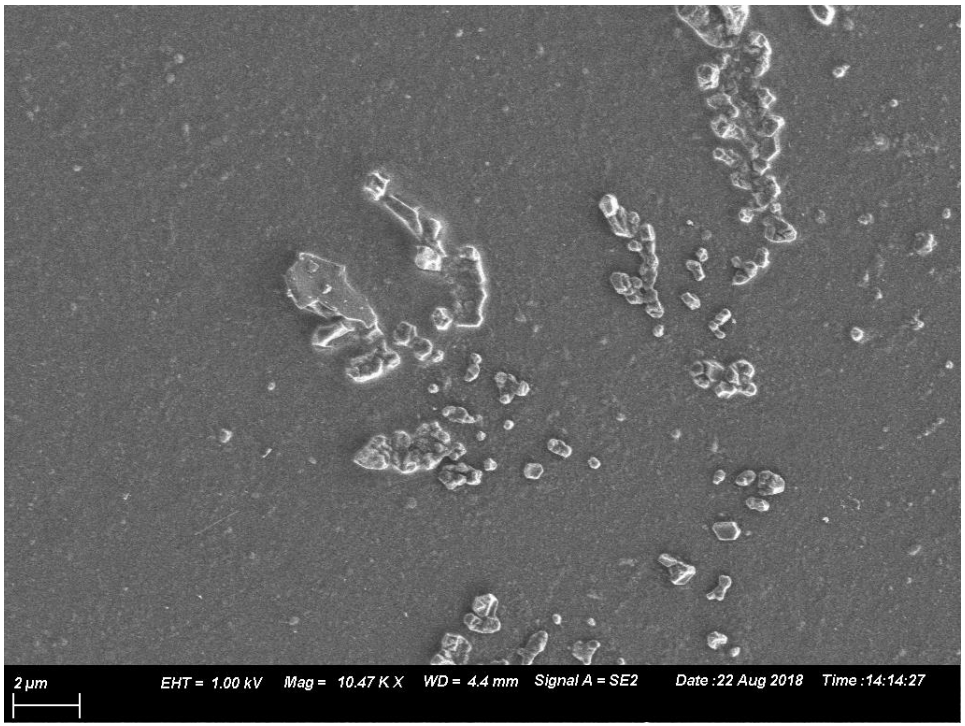

DPM- organic carbon and fly ash

Combustion particulates- organic carbon and fly ash

Figure 69: Electron micrographs for bulk atmospheric PM (DPM and fly ash) from opencast coal mines (Limpopo and Mpumalanga).

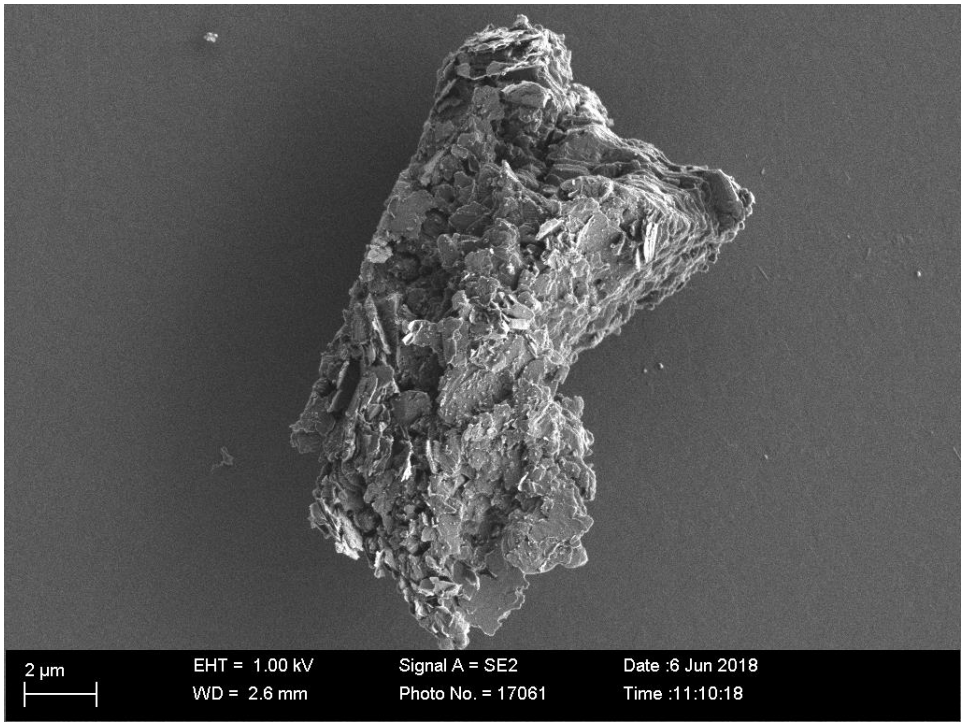

Coal dust

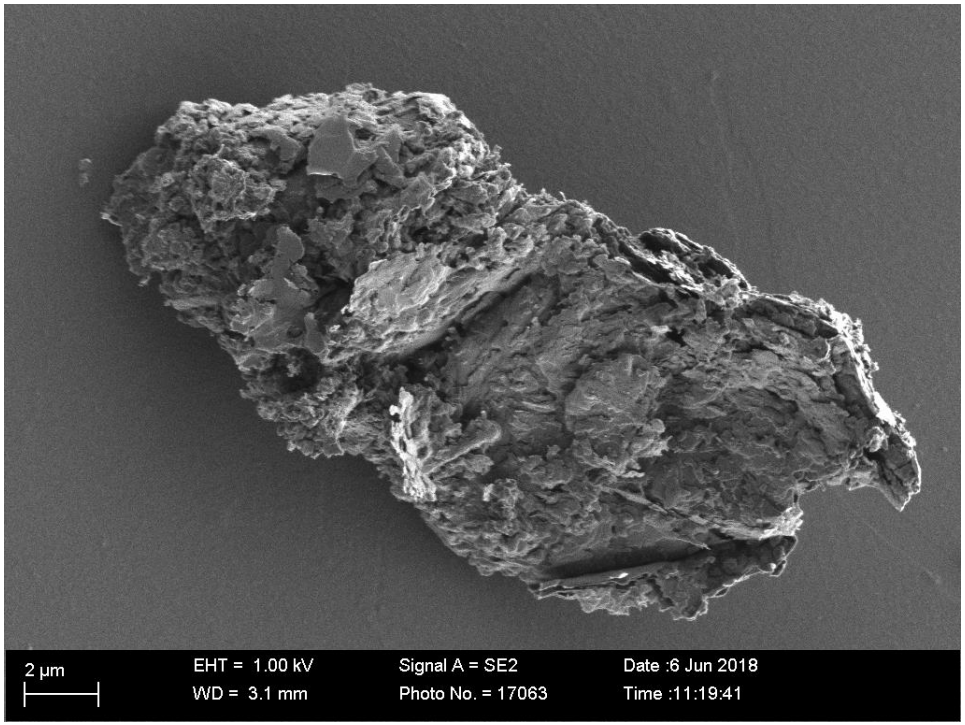

Coal dust

Figure 70: Electron micrographs for individual atmospheric PM (coal dust) from opencast coal mines (Limpopo and Mpumalanga).

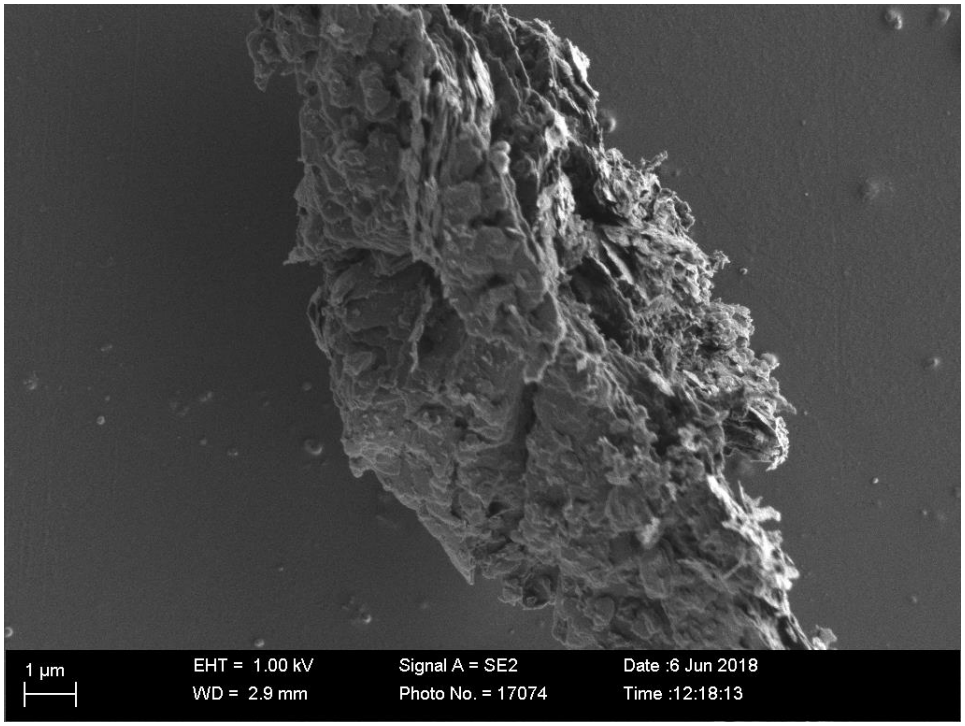

Coal dust

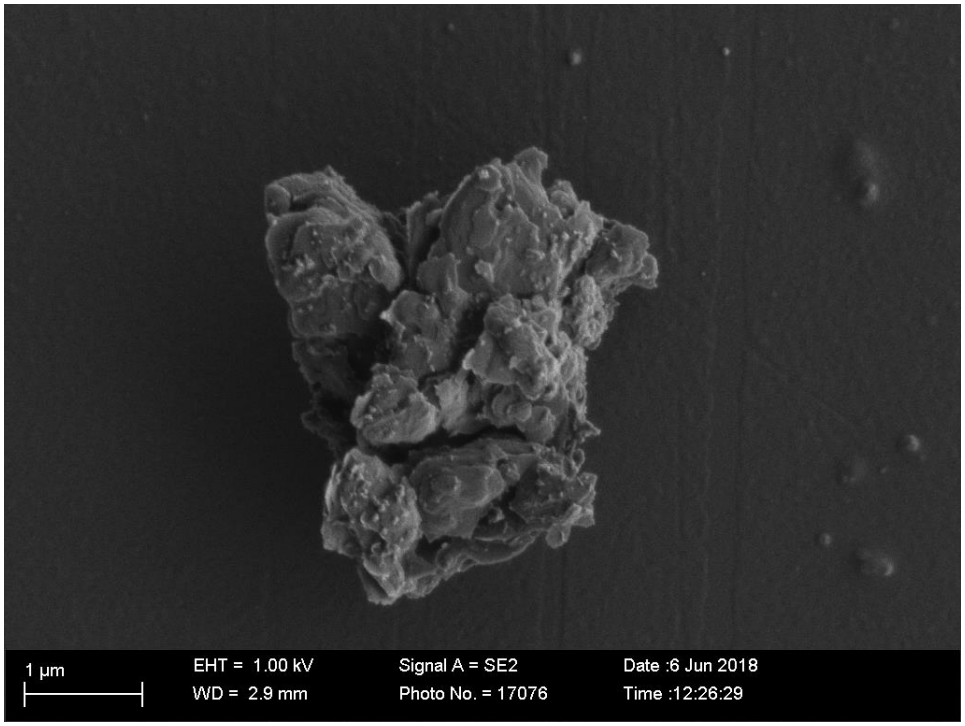

Coal dust

Figure 71: Electron micrographs for individual atmospheric PM (coal dust) from opencast coal mines (Limpopo and Mpumalanga).

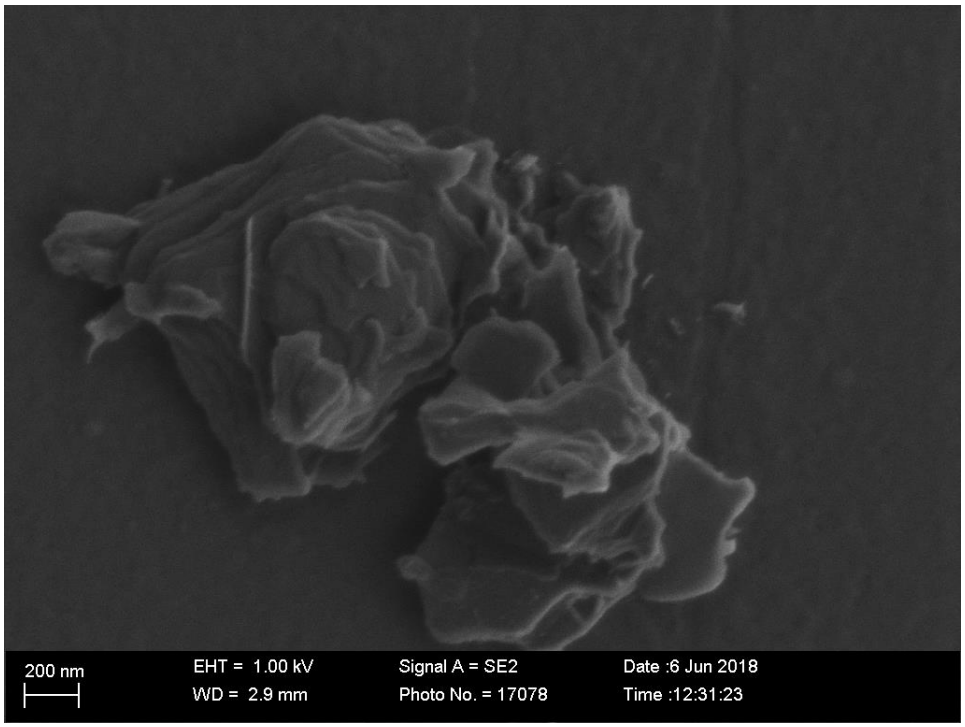

Aluminosilicates

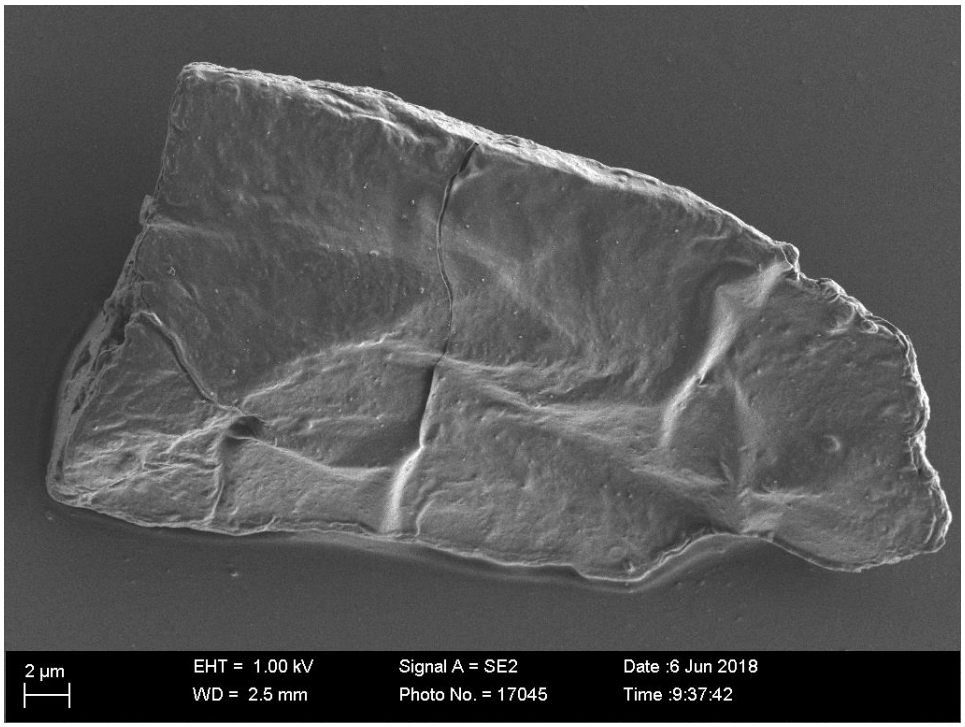

Biological material- organic carbon

Figure 72: Electron micrographs for individual atmospheric PM (aluminosilicates and biological matter) from opencast coal mines (Limpopo and Mpumalanga).

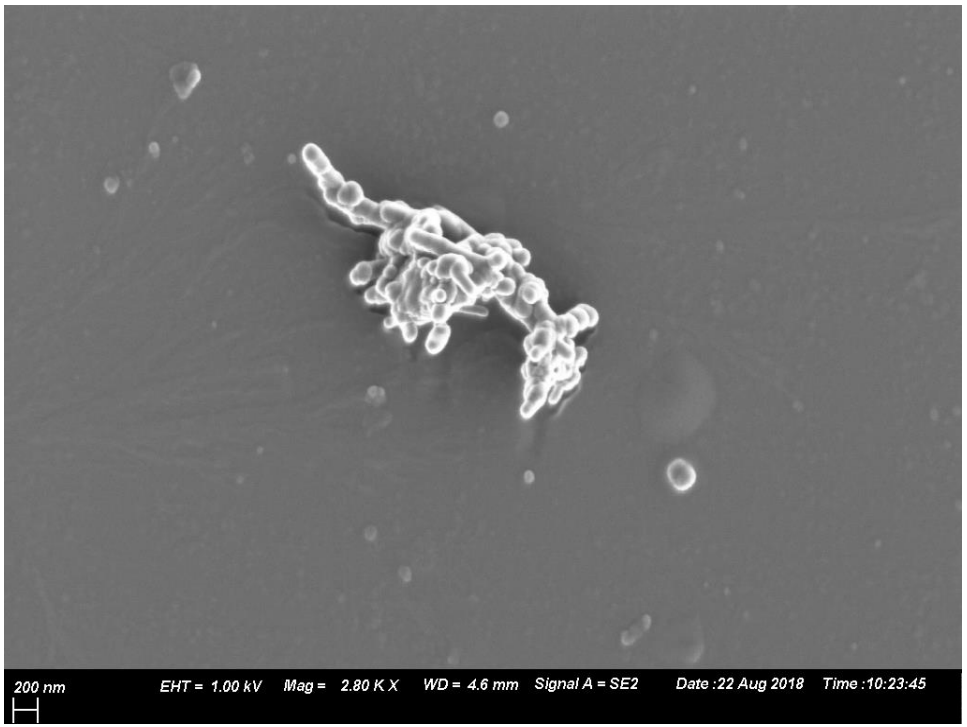

Combustion elemental carbon (DPM)

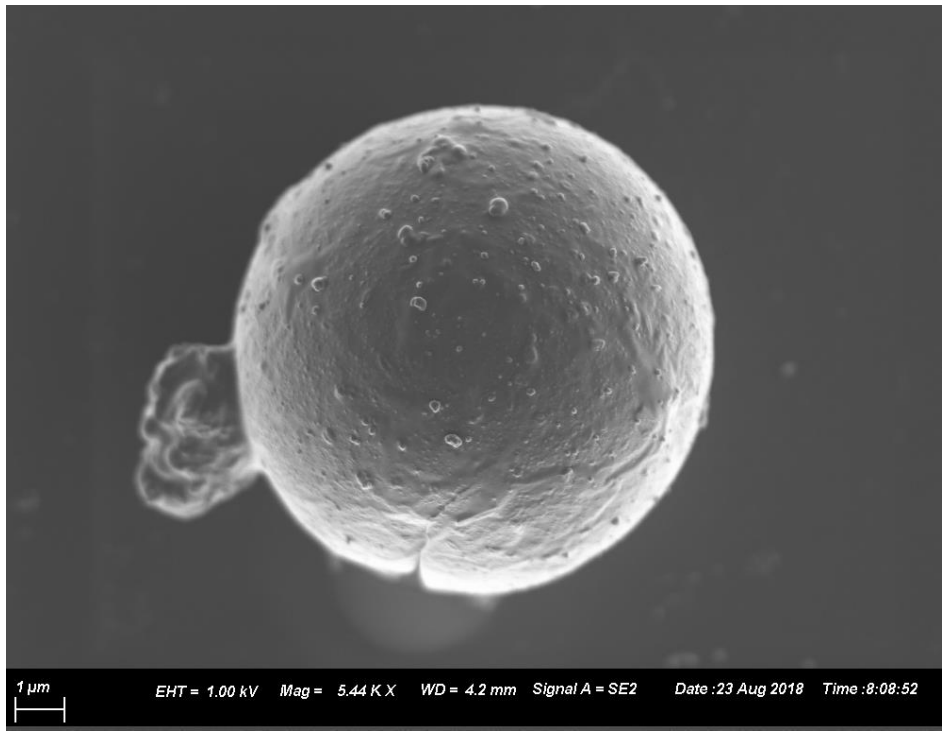

Combustion elemental carbon (fly ash)

Figure 73: Electron micrographs for individual atmospheric PM (combustion spherical particulates) from opencast coal mines (Limpopo and Mpumalanga Province).

4.2.2 Opencast Coal Mining Atmospheric Particulate Matter Samples: EDS

Elemental mapping of selected atmospheric particles from the opencast coal mine samples are shown in Figures 74 to 81. This shows the presence of elements such as C, Mg, Si, O, Cl, Al, S, K and trace amounts of Zn, Fe, Ti and calcium (Ca). The detection of these elements indicates the presence of minerals associated with coal dust. These minerals generally include dolomite ($Ca(CaMg)(CO_3)_2$, quartz in the form of SiO_2, aluminosilicates such as kaolinite ($AlSi_2O_5(OH)_2$), carbonates such as calcites ($CaCO_3$) and illite (KH_3O) (Al, Mg, Fe)$_2$(Si, Al)$_4O_{10}$[(OH)$_2$,(H_2O). Due to the inability of EDS to detect hydrogen, lithium and helium, these are not shown on the spectra.

The analyses show the heterogeneity of the coal dust particulate. This is influenced by local geology i.e different coal seams which influence coal quality. The opencast coal mines included in this study currently exploit coal from the Highveld and Witbank coalfields (Mpumalanga) and the Waterberg coalfields (Limpopo). The Mpumalanga Coalfields have been exploited to the extent that in some areas, low-quality coal indicated by the low carbon content is mined. Most of the particles therefore include some gangue (inorganic mineral) particles with the carbon (Figures 74 to 78), although the varying ratio of Al to Si indicates variation in the composition of the inorganic component. Sodium (Na) and chlorine (Cl) in some of the particles, but not always in stoichiometric ratio corresponding to NaCl, indicates that not all of these elements originate from sea spray. The S content is always less than 1%, indicating a low contribution from secondary atmospheric particulate, as the sulphur content of the coal itself is of the order of 1%.

The spectra of the chain aggregates (Figure 77) indicate a high carbon content. This, as well as the characteristic morphology and the small particle dimensions makes it likely that this is DPM. Particles with a high carbon other than DPM may be of biological origin (Figure 81).

In summary, the EDS results indicate that the atmospheric PM samples captured in coal mine are characterised by carbonaceous and non-carbonaceous material. However, the coupling of chemical composition information obtained from EDS with morphological and particulate dimension information obtained from SEM, does not enable the fingerprinting of the carbon as to its origin.

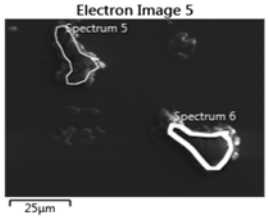

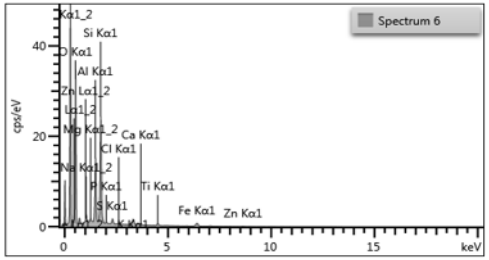

Element	Wt%	Wt%·Sigma	Atomic·%
C	51.52	0.21	62.90
O	31.65	0.18	29.01
Na	0.58	0.03	0.37
Mg	0.25	0.02	0.15
Al	4.11	0.04	2.24
Si	7.43	0.05	3.88
P	0.15	0.02	0.07
S	0.47	0.02	0.21
Cl	0.18	0.02	0.08
K	0.89	0.03	0.33
Ca	0.19	0.02	0.07
Ti	0.48	0.03	0.15

Figure 74: EDS spectrum for individual atmospheric particulate (coal) from opencast coal mining (Mpumalanga).

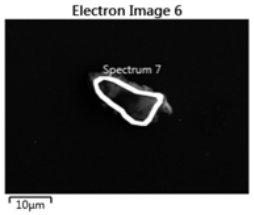

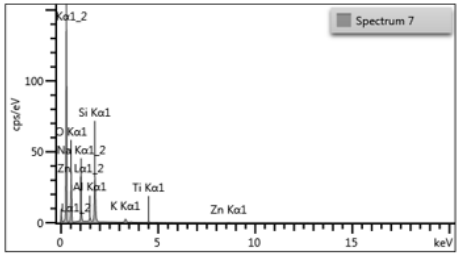

Element	Wt%	Wt% Sigma	Atomic %
C	67.64	0.15	76.45
O	22.71	0.14	19.27
Na	1.17	0.03	0.69
Al	0.43	0.01	0.22
Si	5.63	0.04	2.72
K	0.88	0.02	0.31
Ti	0.40	0.02	0.11
Zn	1.15	0.06	0.24
Total:	100.00		100.00

Figure 75: EDS spectrum for individual particulate (coal) from opencast coal mining (Mpumalanga).

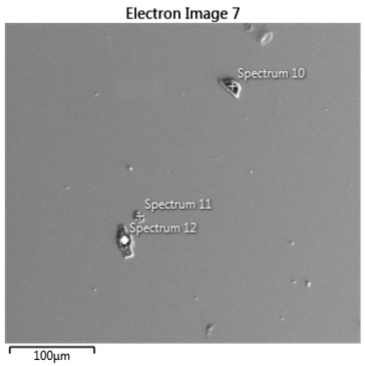

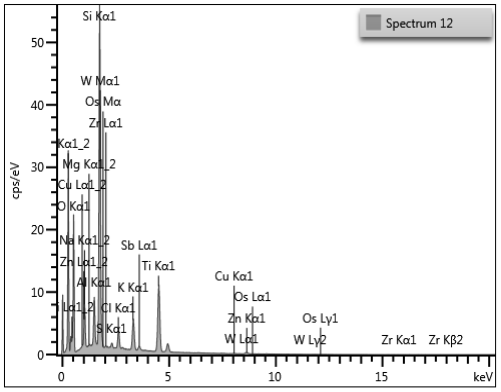

Element	Wt%	Wt%·Sigma	Atomic·%
C	28.05	0.19	48.58
O	13.96	0.10	18.15
Na	1.80	0.04	1.63
Mg	0.08	0.02	0.07
Al	2.72	0.03	2.10
Si	21.99	0.12	16.29
S	0.45	0.03	0.29
Cl	2.03	0.04	1.19
K	4.60	0.05	2.45
Ti	18.76	0.13	8.15
Cu	0.28	0.06	0.09
Zn	1.62	0.09	0.52
Zr	0.62	0.11	0.14
Sb	0.33	0.09	0.06
W	1.58	0.29	0.18
Os	1.12	0.19	0.12
Total:	100.00		100.00

Figure 76: EDS spectrum for individual particulate (coal/gangue) from opencast coal mining (Limpopo).

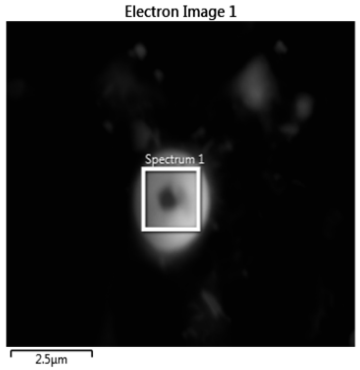

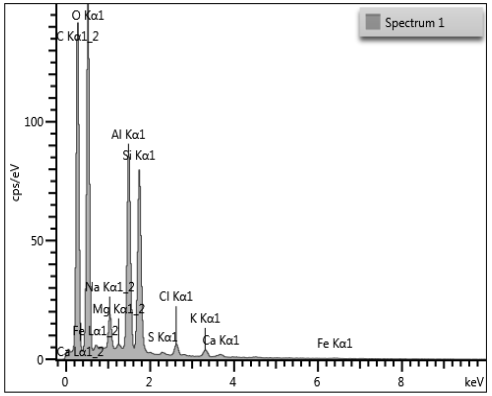

Element	Wt%	Wt% Sigma	Atomic %
C	50.06	0.36	61.66
O	30.55	0.26	28.25
Na	1.35	0.04	0.87
Mg	0.17	0.03	0.10
Al	7.46	0.08	4.09
Si	7.57	0.08	3.99
S	0.11	0.03	0.05
Cl	0.88	0.04	0.37
K	0.81	0.04	0.31
Ca	0.34	0.04	0.13
Fe	0.69	0.18	0.18
Total:	100.00		100.00

Figure 77: EDS spectrum for individual particulates (combustion particle-DPM) from opencast coal mining (Limpopo).

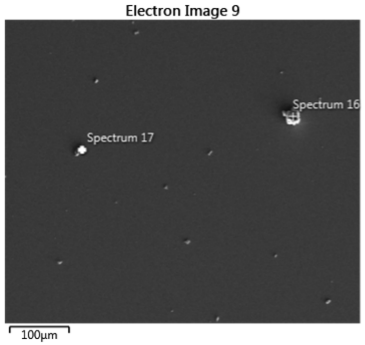

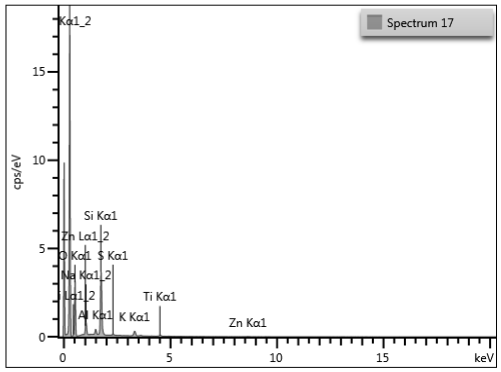

Element	Wt%	Wt% Sigma	Atomic %
C	72.51	0.19	82.68
O	12.31	0.13	10.54
Na	1.10	0.05	0.66
Al	0.71	0.03	0.36
Si	9.44	0.08	4.60
S	0.25	0.03	0.11
K	1.66	0.05	0.58
Ti	0.67	0.06	0.19
Zn	1.35	0.10	0.28
Total:	100.00		100.00

Figure 78: EDS spectrum for individual particulate (coal/gangue) from opencast coal mining (Mpumalanga).

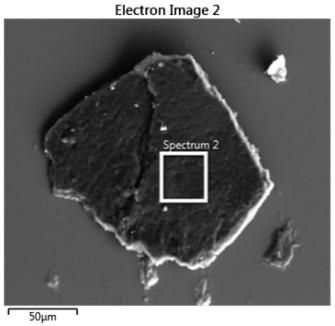

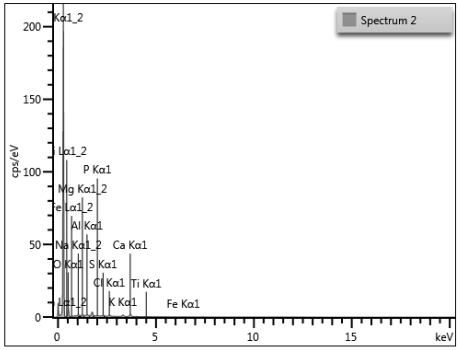

Element	Wt%	Wt% Sigma	Atomic %
C	90.84	0.09	94.98
O	3.97	0.05	3.11
Na	0.28	0.02	0.15
Mg	0.09	0.01	0.04
Al	0.24	0.02	0.11
Si	0.94	0.02	0.42
P	0.05	0.02	0.02
S	0.37	0.02	0.15
Cl	0.48	0.02	0.17
K	0.93	0.03	0.30
Ca	1.52	0.03	0.48
Ti	0.09	0.03	0.02
Fe	0.20	0.04	0.05
Total:	100.00		100.00

Figure 79: EDS spectrum for individual atmospheric particulate (coal) from opencast coal mining (Limpopo).

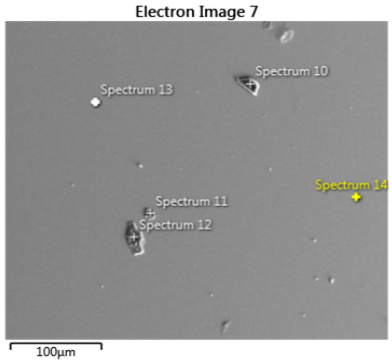

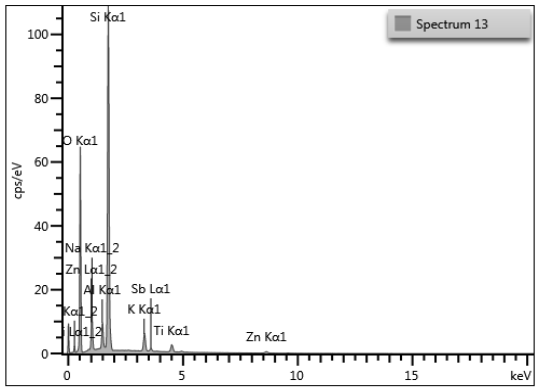

Element	Wt%	Wt%·Sigma	Atomic·%
C	2.00	0.09	3.85
O	32.47	0.12	46.98
Na	1.99	0.05	2.00
Al	2.98	0.04	2.55
Si	45.61	0.13	37.58
K	5.53	0.06	3.27
Ti	4.10	0.07	1.98
Zn	4.66	0.10	1.65
Sb	0.67	0.11	0.13
Total:	100.00		100.00

Figure 80: EDS spectrum for individual particulate (gangue) from opencast coal mine (Limpopo).

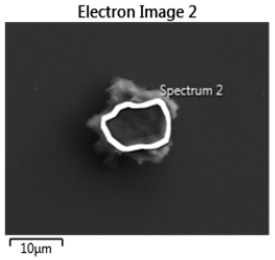

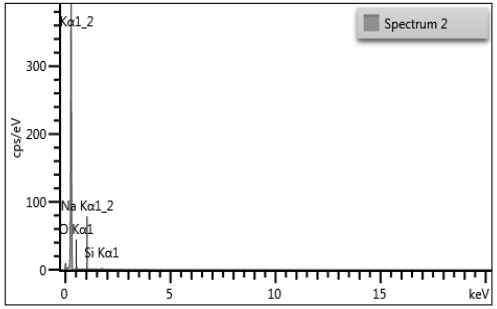

Element	Wt%	Wt% Sigma	Atomic %
C	95.50	0.11	96.70
O	4.12	0.11	3.13
Na	0.08	0.02	0.04
Si	0.30	0.02	0.13
Total:	100.00		100.00

Figure 81: EDS spectrum for individual atmospheric particulate (biological material- carbon) from opencast coal mines (Mpumalanga).

4.2.3 Community Atmospheric Particulate Matter Samples: SEM

Electron micrographs for community atmospheric PM samples (Limpopo and Mpumalanga) are shown for bulk atmospheric particulates in Figures 82 to 85 and individual atmospheric particulates in Figures 86 to 88. Particulate morphology is heterogenous and contains spherical, conical, solid irregular, chain aggregates and linear particulates. Particle dimensions vary from >1 µm to 50 µm indicating the presence of fine and coarse particles.

Coal dust particles are observed in the atmospheric PM samples of the communities of Delpark, Clewer and Marapong (Figure 82). These particles are characterised by serrated edges, a layered appearance and particle dimensions of 5-10 µm, indicating the influence of the mechanical processes associated with opencast coal mining in their formation. However, the percentage of coal dust particulates in the community atmospheric was relatively small: Delpark 15%, Marapong 9% and Clewer 36% and this is due to various coal mining related activities adjacent to this community.

Small quantities of fly ash are detected in two of the community atmospheric PM samples (5% in Clewer and 3% in Marapong) (Figure 83). These are identified by their spherical morphology. The chain agglomerates of <1 µm observed in all the community particulate but particularly at Clewer samples (Figure 84) are identified as DPM emitted from vehicles and other diesel equipment due to their high carbon content. Geological and biological particulates are identified in all the community samples (Figure 87 and Figure 88). The sources of geological material are identified as coal mining activities located adjacent to these communities, as well as unpaved roads and open grounds within the communities.

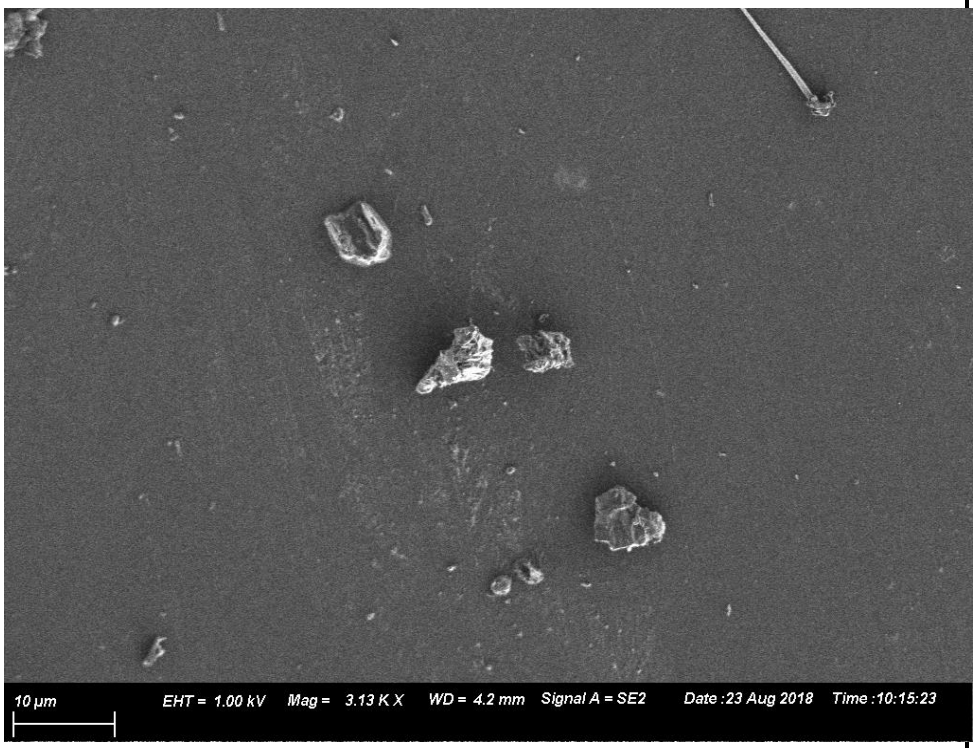

Coal and geological material

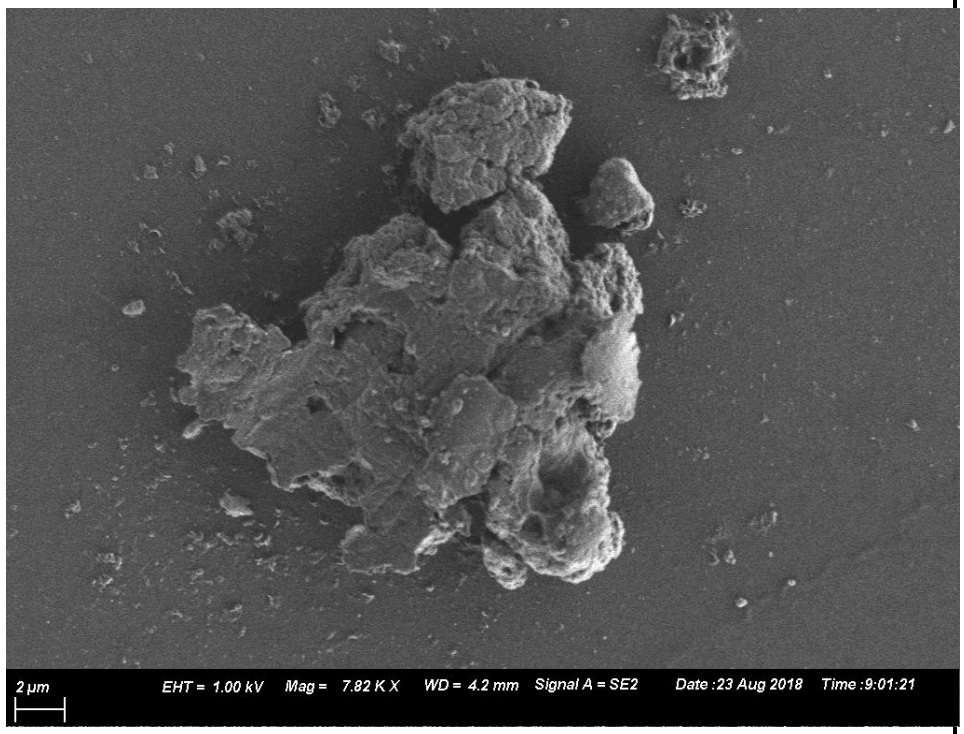

Coal dust

Figure 82: Electron micrographs of community bulk atmospheric PM (Limpopo and Mpumalanga).

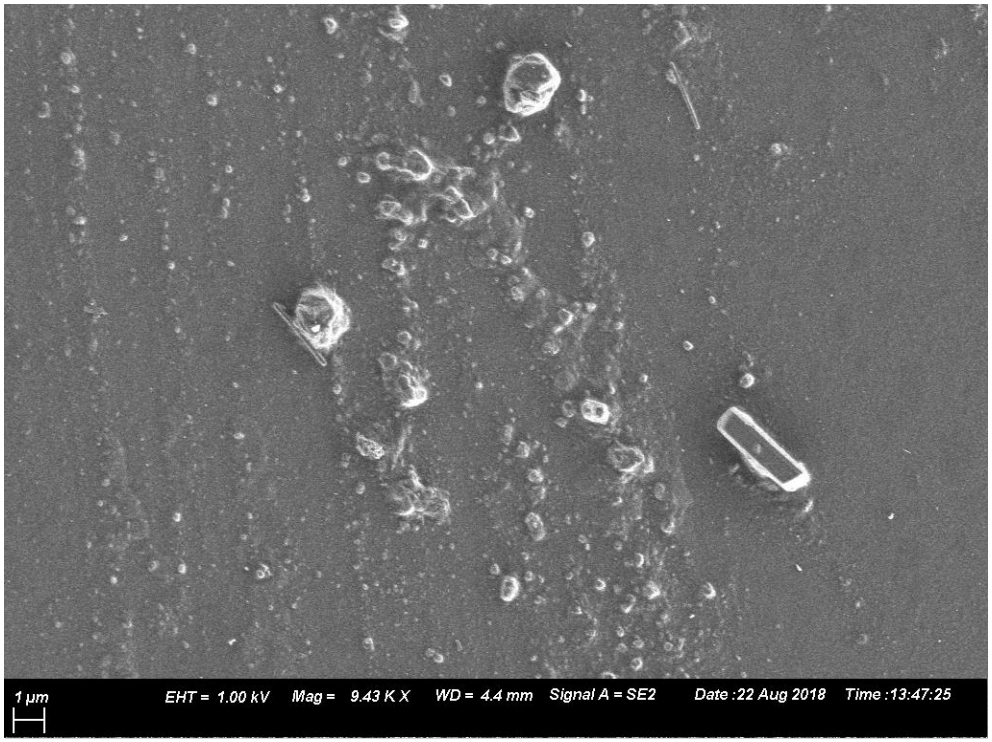

Combustion particulate and fly ash

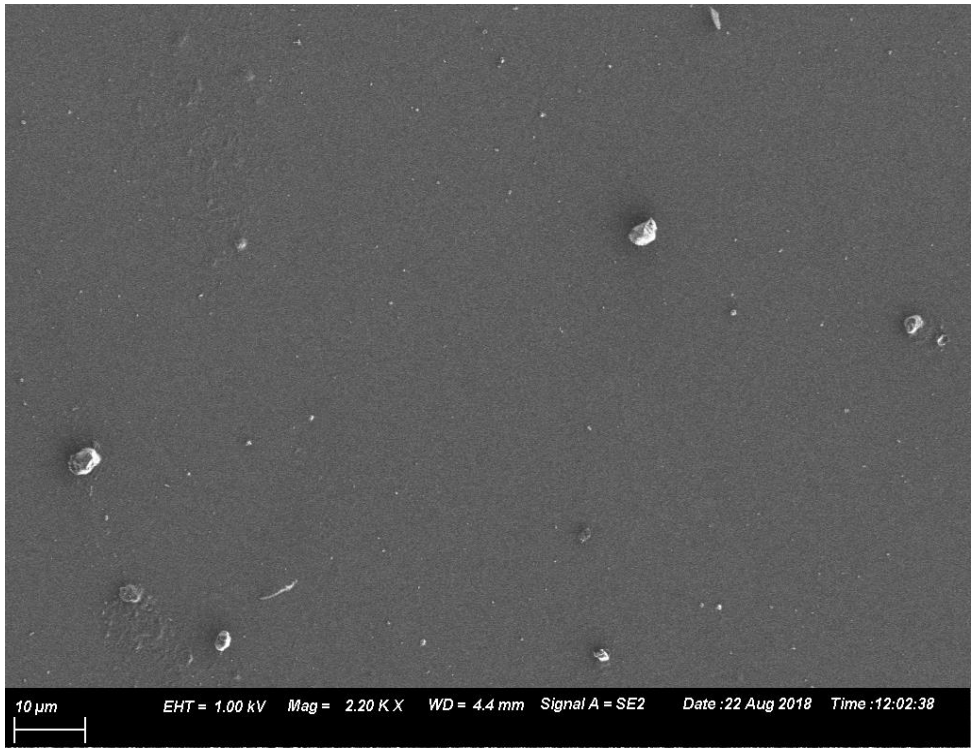

Combustion particulate

Figure 83: Electron micrographs of community bulk atmospheric PM (combustion particulates and fly ash) (Limpopo and Mpumalanga).

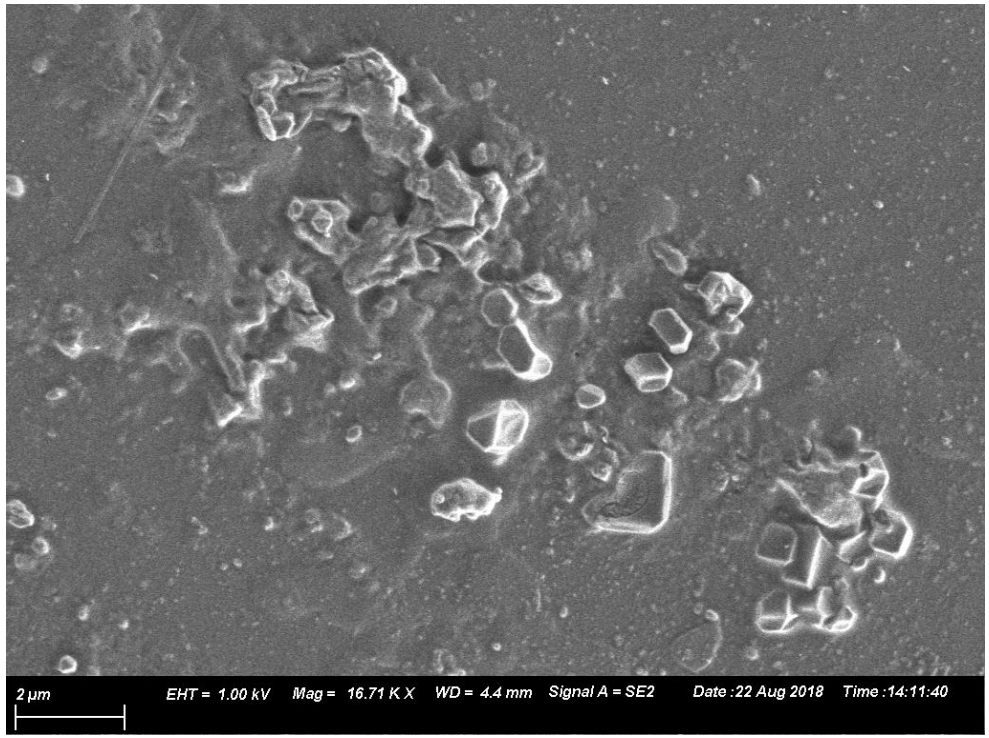

Crystalline geological material

Diesel particulate matter (DPM)

Figure 84: Electron micrographs for community bulk atmospheric PM (crystalline geological material and DPM) (Limpopo and Mpumalanga).

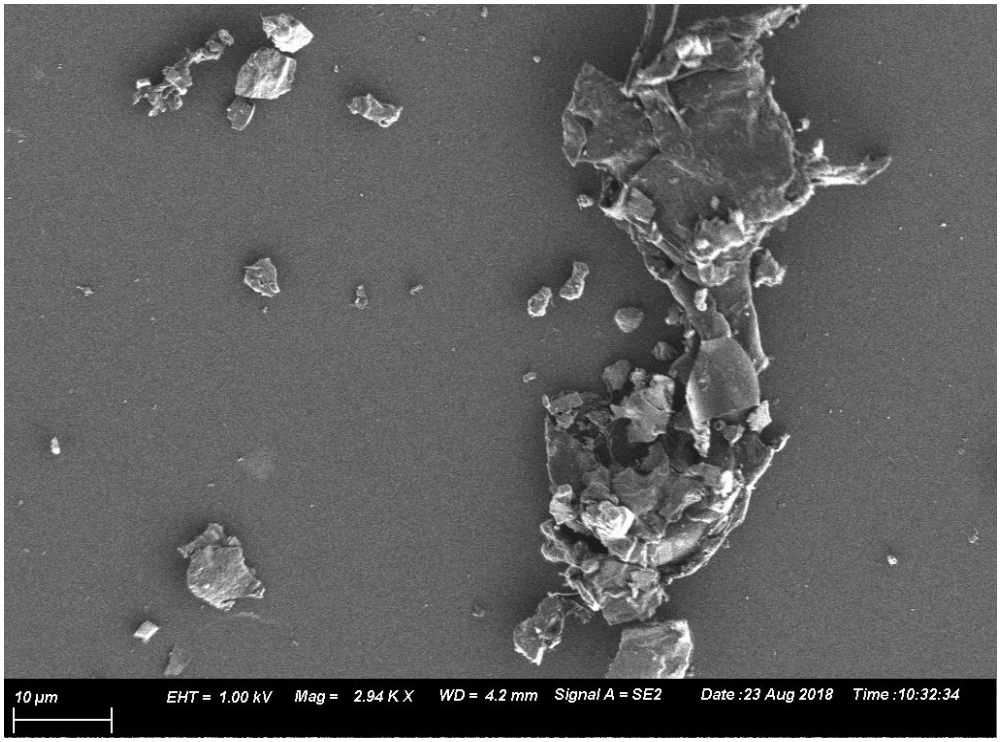

Geological material

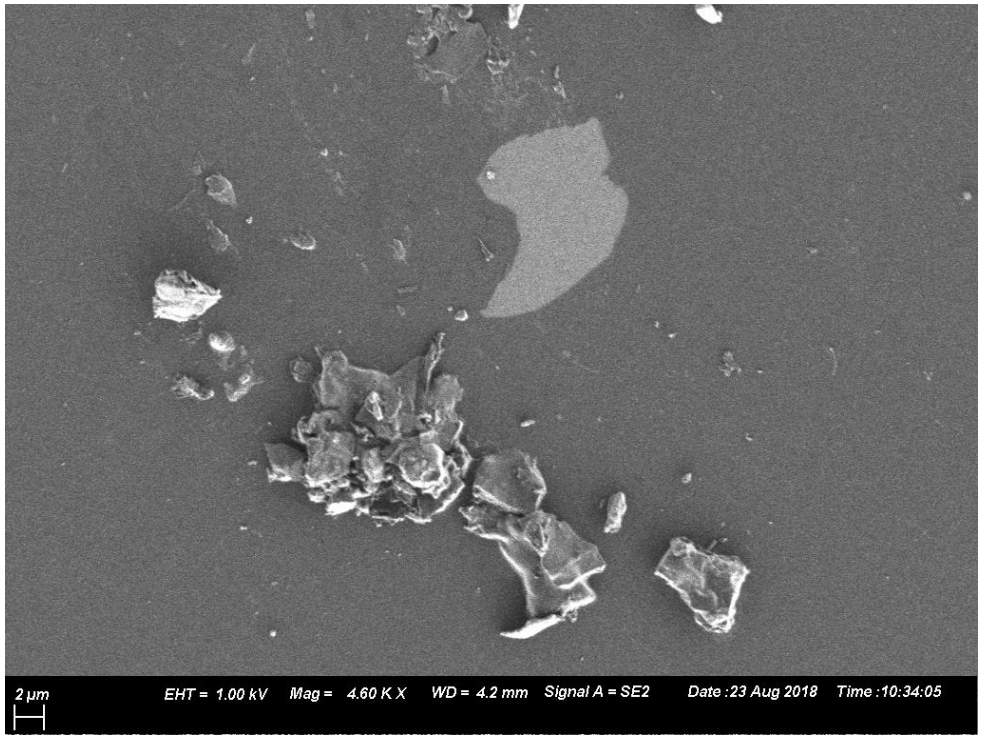

Geological material

Figure 85: Electron micrographs for community bulk atmospheric PM (geological material) (Limpopo and Mpumalanga).

*

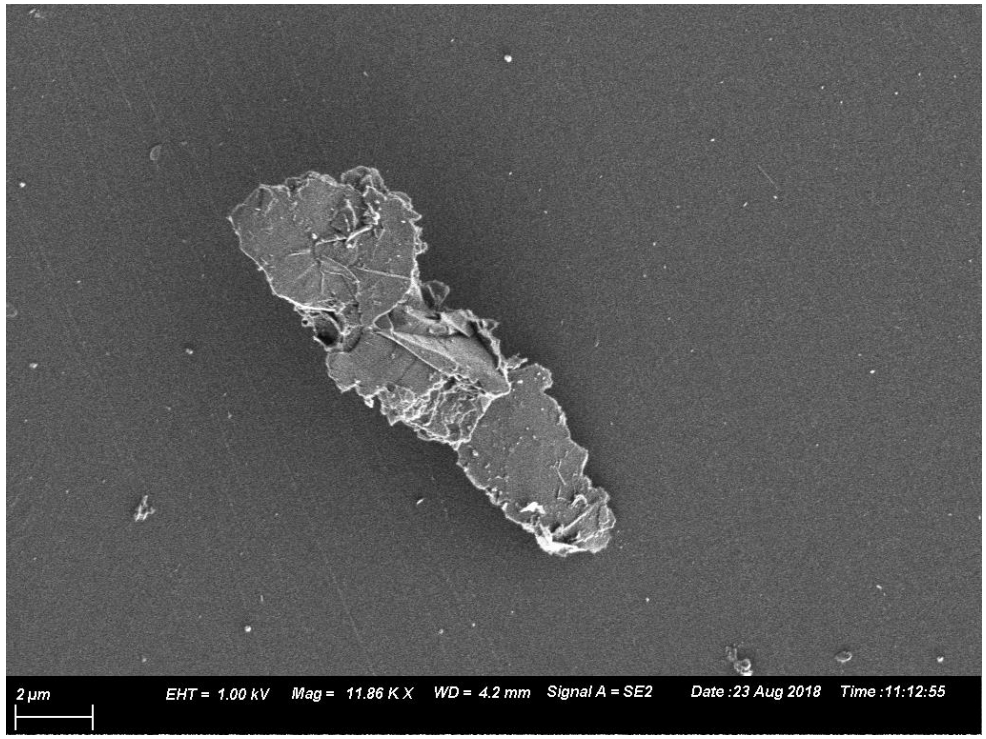

Coal dust

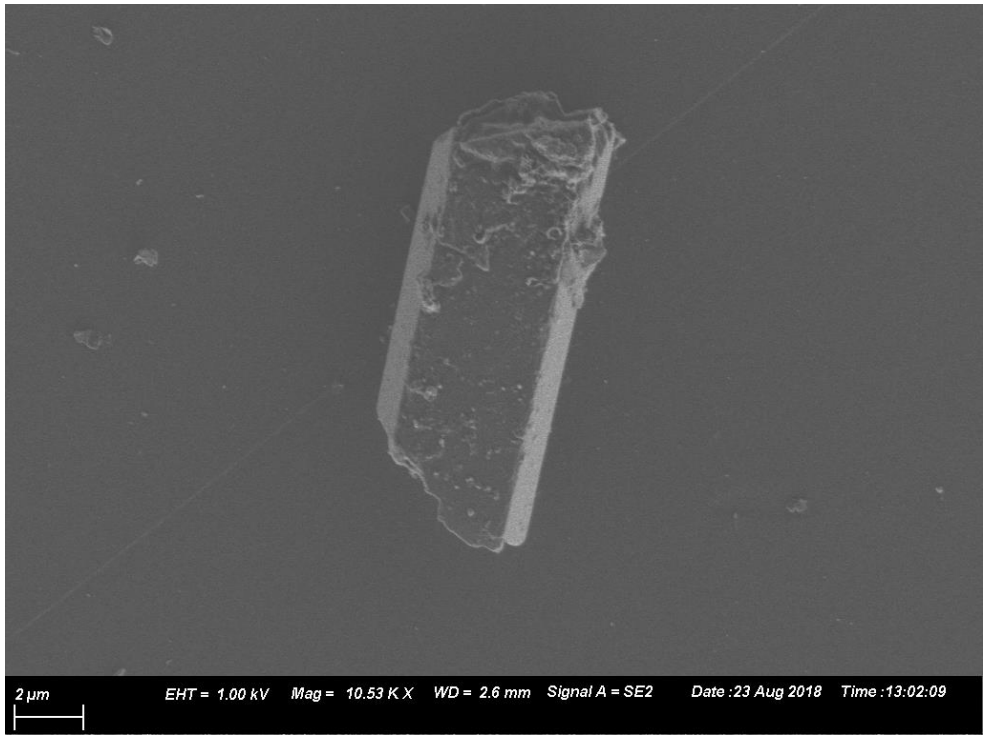

Crystalline material

Figure 86: Electron micrographs for community individual atmospheric PM (coal dust and crystalline material) (Limpopo and Mpumalanga).

Biological material-organic carbon

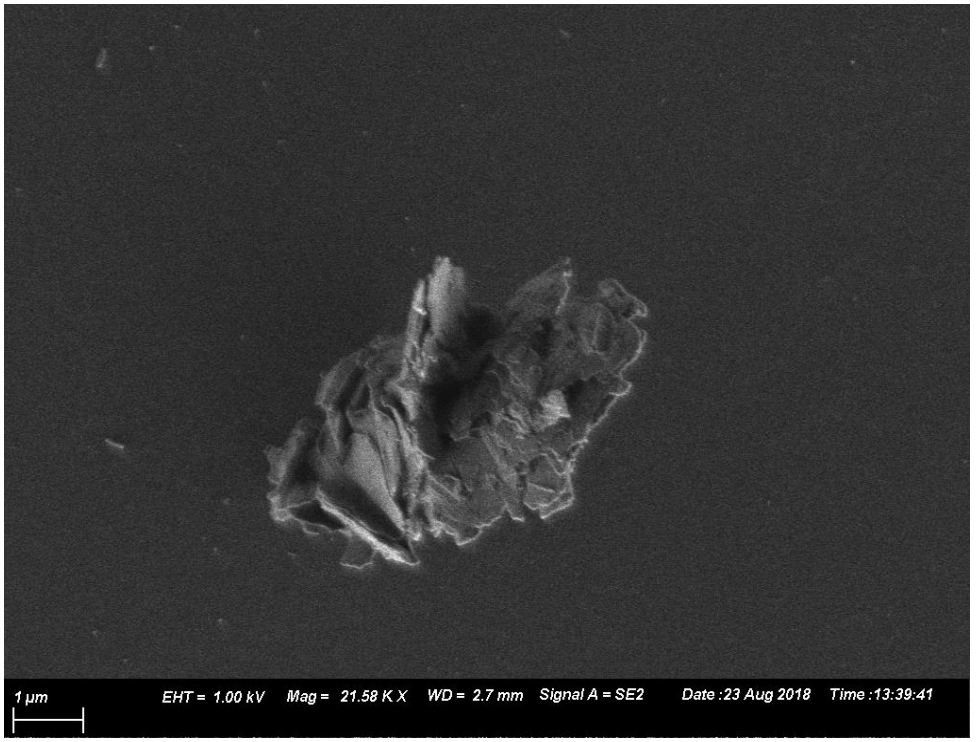

Coal dust

Figure 87: Electron micrographs for community individual atmospheric PM (biological material and coal dust) (Limpopo and Mpumalanga).

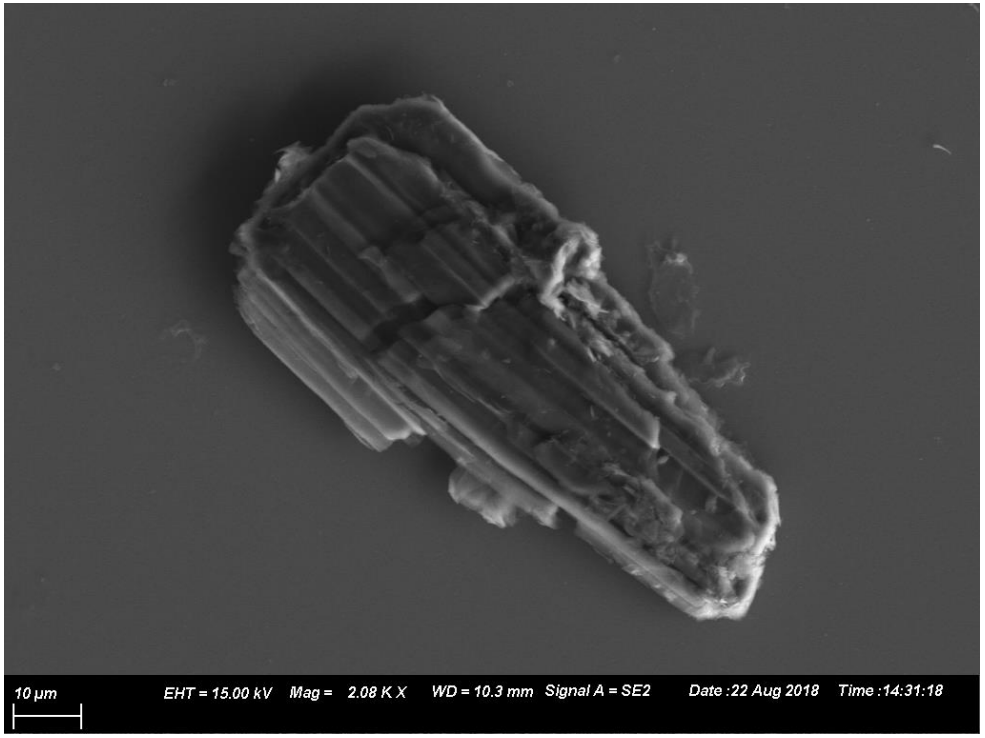

Biological material-organic carbon (also see fig 90)

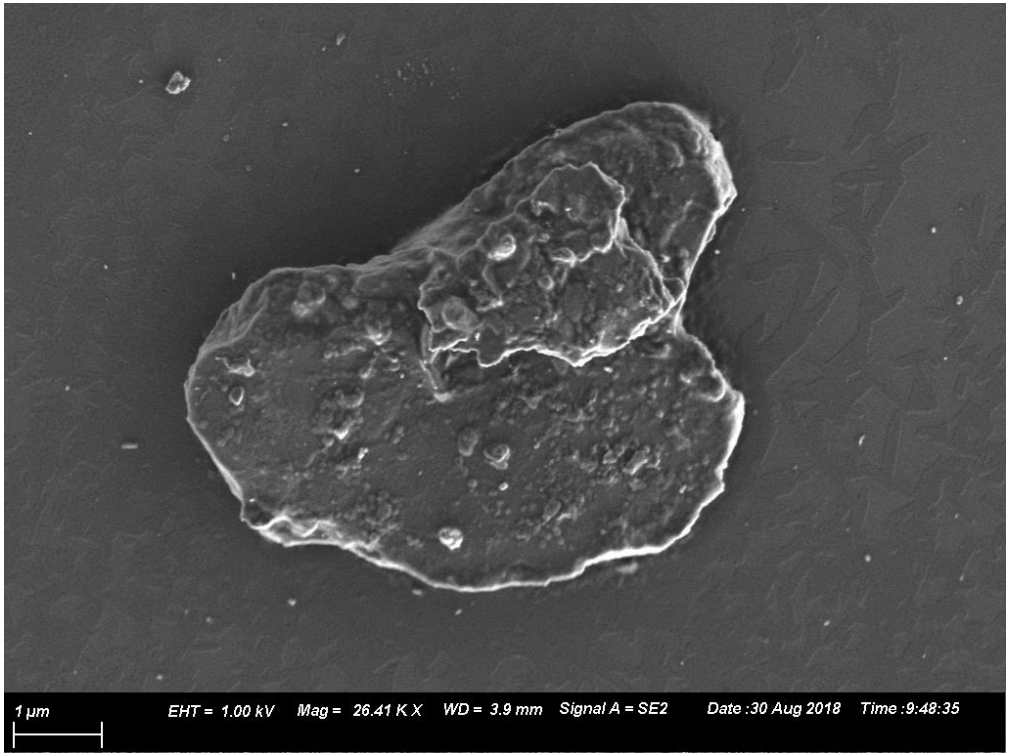

Geological material

Figure 88: Electron micrographs for community individual atmospheric PM (biological and geological material) in Limpopo and Mpumalanga Province.

4.2.4 Community Atmospheric Particulate Matter Samples: EDS

EDS spectra for community atmospheric particulates are shown in Figures 90 to 96. These show the presence of C, Si, O_2, Cl, S and trace amounts of Zn, Fe, Ti and Ca. However, a comparison of the number of particulates with a carbon signature indicates a decrease of 67% from that of the opencast coal mine atmospheric PM samples.

The sulphur content of the coal dust particulates in the community samples is generally higher than that of the opencast coal mine samples (Figure 92 and Figure 94). This could possibly be attributed to combustion related activities such as domestic fuel burning, informal waste incineration (see Figure 89 below), power generation and spontaneous combustion of coal, which may lead to high and localised levels of SO_2 and secondary sulphates. The elemental spectra for the chain aggregates observed during SEM analysis of the community atmospheric PM samples indicate a high carbon content (99% in some cases). The presence of these carbonaceous chain agglomerates signals the presence of DPM from vehicle emissions. Biological material was also observed in the community samples. The carbon content of the biological material varied from 95-99% (Figure 90 and Figure 91).

Figure 89: Domestic fuel burning (Delpark and Clewer) and open burning of waste (Lephalale).

Semi-carbonaceous particulate (Figure 94) may indicate that coal mining operations do impact adjacent communities. In coal mining operations, the pulverisation of coal results in the liberation of pure mineral components or mineral grains that have an association with carbonaceous particulates. The presence of salt crystals with Na and Cl in approximately the stoichiometric ratio of sea salt (Figure 95) may indicate an oceanic origin.

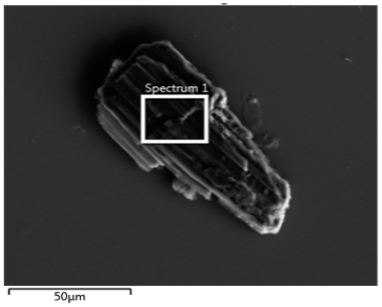

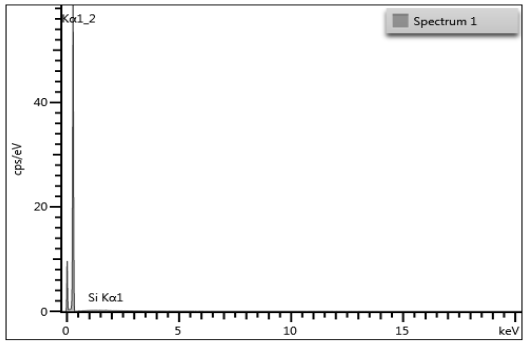

Element	Wt%	Wt% Sigma	Atomic %
C	99.90	0.03	99.96
Si	0.10	0.03	0.04
Total:	100.00		100.00

Figure 90: EDS spectrum for community individual atmospheric particulate (biological material- organic carbon) (Limpopo).

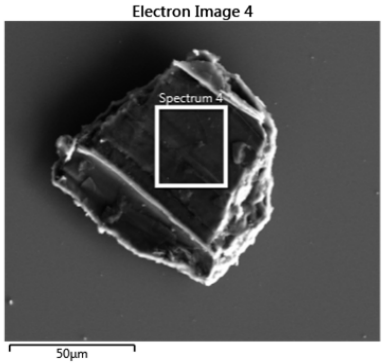

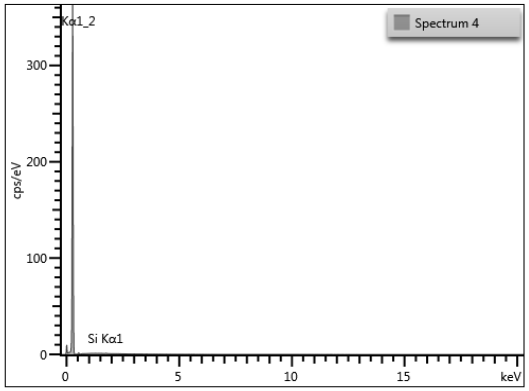

Element	Wt%	Wt% Sigma	Atomic %
C	99.90	0.02	99.96
Si	0.10	0.02	0.04
Total:	100.00		100.00

Figure 91: EDS spectrum for community individual atmospheric particulate (biological material- organic carbon) (Mpumalanga).

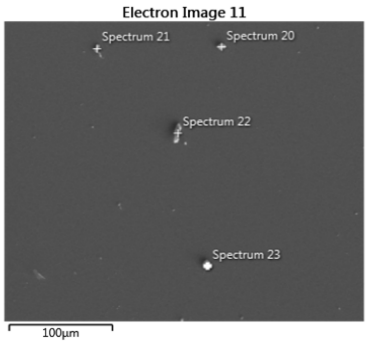

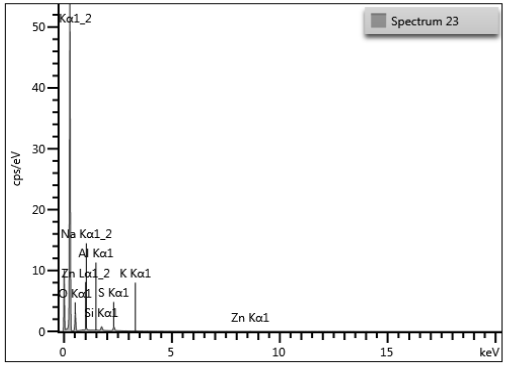

Element	Wt%	Wt% Sigma	Atomic %
C	90.14	0.12	93.60
O	6.72	0.09	5.24
Na	0.17	0.03	0.09
Al	0.07	0.02	0.03
Si	0.88	0.03	0.39
S	1.24	0.04	0.48
K	0.12	0.03	0.04
Zn	0.66	0.07	0.13
Total:	100.00		100.00

Figure 92: EDS spectrum for community individual atmospheric particulate (coal dust) (Mpumalanga).

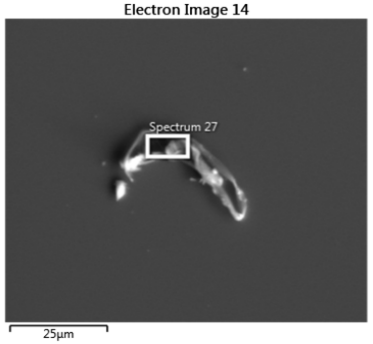

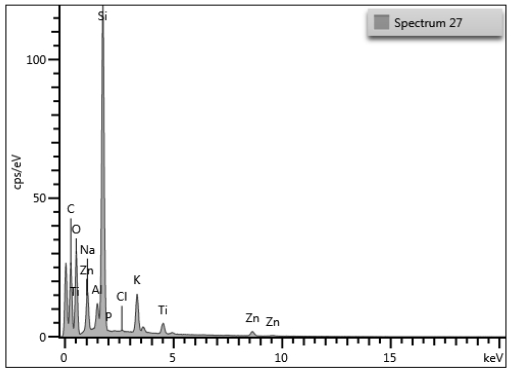

Element	Wt%	Wt%·Sigma	Atomic·%
O	24.81	0.15	39.09
Na	3.99	0.11	4.37
Al	3.52	0.06	3.28
Si	46.52	0.16	41.75
P	0.19	0.05	0.16
Cl	0.27	0.04	0.19
K	9.90	0.08	6.38
Ti	4.30	0.08	2.26
Zn	6.49	0.16	2.50
Total:	100.00		100.00

Figure 93: EDS spectrum for individual atmospheric particulate (geological material or soil) (Limpopo).

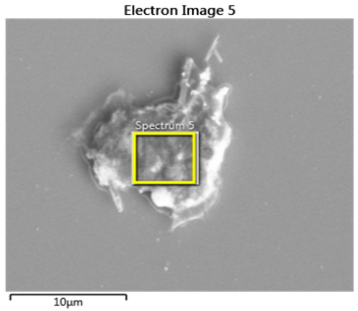

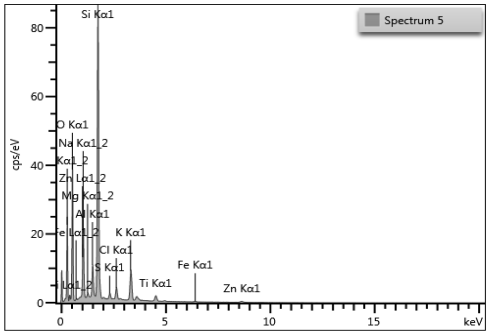

Element	Wt%	Wt%-Sigma	Atomic-%
C	22.08	0.18	36.78
O	20.59	0.11	25.75
Na	4.72	0.06	4.11
Mg	0.39	0.02	0.32
Al	3.02	0.04	2.24
Si	31.92	0.12	22.74
S	0.95	0.03	0.59
Cl	2.19	0.04	1.24
K	7.70	0.07	3.94
Ti	2.52	0.06	1.05
Fe	0.60	0.08	0.22
Zn	3.33	0.11	1.02
Total:	100.00		100.00

Figure 94: EDS spectrum for community individual atmospheric particulates (geological material-semi-carbonaceous) (Mpumalanga).

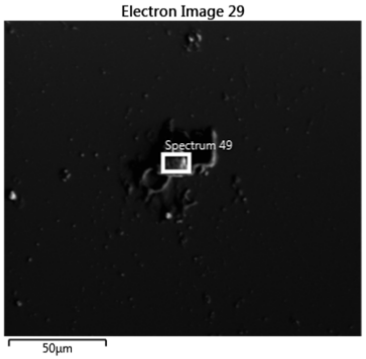

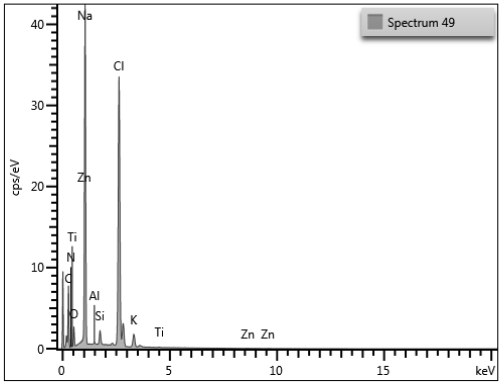

Element	Apparent Concentration	Wt%	Wt% Sigma	Standard Label
N	0.49	0.59	0.12	BN
O	2.29	3.59	0.07	SiO2
Na	28.72	33.98	0.11	Albite
Al	0.09	0.18	0.02	Al2O3
Si	0.87	1.77	0.03	SiO2
Cl	25.71	55.68	0.13	NaCl
K	1.79	4.02	0.06	KBr
Ti	0.07	0.20	0.05	Ti
Zn	0.00	0.00	0.00	Zn
Total:		100.00		

Figure 95: EDS spectrum for community individual atmospheric particulate (salt crystals) (Limpopo).

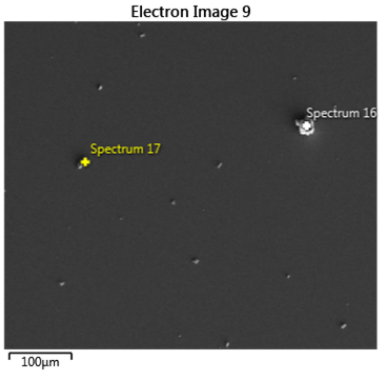

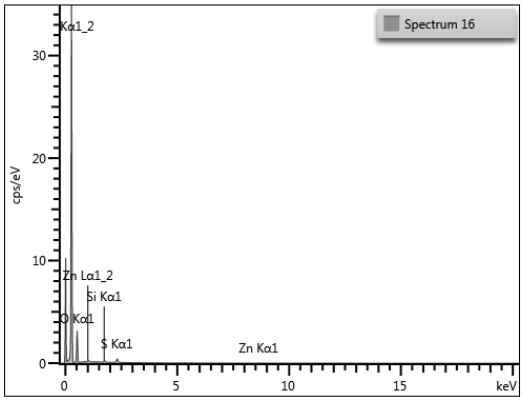

Element	Wt%	Wt%·Sigma	Atomic·%
C	86.54	0.16	90.45
O	11.18	0.14	8.78
Si	0.42	0.03	0.19
S	1.16	0.05	0.46
Zn	0.69	0.07	0.13
Total:	100.00		100.00

Figure 96: EDS spectrum for community individual atmospheric particulate (coal dust- organic carbon) (Limpopo).

4.3 Characterisation of Atmospheric Particulate Matter Through Reflectance Microscopy

4.3.1 Reflectance Microscopy

The analysis of the resin blocks with embedded atmospheric particles obtained from opencast coal mines bulk samples indicates particle diameters of 1 µm to 80 µm (Figure 97). The black particles observed in the reflectance microscope images indicate the presence of coal dust (Figure 97). However, the identification and characterisation of coal dust and non-coal dust particulates using reflectance microscopy is not possible in this research study due to the inability to observe reflectance from the small particles using the available microscope. Consequently, the microscopic analysis of the resin block with the community atmospheric PM samples was not pursued.

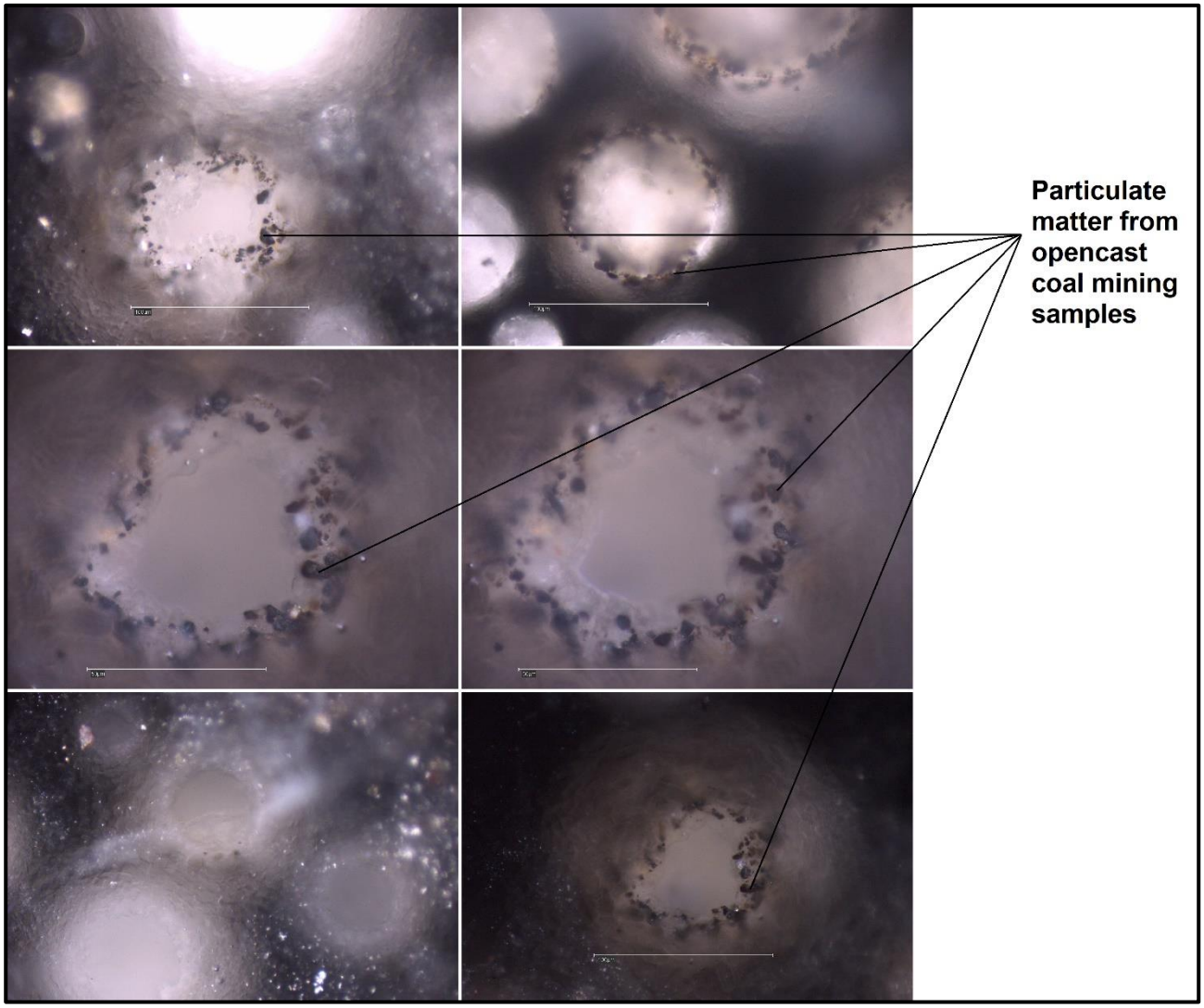

Figure 97: Electron micrographs for coal dust particulates from opencast coal mine atmospheric PM samples.

4.4 Characterisation of Particulate Matter Through X-Ray Photoelectron Microscopy

4.4.1 XPS on Opencast Coal Mining Atmospheric Particulate Samples

High resolution XPS survey spectra were collected for the different opencast mine particulate samples. The survey spectrum of one of the opencast coal mines' atmospheric PM samples is shown in Figure 98. The elements which dominate the surface of the atmospheric PM samples (after sputtering) are O_2 (59%), Si (21%) and C (18%), with 2% Na. The variation in the oxygen/ carbon ratio (O/C) ratio is attributed to significant emissions of oxygen-containing compounds such as CO_2. The presence of Si indicates the presence of oxides such as SiO_2 which is found in geological material and fly ash. The low carbon percentage in the particulate sample is an indicator of the presence of carbonaceous atmospheric PM.

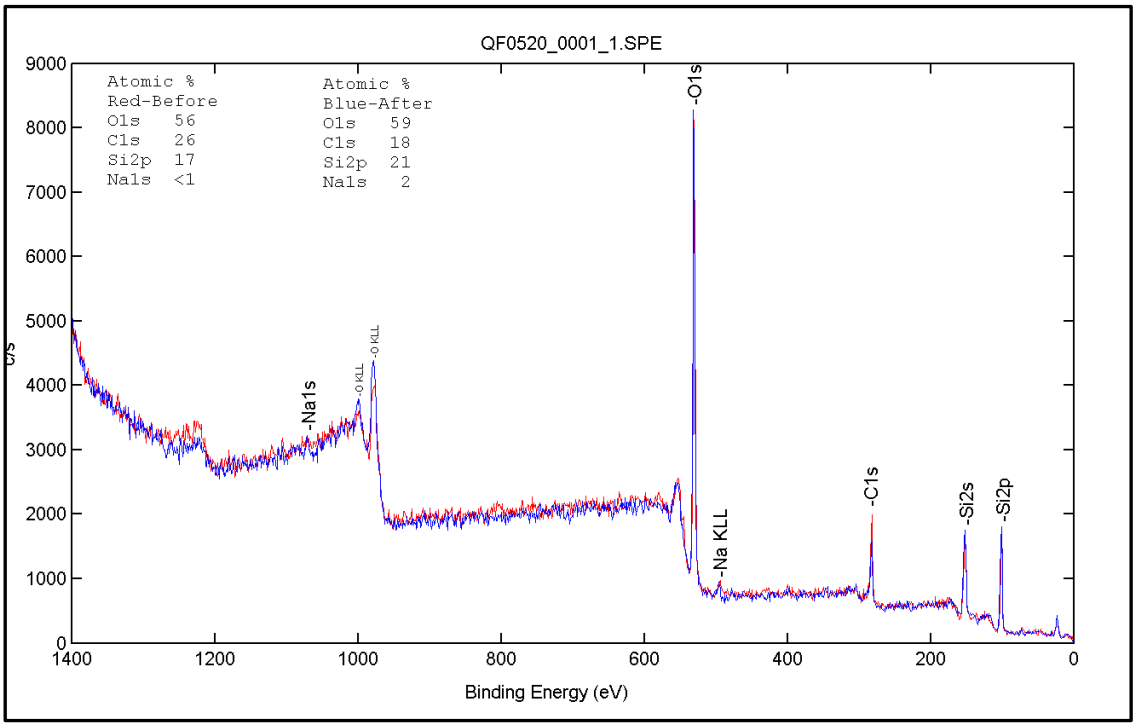

Figure 98: XPS high resolution spectra before (Red) and after (Blue) 2-minute sputter for a coal mine atmospheric PM sample.

The carbon signal or binding energy, after sputtering, varies from 284.5eV (1 peak fit), 284.2eV to 285.6eV (2 peak fit) and 284.1eV to 286.4eV (3 peak fit) (Figure 99). The principal hydrocarbon (C*x*H*y*) peak is assumed to be at 284.6eV. The extension of the carbon signal up to a binding energy of 287.6eV is an indication that carbon is not entirely found in its pure state on the surface of the samples but is bonded to electronegative atoms

such as H and O in chemical compounds. However, H cannot directly be observed in XPS spectra. The relatively low variations observed in the carbon signals or binding energies is an indication that the chemical compounds formed due to the involvement of H with carbonaceous systems exhibit similarities in chemistry. Ultimately, XPS indicates marginal differences between the effects of carbon to carbon (C-C), hydrocarbons (C_xH_y) and carbon to hydrogen (C-H) bonds. The presence of C is an indication of the presence of carbonaceous and semi-carbonaceous atmospheric particulates.

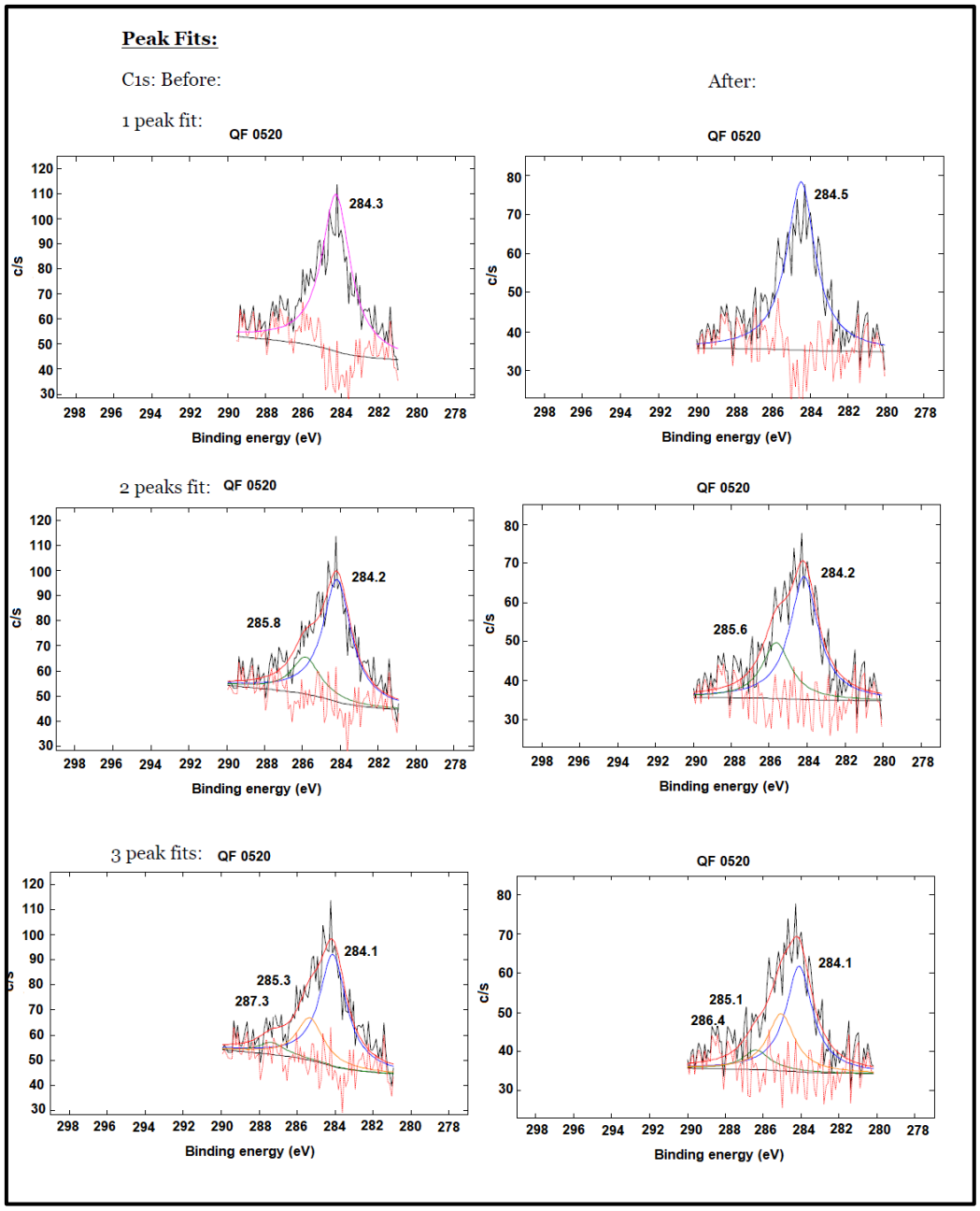

Figure 99: XPS peak fits for carbon binding energy- high resolution spectra before (Red) and after (Blue) 2-minute sputter for an opencast coal mine atmospheric PM sample.

4.4.2 XPS on Community Atmospheric Particulate Samples

High resolution XPS survey spectra, after sputtering, for an atmospheric PM sample from one of the communities is shown in Figure 100. The dominant elements on the surfaces of the atmospheric particulates (after sputtering) are Si (27%), C (14%) and O_2 (58%).The atomic percentage of O_2 is much higher than that of C, Si and Na. Similar to the opencast mine samples, the variation in the oxygen/ carbon ratio (O/C) ratio is attributed to significant emissions of oxygen or oxygen-containing compounds by different sources. These sources include vegetation, coal mining and other industrial activities, CO_2 from spontaneous combustion, incomplete combustion and SiO_2 from overburden and topsoil, power generation (CO_2 and SiO_2-fly ash). Domestic fuel combustion and open burning of waste identified in the different communities are also sources of CO_2 and CO emissions. The total relative weight percentages of Si and O_2 on the sample are in the region of 85%. This is an indication of the presence of geological material and fly ash (SiO_2) in the atmospheric PM samples. Although Na is observed in the sample, it occurs in a lower percentage (<1%) (Figure 100).

The presence of carbon is an indication of the presence of carbonaceous material in this community atmospheric PM sample. The chemical states of carbon in the community sample is identified from high resolution spectra. The carbon signal or binding energy, after sputtering, varies from 284.6eV (1 peak fit), 284eV to 285eV (2 peak fit) and 283.9eV to 287.6eV (3 peak fit) (Figure 101). This extension of the carbon signal up to a binding energy of 287.6eV is an indication that carbon is not entirely found in its pure state on the surface of the atmospheric PM sample and is bonded to atoms such as O and H. The chemical compounds formed from this association indicate the presence of carbonaceous or semi-carbonaceous material. Although different binding energies of carbon are observed, this information is inadequate for the purposes of apportioning the carbon content, as the differences observed in the XPS results are due to chemical bonding of carbon to other elements and not differences associated to different chemical states of carbon itself.

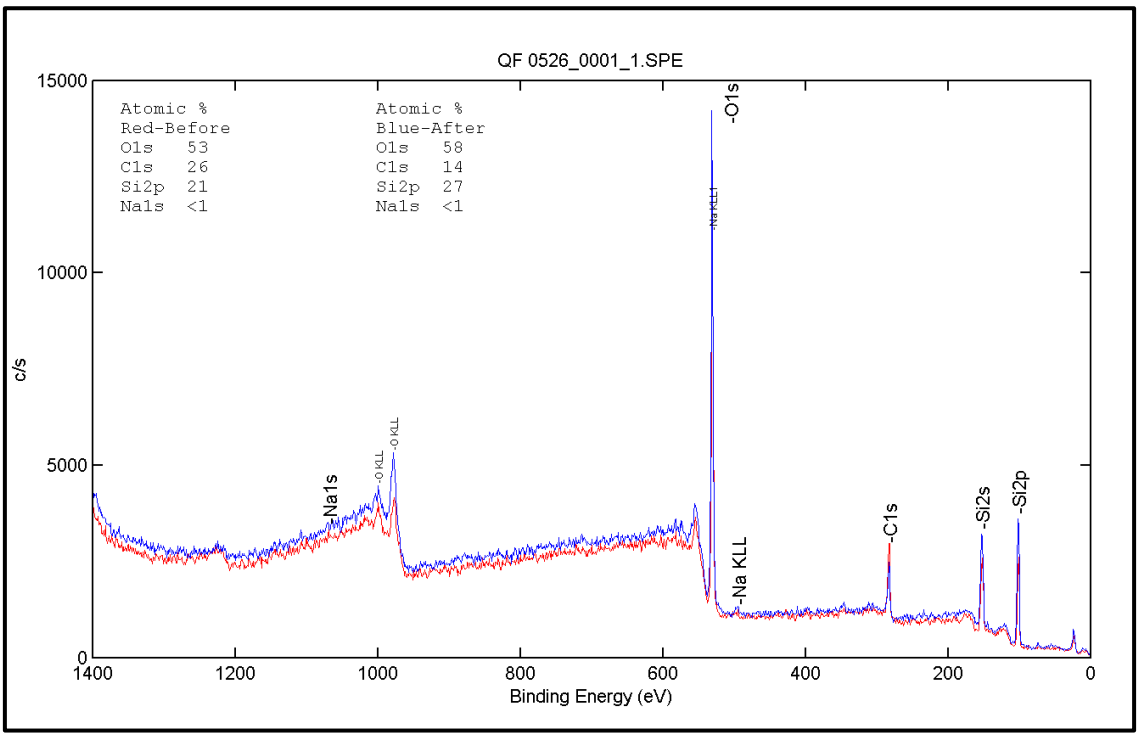

Figure 100: XPS high resolution spectra before (Red) and after (Blue) 2-minute sputter for a community atmospheric PM sample.

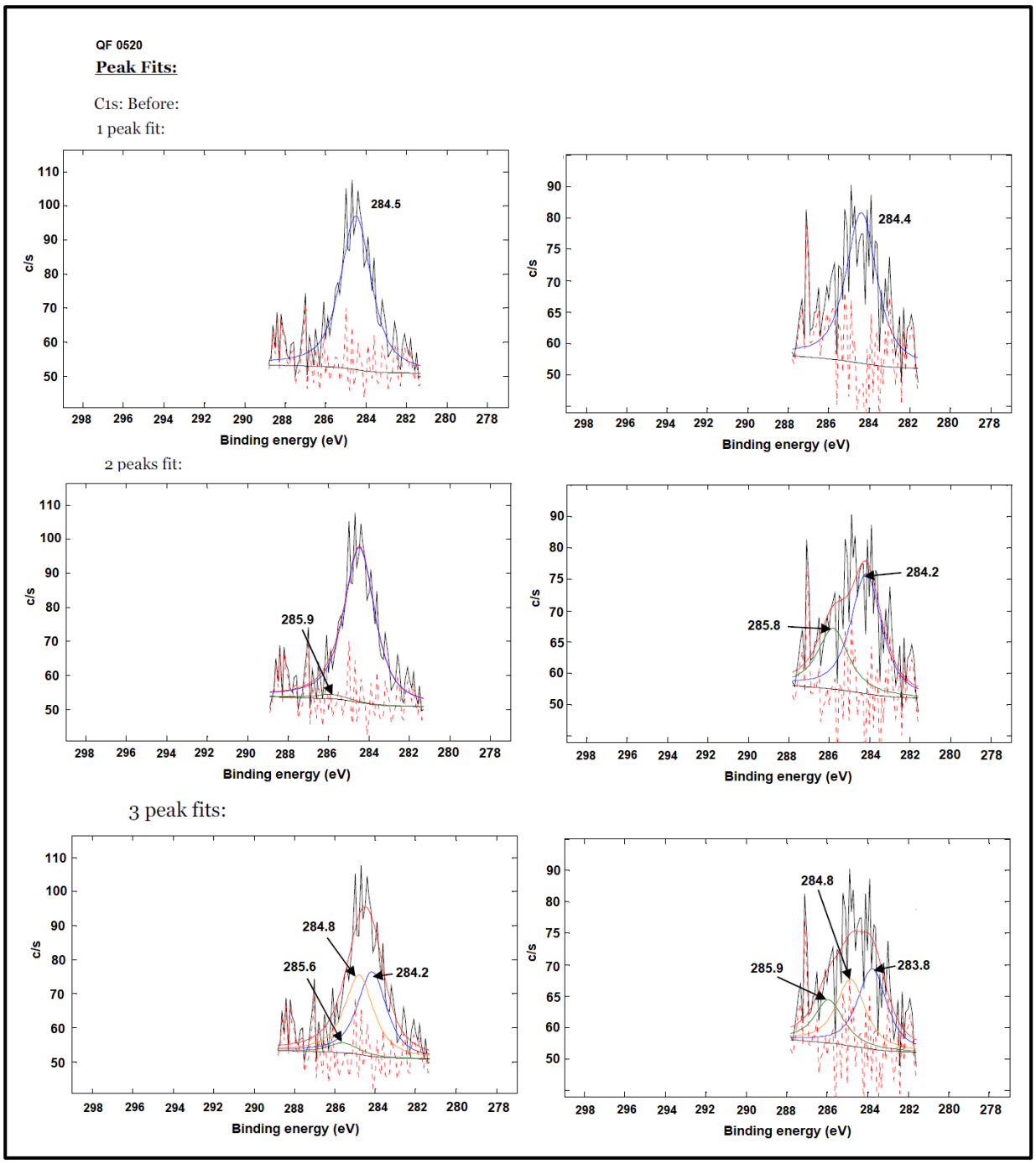

Figure 101: XPS peak fits for carbon binding energy- high resolution spectra before (Red) and after (Blue) 2-minute sputter for a community particulate sample.

4.5 Optical Microscopy: Characterisation of Atmospheric Particulate Matter

4.5.1 Opencast Coal Mining Atmospheric Particulate Matter

Optical microscopy images of atmospheric PM obtained by passive sampling from opencast coal mining operations in Mpumalanga and Limpopo are shown in Figure 102 and Figure 103 respectively. These images lack detail due to limitations of the optical microscope (diffraction limit, poor resolution and small depth of focus). However, the morphological characteristics of the particulates may be observed and vary from linear, spherical, solid irregular to chain agglomerates. Particle dimensions vary from 2 to over 100 µm.

A comparison of the atmospheric PM morphological characteristics observed during SEM analysis and optical microscopy indicates that less detail is observed on the optical microscopy results. However, the presence of solid irregular atmospheric particulates (coarse particles) is attributed to opencast mining mechanical activities such as excavation, drilling and blasting, crushing and screening, exposed areas or ground, material handling and stockpiles. The sources of observed spherical particulates and chain agglomerates are probably attributable to combustion related activities such as spontaneous combustion of coal, products of combustion from industrial activities, power generation and vehicle emissions.

The limitations associated with the optical microscope mean that this technique cannot be used for apportionment between the mine-related and the community-related sources. Some information that can be obtained from this technique is provided in the following sections. Tables 13 to 15 provide the particle size analysis of the passively collected samples from the opencast coal mines. The similarity in particle size distribution between the different mines indicates that opencast coal mining activities and their mechanical nature are generally similar and result in the emission of a significant number of coarse particles. An example of further statistical analysis is given in Table 16. The relatively high standard deviation is due to limitations in the method, particularly limitations associated with the particulate recognition feature of Axio-Imager, the software adopted for optical microscopy analysis.

Table 13: Atmospheric PM size distribution (Mpumalanga Opencast Coal Mine 1).

Class	>=	<	Absolute number of particles	Number (%)	Number sum
2-5	2	5	555	58	555
5-7	5	7	191	20	746
7-10	7	10	101	11	847
10-15	10	15	59	6	906
15-30	15	30	44	5	950

Table 14: Atmospheric PM size distribution (Mpumalanga Opencast Coal Mine 2).

Class	>=	<	Absolute number of particles	Number (%)	Number sum
2-5	2	5	583	58	583
5-7	5	7	197	20	780
7-10	7	10	115	11	895
10-15	10	15	64	6	959
15-30	15	30	49	5	1008

Table 15: Atmospheric PM size distribution (Limpopo Opencast Coal Mine).

Class	>=	<	Absolute number of particles	Number (%)	Number sum
2-5	2	5	527	49	527
5-7	5	7	229	21	756
7-10	7	10	162	15	918
10-15	10	15	104	10	1022
15-30	15	30	59	5	1081

Table 16: Statistical analysis for atmospheric PM sample (Mpumalanga Opencast Coal Mine 1).

Parameter	Feret maximum (µm)
Minimum	2.24
Maximum	177.38
Mean	7.09
Count	963.00
Sum	6827.60
Standard Deviation	28.60
Range	175.14
Sum Square	835102.03
Variance	817.77
25-Quartile	3.44
50-Quartile (Median)	4.38
75-Quartile	6.72
10-Percentile	2.72
90-Percentile	11.31
1-Percentile	2.24
99-Percentile	32.49
Kurtosis	894.28
Skewness	29.38

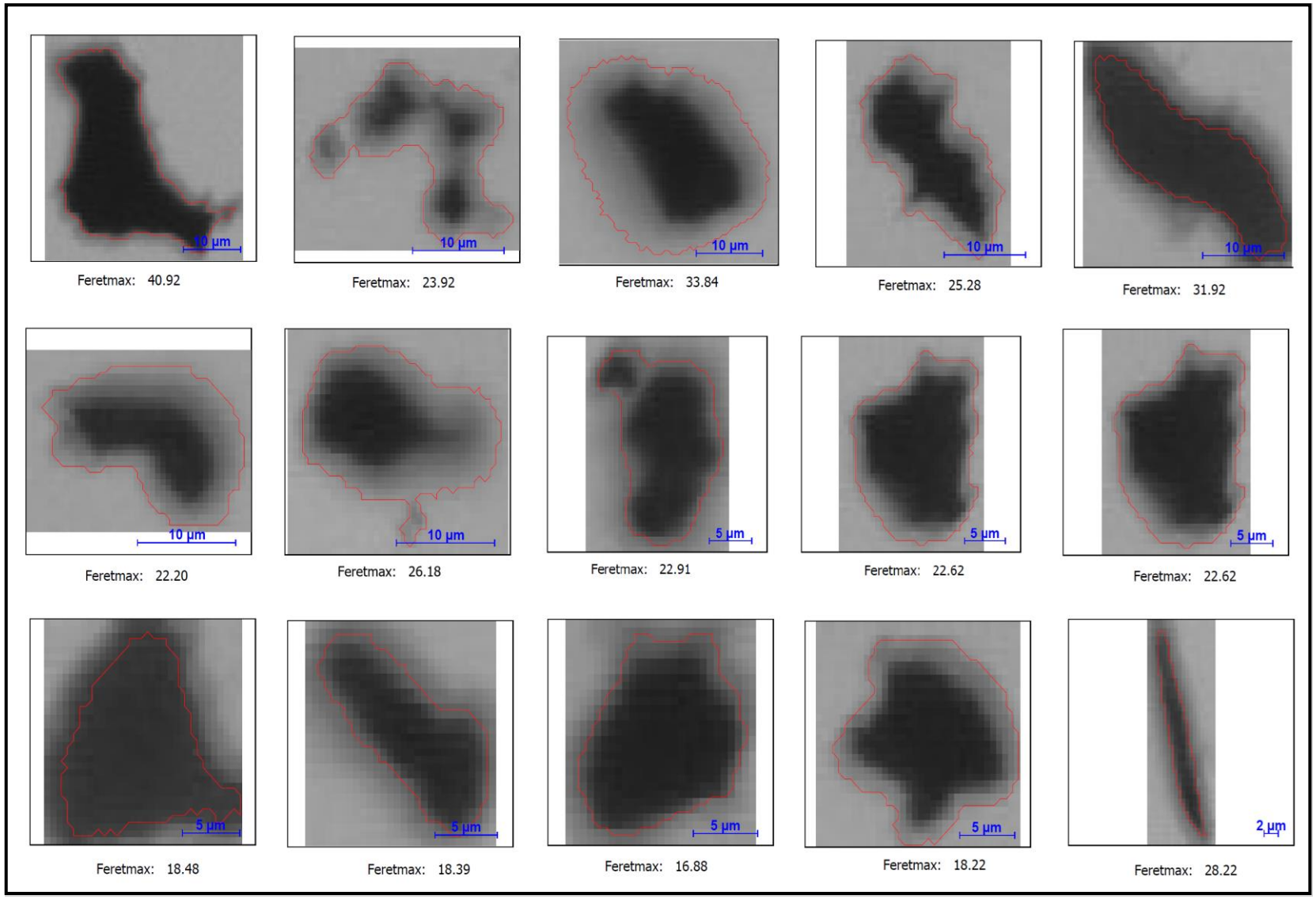

Figure 102: Opencast coal mine atmospheric PM morphologies and particle dimensions (Mpumalanga Mine 1 and Mine 2).

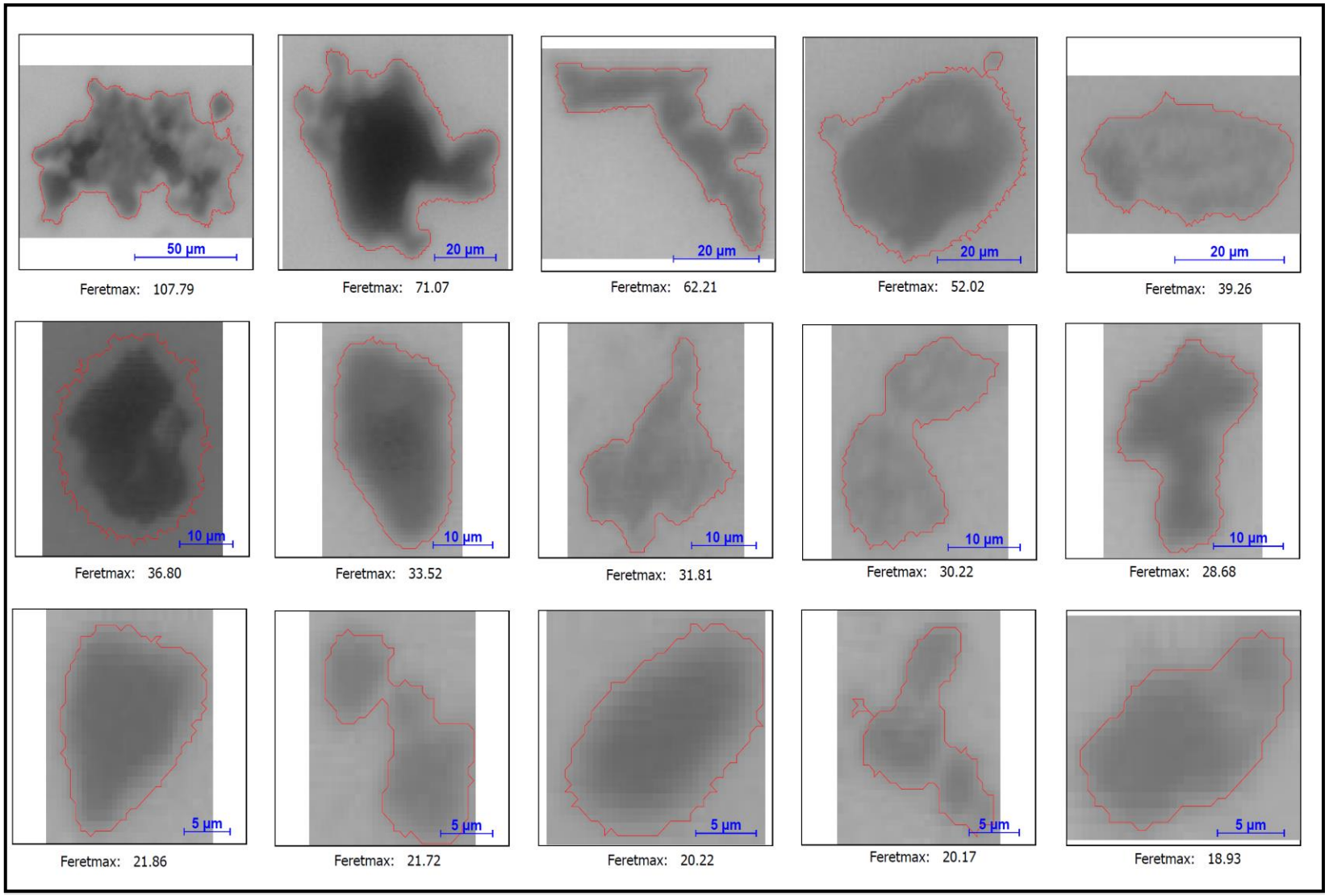

Figure 103: Opencast coal mine atmospheric PM morphologies and particle dimensions (Limpopo Mine).

For example, particulates located adjacently are interpreted as one large particle by the software, resulting in distortions of particulate characteristics. The physical limitation regarding the recognition and counting of particles smaller than 2.5 µm (and hence the accuracy of the particle size distribution) imposed by optical microscopy are further discussed in the following section.

4.5.1.1 Atmospheric PM Concentrations for Opencast Coal Mines: Passive Sampling

At the maximum magnification for practical use on the optical microscope (200X, particles smaller than 2.5 µm are not individually distinguishable and the concentrations calculated from this technique are more correctly indicated as $PM_{10-2.5}$. The calculated average daily $PM_{10-2.5}$ concentrations for the opencast coal mines' atmospheric PM samples range from 82 (79-85) µg/m³ to 111 (108-113) ug/m³ in Mpumalanga and from 91 µg/m³ to 103 ug/m³ in Limpopo (Figure 104).

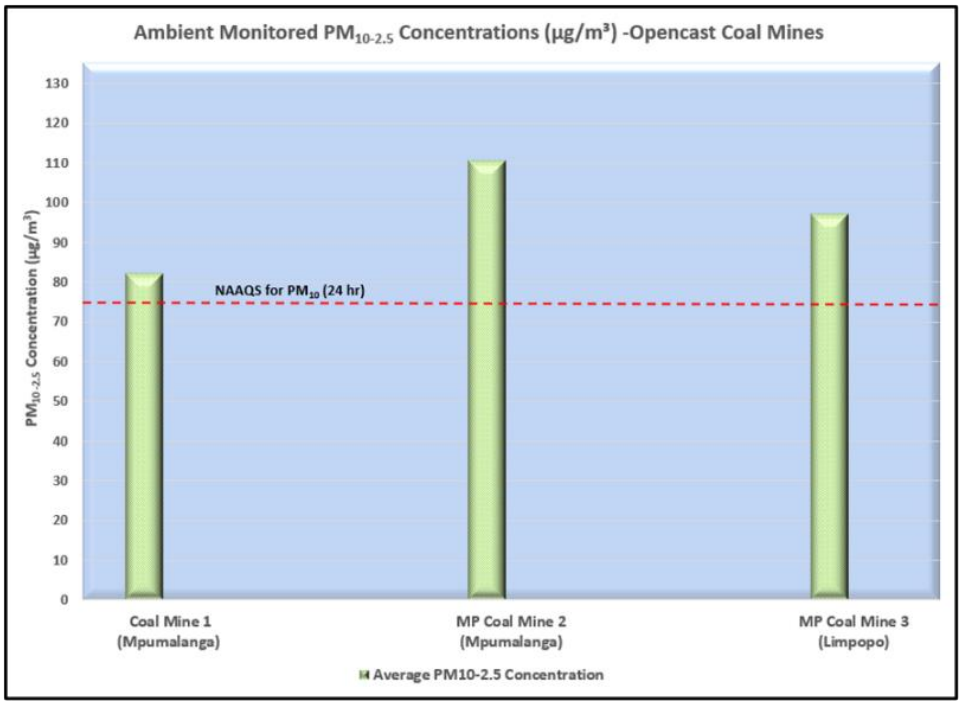

Figure 104: Average $PM_{10-2.5}$ concentrations for the opencast coal mines (passive sampling).

A comparison of the calculated average daily $PM_{10-2.5}$ concentrations to the PM_{10} daily (24 hour) standard or NAAQS of 75 ug/m³ indicates exceedances for all the opencast coal mine atmospheric PM samples. The note made earlier regarding the accuracy of the technique for small particles used here should be observed. It should also be noted that passive

sampling was not undertaken at the opencast mines' fence-lines or boundaries, but in the vicinity of fugitive dust sources, and the NAAQS are not applicable there.

4.5.1.2 Atmospheric PM concentrations for Opencast Coal Mines: Active Sampling

Average daily PM_{10} concentrations for the opencast coal mining operations range from 93 µg/m³ to 136 ug/m³ (Figure 105). PM_{10} daily concentrations range from 108 µg/m³ to 121 ug/m³ for the opencast coal mine located in the Limpopo Province. The PM_{10} daily concentrations for the Mpumalanga opencast coal mines range from 87 µg/m³ to 98 µg/m³ for Coal Mine 1 and 125 µg/m³ to 146 µg/m³ for Coal Mine 2. These concentrations exceed the PM_{10} daily NAAQS, but again the NAAQS are not applicable at the sampling locations, which were specifically selected to be representative of fugitive dust emission from mining sources.

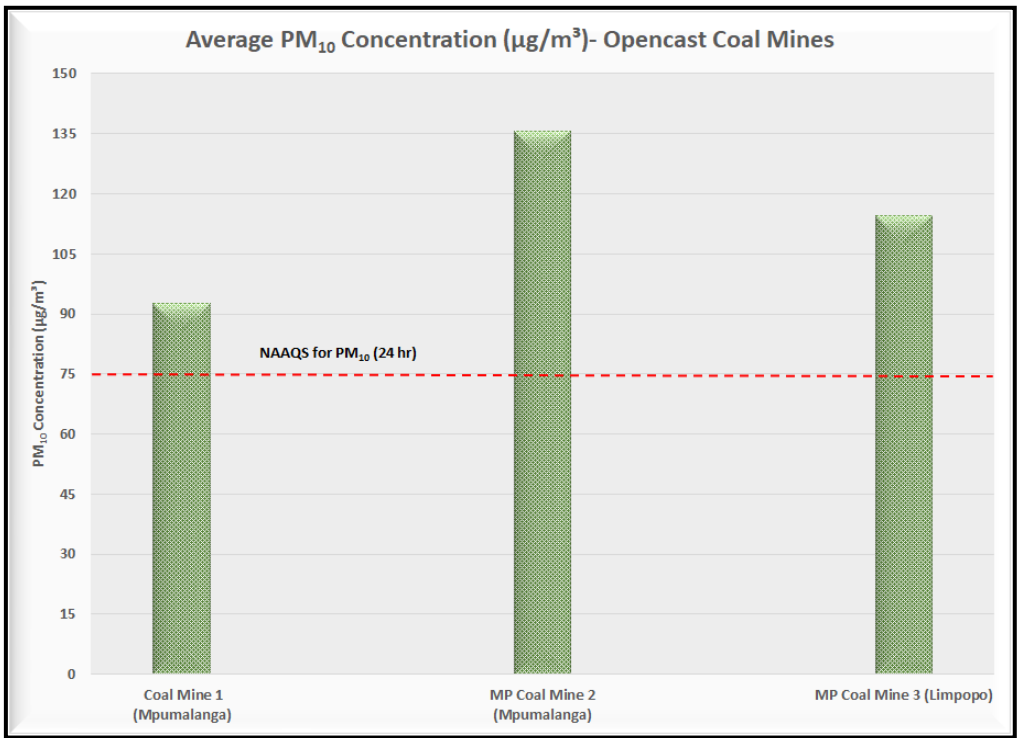

Figure 105: Average PM_{10} concentrations for the opencast coal mines (active sampling).

A comparison of the PM_{10} daily concentrations from the passive sampling and active sampling, indicates higher active monitoring concentrations by margins ranging from 12-22%. These differences are not an indication of passive sampler limitations only, but may also be due to source specific characteristics, different micro-site dispersion potentials in various areas of the opencast coal mines and passive sampler placement in different areas

or sources within the opencast coal mines, as active and passive samplers were not co-located.

4.5.2 Atmospheric Particulate Matter from Communities

The morphological characteristics and particulate dimensions for atmospheric PM sampled from communities located adjacent to opencast coal mines in Mpumalanga and Limpopo are shown in Figures 106 to 108. Tables 17 to 19 provide the particle size distribution. The morphological characteristics of the atmospheric particulates range from solid irregular, linear, spherical and agglomerates. The same method limitations as for the mining samples apply here. Again, one example of further statistical analysis of the images is provided in Table 20. Generally, the particles for the community samples are smaller than those for the mine samples; this can be attributed to the difference in sources, which for the community samples may include power generation and other combustion related industrial activities, domestic fuel burning and open burning of waste.

4.5.2.1 Atmospheric PM Concentrations for Communities: Passive Sampling

The $PM_{10-2.5}$ daily concentrations for Marapong range from 54 µg/m³ to 68 µg/m³; for Delpark, from 35 µg/m³ to 58 ug/m³ and for Clewer 63 µg/m³ to 82 µg/m³ (Figure 109). The average daily concentrations results indicate no exceedances of the PM_{10} daily NAAQS of 75 µg/m³ in any of the communities. The results presented above are for a short term 24-hour monitoring campaign and not a continuous, long-term campaign. The concentrations are therefore not a true reflection of long-term concentrations in the communities.

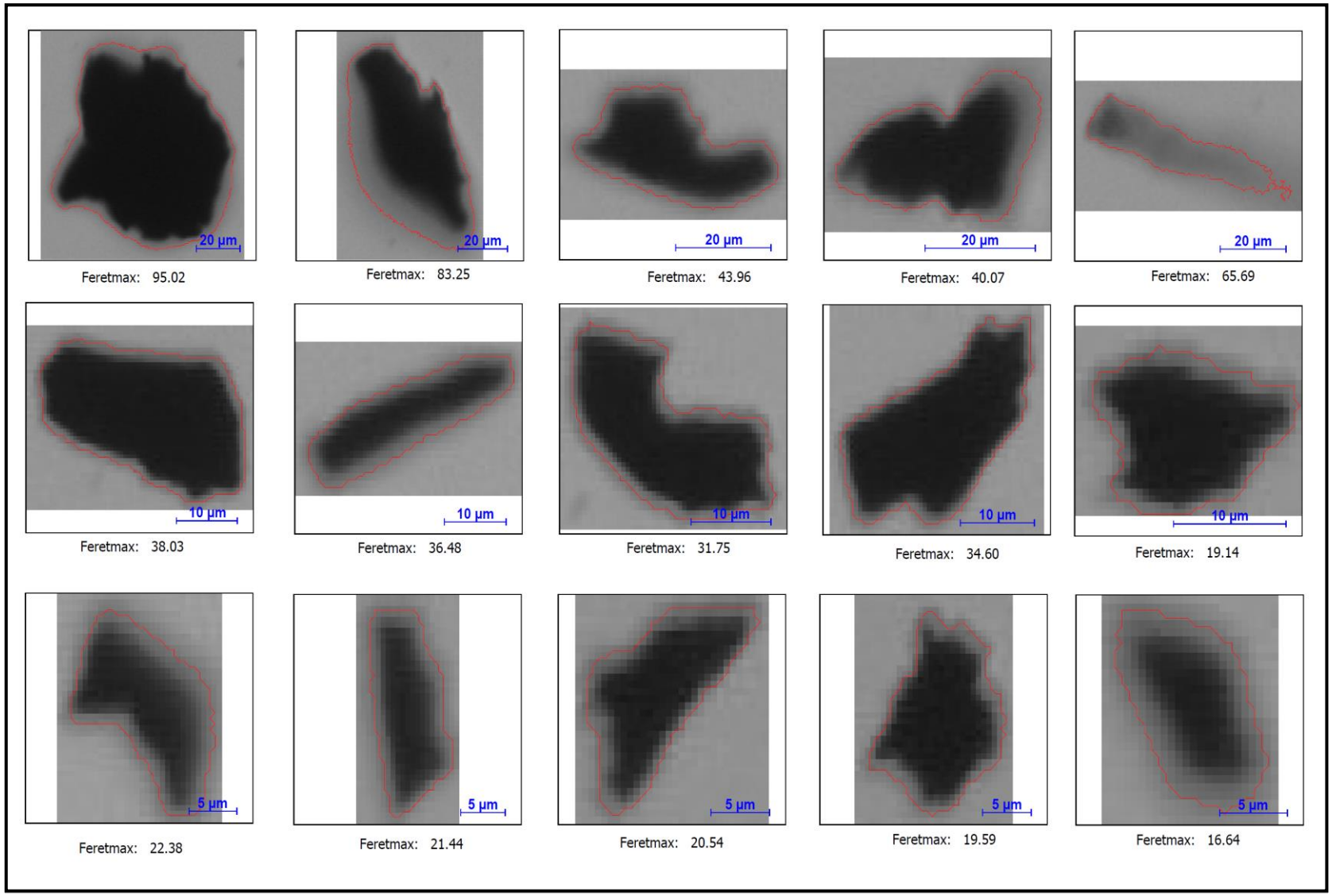

Figure 106: Atmospheric PM size distribution (Clewer, Mpumalanga).

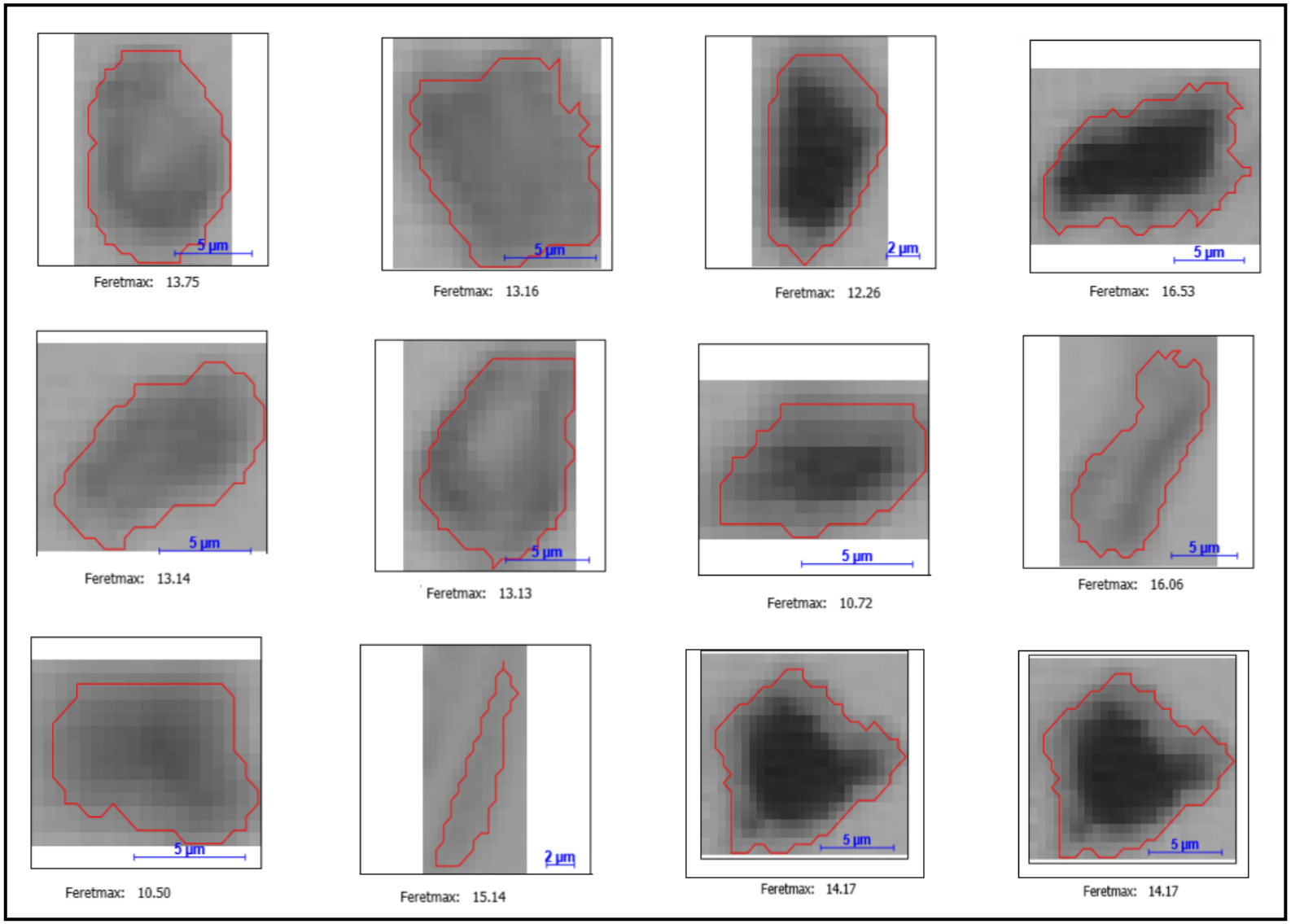

Figure 107: Atmospheric PM size distribution (Delpark, Mpumalanga).

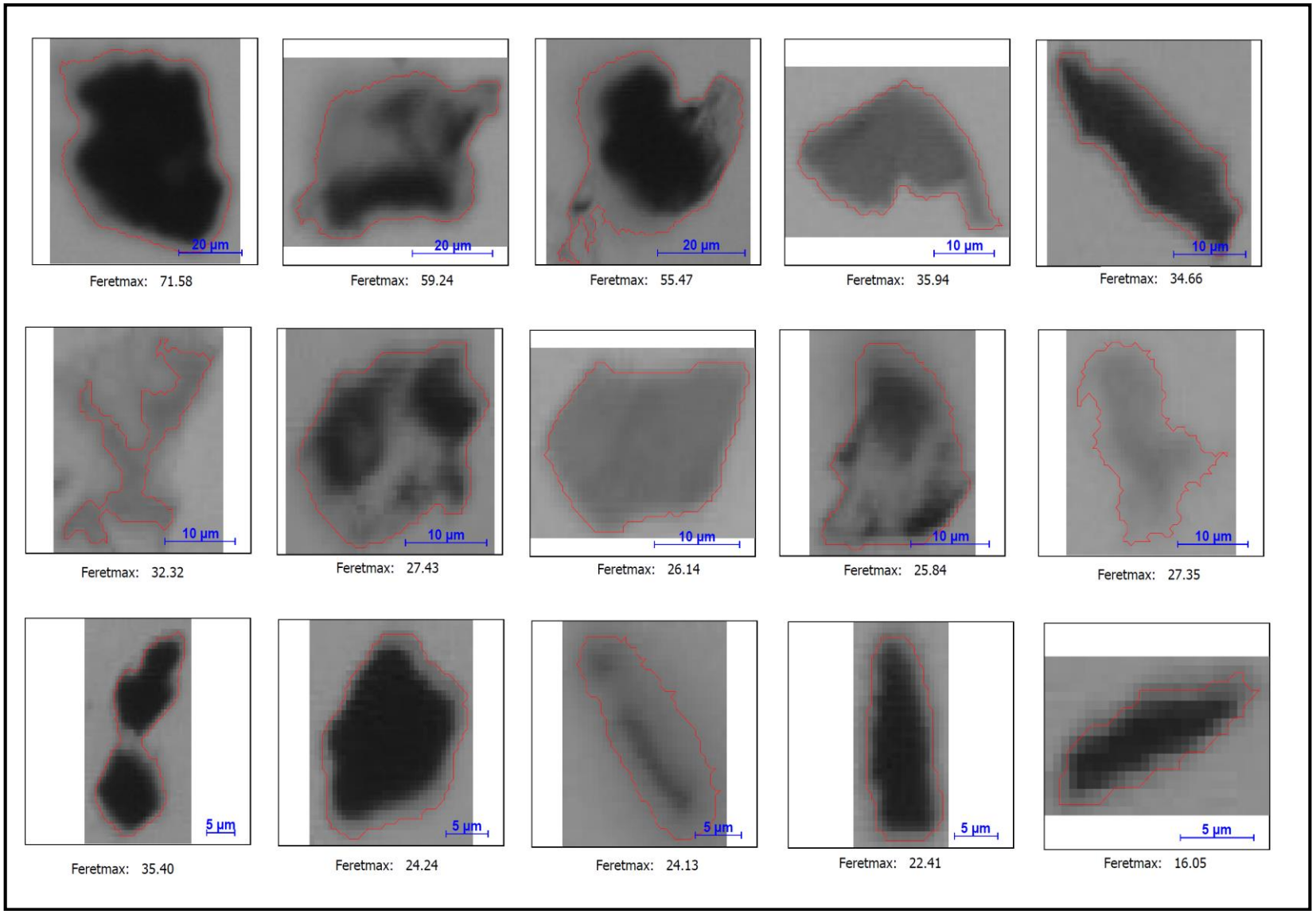

Figure 108: Atmospheric PM size distribution (Marapong, Limpopo).

Table 17: Atmospheric PM size distribution (Clewer, Mpumalanga).

Class	>=	<	Absolute number of particles	Number (%)	Number sum
2-5	2	5	696	59	696
5-7	5	7	213	18	909
7-10	7	10	153	13	1062
10-15	10	15	66	6	1128
15-30	15	30	46	4	1174

Table 18: Atmospheric PM size distribution (Delpark, Mpumalanga).

Class	>=	<	Absolute number of particles	Number (%)	Number sum
2-5	2	5	597	57	795
5-7	5	7	198	19	993
7-10	7	10	162	15	1155
10-15	10	15	58	5	1213
15-30	15	30	41	4	1254

Table 19: Atmospheric PM size distribution (Marapong, Mpumalanga).

Class	>=	<	Absolute number of particles	Number (%)	Number sum
2-5	2	5	434	59	434
5-7	5	7	132	18	566
7-10	7	10	84	11	650
10-15	10	15	50	7	700
15-30	15	30	39	5	739

Table 20: Statistical analysis for atmospheric PM sample (Clewer, Mpumalanga).

Parameter	Feret maximum (µm)
Minimum	2.24
Maximum	95.02
Mean	6.00
Count	1183.00
Sum	7103.35
Standard Deviation	5.96
Range	92.77
Sum Square	84693.98
Variance	35.57
25-Quartile	3.17
50-Quartile (Median)	4.24
75-Quartile	6.63
10-Percentile	2.72
90-Percentile	10.02
1-Percentile	2.31
99-Percentile	28.57
Kurtosis	78.13
Skewness	6.98

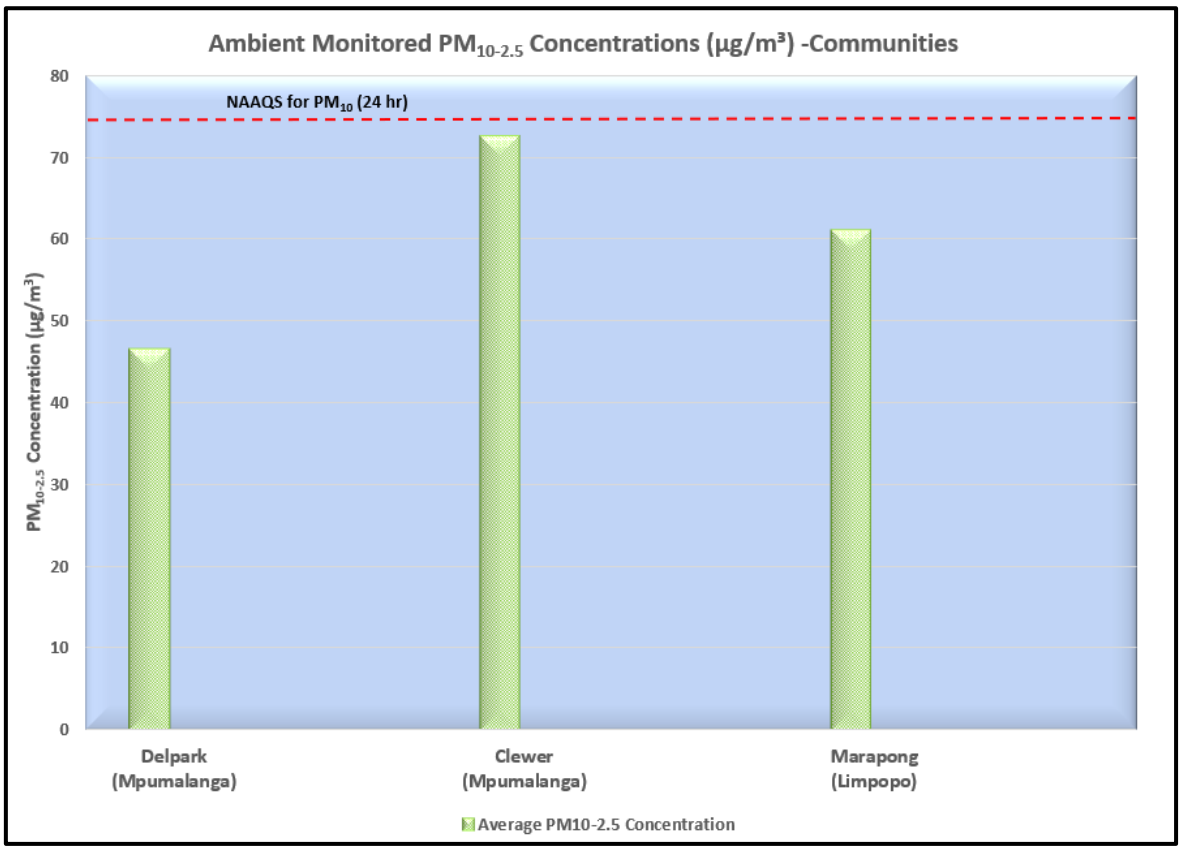

Figure 109: Average $PM_{10-2.5}$ concentrations at the communities of Clewer, Delpark and Marapong.

4.5.2.2 Atmospheric PM Concentrations for Communities: Active Sampling

The calculated PM_{10} daily average concentrations range from 59 µg/m³ to 90 ug/m³ (Figure 110). PM_{10} daily concentrations for Marapong range from 63 µg/m³ to 71 µg/m³. For Delpark, PM_{10} daily concentrations range from 56 µg/m³ to 62 ug/m³ and 76 µg/m³ to 103 µg/m³ for Clewer (Figure 110). The PM_{10} daily NAAQS is exceeded at the community area of Clewer by a margin of 17%. A comparison of the PM_{10} concentrations from the passive sampling and active sampling campaigns indicates that higher concentrations are recorded for the active monitoring campaigns (differences of between 9- 20%). As is the case with the opencast coal mine samples, the differences are not only due to passive sampler limitations, but also different source characteristics, differences in micro-site dispersion potentials and different passive sampler placement within the opencast mines.

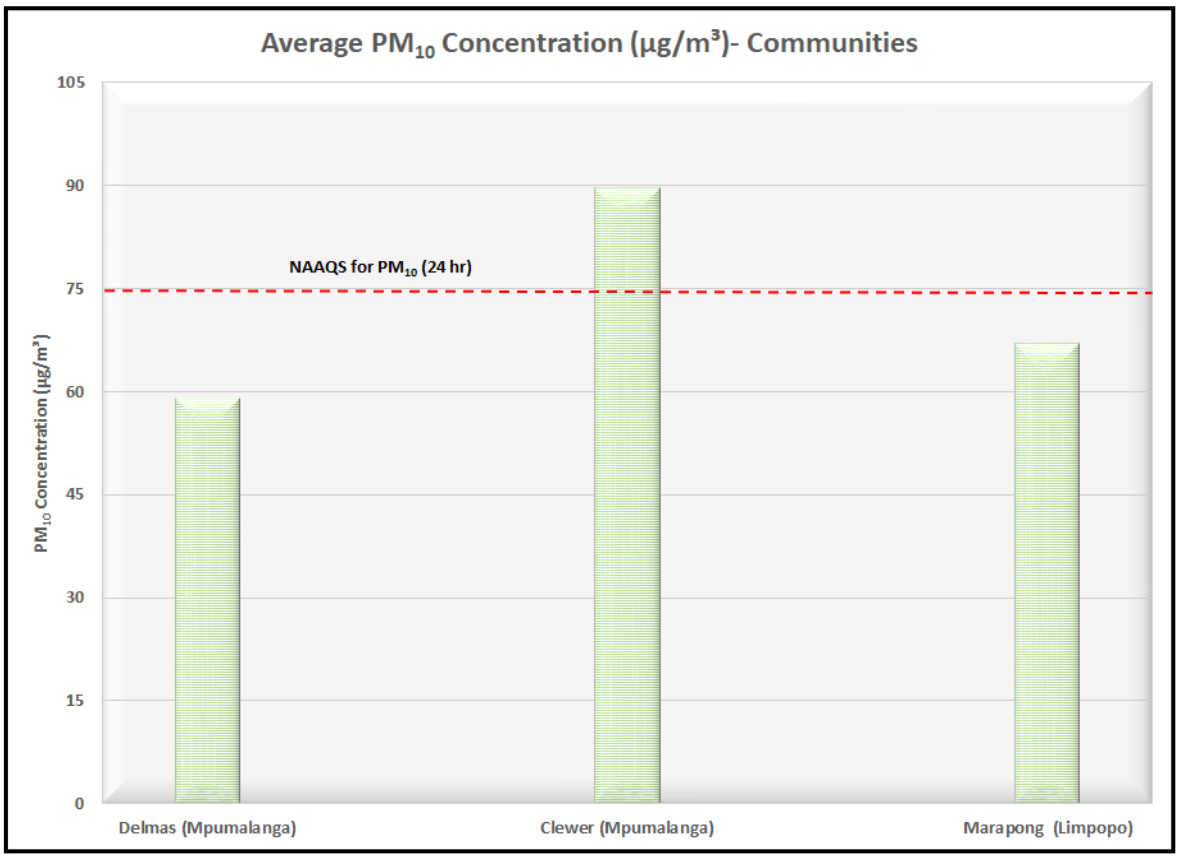

Figure 110: Average PM_{10} concentrations at the communities of Clewer, Delpark and Marapong.

4.6 Raman Spectroscopy

Raman spectroscopy is undertaken to attempt to differentiate between EC and OC in the atmospheric PM samples. Due to their sensitivity to modifications, it was envisaged that the D and G wavelength bands which are characteristic to carbonaceous material and are easily identified during Raman spectroscopy, might be instrumental in this differentiation.

The undeconvoluted Raman spectra and normalised intensities for the atmospheric PM samples from opencast coal mines and adjacent communities are shown in Figure 111 and Figure 112. The graphitic band, G, which occurs at approximately 1600 cm^{-1}, is observed in the spectra for all opencast coal mines and communities' particulate samples. This is an indication that some of the carbon in the atmospheric PM samples is highly ordered and exhibits a high degree of crystallinity. The G band generally corresponds to a more ordered graphitic structure, whereas the D bands are normally associated with defects i.e chemical and structural defects in the crystal lattice.

The D band wavelength is also observed, particularly in the opencast coal mining samples, at approximately 1360 cm^{-1} (Figure 111). The D band is generally associated with disordered and amorphous carbons ie. structural and chemical defects in the carbon crystal lattice and carbon bonding with other non-carbon atoms such as H and O. The presence of these non-carbon atoms in atmospheric PM samples is observed in the XPS results section of the research study (Section 4.4.1 and Section 4.4.2).

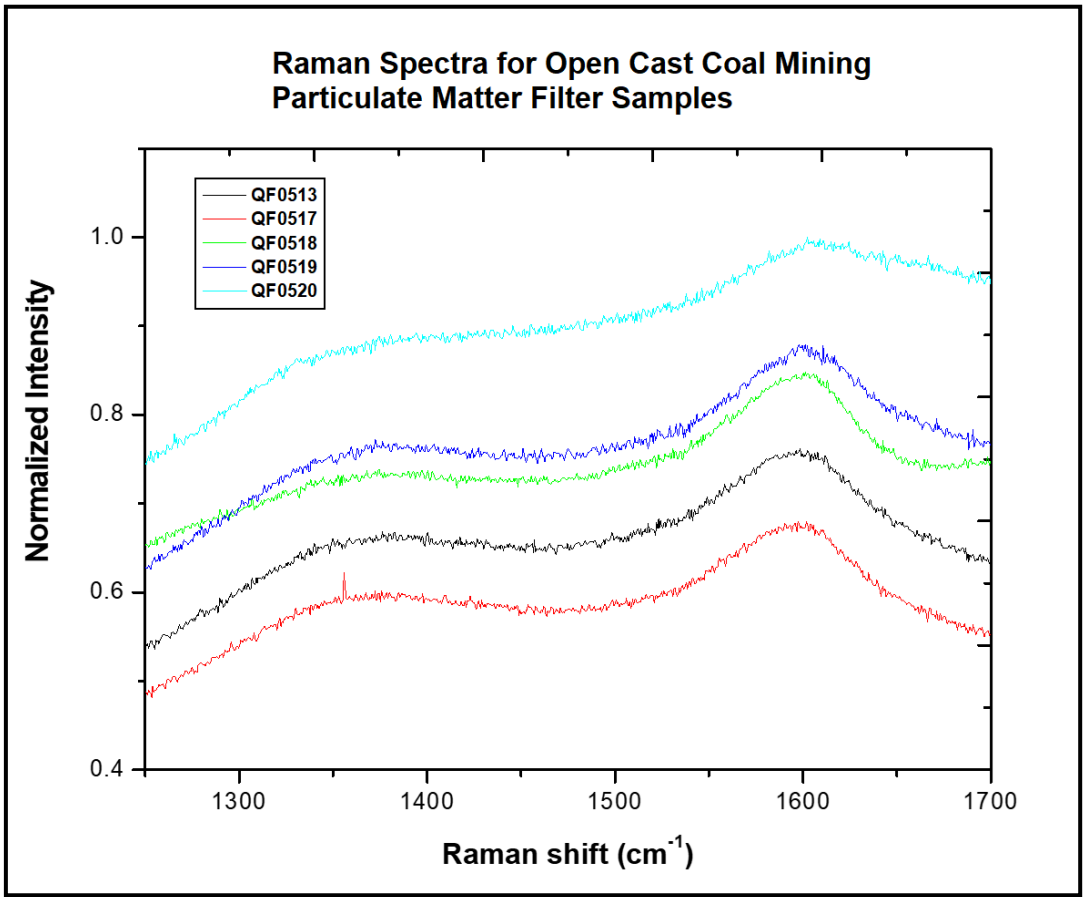

Figure 111: Undeconvoluted Raman spectra for coal mining atmospheric PM filter samples.

The Raman spectra for the community atmospheric PM samples indicates an extra band of approximately 1720 cm^{-1} (Figure 112). The origin of this band could be a shifted G band due to the presence of impurities in the graphitic structure and a change in electronic states in some planes. Slight differences are also observed in the intensities of the Raman signals.

Blank Teflon filters indicate 5 bands at 294 cm^{-1}, 386 cm^{-1}, 737 cm^{-1}, 1216 cm^{-1}, 1301 cm^{-1} and 1379 cm^{-1}. These bands do not occur in the spectra shown above and it is inferred that the high concentration of atmospheric PM on the Teflon filter masks the contribution of the Teflon.

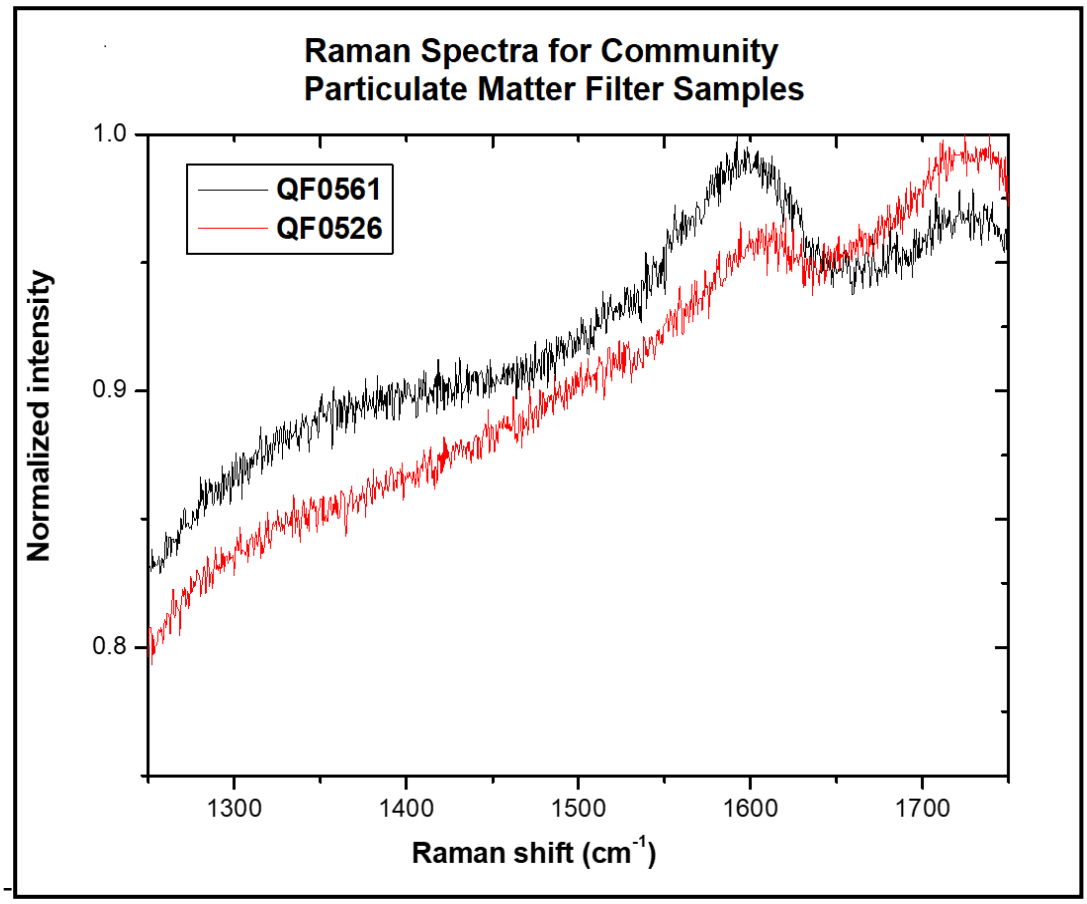

Figure 112: Undeconvoluted Raman spectra for two community atmospheric PM filter samples.

The observed Raman spectra for atmospheric PM from opencast coal mines and adjacent communities indicates the presence of carbonaceous material, but do not show sufficient differences to enable source apportionment based on the carbon content.

4.7 Thermogravimetric Analysis

The thermogravimetry analysis (TGA) and differentiated thermogravimetry (DTG) results for the atmospheric PM samples for the opencast coal mines and communities are shown in Figures 113 to 120. The observed DTG results for the air and N_2 runs indicate different stages of mass loss in these atmospheric PM samples.

The observed stages of mass loss include the following;

- Below 200°C- this stage involves the loss of water and other substances which evaporate between ambient temperatures and 200°C, as well as the release of gases from the sample.

- Devolatilisation or evolution of organic content at temperatures of between 200°C-600°C. The peaks observed at approximately 300°C and 310°C, particularly in the opencast coal mining atmospheric PM samples, are OC peaks which correspond to the volatilisation of organics with lower molecular weights. The peaks observed at approximately 475°C correspond to the initial decomposition and volatilisation of species with high molecular weights. Furthermore, this range is characterised by rapid increases and decreases in the DTG%/ minute which is attributed to devolatisation and other chemical reactions.
- Above 600°C- this stage involves the evolution of less volatile components such as graphite which burns at temperatures higher than 600°C. This is an indication of the presence of EC from incomplete combustion. However, OC and EC can still be components of the volatilised material at this stage as both may contain graphite.

Differences in the DTG results for the air runs and N_2 runs are also observed, with more gradual peaks being observed in the N_2 runs. This is attributed to little or no interference with the atmospheric PM samples during thermal treatment as N_2 is an inert gas. On the other hand, the use of air for purging may expose the sample to oxidative conditions which may influence or impact chemical reactions. This impact can potentially result in endothermic and exothermic reactions which affect temperature and rate of mass loss.

The thermogravimetry percentage (TG%) for most of the samples varies from 1-4% for both the air and N_2 runs. The mass loss of the particulates is also observed to occur within less than a minute. Typically, the smaller the carbon particles, the earlier and the faster they burn.

There is an indication that the differentiation of EC and OC in the atmospheric PM samples is achieved, albeit qualitatively, through TGA/DTG. However, the difference between samples from the different mines and the difference between different communities makes the use of this technique as a generally applicable carbon apportionment tool problematical.

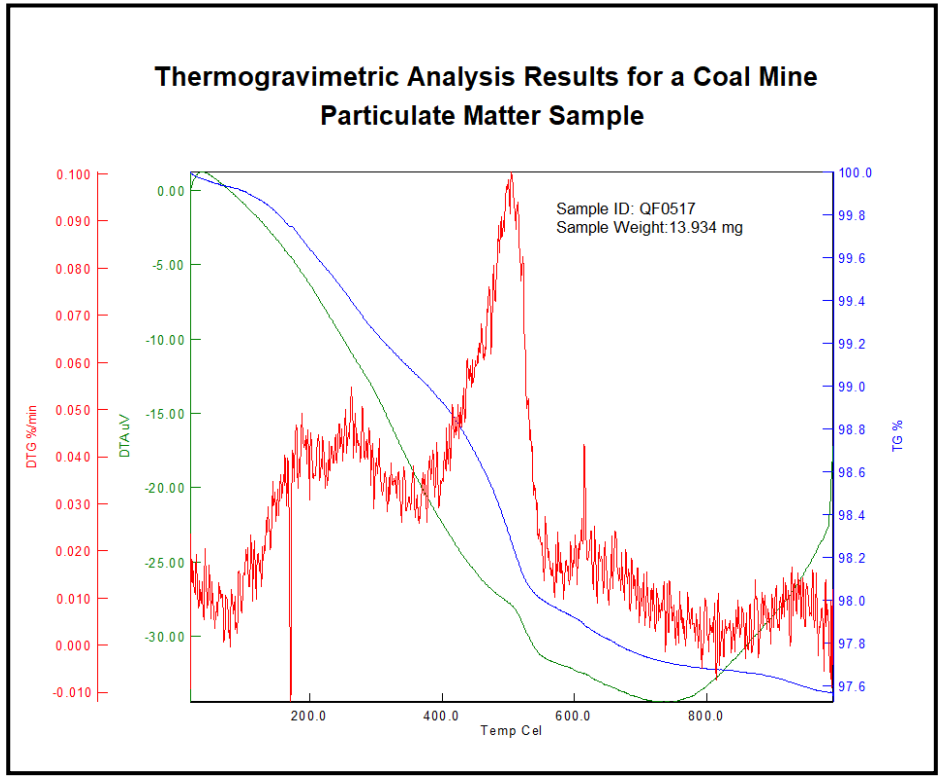

Figure 113: Thermogravimetric analysis (air run) of opencast coal mining atmospheric PM filter sample (Mpumalanga Province).

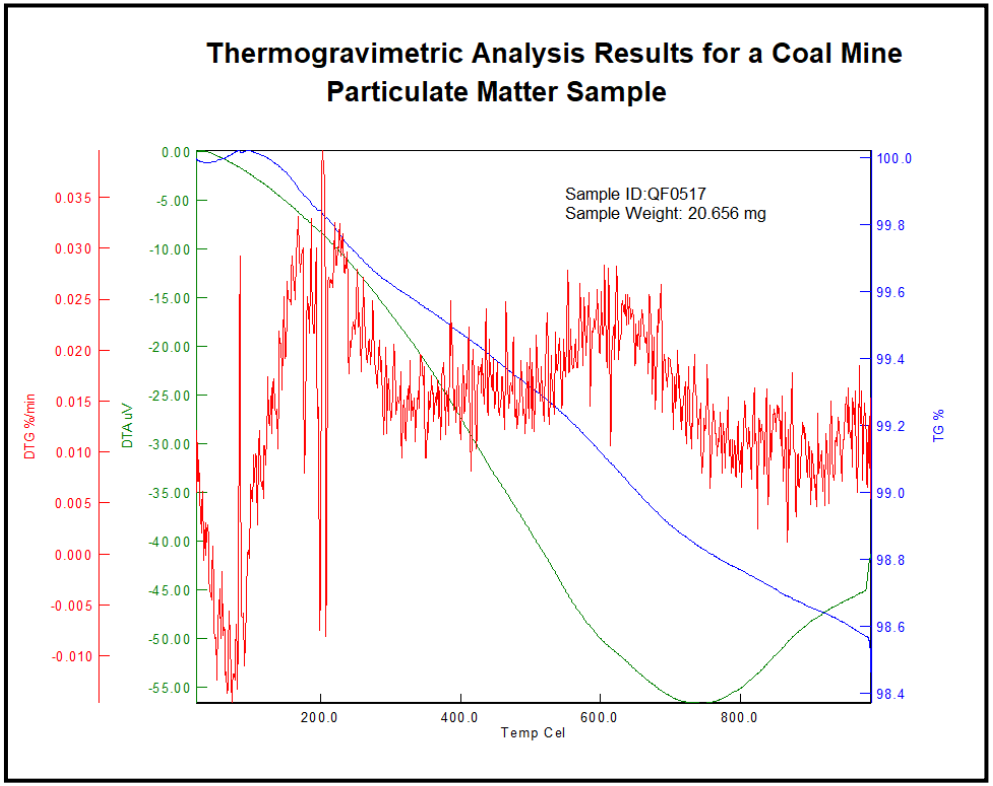

Figure 114: Thermogravimetric analysis (nitrogen run) of opencast coal mining atmospheric PM filter sample (Mpumalanga Province).

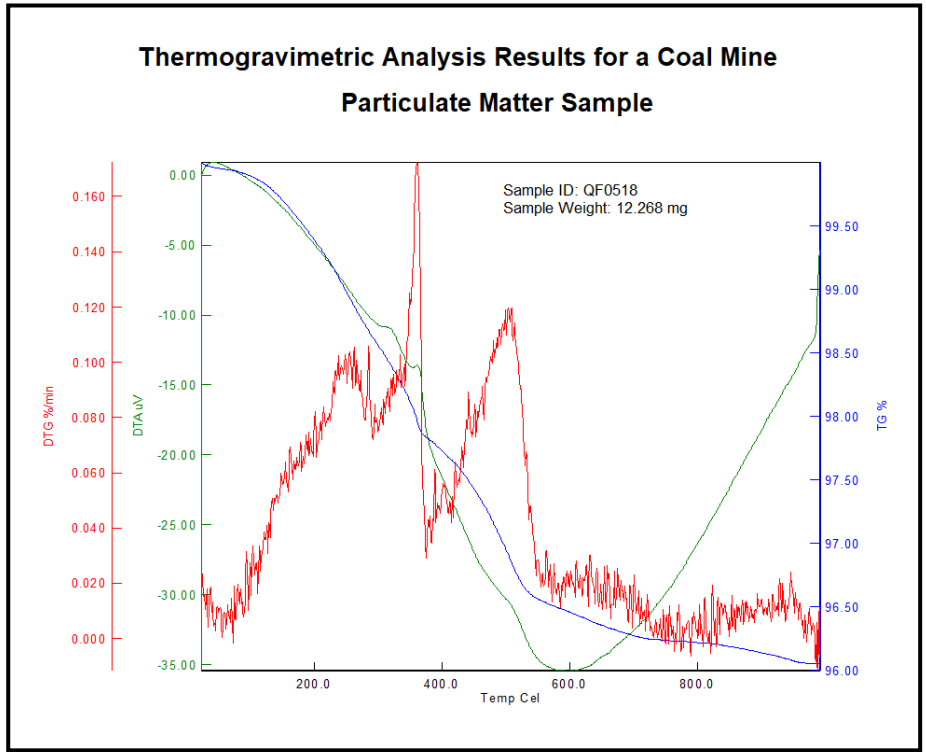

Figure 115: Thermogravimetric analysis (air run) of opencast coal mining atmospheric PM filter sample (Mpumalanga Province).

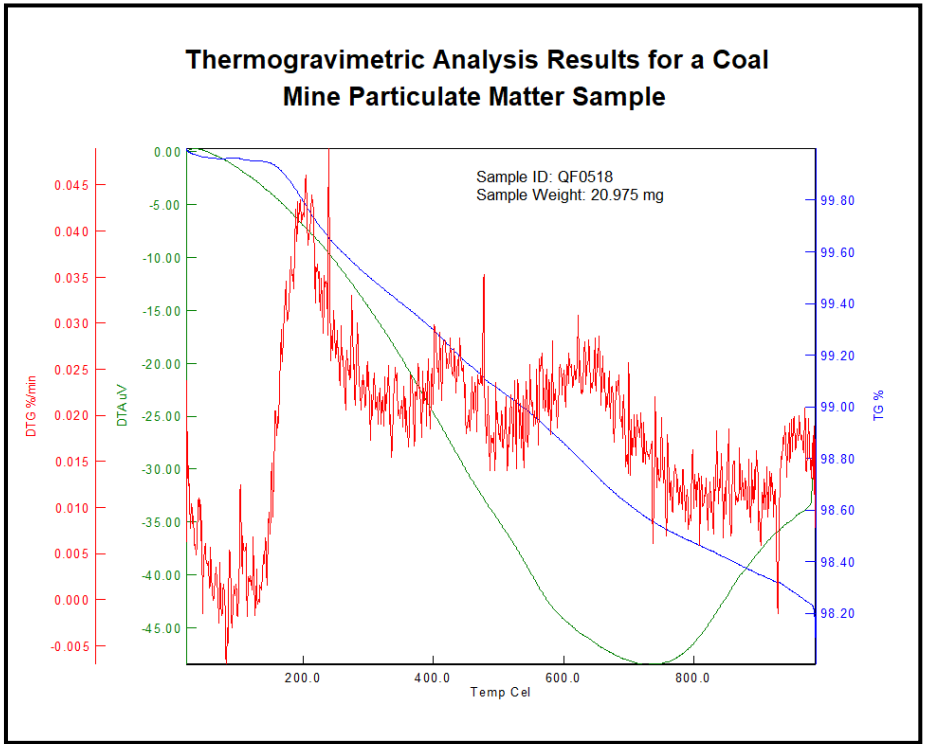

Figure 116: Thermogravimetric analysis (nitrogen run) of opencast coal mining atmospheric PM filter sample (Mpumalanga Province).

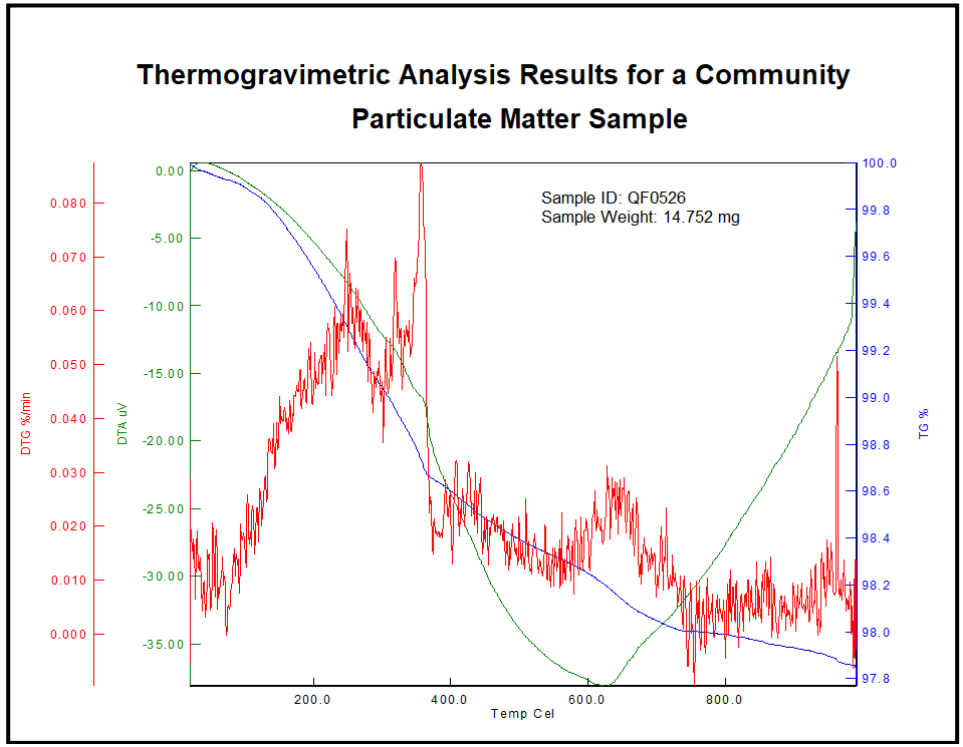

Figure 117: Thermogravimetric analysis (air run) of community atmospheric PM filter sample (Mpumalanga Province).

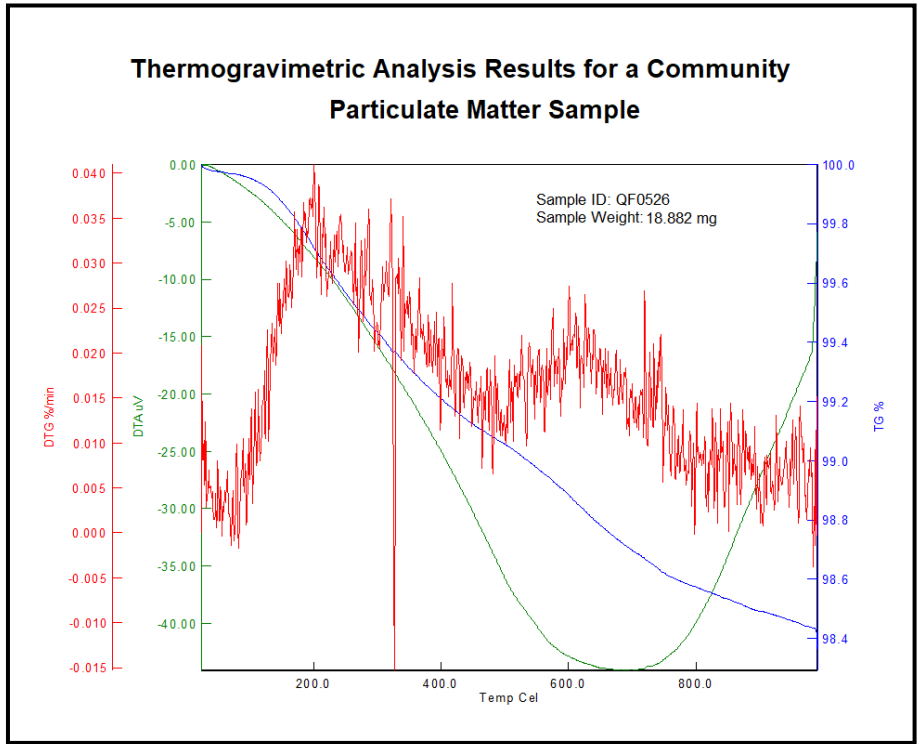

Figure 118: Thermogravimetric analysis (nitrogen run) of community atmospheric PM filter sample (Mpumalanga Province).

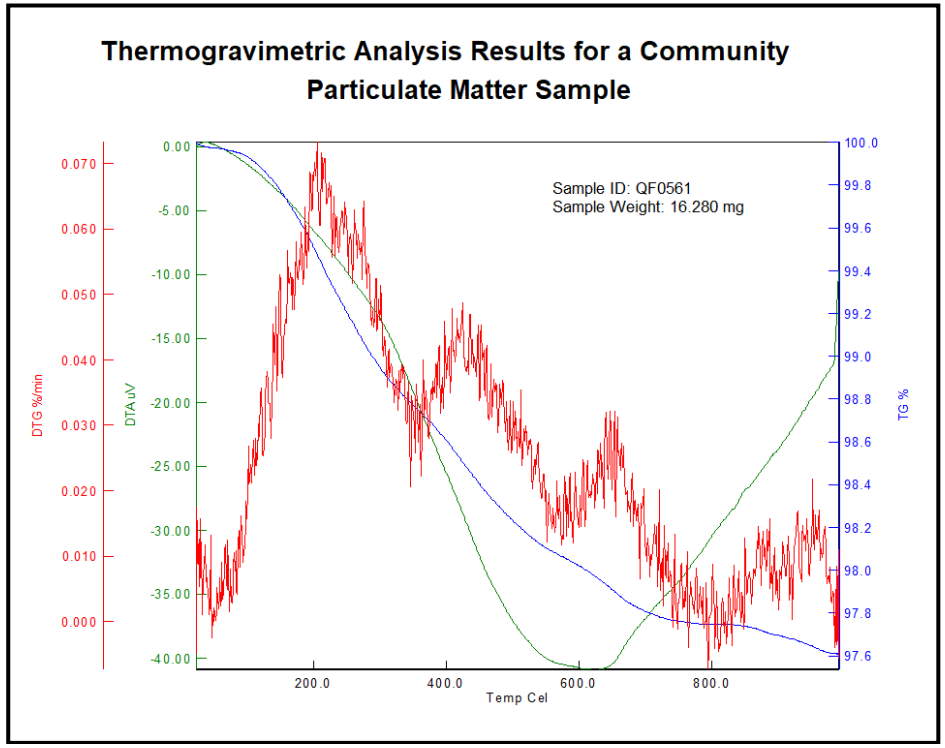

Figure 119: Thermogravimetric analysis (air run) of community atmospheric PM filter sample (Limpopo Province).

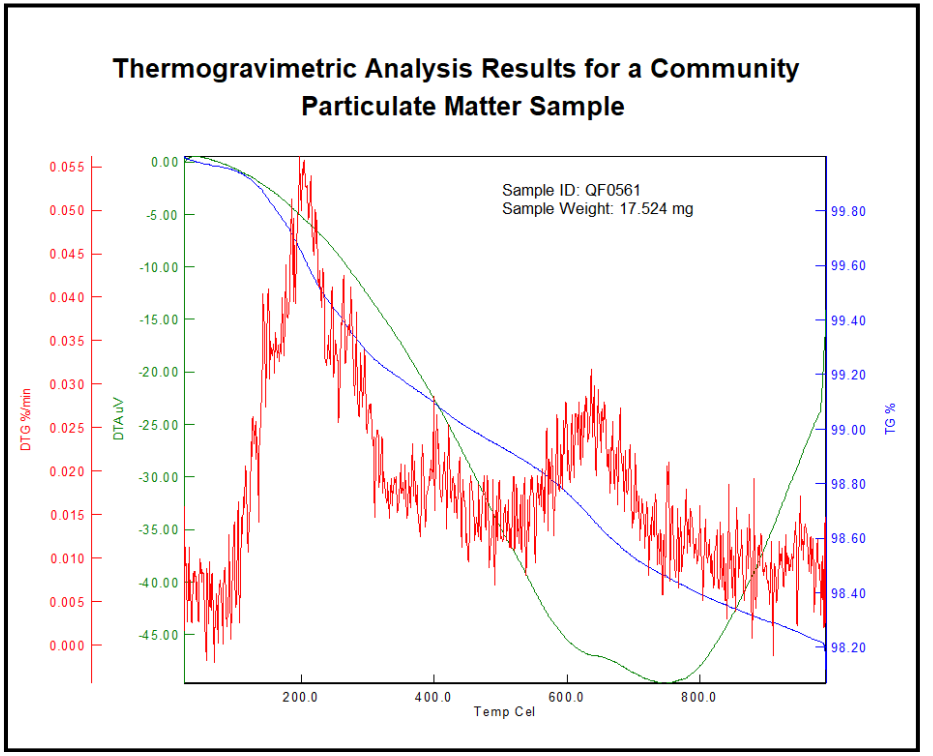

Figure 120: Thermogravimetric analysis (nitrogen run) of community atmospheric PM filter sample (Limpopo Province).

4.8 Isotope Ratio Mass Spectrometry

4.8.1 Opencast Coal Mining and Community Atmospheric PM Samples

The carbon and nitrogen isotope fingerprints from the atmospheric PM samples collected on the quartz filters from opencast coal mines and adjacent communities are presented in Table 21 and illustrated in Figure 121. For the atmospheric PM samples collected from the opencast coal mines, the carbon isotope fingerprint of $\delta^{13}C$ ranges from -25.28‰ to -21.48‰. The carbon isotope fingerprint of the community atmospheric PM samples ranges from -27.63‰ to -23.55‰. Higher $\delta^{13}C$ values are observed for the opencast coal mines' atmospheric PM samples compared to the community samples.

Once the samples containing mainly overburden (soil) particulate are removed (samples A309 and A313), the mine and residential area samples have distinct characteristic fingerprints, with the community samples having higher $\delta^{15}N$ values than the coal samples. The high $\delta^{15}N$ values for the residential areas of Marapong (average annual precipitation 437 mm), Clewer (average annual precipitation 693 mm) and Delpark (average annual precipitation 1230 mm) are unexpected. Amundsen *et al* (2003) indicate the South African average for soils to be 6.2 to 7.6‰, while they found values to decrease with increased annual precipitation. Savard *et al* (2017) give a value of 3.4 to 6.1‰ for coal-fired power station emissions, while Moroeng *et al* (2018) give a value of 2.66‰ for Witbank no 4 seam coal, which is the predominant coal at Opencast Coal Mines 2 and 3. This suggests a contribution by biomass-related particulates for the residential samples as would be expected and confirmed by the $\delta^{13}C$ value (see below) for the more rural area around Marapong, but not for Clewer and Delpark where biomass is less readily available; the $\delta^{15}N$ for C_3 and C_4 biomass-related PM_{10} is given as 13.7 ± 2.2‰ by Mkoma *et al* (2013), while for C_4 biomass-related particulate Bikkina *et al* (2016) give a value of 11.5±2.1‰. The $\delta^{15}N$ isotope ratios for the opencast coal atmospheric PM samples are lower than those for the residential samples, but higher than that given for South African coals by Moroeng *et al* (2018) at 2.66‰. This may be due to the extensive use of liquid fuels (diesoline) in opencast coal mining, for which the $\delta^{15}N$ is given as between 3.9 and 5.4±0.5‰ by Widory (2007), or to the presence of mineral dust in the mine samples.

The carbon isotope fingerprint ratios for the opencast coal mines' atmospheric PM samples were within the $\delta^{13}C$ ranges measured for coal in various parts of the world (-27.4‰ to –

23.7‰) (Suto & Kawashima, 2016; Garbarienė *et al.*, 2016). For the coal mined at mines 2 and 3, Moroeng *et al* (2018) give a value of -23.27‰. The impact of coal combustion products cannot be distinguished from coal dust itself, values for atmospheric particulates related to coal combustion are given as -23.5±1.3 (Andersson 2015; Fang & Andersson 2017) and -24.5±0.5‰ (Garbarienė *et al.*, 2016, Engelbrecht *et al.*, 2002). The lower carbon isotope values for the residential area, especially for the rural area (sample A310) can be attributed to the use of biomass (mainly wood) or the contribution of traffic-derived particulate. The $\delta^{13}C$ values for wood is given by Garbarienė *et al* (2016) as -26 to -27‰, with little fractionation with combustion, while Bikkina *et al* give a value of -25.8±0.5‰ for C_4 plant-related combustion particulate. For traffic-related particulate, Engelbrecht *et al* (2002) provide a $\delta^{13}C$ value of -28 to -29‰.

Table 21: Isotope ratio mass spectroscopy results for atmospheric PM samples

Sample ID	Weight	$\delta^{15}N$ (‰)	%N	$\delta^{13}C$ (‰)	%C	C/N ratio
A301 Opencast Coal Mine 1 Sample 1	10,1	7,8	0,13	-23,5	1,21	10,8
A302 Delpark Community	12,4	17,5	0,24	-23,6	2,89	14,3
A304 Clewer Community	17,6	10,5	0,03	-23,6	0,53	18,4
A306 Opencast Coal Mine 1 Sample 2 (plant area)	10,7	4,1	0,06	-23,4	1,80	34,8
A307 Opencast Coal Mine 2 Sample 1 (overloaded)	2,8	2,8	1,37	-21,6	56,55	48,1
A309 Opencast Coal Mine 1 (overburden area)	13,0	14,4	0,08	-24,2	1,08	16,5
A310 Marapong Community	14,6	15,4	0,07	-27,6	0,83	14,7
A311 Opencast Coal Mine 3 Sample 1	10,0	7,1	0,23	-22,8	5,27	27,1
A312 Opencast Coal Mine 2 Sample 2	12,9	5,8	0,39	-21,5	12,87	38,9
A313 Opencast Coal Mine 3 Sample 2 (overburden area)	16,4	16,1	0,04	-25,3	0,33	9,7
Opencast Coal Mine 2 Additional Sample 2	2,8	1,5	1,02	-22,6	33,58	38,5
Opencast Coal Mine 3 Additional Sample	9,8	5,95	0,46	-21,6	16,32	41,2

4.8.2 Statistical Analysis for IRMS Results

The standard deviation results are shown in Table 22 (Merck Standard) and Table 23 (DL-Valine Standard). The standard deviation for the Merck Standard is 0.06 for the nitrogen peak and 0.05 for the carbon peak. For the DL-Valine Standard, the standard deviation for

the nitrogen peak is 0.04 and 0.08 for the carbon peak. The standard deviation results for both standards indicate that the peak values for carbon and nitrogen differ by a small margin from the mean peak values. The small standard deviations are an indication of the high accuracy of the analysis technique.

Table 22: Standard deviation (Merck Standard)

Sample ID	Standard	Weight	N peak	$\delta^{15}N$ (‰)	C peak	$\delta^{13}C$ (‰)
A301 Opencast Coal Mine 1 Sample 1	Merck	0,23	25,52	7,96	28,54	-20,35
A302 Delpark Community	Merck	0,43	49,14	7,78	55,41	-20,20
A304 Clewer Community	Merck	0,60	70,65	7,95	79,36	-20,18
A306 Opencast Coal Mine 1 Sample 2	Merck	0,20	23,99	7,84	26,27	-20,29
A307 Opencast Coal Mine 2 Sample 1	Merck	0,62	73,44	7,85	82,38	-20,27
A309 Opencast Coal Mine 1 Sample 3	Merck	0,45	53,96	7,92	59,22	-20,25
A310 Marapong Community	Merck	0,45	52,97	7,89	59,49	-20,28
Opencast Coal Mine 2 Additional Sample	Merck	0,22	26,38	7,93	28,88	-20,26
Mean				**7,89**		**-20,26**
Standard deviation				**0,06**		**0,05**

Merck Standard deviation not calculated for the following samples;
A311 (Opencast Coal Mine 3- Sample 1), A312 (Opencast Coal Mine 2- Sample 2), A313 (Opencast Coal Mine 3 Sample 2) and Additional Opencast Coal Mine 3 Sample due to high filter particulate loading.

Table 23: Standard deviation (DL-Valine Standard)

Sample ID	Standard	Weight	N peak	$\delta^{15}N$ (‰)	C peak	$\delta^{13}C$ (‰)
A301 Opencast Coal Mine 1 Sample 1	DL-Valine	0,22	20,34	-6,13	35,29	-10,57
A302 Delpark Community	DL-Valine	0,41	37,16	-6,19	64,51	-10,54
A304 Clewer Community	DL-Valine	0,63	56,57	-6,13	99,86	-10,64
A306 Opencast Coal Mine 1 Sample 2	DL-Valine	0,24	21,95	-6,16	37,11	-10,65
A307 Opencast Coal Mine 2 Sample 1	DL-Valine	0,61	56,56	-6,17	98,54	-10,47
A309 Opencast Coal Mine 1 Sample 3	DL-Valine	0,44	39,79	-6,11	68,66	-10,45
A310 Marapong Community	DL-Valine	0,42	38,39	-6,11	66,53	-10,65
Opencast Coal Mine 2 Additional Sample	DL-Valine	0,24	21,77	-6,20	37,49	-10,60
Mean				**-6,15**		**-10,57**
Standard deviation				**0,04**		**0,08**

DL-Valine Standard deviation not calculated for the following samples;
A311 (Opencast Coal Mine 3- Sample 1), A312 (Opencast Coal Mine 2- Sample 2), A313 (Opencast Coal Mine 3 Sample 2) and Additional Opencast Coal Mine 3 Sample due to high filter particulate loading.

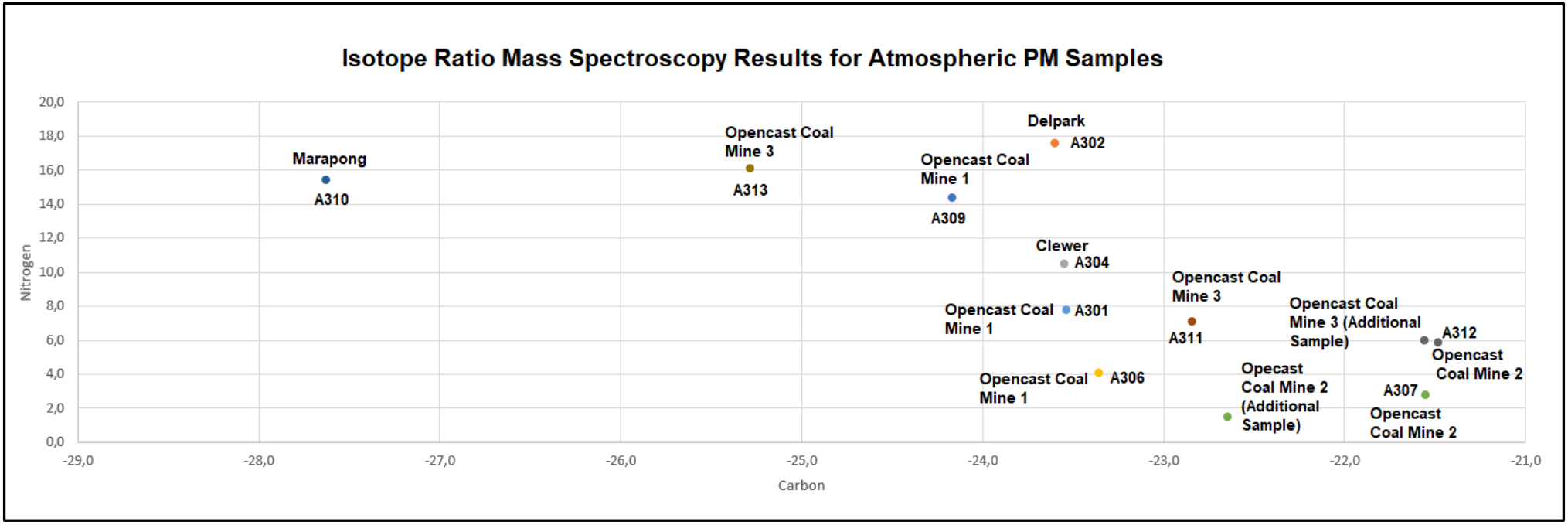

Figure 121: Isotope ratio mass spectroscopy results for opencast coal mines and adjacent communities

4.9 Thermal Optical Characterisation of Brown/Organic Carbon and Elemental Carbon

The OC, EC and TC concentrations (µg/cm^{-2}) obtained from the thermal optical analysis of the opencast coal mines and adjacent communities' atmospheric PM samples are shown in Table 24 below.

Table 24: Organic, elemental and total carbon concentrations for the opencast coal mines and adjacent communities atmospheric PM samples

Sample ID	OC (ug/sq cm)	EC (ug/sq cm)	TC (ug/sq cm)	OC/EC Ratio
A301 Opencast Coal Mine 1 Sample 1	24	16	39	1.53
A302 Delpark Community	112	25	136	4.50
A304 Clewer Community	21	4	25	6.03
A306 Opencast Coal Mine 1 Sample 2	30	19	48	1.60
A307 Opencast Coal Mine 2 Sample 1 (filter overloaded)	4,7E+09	5,1E+09	9,9E+09	0.92
A309 Opencast Coal Mine 1 Sample 3 (overburden area)	33	7	40	5.01
A310 Marapong Community	24	3	27	8.13
A311 Opencast Coal Mine 3 Sample 1	91	58	150	1.56
A312 Opencast Coal Mine 2 Sample 2	285	310	596	0.92
A313 Opencast Coal Mine 3 Sample 2 (overburden area)	16	3	19	5.61

*Opencast coal mines samples collected close to overburden areas and hence the low carbon content
Opencast Coal Mine 2 Additional Sample 2 and Opencast Coal Mine 3 Additional Sample not analysed during thermal optical analysis

4.9.1 Opencast Coal Mining Atmospheric PM Samples

Thermograms for the atmospheric PM samples are shown in Figures 122 to 124. The four traces correspond to flame ionisation detector 1 (FD1), flame ionisation detector 2 (FD2), temperature and laser (filter transmittance). The peaks correspond to pyrolytic carbon, OC) and EC. The methane calibration peak is the final peak for all the samples. The split between OC and EC is evident in all the thermograms, with EC being the carbon that is volatilized after the split. The occurrence of the OC and EC split is different for all the atmospheric PM samples due to differences in the concentrations of OC and EC in each sample, which in

turn depend on the sources of carbon in the sampling area. The OC, EC and TC concentrations (µg/cm-²) and the OC/EC ratio obtained from the thermal optical analysis of the opencast coal mines and adjacent communities' atmospheric PM samples are shown in Table 24 above. The concentrations of OC in the opencast coal mines' atmospheric PM samples range from 24-285 µg/cm^{-2}, with the highest concentrations reported for the Mpumalanga opencast mines. The EC concentrations range from 3-310 µg/cm^{-2}. Not taking samples that represent mainly overburden (A309 and A313) into account, OC/EC ratios confirm the observations of the IRMS analysis. Mine samples have a low ratio, commensurate with the ratio between volatile matter and fixed carbon in the coal before combustion. The filters for the samples from Mine 2 were both overloaded, and the results are accordingly less accurate. The best range for the deposit concentration is 5-400 µg/cm-² for OC and 1-15 µg/cm-² for EC. Concentrations of OC that are greater than this range may result in exceedances of the detection limits of the OC/EC instrument and interference with the EC measurements, particularly when low concentrations of EC are found in the sample (Desert Research Institute, 2019).

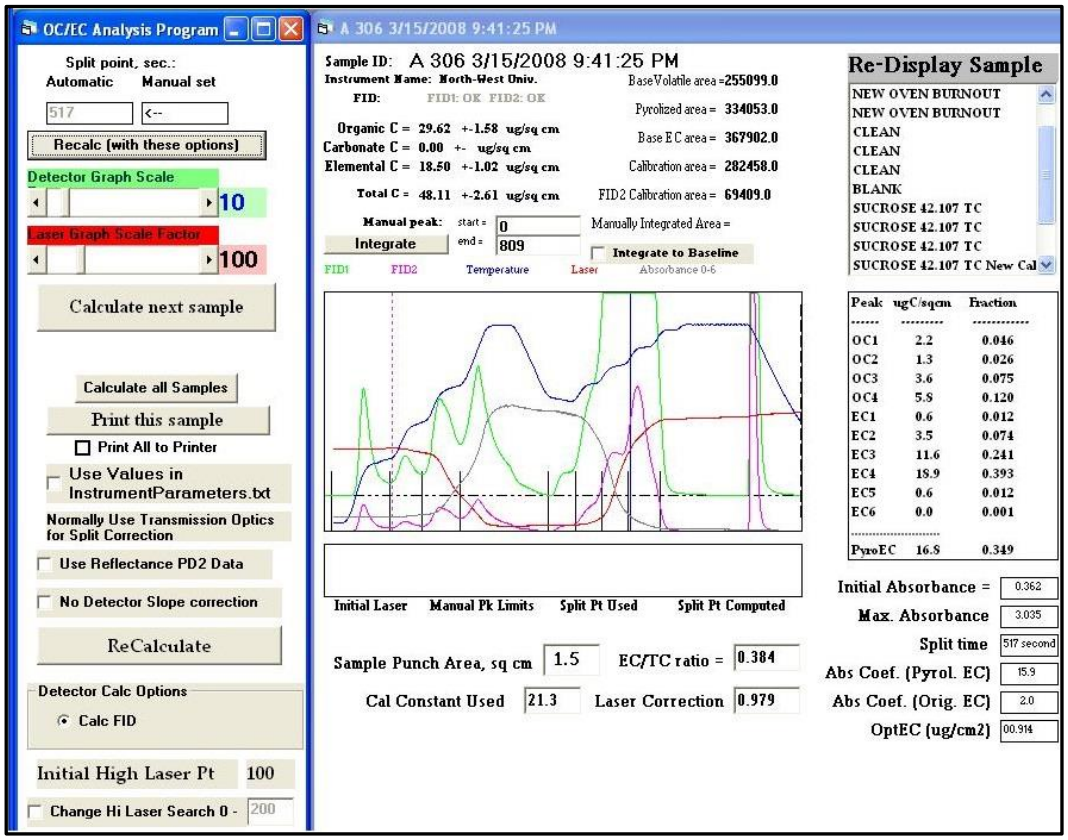

Figure 122: Thermogram for atmospheric PM samples (Opencast Coal Mine 1).

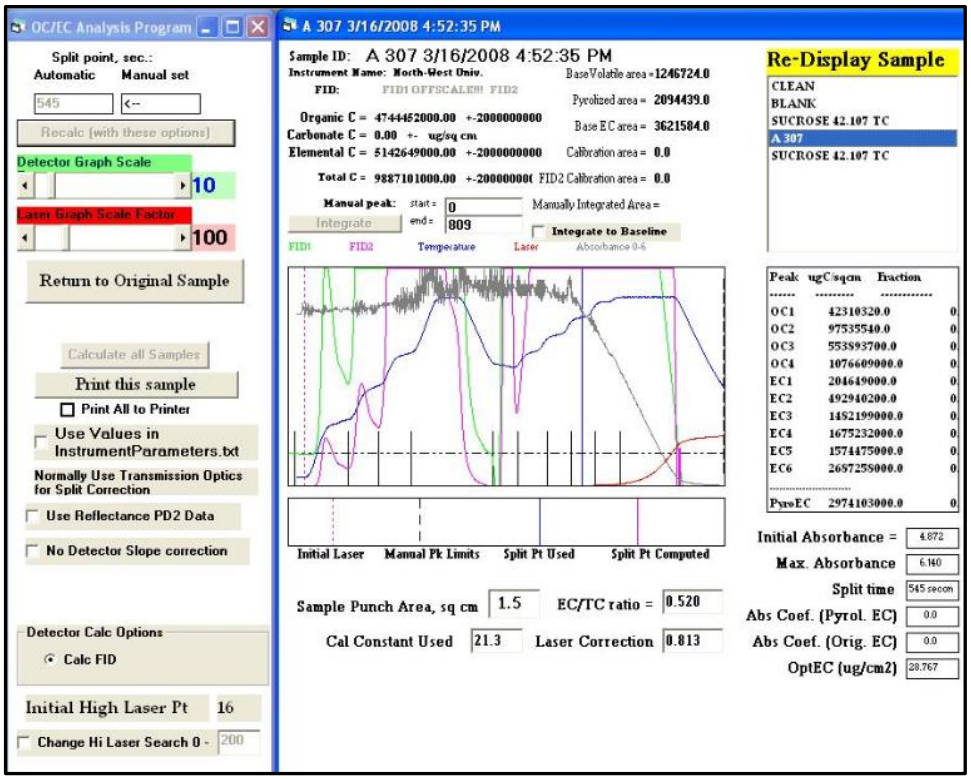

Figure 123: Thermogram for atmospheric PM samples (Opencast Coal Mine 2)

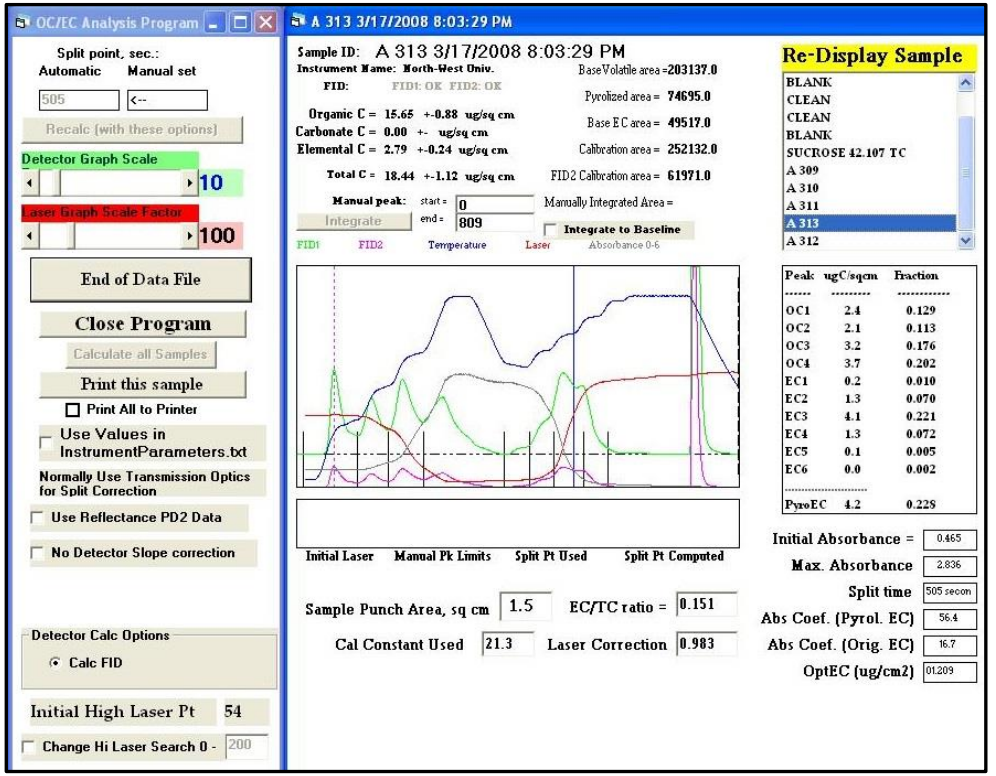

Figure 124: Thermogram for atmospheric PM samples (Opencast Mine 3).

4.9.2 Community Atmospheric PM Samples

The thermograms for the community samples are shown in Figures 125 to 127. The concentrations of OC for the adjacent communities' atmospheric PM samples range from 21-112 µg/cm^{-2}, with the highest concentrations reported for communities located in Mpumalanga (Table 24). The EC concentrations range from 3-25 µg/cm^{-2}. The recorded concentrations for EC are lower for the community of Marapong compared to Clewer and Delpark. The recorded OC/EC ratios for the communities' atmospheric PM samples range from 4 to 8, which clearly distinguishes them from the samples taken in or near the opencast coal mines. Samples from the residential communities have higher values, but source contributions cannot be determined from this ratio only. Sources that may contribute are coal combustion at OC/EC of 7.0, liquid fuel combustion at 9.7 (Engelbrecht *et al*., 2002), C_3 biomass at 16±5 and C_4 biomass (grasses) at 18±4 (Salma *et al*., 2017). The higher ratio for Marapong would suggest a higher contribution by the latter two sources.

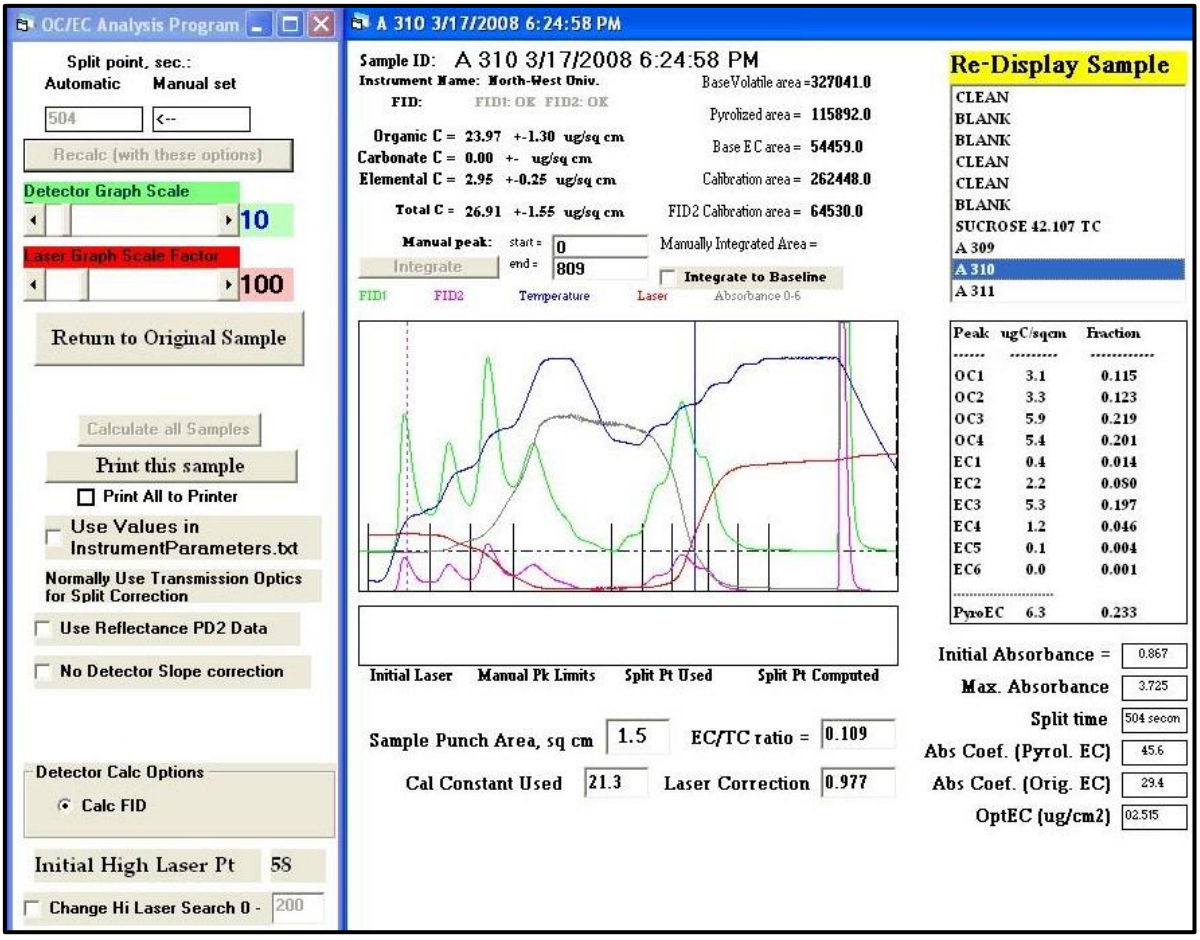

Figure 125: Thermogram for community atmospheric PM samples (Marapong, Limpopo).

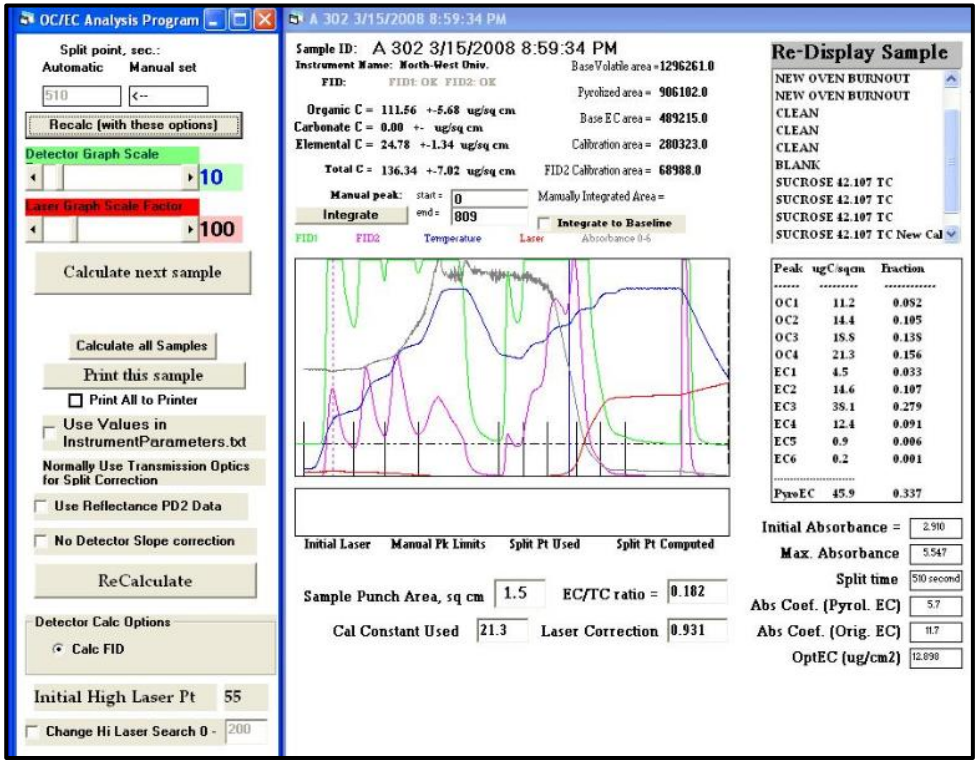

Figure 126: Thermogram for atmospheric PM samples from Delpark, Mpumalanga.

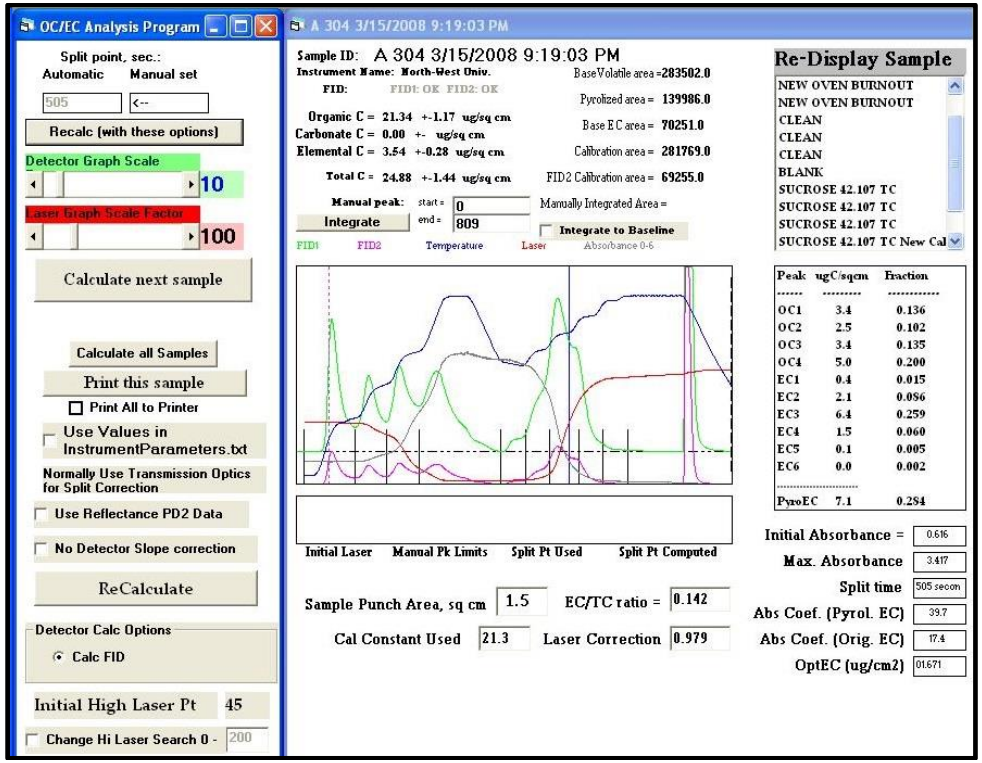

Figure 127: Thermogram for atmospheric PM samples from Clewer, Mpumalanga.

It is evident that thermal optical analysis of the carbon in atmospheric samples in combination with IRMS in principle allows the source of the carbon to be determined.

5 DISCUSSION

5.1 Introduction

Various sources of carbonaceous aerosols exist in the Highveld Priority Area and the Waterberg Bojanala Priority Area. These include biological, geological and combustion related sources such as power generation, chemical industries, smelters, biomass burning, domestic fuel burning and open burning of waste. The main objective of the study was to distinguish between carbon from coal mining and carbon from other sources in coal mining regions through the characterisation of the carbonaceous component of atmospheric PM. Various microscopic, spectroscopic, thermogravimetric and thermal optical techniques were applied. This section discusses the results obtained.

5.2 Characterisation of Atmospheric Particulate Matter Samples: SEM-EDS

The application of SEM-EDS for the analysis of atmospheric PM from opencast coal mines and adjacent communities in Mpumalanga and Limpopo culminated in the determination of the chemical composition, morphological and dimensional characteristics of individual atmospheric PM. This enabled the identification and grouping of atmospheric particles from the opencast coal mines and communities under the following categories;

- Coal dust particulates (carbonaceous), semi-carbonaceous and non-coal dust particulates. The categorisation of coal dust particles was based on morphological, particle dimensions and elemental composition characteristics obtained from SEM-EDS. The coal dust particulates had characteristic sharp serrated edges, and a layered appearance which is characteristic of sedimentary rocks (coal is an organic sedimentary rock). The morphology and size of coal dust particulates is obviously influenced by the mechanical processes employed during opencast coal mining activities which result in the emission of coarse coal dust particulates and other forms of dust.
- Aluminosilicate particles which generally contain Ca, Si or Al and are characterised by rough angular and polyhedral shapes. The sources of these particulates were identified as crustal, soils and road dust. Other identified elements which can be found in smaller concentrations within the aluminosilicates included Mg, Na and Mn.
- Biological particles which were characterised by high levels of C and O and had different shapes i.e., spherical and angular.

- Diesel particulate matter or DPM containing high levels of carbon. The fine agglomerates of carbonaceous material observed in the opencast coal mines and communities' atmospheric particulate samples were identified as DPM. This is in line with findings from other SEM-EDS studies which indicate that the contents of DPM generally include very fine carbonaceous matter (1 µm or less) which agglomerates in chains. Sources of these particulates were identified as domestic fuel burning and vehicle emissions. DPM is a good indicator or tracer for vehicle emissions.
- Metal oxides which were characterised by the presence of Zn, Fe, Cu, Ti and are generally of crustal and anthropogenic origin. The anthropogenic sources of these aerosols can be identified as industrial activities, power generation, vehicle emissions, etc. In highly industrialised regions such as the Highveld Priority Area, various industrial sources contribute significantly to emissions of metal oxides.
- Salt particles which consist mainly of NaCl and are characterised by linear and angular shapes. The source of these particles was identified as marine aerosols.

The atmospheric particulates constitute a complex mixture in chemical composition, dimensions and morphology depending on their sources. This complexity has been alluded to in most SEM-EDS studies.

Coal dust particulates were identified from the community atmospheric PM samples, particularly in the case of Clewer. This community is located adjacent to coal mines and a coal rail siding and the presence of coal dust particulates in the atmospheric PM samples derived from this community is an indication that fugitive emissions from coal mining and associated activities contribute to atmospheric PM levels in this community.

The identified non-coal dust particulates and semi-carbonaceous material in the opencast coal mining samples was an indication that some of the mining related activities such as overburden and topsoil removal contributed significantly to particulate emissions, including fine particulate (2.5 µm or less). The sources of this fine particulate matter in opencast coal mining include re-suspended particulates within the mining operations, primary and secondary anthropogenic combustion remnants, products of vehicle emissions and spontaneous combustion. Previous studies have identified resuspension of particulates as a significant source of fine atmospheric PM in coal mines and this contributes to high levels of dust from the mine roads (both paved and unpaved). The removal of material which can

be resuspended on the roads through mechanical sweeping will reduce emissions and prevent further resuspension of material.

The sources of the particulate from the communities' samples were identified as industrial activities, coal mining, power generation, domestic fuel combustion and open burning of waste. This was an indication that various sources contributed to atmospheric PM levels, particularly in communities located in the Highveld Priority Area in Mpumalanga (Clewer and Delpark).

Given the contribution of various sources to atmospheric PM in these communities, it is important that ambient air quality management takes into consideration site dispersion potential. Pollution plumes from opencast coal mines and other sources of emissions may travel in the direction of the communities, particularly in Clewer with predominant easterly and south easterly winds, and in Delpark with easterly winds, blowing from mine sites towards residential areas. The differentiation between particulates arising from mines and from other sources could however, not be achieved through the application of SEM-EDS only, although qualitative differentiation could in some instances be achieved for the particles resulting from vehicle emissions, power generation, industrial activities, open burning of waste and biomass burning. As an example, atmospheric particulates which exhibited morphological characteristics such as spherical shapes, chain agglomerates (DPM) and chemical compositions which indicated their carbonaceous nature, were identified as internal combustion-engine related. Previous studies indicate that 90% of this DPM has a diameter of less than 1 µm and primarily contains OC, EC, hydrocarbons (condensed and adsorbed) and sulphates. This is in agreement with the findings of this research study with regards to the characteristics of DPM and its components which include EC and OC. The presence of OC and EC in the atmospheric PM samples was also corroborated by the thermal optical analysis results.

Limitations associated with the application of SEM-EDS during the study included relatively poor sensitivity of EDS to elements which were present in low quantities in the atmospheric PM samples and the fact that prior to analysis with SEM, sample coating was undertaken to increase sample conductivity. However, wavelength dispersive X-ray spectroscopy (WDS), a technique that has better capability in terms of detecting light elements such as H can be used as an alternative to SEM-EDS. One other limitation associated with SEM-EDS is the

inability of the technique to provide molecular structure information and to differentiate between elements and compounds. For example, SEM-EDS detected sulphur-containing particulates but did not have the ability to differentiate between elemental sulphur and sulphur compounds such as sulphates.

5.3 Characterisation of Atmospheric Particulate Matter Using Reflectance Microscopy

In this research study, reflectance analysis of the atmospheric PM samples did not yield any reflectance results due to the resolution limits of the light microscope. Although the microscopic images indicated the presence of black atmospheric particulates which were qualitatively identified as coal dust particulates, it was not possible to obtain a clear image on which to conduct reflectance analysis for the identification of coal dust and non-coal dust particulates. It is envisaged that the research work currently being undertaken by CSIRO will provide more insight and knowledge on the application of reflectance microscopy for the characterisation of coal dust in urban dust samples.

In addition to the challenges associated with the resolution limits presented by the reflectance microscope used in this study, the lack of a standard methodology for mounting small amounts (<20 mg) of atmospheric PM samples for the purposes of reflectance microscope analysis was also identified as a challenge.

However, given the recent developments in the field of microscopy and techniques for dust analysis, it is envisaged that improvements in the use of reflectance microscopy for the characterisation of coal dust and other atmospheric particulates will eventually result in generally accessible methods.

5.4 Characterisation of Atmospheric Particulate Matter Using Optical Microscopy

The characterisation of atmospheric PM through optical microscopy and the Zeiss AxioImager software yielded results which indicated atmospheric particulate morphology and dimensions (Ferret diameter). However, the level of detail obtained on atmospheric PM was limited, especially when compared to the level of detail that was obtained through SEM-EDS. These limitations include poor resolution limits, poor surface view of particulates and

magnification limits. The resolution limits were quite evident when at 200X magnification, the particulate images became distorted and there was increasing difficulty in distinguishing the particulates' morphological details as shown in the results section of the study.

Optical microscopy is therefore limited to instances where economical methods are required to do widespread surveys of particulate concentration and size distribution. The standard particle image analysis software available from the public domain and from microscope suppliers increases the productivity in these applications.

5.5 Characterisation of Atmospheric Particulate Matter Using Raman Spectroscopy

The analysis of samples using Raman spectroscopy focused on the carbonaceous component of atmospheric PM for the purposes of differentiating the OC and EC fractions. The Raman spectra for all the atmospheric PM samples (opencast coal mines and communities) indicated identical carbon wavelengths or signatures for amorphous carbon band, D, which was observed at 1360 cm^{-1}. The D band was particularly evident in the opencast coal mine atmospheric PM samples. The graphitic band, G, was observed in all the atmospheric PM samples at approximately 1600 cm^{-1}. The D band is generally associated with disordered and amorphous carbons i.e. structural and chemical defects in the carbon crystal lattice and carbon bonding with other non-carbon atoms such as H and O. There are different potential sources of amorphous carbon (a-C) and these include non-combustion related activities. Given that non-combustion related activities can also be sources of a-C, biological material and opencast coal mining activities were identified as sources of OC. Previous investigations also indicate that the different potential sources of amorphous carbon (a-C) and OC include non-combustion related activities and incomplete combustion of organic material such as plant and animal material.

On the other hand, EC is generally formed through combustion processes such as power generation, vehicle emissions, spontaneous combustion in coal mines and other industrial activities. During combustion of carbonaceous material, temperature increases result in the expulsion of chemical defects from the crystal lattice while the carbon remnants undergo re-organisation to form a more ordered carbon structure which transforms into highly ordered graphite during the metamorphism stage. It is this graphitic component that provides the G band signals in carbonaceous material. In this study, the G band was therefore linked to the

presence of EC in the atmospheric PM samples. The application of Raman for the purposes of differentiating EC and OC, was qualitatively achieved in this study. Previous studies have also shown that Raman can be applied for the purposes of differentiating between EC and OC. Potgieter-Vermaak (2006) and Van Grieken (2006), have shown that modern techniques such as Raman micro-spectroscopy can also be applied for the analysis of individual atmospheric particulates (Ivleva *et al*., 2007). Individual particulate analysis is achieved through the combination of the spatial resolution of an optical microscope and the analytical capabilities of Raman spectroscopy. However, Raman spectroscopy on its own provided insufficient information for source apportionment of the carbon-containing particulate.

5.6 Characterisation of Atmospheric Particulate Matter Using X-ray Photoelectron Microscopy

High resolution survey spectra collected from opencast coal mines and community particulate samples indicated that O_2, C, Fe and Si dominated the surface chemical composition of the atmospheric particulates. The presence of these elements has also been detected in XPS studies on respirable coal dust. However, the differentiation of EC and OC could not be undertaken using XPS. The varying carbon signals or binding energies observed in the XPS spectra for the atmospheric PM samples from opencast coal mines and communities were not due to differences between EC and OC signatures. The signals were an indication that the carbon was likely to be bonded to more electronegative atoms such as H and O. Although the binding energy provided an indication of the chemical state of carbon on the surface of all the atmospheric PM samples, it could not be applied for the purposes of differentiating the source of the carbon. This said, a considerable number of previous studies are in wide agreement that the surface composition of atmospheric particulates is crucial for the understanding of atmospheric processes such as scavenging and adsorption (Song & Peng 2009).

5.7 Characterisation of Atmospheric Particulate Matter: Thermogravimetric Analysis

The differentiation of OC and EC in atmospheric PM samples collected from opencast coal mines and communities was qualitatively achieved through TGA analysis. Given that in most

speciation studies, the differentiation between OC and EC is generally achieved through the application of TGA, the expectation was that TGA could also be applied successfully in the study, as previously undertaken on samples such as crushed coal powders whose constituents are not submicron particulates as is the case in this research study. In addition, the atmospheric PM sample sizes collected during this study were too small for TGA to fully resolve minute mass losses that reveal the differences in composition and enable the accurate differentiation of OC and EC.

However, thermal optical analysis, as shown in this study, is a superior technique for the differentiation of OC and EC which can be employed instead of TGA for the characterisation of the carbonaceous component of atmospheric PM.

5.8 Characterisation of Atmospheric Particulate Matter: Isotope Ratio Mass Spectrometry

The application of IRMS in this research study indicated clear differences in mine-related and community-related carbon and nitrogen isotope abundances. Community samples have consistently lower (more negative) $\delta^{13}C$ ratios and higher $\delta^{15}N$ ratios than samples taken in the coal processing areas (as opposed to overburden-processing) areas, with the possibility of the development of a characteristic $\delta^{13}C/ \delta^{15}N$ index. Isotope ratio techniques therefore seem to be potentially robust and powerful tools for this identification. In addition, a considerable literature base exists on the abundances for different soils and carbon-containing substances, including coal, combustion products from different fossil fuels and biological materials, which will assist future source apportionment exercises.

In South Africa, domestic fuel burning is a major source of various air pollutants, including NO_x, particularly in areas where coal, paraffin and wood are utilised as sources of energy. In the adjacent communities selected for the study, particularly Clewer and Delpark, domestic fuel burning was observed during the sampling campaign. Biomass-related atmospheric PM for the community samples is confirmed by the ($\delta^{13}C$) value for the more rural area around Marapong, but not for Clewer and Delpark where biomass is less readily available.

5.9 Characterisation of Atmospheric Particulate Matter: Thermal Optical Techniques

Thermal optical analysis enabled the quantification and differentiation of OC and EC in the atmospheric PM samples. Generally, mine samples have a much lower OC/EC ratio than combustion-related sources. Therefore, it may be possible to distinguish between different coal fields and/or mines based on a more detailed analysis. The limited number of samples taken in this exploratory study did not allow the exact combustion source for the high OC/EC ratios in the residential samples to be determined. There is an indication that the contribution of biomass in the rural village is higher than that in the urban areas, where coal use is more prevalent. The results of the thermal optical analysis therefore, corroborate those of IRMS.

Complexities still exist in fully characterising atmospheric PM through thermal optical analysis and the OC and EC components of $PM_{2.5}$ and PM_{10} are the most uncertain with respect to sampling and analysis (Huebert and Charlson, 2000; Jacobson *et al*., 2000; Turpin *et al*., 1994).

6 CONCLUSIONS AND RECOMMENDATIONS

6.1 CONCLUSIONS

Given the complexities associated with atmospheric PM i.e. health and environmental impacts, toxicity, various sources, different particle sizes, mode of formation, atmospheric conversion and formation of other secondary particulates with different chemistries, sophisticated and modern techniques are necessary for understanding atmospheric PM. The main objective of the research study was the distinguishing of carbon from coal mining and carbon from other sources such as biological and combustion sources in coal mining regions, i.e characterisation of the carbonaceous component of atmospheric PM, through the application of various microscopic, spectroscopic, thermogravimetric and thermal optical techniques.

SEM-EDS, IRMS, TGA, XPS and Raman spectroscopy were applied to actively and passively collected samples. SEM-EDS proved to be a powerful tool and provided a wealth of information and insight on the morphological, dimensional and chemical composition characteristics of the atmospheric PM samples. However, thermal optical analysis was the only technique which enabled the quantification and differentiation of OC and EC. IRMS enabled the differentiation between atmospheric PM from the opencast coal mines and different communities. The findings indicate that currently, no single technique is available to unambiguously identify particulates arising from coal mining and other human activities, but that a combination of thermal optical analysis and IRMS, with corroboration from some of the other techniques such as SEM-EDS, will enable this identification and determination of the origin of carbon in atmospheric particulate PM.

The locally developed passive samplers that were employed in the research study for atmospheric PM sampling in opencast coal mining operations and adjacent communities provided individual particles that were later analysed using SEM-EDS and optical microscopy.

6.2 RECOMMENDATIONS

- Passive samplers can be used in various parts of South Africa and could be utilised to supplement existing ambient monitoring networks, especially in the priority air quality management areas and other areas which lack air quality ambient monitoring equipment. The problem of inadequate ambient monitoring stations is a common occurrence in South Africa and other developing countries due to critical socio-economic factors such as poverty alleviation, lack of resources, particularly financial resources. This necessitates the development of cost-effective monitoring technologies such as the locally developed passive samplers employed in this research study. The wealth of information obtained from SEM-EDS as shown in this study and previous studies can be utilised and applied for the purposes of air quality management, community education and awareness, health and environmental management, especially in highly industrialised regions such as the Highveld Priority Area. For the coal mining industry, this information will provide understanding on how coal dust and other types of particulate matter affect the environment, health and wellbeing of employees and communities living adjacent to coal mining operations. This information can also be critical to the coal mining industry for the designing of effective mitigation measures for the prevention and control of fugitive dust associated with coal mining operations (Appendix A).

- The use of this SEM-EDS is limited in South Africa. It is recommended that regional and local air quality management plans developed by state institutions, particularly in air quality management priority areas, take into consideration existing information from SEM-EDS studies. If this information is not available, efforts should be directed towards the undertaking of such studies. The current PM NAAQS are only mass based and are therefore, not suitable for the unique characterisation of health risks, particularly in heavily polluted areas such as the Highveld Priority Area. Industries can also apply SEM-EDS to fully understand the impacts of their activities on local and regional ambient air quality and more crucially, impacts on communities adjacent to their operations. This is critical given growing public and sustainability concerns over the role of industries in the degradation of ambient air quality and the environment in general, and the need for the identification or characterisation of ‘new’ and ‘ultrafine’ particulates which can have major impacts on health and the environment.

- There are no standardised methods for the characterisation of coal dust. Currently, coal dust particulates are identified through chemical analysis as there is no distinguishable/unique tracer to the source. The lack of an elemental ratio that can be utilised to differentiate coal particulates from other non-coal particulates exacerbates the problem. Although thermal optical analysis allowed the quantification of OC and EC in the atmospheric PM samples, coal dust particulates could not be identified uniquely through the application of thermal optical analysis only as currently there is no comprehensive thermal optical signature for coal dust. A combination of thermal optical analysis and IRMS seems the most promising approach and further research on how the results of these techniques can be combined to provide a 'coal fingerprint', potentially fine-tuned to specific coal fields, is recommended. This might also contribute towards the characterisation and understanding of vehicle emissions, particularly DPM and other components such as soot, as well as contributions from biomass burning from veld fires and agricultural activities.
- The study highlights challenges associated with the application of techniques that are traditionally designed for the analysis of large samples of materials, crushed powders, etc., and not necessarily atmospheric PM analysis. This challenge was evident during Raman, reflectance and TGA analysis. It is recommended that further research be undertaken on developing new techniques and improving existing techniques to accommodate atmospheric PM analysis. One of the critical factors is the choice of filter material to avoid interferences during particle analysis and to ensure filter media compatibility for atmospheric PM monitoring and sample analysis procedures/ protocols. It is therefore, recommended that any future research on the characterisation of atmospheric PM takes these compatibility issues into account.

7 REFERENCES

ACTTR Technology (2015) *What Are The Common Applications By Thermal Analysis?* Available at: http://www.acttr.com/en/en-faq/en-faq-thermal-analysis/189-en-faq-thermal-analysis-applications.html (Accessed: 26 November 2019).

Adams, K. M. (1994) Chemical characterisation of atmospheric particles, in *European Research Course on Atmospheres*. Grenoble, France.

Adams, P. J., Seinfeld, J. H. and Koch, D. M. (1999) Global concentrations of tropospheric sulfate, nitrate, and ammonium aerosol simulated in a general circulation model, *The Journal of Geophysical Research*, 104(13), pp. 719–823.

Agarwal, U. P. and Atalla, R. H. (1995) Raman Spectroscopy, in Conners, T. E. and Banerjee, S. (eds) *Surface analysis of paper*. Boca Raton, FL: CRC Press, Inc, pp. 152–181.

Ahmed, M., Guo, X. and Zhao, X. M. (2017) Spectroscopic and microscopic characterization of atmospheric particulate matter, *Instrumentation Science and Technology*. Informa UK Limited, 45(6), pp. 659–682. doi: 10.1080/10739149.2017.1308377.

Ahuja, D. and Tatsutani, M. (2009) Sustainable energy for developing Countries, *Sapiens*, 2(1), p. Online. Available at: http://journals.openedition.org/sapiens/823.

Akatsu, M. (2015) The Problem of Air Pollution During the Industrial Revolution: A Reconsideration of the Enactment of the Smoke Nuisance Abatement Act of 1821, *Monograph Series of the Socio-Economic History Society, Japan*. Springer Japan, pp. 85–109. doi: 10.1007/978-4-431-55507-0_4.

Albarakat, R and Lakshmi, V (2019) Monitoring Dust Storms in Iraq Using Satellite Data, *Sensors*. MDPI AG, 19(17), p. 3687. doi: 10.3390/s19173687.

Albers, P. N., Wright, C. Y., Voyi, K. V. V. and Mathee, A. (2015) Household fuel use and child respiratory ill health in two towns in Mpumalanga, South Africa, *South African Medical Journal*. South African Medical Association NPC, 105(7), pp. 573–577. doi: 10.7196/SAMJnew.7934.

Allen, T. (2003) Powder sampling, in *Powder Sampling and Particle Size Determination*. Elsevier, pp. 1–55. doi: 10.1016/B978-044451564-3/50003-6.

AME Staff (2018) *TGA Analysis or Thermogravimetric Analysis*, *Anderson Materials Evaluation, Inc.* Available at: http://www.andersonmaterials.com/tga.html (Accessed: 29 November 2019).

Al Ameri, I. D. S., Briant, R. M. and Engels, S. (2019) Drought severity and increased dust storm frequency in the Middle East: a case study from the Tigris–Euphrates alluvial plain, central Iraq, *Weather*. Wiley. doi: 10.1002/wea.3445.

Amponsah-Dacosta, F. (1997) *Cost Effective Strategies for Dust Control in an Opencast Coal Mine*. University of the Witwatersrand, Johannesburg, South Africa.

Andersson, A., Deng, J., Du, K., Zheng, M., Yan, C., Sköld, M. and Gustafsson, Ö. (2015) Regionally-Varying Combustion Sources of the January 2013 Severe Haze Events over Eastern China. Environ. Sci. Technol. 49, 2038−2043 doi:10.1021/es503855e

Anderson, J. O., Thundiyil, J. G. and Stolbach, A. (2012) Clearing the Air: A Review of the Effects of Particulate Matter Air Pollution on Human Health, *Journal of Medical Toxicology*. Springer Science and Business Media LLC, 8(2), pp. 166–175. doi: 10.1007/s13181-011-0203-1.

Anderson Materials Evaluation Inc. (2018) *Thermal analysis*. Available at: http://www.andersonmaterials.com (Accessed: 3 April 2019).

Andrade, F., Orsini, C. and Maenhaut, W. (1993) Receptor modeling for inhalable atmospheric particles in Sao Paulo, Brazil, *Nuclear Inst. and Methods in Physics Research, B*. Elsevier BV, 75(1–4), pp. 308–311. doi: 10.1016/0168-583X(93)95665-R.

Andrade, J. D. (ed.) (1985a) *Surface and Interfacial Aspects of Biomedical Polymers*, *Surface and Interfacial Aspects of Biomedical Polymers*. Boston, MA: Springer US. doi: 10.1007/978-1-4684-8610-0.

Andrade, J. D. (1985b) X-ray Photoelectron Spectroscopy (XPS) BT- Surface and Interfacial Aspects of Biomedical Polymers: Volume 1 Surface Chemistry and Physics, in *Surface and Interfacial Aspects of Biomedical Polymers*. Boston, MA: Springer US, pp. 105–195. doi: 10.1007/978-1-4684-8610-0_5.

Andreae, M. O. and Gelencsér, A. (2006) Black carbon or brown carbon? The nature of light-absorbing carbonaceous aerosols, *Atmospheric Chemistry and Physics*. Copernicus GmbH, 6(10), pp. 3131–3148. doi: 10.5194/acp-6-3131-2006.

Aneja, V. P., Isherwood, A. and Morgan, P. (2012) Characterization of particulate matter (PM 10) related to surface coal mining operations in Appalachia, *Atmospheric Environment*. Elsevier BV, 54, pp. 496–501. doi: 10.1016/j.atmosenv.2012.02.063.

Appleton, T. J., Kingman, S. W., Lowndes, I. S. and Silvester, S. A. (2006) The development of a modelling strategy for the simulation of fugitive dust emissions from in-pit quarrying activities: A UK case study, *International Journal of Mining, Reclamation and Environment*. Informa UK Limited, 20(1), pp. 57–82. doi: 10.1080/13895260500396404.

Aspeling, C. P. and Adamski, S. A. (2002) The backfilling of spontaneous combustible material into pre-built compartments at Grootegeluk Coal Mine, in *Open Cut Coal Conference*. Mackay, Queensland,.

Assael, M. J., Melas, D. and Kakosimos, K. E. (2010) Monitoring particulate matter concentrations with passive samplers: Application to the Greater Thessaloniki area, *Water, Air, and Soil Pollution*. Springer Science and Business Media LLC, 211(1–4), pp. 395–408. doi: 10.1007/s11270-009-0308-1.

Averitt, P. (1975) *Coal Resources of the United States, January 1, 1974.*, *U S Geol Surv Bull*. US Geological Survey. doi: 10.3133/b1412.

Baeten, V. and Dardenne, P. (2002) Spectroscopy: Developments in instrumentation and analysis, *Grasas y Aceites*. Departmento de Publicaciones del CSIC, 53(1), pp. 45–63. doi: 10.3989/gya.2002.v53.i1.289.

Ballentine, D. C., Macko, S. A., Turekian, V. C., Gilhooly, W. P. and Martincigh, B. (1996) Compound specific isotope analysis of fatty acids and polycyclic aromatic hydrocarbons in aerosols: Implications for biomass burning, *Organic Geochemistry*. Elsevier BV, 25(1-2–2 pt 5), pp. 97–104. doi: 10.1016/S0146-6380(96)00110-6.

Balmer, M. (2007) Household coal use in an urban township in South Africa, *Journal of Energy in Southern Africa*, 18(3), pp. 27–32. doi: 10.17159/2413-3051/2007/v18i3a3382.

Baltensperger, U., Nyeki, S. and Kalberer, M. (2007) *Atmospheric particulate matter*, *Handbook of Atmospheric Science: Principles and Applications*. Cambridge. doi: 10.1002/9780470999318.ch9.

Banerjee, S. P. (1994) *TSP emission factors for different mining activities for air quality impact prediction as collated from different sources*, *Minetech*.

Barraza, F. (2018) *Human exposure assessment related to oil activities in Ecuador : from the air quality monitoring to the study of metallic contaminants transfer in the soil-plant Fiorella Barraza Castelo To cite this version : HAL Id : tel-01668502*. Universite Toulouse 3 Paul Sabatier. Available at: https://tel.archives-ouvertes.fr.

Barston, R. P. (2019) The Paris agreement, in *Modern Diplomacy*. Fifth Edit. New York, NY: Routledge, pp. 492–505. doi: 10.4324/9781351270090-20.

Batonneau, Y., Sobanska, S., Laureyns, J. and Bremard, C. (2006) Confocal microprobe Raman imaging of urban tropospheric aerosol particles, *Environmental Science and Technology*. American Chemical Society (ACS), 40(4), pp. 1300–1306. doi: 10.1021/es051294x.

Benson, S., Lennard, C., Maynard, P. and Roux, C. (2006) Forensic applications of isotope ratio mass spectrometry - A review, *Forensic Science International*. Elsevier BV, 157(1), pp. 1–22. doi: 10.1016/j.forsciint.2005.03.012.

Berto, D., Rampazzo, F., Gion, C., Noventa, S., Formalewicz, M., Ronchi, F., Traldi, U. and Giorgi, G. (2019) Elemental Analyzer/Isotope Ratio Mass Spectrometry (EA/IRMS) as a Tool to Characterize Plastic Polymers in a Marine Environment, in *Plastics in the Environment*. IntechOpen. doi: 10.5772/intechopen.81485.

Birch, M. E. and Cary, R. A. (1996) Elemental Carbon-Based Method for Monitoring Occupational Exposures to Particulate Diesel Exhaust, *Aerosol Science and Technology*. Informa UK Limited, 25(3), pp. 221–241. doi: 10.1080/02786829608965393.

Bikkina, S., Kawamura, K. and Manmohan S. (2016) Stable carbon and nitrogen isotopic composition of fine mode aerosols (PM2.5) over the Bay of Bengal : impact of continental sources. *31* 68 pp 31518-31533 doi 10.3402/tellusb.v68.31518.

Bitkolov, A. Z. (1969) Wind and temperature stratification of quarry atmospheres, *Soviet Mining Science*. Springer Science and Business Media LLC, 5(5), pp. 546–551. doi: 10.1007/BF02501273.

Blanco, C., Casal, E., Granda, M. and Menéndez, R. (2003) Influence of fibre-matrix interface on the fracture behaviour of carbon-carbon composites, *Journal of the European Ceramic Society*. Elsevier BV, 23(15), pp. 2857–2866. doi: 10.1016/S0955-2219(03)00298-X.

Bloss, W. (2014) *Atmospheric particulate matter. ECG Environmental Briefs, ECGEB No. 4*. Birmingham. Available at: https://www.envchemgroup.com/eb4-atmospheric-particulate-matter.html (Accessed: 12 February 2019).

Boubel, R. W., Fox, D. L., Turner, D. B. and Stern, A. C. (1994) Air Pollution Monitoring and Surveillance, *Fundamentals of Air Pollution*. Elsevier, pp. 216–228. doi: 10.1016/b978-0-08-050707-1.50019-6.

Bray, C. D., Battye, W., Uttamang, P., Pillai, P. and Aneja, V. P. (2017) Characterization of particulate matter (PM2.5 and PM10) relating to a coal power plant in the boroughs of Springdale and Cheswick, PA, *Atmosphere*. MDPI AG, 8(10), p. 186. doi: 10.3390/atmos8100186.

Briggs, D. and Seah, M. P. (1990) *Practical Surface Analysis, Auger and X-ray Photoelectron Spectroscopy*. Second Edi. Edited by D. Briggs and M. . Seah. Available at: https://www.amazon.com/Practical-Surface-Analysis-Photoelectron-Spectroscopy/dp/0471920819.

Brodie, C. (2018) *EA-IRMS: Using isotope fingerprints to track sources of PM2.5 in air pollution*. Germany: Thermo Fisher Scientific. Available at: https://assets.thermofisher.com/TFS-Assets/CMD/Application-Notes/ab-30482-ea-irms-isotope-fingerprints-air-pollution-ab30482-en.pdf.

Brown, R. C., Hemingway, M. A., Wake, D. and Thorpe, A. (1996) Electret-based passive dust sampler: Sampling of organic dusts, *Analyst*. Royal Society of Chemistry (RSC), 121(9), pp. 1241–1246. doi: 10.1039/an9962101241.

Brown, R. H. (1993) The use of diffusive samplers for monitoring of ambient air: Position paper on their environmental potential and the need for further research (technical report), *Pure and Applied Chemistry*. Walter de Gruyter GmbH, 65(8), pp. 1859–1874. doi: 10.1351/pac199365081859.

Brown, S., Iverson, L. R., Prasad, A. and Liu, D. (1993) Geographical distributions of carbon in biomass and soils of tropical asian forests, *Geocarto International*. Informa UK Limited, 8(4), pp. 45–59. doi: 10.1080/10106049309354429.

Bumbrah, G. S. and Sharma, R. M. (2016) Raman spectroscopy – Basic principle, instrumentation and selected applications for the characterization of drugs of abuse, *Egyptian Journal of Forensic Sciences*. Springer Nature, 6(3), pp. 209–215. doi: 10.1016/j.ejfs.2015.06.001.

Buzgar, N., Apopei, A. I. and Buzatu, A. (2009) *Advantages and disadvantages of Raman Spectroscopy - Romanian Database of Raman Spectroscopy*. Available at: http://www.rdrs.ro/blog/articles/advantages-disadvantages-raman-spectroscopy/ (Accessed: 28 November 2019).

Cabada, J. C., Pandis, S. N., Subramanian, R., Robinson, A. L., Polidori, A. and Turpin, B. (2004) Estimating the Secondary Organic Aerosol Contribution to PM2.5 Using the EC Tracer Method. Special Issue of Aerosol Science and Technology on Findings from the Fine Particulate Matter Supersites Program, *Aerosol Science and Technology*. Informa UK Limited, 38(sup1), pp. 140–155. doi: 10.1080/02786820390229084.

Cao, J., Wang, Y., Zhang, X., Lee, S., Ho, K., Cao, Y. and Li, Y. (2004) Analysis of carbon isotopes in airborne carbonate and implications for aeolian sources, *Chinese Science Bulletin*. Springer Science and Business Media LLC, 49(15), pp. 1637–1641. doi: 10.1007/bf03184135.

Cao, J., Lee, S. C., Chow, J. C., Watson, J. G., Ho, K. F., Zhang, R. J., Jin, Z. D., Shen, Z. X., Chen, G. C., Kang, Y. M., Zhou, S. C., Zhang, L. Z., Qi, S. H., Dai, M. H., Cheng, Y. and Hu, K. (2007) Spatial and seasonal distributions of carbonaceous aerosols over China, *Journal of Geophysical Research Atmospheres*. American Geophysical Union (AGU), 112(22), p. D22S11. doi: 10.1029/2006JD008205.

Cao, J., Chow, J. C., Tao, J., Lee, S. cheng, Watson, J. G., Ho, K. fai, Wang, G. hui, Zhu, C. shu and Han, Y. ming (2011) Stable carbon isotopes in aerosols from Chinese cities: Influence of fossil fuels, *Atmospheric Environment*. Elsevier BV, 45(6), pp. 1359–1363. doi: 10.1016/j.atmosenv.2010.10.056.

Capes, G., Murphy, J. G., Reeves, C. E., McQuaid, J. B., Hamilton, J. F., Hopkins, J. R., Crosier, J., I.Williams, P. and Coe, H. (2009) Secondary organic aerosol from biogenic VOCs over West Africa during AMMA, *Atmospheric Chemistry and Physics*. Copernicus GmbH, 9(12), pp. 3841–3850. doi: 10.5194/acp-9-3841-2009.

Carras, J. N., Day, S., Saghafi, A. and Roberts, O. C. (2005) Spontaneous Combustion in Open Cut Coal Mines- Recent Australian Research Spontaneous Combustion in Open Cut Coal Mines, in Carras, J. . et al. (eds) *COAL2005 Conference*, pp. 195–200.

Carter, J. F. and Barwick, V. J. (2011) *Good practice guide for isotope ratio Mass Spectrometry*, *FIRMS Network*. Edited by J. . Carter and V. . Barwick. FIRMS. doi: 10.1016/j.forc.2018.10.005.

Casuccio, G. S., Schlaegle, S. F., Lersch, T. L., Khosah, R. P., Robinson, A. L., Treado, P. J. and Martello, D. V (2002) Characterisation of Ambient Particulate Matter Using Electron Microscopy and Raman Spectroscopy Techniques, in *NETL Conference on PM2 (Vol. 5).* Pittsburgh. Available at: citeseerx.ist.psu.edu.

Casuccio, G. S., Schlaegle, S. F., Lersch, T. L., Huffman, G. P., Chen, Y. and Shah, N. (2004) Measurement of fine particulate matter using electron microscopy techniques, *Fuel Processing Technology*. Elsevier BV, 85(6–7), pp. 763–779. doi: 10.1016/j.fuproc.2003.11.026.

Cavalli, F., Viana, M., Yttri, K. E., Genberg, J. and Putaud, J. P. (2010) Toward a standardised thermal-optical protocol for measuring atmospheric organic and elemental carbon: The EUSAAR protocol, *Atmospheric Measurement Techniques*. Copernicus GmbH, 3(1), pp. 79–89. doi: 10.5194/amt-3-79-2010.

Cavalli, F., Alastuey, A., Areskoug, H., Ceburnis, D., Čech, J., Genberg, J., Harrison, R. M., Jaffrezo, J. L., Kiss, G., Laj, P., Mihalopoulos, N., Perez, N., Quincey, P., Schwarz, J., Sellegri, K., Spindler, G., Swietlicki, E., Theodosi, C., Yttri, K. E., Aas, W. and Putaud, J. P. (2016) A European Aerosol Phenomenology -4: Harmonized Concentrations of Carbonaceous Aerosol at 10 Regional Background Sites Across Europe, *Atmospheric Environment*. Elsevier BV, 144, pp. 133–145. doi: 10.1016/j.atmosenv.2016.07.050.

Ceburnis, D., Masalaite, A., Ovadnevaite, J., Garbaras, A., Remeikis, V., Maenhaut, W., Claeys, M., Sciare, J., Baisnée, D. and O'Dowd, C. D. (2016) Stable isotopes measurements reveal dual carbon pools contributing to organic matter enrichment in marine aerosol, *Scientific Reports*. Springer Science and Business Media LLC, 6(1). doi: 10.1038/srep36675.

Cecala, A. B., O'Brien, A. D., Schall, J., Colinet, J. F., Fox, W. R., Franta, R. J., Joy, J., Reed, W. R., Reeser, P. W., Rounds, J. R. and Schultz, M. J. (2012) *Dust Control Handbook for Industrial Minerals Mining and Processing. RI 9689- Report of Investigations/2012. Department of Health and Human Services*.

Chatterton, T., Dorling, S., Lovett, A. and Stephenson, M. (2002) The Relative Influences of Primary and Secondary Particulates to Urban Air Quality in the United Kingdom, in *Urban Air Quality — Recent Advances*. Dordrecht: Springer Netherlands, pp. 173–187. doi: 10.1007/978-94-010-0312-4_13.

Chaudhuri, S. N. (2016) Coal Macerals, *Encyclopedia of Mineral and Energy Policy*. Springer Berlin Heidelberg, pp. 1–5. doi: 10.1007/978-3-642-40871-7_93-1.

Chaulya, S. K. (2004) Assessment and management of air quality for an opencast coal mining area, *Journal of Environmental Management*. Elsevier BV, 70(1), pp. 1–14. doi: 10.1016/j.jenvman.2003.09.018.

Chaulya, S. K. (2005) Air quality status of an open pit mining area in India, *Environmental Monitoring and Assessment*. Springer Science and Business Media LLC, 105(1–3), pp. 369–389. doi: 10.1007/s10661-005-4345-y.

Chen, L.-W. A., Chow, J. C., Watson, J. G., Moosmuller, H. and Arnott, W. P. (2004) Modeling reflectance and transmittance of quartzfiber filter samples containing elemental carbon particles: Implications for thermal/optical analysis, *Journal of Aerosol Science*, 35(6), pp. 765–780. Available at: http://www.patarnott.com/pdf/ModelingFilterChen.pdf (Accessed: 29 November 2019).

Chinthala, S. and Khare, M. (2011) Particle Dispersion Within a Deep Opencast Coal Mine, in *Air Quality-Models and Applications*. In Tech. doi: 10.5772/16326.

Chow, J. C., Watson, J. G., Lowenthal, D. H., Solomon, P. A., Magliano, K. L., Ziman, S. D. and Willard Richards, L. (1992) PM10 source apportionment in California's San Joaquin valley, *Atmospheric Environment Part A, General Topics*. Elsevier BV, 26(18), pp. 3335–3354. doi: 10.1016/0960-1686(92)90350-T.

Chow, J. C., Watson, J. G., Pritchett, L. C., Pierson, W. R., Frazier, C. A. and Purcell, R. G. (1993) The DRI thermal/optical reflectance carbon analysis system: Description, evaluation and applications in US Air quality studies, *Atmospheric Environment Part A, General Topics*. Elsevier BV, 27(8), pp. 1185–1201. doi: 10.1016/0960-1686(93)90245-T.

Chow, J. C., Watson, J. G., Lu, Z., Lowenthal, D. H., Frazier, C. A., Solomon, P. A., Thuillier, R. H. and Magliano, K. (1996) Descriptive analysis of PM2.5 and PM10 at regionally representative locations during SJVAQS/AUSPEX, *Atmospheric Environment*. Elsevier BV, 30(12), pp. 2079–2112. doi: 10.1016/1352-2310(95)00402-5.

Chow, J. C. and Watson, J. G. (2002) Review of PM2.5 and PM10 apportionment for fossil fuel combustion and other sources by the Chemical Mass Balance receptor model, *Energy & Fuels*. American Chemical Society (ACS), 16(2), pp. 222–260. doi: 10.1021/ef0101715.

Christensen, S., Durrant, N., O'Connor, P. and Phillips, A. (2011) Regulating greenhouse gas emissions from coal mining activities in the context of climate change, *Environmental and Planning Law Journal*, 28(6), pp. 381–415.

Coal Terminal Action Group (Australia) (2013) *Characterisation of Coal Dust*. Available at: https://thegenerator.news/coal-terminal-action-group-2 (Accessed: 27 March 2018).

Coats, A. W. and Redfern, J. P. (1963) Thermogravimetric analysis. A review, *The Analyst*. Royal Society of Chemistry (RSC), 88(1053), pp. 906–924. doi: 10.1039/AN9638800906.

Coetsee-Hugo, L. (2016) *Scanning ESCA Microprobe - Report*. University of the Free State.

Cohen, D. D., Stelcer, E., Hawas, O. and Garton, D. (2004) IBA methods for characterisation of fine particulate atmospheric pollution: A local, regional and global research problem, *Nuclear Instruments and Methods in Physics Research, Section B: Beam Interactions with Materials and Atoms*. Elsevier BV, 219–220(1–4), pp. 145–152. doi: 10.1016/j.nimb.2004.01.043.

Cohen, D. D., Crawford, J., Stelcer, E. and Bac, V. T. (2010) Characterisation and source apportionment of fine particulate sources at Hanoi from 2001 to 2008, *Atmospheric Environment*. Elsevier BV, 44(3), pp. 320–328. doi: 10.1016/j.atmosenv.2009.10.037.

Colarco, P., Da Silva, A., Chin, M. and Diehl, T. (2010) Online simulations of global aerosol distributions in the NASA GEOS-4 model and comparisons to satellite and ground-based aerosol optical depth, *Journal of Geophysical Research Atmospheres*. American Geophysical Union (AGU), 115(14). doi: 10.1029/2009JD012820.

Contini, D., Vecchi, R. and Viana, M. (2018) Carbonaceous aerosols in the atmosphere, *Atmosphere*. MDPI AG, 9(5), p. 181. doi: 10.3390/atmos9050181.

Cowherd, C. and Englehart, J. (1985) *Size -Specific Particulate Emission Factors for Industrial and Rural Roads*. Cincinnati, Ohio. Available at: https://nepis.epa.gov.

Crippa, M., DeCarlo, P. F., Slowik, J. G., Mohr, C., Heringa, M. F., Chirico, R., Poulain, L., Freutel, F., Sciare, J., Cozic, J., Di Marco, C. F., Elsasser, M., Nicolas, J. B., Marchand, N., Abidi, E., Wiedensohler, A., Drewnick, F., Schneider, J., Borrmann, S., Nemitz, E., Zimmermann, R., Jaffrezo, J. L., Prévôt, A. S. H. and Baltensperger, U. (2013) Wintertime aerosol chemical composition and source apportionment of the organic fraction in the metropolitan area of Paris, *Atmospheric Chemistry and Physics*. Copernicus GmbH, 13(2), pp. 961–981. doi: 10.5194/acp-13-961-2013.

Cubukçu, H. E., Ersoy, O., Aydar, E. and Çakir, U. (2008) WDS versus silicon drift detector EDS: A case report for the comparison of quantitative chemical analyses of natural silicate minerals, *Micron*. Elsevier BV, 39(2), pp. 88–94. doi: 10.1016/j.micron.2006.11.004.

Currie, L. A., Benner, B. A., Kessler, J. D., Klinedinst, D. B., Klouda, G. A., Marolf, J. V., Slater, J. F., Wise, S. A., Cachier, H., Cary, R., Chow, J. C., Watson, J., Druffel, E. R. M., Masiello, C. A., Eglinton, T. I., Pearson, A., Reddy, C. M., Gustafsson, Ö., Quinn, J. G., Hartmann, P. C., Hedges, J. I., Prentice, K. M., Kirchstetter, T. W., Novakov, T., Puxbaum, H. and Schmid, H. (2002) A critical evaluation of interlaboratory data on total, elemental, and isotopic carbon in the carbonaceous particle reference material, NIST SRM 1649a, *Journal of Research of the National Institute of Standards and Technology*. National Institute of Standards and Technology (NIST), 107(3), pp. 279–298. doi: 10.6028/jres.107.022.

D'Almeida, G. A., Koepke, P. and Shettle, E. P. (1991) *Atmospheric Aerosols: Global Climatology and Radiative Characteristics (Studies in Geophysical Optics and Remote Sensing)*. A Deepak Pub. Available at: http://www.worldcat.org/isbn/0937194220.

Dai, S., Bi, X., Chan, L. Y., He, J., Wang, B., Wang, X., Peng, P., Sheng, G. and Fu, J. (2015) Chemical and stable carbon isotopic composition of PM2.5 from on-road vehicle emissions in the PRD region and implications for vehicle emission control policy, *Atmospheric Chemistry and Physics*. Copernicus GmbH, 15(6), pp. 3097–3108. doi: 10.5194/acp-15-3097-2015.

Dass, C. (2007) *Fundamentals of Contemporary Mass Spectrometry*. John Wiley & Sons, Inc. doi: 10.1002/0470118490.

Davies, T. C. and Mundalamo, H. R. (2010) Environmental health impacts of dispersed mineralisation in South Africa, *Journal of African Earth Sciences*. Elsevier BV, 58(4), pp. 652–666. doi: 10.1016/j.jafrearsci.2010.08.009.

Davis, A. (1978) *The Measurement of Reflectance of Coal Macerals: Its Automation and Significance*. Volume 10. Department of Energy, 1978. doi: 10.2172/6074074.

Davis, A., Mitchell, G. D., Derbyshire, F. J., Rathbone, R. F. and Lin, R. (1991) Optical properties of coals and liquefaction residues as indicators of reactivity, *Fuel*. Elsevier BV, 70(3), pp. 352–360. doi: 10.1016/0016-2361(91)90122-q.

Department of Energy (DoE) (2015) *Coal Resources: Overview*, *Department of Energy (DoE)*. doi: http://www.energy.gov.za//files/coal_frame.html.

Department of Energy (DoE) (2019) *Integrated Resource Plan 2019*, *Department of Energy (DoE)*. doi: http://dx.doi.org/9771682584003-32963.

Department of Environment, Food and Rural Affairs (DEFRA) (1993) *Urban Air Quality in the United Kingdom. First Report of the Quality of Urban Air Review Group.* London. Available at: https://uk-air.defra.gov.uk/library/reports?report_id=56.

Department of Environmental Affairs (DEA) (2004) *National Environmental Management: Air Quality Act, 2004 (Act No. 39 of 2004)*. Government Gazette 39805, Notice R250,South Africa: Department of Environmental Affairs. Available at: www.saaqis.org.za › documents.

Department of Environmental Affairs (DEA) (2011) *The Highveld Priority Area Air Quality Management Plan*, *Management*. Available at: http://www.saaqis.org.za/documents/HIGHVELD PRIORITY AREA.

Department of Environmental Affairs (DEA) (2014) *The Waterberg-Bojanala Priority Area Air Quality Management Plan: Baseline Characterisation*. Available at: www.saaqis.org.za.

Department of Environmental Affairs (DEA) (2016a) *Department of Environmental Affairs, 2016: Air Quality Monitoring Overview for the HPA.* Emalahleni.

Department of Environmental Affairs (DEA) (2016b) *Department of Environmental Affairs, 2016: Ambient Air Quality Monitoring- Highveld Priority Area Multi-Stakeholder Reference Group.* Richards Bay. Available at: https://saaqis.environment.gov.za (Accessed: 29 November 2019).

Department of Environmental Affairs (DEA) (2017) *The Management of Air Quality in South Africa*. Available at: www.saaqis.org.za (Accessed: 29 November 2019).

Department of Environmental Affairs (DEA) (2018a) Ambient Air Quality Monitoring Overview for the Waterberg -Bojanala Priority Area., in *Waterberg -Bojanala Priority Area Multi Stakeholder Reference Group*. Rustenburg: Department of Environmental Affairs, p. 12.

Department of Environmental Affairs (DEA) (2018b) *South African Air Quality Information System (SAAQIS)*. Available at: www.saaqis.org.za (Accessed: 29 November 2019).

Department of Mineral Resources (DMR) (2016a) *South African Mineral Industry (2016/2017)*. Available at: https://www.dmr.gov.za/LinkClick.aspx?fileticket=pBSna_Tf58Q%3D&portalid=0 (Accessed: 13 January 2019).

Department of Mineral Resources (DMR) (2016b) Type, distribution and use of coal in South Africa, in *35th International Geological Congress (IGC)*. Cape Town.

Desert Research Institute (2019) *EAF Capabilities- Carbon Analysis (TOR/TOT)*. Available at: https://www.dri.edu/eaf-lab (Accessed: 29 November 2019).

Dockery, D. W. and Pope, C. A. (1994) Acute Respiratory Effects of Particulate Air Pollution, *Annual Review of Public Health*. Annual Reviews, 15(1), pp. 107–132. doi: 10.1146/annurev.pu.15.050194.000543.

Dockery, D. W. and Stone, P. H. (2007) Cardiovascular risks from fine particulate air pollution, *New England Journal of Medicine*. Massachusetts Medical Society, 356(5), pp. 511–513. doi: 10.1056/NEJMe068274.

Dougall, A. W. and Mmola, M. (2015) Identification of key performance areas in the Southern African surface mining delivery environment, *Journal of the Southern African Institute of Mining and Metallurgy*. Academy of Science of South Africa, 115(11), pp. 1001–1006. doi: 10.17159/2411-9717/2015/v115n11a3.

Dresser, A. L. and Huizer, R. D. (2011) CALPUFF and AERMOD model validation study in the near field: Martins Creek revisited, *Journal of the Air & Waste Management Association*. Informa UK Limited, 61(6), pp. 647–659. doi: 10.3155/1047-3289.61.6.647.

Durant, A. J., Quéré, C. L., Hope, C. and Friend, A. D. (2011) Economic value of improved quantification in global sources and sinks of carbon dioxide, *The Royal Society*, 369(1943), pp. 1967–1979. doi: https://doi.org/10.1098/rsta.2011.0002.

Earth.org (2018) *Typical opencast coal mining activities*. Available at: www.earth.org (Accessed: 19 March 2019).

Eberhardt, C. and Clarke, A. (2002) *Microscopy Techniques for Materials Science*, *Microscopy Techniques for Materials Science*. CRC Press. doi: 10.1201/9781439823231.

Ebert, M., Weinbruch, S., Hoffmann, P. and Ortner, H. M. (2004) The chemical composition and complex refractive index of rural and urban influenced aerosols determined by individual particle analysis, *Atmospheric Environment*, 38(38), pp. 6531–6545. doi: 10.1016/j.atmosenv.2004.08.048.

Ebert, M., Müller-Ebert, D., Benker, N. and Weinbruch, S. (2012) Source apportionment of aerosol particles near a steel plant by electron microscopy, *Journal of Environmental Monitoring*. Royal Society of Chemistry (RSC), 14(12), p. 3257. doi: 10.1039/c2em30696d.

Edwards, R. M. (2008) United Nations Environment Programme (UNEP), in Philander, S. (ed.) *Encyclopedia of Global Warming and Climate Change*. Thousand Oaks, California: SAGE Publications, Inc. doi: 10.4135/9781412963893.n654.

Egerton, R.F. (2005) *Physical Principles of Electron Microscopy. An Introduction to TEM, SEM, and AEM*. Springer US. doi: 10.1007/B136495.

Egerton, Ray F. (2005) TEM Specimens and Images, in *Physical Principles of Electron Microscopy*. Boston, MA: Springer US, pp. 93–124. doi: 10.1007/0-387-26016-1_4.

Engelbrecht, J.P., Swanepoel, L., Chow, J.C., Watson, J.G. and Egami, R.T. (2002) The comparison of source contributions from residential coal and low-smoke fuels, using CMB modeling, in South Africa. *Envl Sci & Policy* 5 157–167.

Engel-Cox, J., Kim Oanh, N. T., van Donkelaar, A., Martin, R. V and Zell, E. (2013) Toward the next generation of air quality monitoring: Particulate matter, *Atmospheric Environment*. Elsevier BV, 80, pp. 584–590. doi: 10.1016/j.atmosenv.2013.08.016.

Engelstaedter, S., Tegen, I. and Washington, R. (2006) North African dust emissions and transport, *Earth-Science Reviews*. Elsevier BV, 79(1–2), pp. 73–100. doi: 10.1016/j.earscirev.2006.06.004.

Escamilla, J. A. H. (2015) Particulate Matter: Capture and Quantification in Natural and Anthropogenic Sources, *Journal of Environmental & Analytical Toxicology*. OMICS Publishing Group, 05(04). doi: 10.4172/2161-0525.1000281.

Eskom (2018) *Electricity Generation*. Available at: http://www.eskom.co.za (Accessed: 12 January 2019).

Fang, W., Andersson, A., Zheng, M., Lee, M., Holmstrand, H., Kim, S., Du, K. and Gustafsson, Ö. (2017) Divergent Evolution of Carbonaceous Aerosols during Dispersal of East Asian Haze. Scientific Reports 7 10422-10433 doi:10.1038/s41598-017-10766-4

Farrants, G., Reith, A., Schüler, B. and Feren, K. (1988) A simple, direct method for the collection of particles from air samples for transmission electron microscopy and digital image analysis, *Journal of Microscopy*. Wiley, 149(2), pp. 159–164. doi: 10.1111/j.1365-2818.1988.tb04572.x.

Felix, J. D., Elliott, E. M. and Shaw, S. L. (2012) Nitrogen Isotopic Composition of Coal-Fired Power Plant NOx: Influence of Emission Controls and Implications for Global Emission Inventories, *Environmental Science & Technology*. American Chemical Society (ACS), 46(6), pp. 3528–3535. doi: 10.1021/es203355v.

Fergusson, J. E. and Kim, N. D. (1991) Trace elements in street and house dusts: Sources and speciation, *Science of the Total Environment, The*, 100(C), pp. 125–150. doi: 10.1016/0048-9697(91)90376-P.

Ferralis, N. (2010) Probing mechanical properties of graphene with Raman spectroscopy, *Journal of Materials Science*. Springer Nature, 45(19), pp. 5135–5149. doi: 10.1007/s10853-010-4673-3.

Ferreira, T. M., Forti, M. C. and Alcaide, R. L. M. (2013) Inhalable particulate matter characterization in a medium-sized urban region in Brazil (São José dos Campos Town) - Part I: Morphology, *Química Nova*. FapUNIFESP (SciELO), 36(9), pp. 1380–1387. doi: 10.1590/s0100-40422013000900018.

Finkelman, R. B., Orem, W., Castranova, V., Tatu, C. A., Belkin, H. E., Zheng, B., Lerch, H. E., Maharaj, S. V and Bates, A. L. (2002) Health impacts of coal and coal use: Possible solutions, *International Journal of Coal Geology*. Elsevier BV, 50(1–4), pp. 425–443. doi: 10.1016/s0166-5162(02)00125-8.

Forster, P. (2007) *Changes in atmospheric constituents and in radiative forcing: In Climate Change 2007: The Physical Science Basis. Contribution of Working Group I to the Fourth Assessment Report of the Intergovernmental Panel on Climate Change. Edited by: Solomon, S., Qin*. Geneva, Switzerland. Available at: http://www.cgd.ucar.edu/events/20130729/files/Forster-Ramaswamy-etal-2007.pdf (Accessed: 16 April 2019).

Freyer, H. D. (1978) Seasonal trends of NH_4^+ and NO_3^- nitrogen isotope composition in rain collected at Jülich, Germany, *Tellus*. Informa UK Limited, 30(1), pp. 83–92. doi: 10.3402/tellusa.v30i1.10319.

Garbarienė,I., Šapolaitė, J., Garbaras, A., Ežerinskis, Ž., Pocevičius, M., Krikščikas, L., Plukis, A. and Remeikis, V. (2016) Origin Identification of Carbonaceous Aerosol Particles by Carbon Isotope Ratio Analysis. *Aerosol and Air Quality Res*, 16: 1356–1365 doi: 10.4209/aaqr.2015.07.0443

Garbaras, A. (2008) Tracing of atmospheric aerosol sources using stable carbon isotopes, *Lithuanian Journal of Physics*. Lithuanian Academy of Sciences, 48(3), pp. 259–264. doi: 10.3952/lithjphys.48309.

Garbaras, A., Masalaite, A., Garbariene, I., Ceburnis, D., Krugly, E., Remeikis, V., Puida, E., Kvietkus, K. and Martuzevicius, D. (2015) Stable carbon fractionation in size-segregated aerosol particles produced by controlled biomass burning, *Journal of Aerosol Science*. Elsevier BV, 79, pp. 86–96. doi: 10.1016/j.jaerosci.2014.10.005.

Garland, R. M., Naidoo, M., Sibiya, B. and Oosthuizen, R. (2017) Air quality indicators from the Environmental Performance Index: Potential use and limitations in South Africa, *Clean Air Journal*, 27(1), pp. 33–41. doi: 10.17159/2410-972X/2017/v27n1a8.

Gatari, M. J., Boman, J., Wagner, A., Janhäll, S. and Isakson, J. (2006) Assessment of inorganic content of PM2.5 particles sampled in a rural area north-east of Hanoi, Vietnam, *Science of The Total Environment*. Elsevier BV, 368(2–3), pp. 675–685. doi: 10.1016/j.scitotenv.2006.04.004.

Gautam, S., Patra, A. K., Sahu, S. P. and Hitch, M. (2016) Particulate matter pollution in opencast coal mining areas: A threat to human health and environment, *International Journal of Mining, Reclamation and Environment*. Informa UK Limited, 32(2), pp. 75–92. doi: 10.1080/17480930.2016.1218110.

Gautam, S., Prusty, B. K. and Patra, A. K. (2012) Pollution Due To Particulate Matter From Mining Activities, *Recycling and sustainable development*, 5(5), pp. 53–58. doi: 504.3:622.015.

Genc, B. and Cook, A. (2015) Spontaneous combustion risk in South African coalfields, *Journal of the Southern African Institute of Mining and Metallurgy*. Academy of Science of South Africa, 115(7), pp. 563–568. doi: 10.17159/2411-9717/2015/V115N7A1.

Genga, A. F., Baglivi, F., Siciliano, M., Siciliano, T., Aiello, D. and Tortorella, C. (2013) Chemical and Morphological Study of Particulate Matter Analysed by SEM-EDS, in *4th Imeko TC19 Symposium on Environmental Instrumentation and Measurements June 3-4*. Lecce, Italy, p. 4. doi: :9788896515204.

George, I. J. and Abbatt, J. P. D. (2010) Heterogeneous oxidation of atmospheric aerosol particles by gas-phase radicals, *Nature Chemistry*. Springer Science and Business Media LLC, 2(9), pp. 713–722. doi: 10.1038/nchem.806.

Ghose, M. K. (2002) Air Pollution Due to Opencast Coal Mining and the Characteristics of Air-Borne Dust-An Indian Scenario, *International Journal of Environmental Studies*. Informa UK Limited, 59(2), pp. 211–228. doi: 10.1080/00207230210927.

Ghose, M. K. and Majee, S. R. (2000) Assessment of the impact on the air environment due to opencast coal mining- an Indian case study, *Atmospheric Environment*. Elsevier BV, 34(17), pp. 2791–2796. doi: 10.1016/s1352-2310(99)00302-7.

Ghose, M. K. and Majee, S. R. (2007) Characteristics of Hazardous Airborne Dust Around an Indian Surface Coal Mining Area, *Environmental Monitoring and Assessment*. Springer Science and Business Media LLC, 130(1–3), pp. 17–25. doi: 10.1007/s10661-006-9448-6.

Giere, R. and Querol, X. (2010) Solid Particulate Matter in the Atmosphere, *Elements*. Mineralogical Society of America, 6(4), pp. 215–222. doi: 10.2113/gselements.6.4.215.

Goldstein, J., Newbury, D., Joy, D., Lyman, C., Echlin, C., Lifshin, E., Sawyer, L. and Michael, J. (2003) *Scanning Electron Microscopy and X-Ray Microanalysis*. Third, *Microscopy and Microanalysis*. Third. Springer US. Available at: http://dx.doi.org/10.1017/s1431927603030617 (Accessed: 20 June 2019).

Google Earth (2018) *Maps*.

Górka, M., Jędrysek, M. O., Maj, J., Worobiec, A., Buczyńska, A., Stefaniak, E., Krata, A., Van Grieken, R., Zwoździak, A., Sówka, I., Zwoździak, J. and Lewicka-Szczebak, D. (2009) Comparative assessment of air quality in two health resorts using carbon isotopes and palynological analyses, *Atmospheric Environment*. Elsevier BV, 43(3), pp. 682–688. doi: 10.1016/j.atmosenv.2008.09.056.

Górka, M., Rybicki, M., Simoneit, B. R. T. and Marynowski, L. (2014) Determination of multiple organic matter sources in aerosol PM10 from Wrocław, Poland using molecular and stable carbon isotope compositions, *Atmospheric Environment*. Elsevier BV, 89, pp. 739–748. doi: 10.1016/j.atmosenv.2014.02.064.

Goudie, A. S. and Middleton, N. J. (1992) The changing frequency of dust storms through time, *Climatic Change*. Springer Nature, 20(3), pp. 197–225. doi: 10.1007/bf00139839.

Grainger, C. and Meroney, R. N. (1993) Dispersion in an open-cut coal mine in stably stratified flow, *Boundary-Layer Meteorology*. Springer Nature, 63(1–2), pp. 117–140. doi: 10.1007/bf00705379.

Grassi, C., Narducci, P. and Tognott, L. (2004) Atmospheric Particulate Matter By SEM-EDX, in *World Clean Air and Environmental Protection Congress*. Pisa, Italy, p. 6. Available at: http://www.umad.de/infos/cleanair13/pdf/full_273.pdf (Accessed: 24 May 2019).

Gray, H. A., Cass, G. R., Huntzicker, J. J., Heyerdahl, E. K. and Rau, J. A. (1986) Characteristics of atmospheric organic and elemental carbon particle concentrations in Los Angeles, *Environmental Science & Technology*. American Chemical Society (ACS), 20(6), pp. 580–589. doi: 10.1021/es00148a006.

Greeley, R. and Iversen, J. D. (1985) Wind as a Geological Process on Earth, Mars, Venus and Titan. Cambridge Planetary Science Series No. 4., *Geological Magazine*. Cambridge University Press (CUP), 122(5), pp. 578–579. doi: 10.1017/s0016756800035640.

Groot, P. de (ed.) (2004) *Handbook of Stable Isotope Analytical Techniques, Volume I*. First. Elsevier Science. Available at: https://www.elsevier.com/books/handbook-of-stable-isotope-analytical-techniques/de-groot/978-0-444-51114-0 (Accessed: 25 March 2018).

Guedes, A., Valentim, B., Prieto, A. C., Rodrigues, S. and Noronha, F. (2010) Micro-Raman spectroscopy of collotelinite, fusinite and macrinite, *International Journal of Coal Geology*. Elsevier BV, 83(4), pp. 415–422. doi: 10.1016/j.coal.2010.06.002.

Gustian, I., Angasa, E., Agustini, D., Maryanti, E. and Fitriani, D. (2015) Preparation of Fe-intercalated Graphite Based on Coal Tailings, Dimensional Structure, *Aceh International Journal of Science and Technology*. Institute of Postgraduate Studies, Syiah Kuala University, 4(3), pp. 88–92. doi: 10.13170/aijst.4.3.3017.

Hamilton, R. S. and Mansfield, T. A. (1993) The soiling of materials in the ambient atmosphere, *Atmospheric Environment. Part A. General Topics*. Elsevier BV, 27(8), pp. 1369–1374. doi: 10.1016/0960-1686(93)90263-x.

Hanekom, E., Liebenberg, A. and de Vries, M. (2016) An Extended Farm Site Development Method, *South African Journal of Science*. Academy of Science of South Africa, Volume 112(Number 9/10). doi: 10.17159/sajs.2016/20150427.

Hanlon, W. W. (2016) *Coal Smoke and the Costs of the Industrial Revolution*. National Bureau of Economic Research. doi: 10.3386/w22921.

Hartmann, S., O'Brien, G., Warren, K. and Krahenbuhl, G. (2016) Characterisation of urban dust samples using reflected light microscopy methods, *Air Quality and Climate Change*, 50(3), p. 34.

Hatch, C. D., Gierlus, K. M., Schuttlefield, J. D. and Grassian, V. H. (2008) Water adsorption and cloud condensation nuclei activity of calcite and calcite coated with model humic and fulvic acids, *Atmospheric Environment*. Elsevier BV, 42(22), pp. 5672–5684. doi: 10.1016/j.atmosenv.2008.03.005.

Heaton, T. H. E. (1987) 15N/14N ratios of nitrate and ammonium in rain at Pretoria, South Africa, *Atmospheric Environment (1967)*. Elsevier BV, 21(4), pp. 843–852. doi: 10.1016/0004-6981(87)90080-1.

Heaton, T. H. E. (1990) 15N/14N ratios of NOx from vehicle engines and coal-fired power stations, *Tellus B*. Informa UK Limited, 42(3), pp. 304–307. doi: 10.1034/j.1600-0889.1990.00007.x-i1.

Helmenstine, M. (2018) *Spectroscopy Introduction*. Available at: https://www.thoughtco.com/introduction-to-spectroscopy (Accessed: 23 January 2019).

Hemby, J., Sasser, E., Adler, K., Anenberg, S., Bailey, C., Brockman, L., Chappell, L., DeAngelo, B., Damberg, R., Dawson, J., Frank, N., Geller, M., Hagler, G., Hemming, B., Jantarasami, L., Luben, T., Mitchell, J., Moss, J., Rao, V. and Witosky, M. (2012) *Report to Congress on Black Carbon March 2012*. Available at: https://cfpub.epa.gov/si/si_public_record_report.cfm?Lab=OAQPS&dirEntryID=240148 (Accessed: 4 May 2019).

Hitachi Construction (2018) *Excavation*. Available at: www.hitachiconstruction.com, (Accessed: 23 September 2018).

Horvath, H. (1993) Atmospheric light absorption-A review, *Atmospheric Environment. Part A. General Topics*. Elsevier BV, 27(3), pp. 293–317. doi: 10.1016/0960-1686(93)90104-7.

Huebert, B. and Charlson, R. J. (2000) Uncertainties in data on organic aerosols, *Tellus B*. Informa UK Limited, 52(5), pp. 1249–1255. doi: 10.1034/j.1600-0889.2000.01146.x.

Huertas, J. I., Camacho, D. A. and Huertas, M. E. (2012) Standardized emissions inventory methodology for open-pit mining areas, *Environmental Science and Pollution Research*. Springer Science and Business Media LLC, 19(7), pp. 2784–2794. doi: 10.1007/s11356-012-0778-3.

Huertas, J. I., Huertas, M. E. and Solís, D. A. (2012) Characterization of airborne particles in an open pit mining region, *Science of The Total Environment*. Elsevier BV, 423, pp. 39–46. doi: 10.1016/j.scitotenv.2012.01.065.

Hutton, B. M. and Williams, D. E. (2000) Assessment of X-ray photoelectron spectroscopy for analysis of particulate pollutants in urban air, *The Analyst*. Royal Society of Chemistry (RSC), 125(10), pp. 1703–1706. doi: 10.1039/b005872f.

Hwang, I. and Hopke, P. K. (2007) Estimation of source apportionment and potential source locations of PM2.5 at a west coastal IMPROVE site, *Atmospheric Environment*. Elsevier BV, 41(3), pp. 506–518. doi: 10.1016/j.atmosenv.2006.08.043.

Iminco (2018) *Open Cut and Underground Mining*. Available at: http://iminco.net/open-cut-and-underground-mining/ (Accessed: 3 November 2018).

Impact Analytical (2018) *TGA Analysis-Sample Characterization Using Thermogravimetric Analysis (TGA)*. Available at: https://www.impactanalytical.com (Accessed: 29 November 2019).

International ASTM (2016) *Standard Practice for General Techniques of Thermogravimetric Analysis (TGA) Coupled with Infrared Analysis (TGA/IR)*. West Conshohocken: ASTM International. doi: 10.1520/e2105-00.

International Energy Agency (IEA) (2016) World Energy Outlook 2016, *World Energy Outlook*. OECD. doi: 10.1787/weo-2016-en.

International Energy Agency (IEA) (2017a) *Coal 2017- Analysis and Forecasts to 2022*. Paris : OECD/IEA, 2017. Available at: www.iea.org.

International Energy Agency (IEA) (2017b) *Coal 2017*, *Market Report Series*. Available at: https://www.iea.org (Accessed: 11 October 2018).

International Energy Agency (IEA) (2017c) Coal Information 2017, *Coal Information*. OECD. doi: 10.1787/coal-2017-en.

International Mining Industrial Photographer (2017) *Coal Mining*. Available at: https://miningindustrialphotographer.com.

Ionel, I. and Popescu, F. (2010) *Methods for Online Monitoring of Air Pollution Concentration*, *Air Quality*. Sciyo. doi: 10.5772/9754.

Ivleva, N. P., McKeon, U., Niessner, R. and Pöschl, U. (2007) Raman Microspectroscopic Analysis of Size-Resolved Atmospheric Aerosol Particle Samples Collected with an ELPI: Soot, Humic-Like Substances, and Inorganic Compounds, *Aerosol Science and Technology*. Informa UK Limited, 41(7), pp. 655–671. doi: 10.1080/02786820701376391.

Jacobson, M. C., Hansson, H.-C., Noone, K. J. and Charlson, R. J. (2000) Organic atmospheric aerosols: Review and state of the science, *Reviews of Geophysics*. American Geophysical Union (AGU), 38(2), pp. 267–294. doi: 10.1029/1998rg000045.

Jaenicke, R. (1980) Atmospheric aerosols and global climate, *Journal of Aerosol Science*. Elsevier BV, 11(5–6), pp. 577–588. doi: 10.1016/0021-8502(80)90131-7.

Janssen, N. A. H., Hoek, G., Simic-Lawson, M., Fischer, P., Bree, L. van, Brink, H. ten, Keuken, M., Atkinson, R. W., Anderson, H. R., Brunekreef, B. and Cassee, F. R. (2011) Black Carbon as an Additional Indicator of the Adverse Health Effects of Airborne Particles Compared with PM10 and PM2.5, *Environmental Health Perspectives*. Environmental Health Perspectives, 119(12), pp. 1691–1699. doi: 10.1289/ehp.1003369.

Jeffrey, L. S. (2005) Characterization of the coal resources of South Africa, *Journal of the Southern African Institute of Mining and Metallurgy*, 105(2), pp. 95–102. Available at: https://journals.co.za/content/saimm/105/2/AJA0038223X_3050 (Accessed: 8 December 2017).

Jia, G. and Jia, J. (2014) Atmospheric Residence Times of the Fine-aerosol in the Region of South Italy Estimated from the Activity Concentration Ratios of 210Po/210Pb in Air Particulates, *Journal of Analytical & Bioanalytical Techniques*. OMICS Publishing Group, 5(6). doi: 10.4172/2155-9872.1000216.

Jimoda, L. A. (2012) Effects of particulate matter on human health, the ecosystem, climate and materials: A review, *Working and Living Environmental Protection*, 9(1), pp. 27–44. Available at: http://facta.junis.ni.ac.rs.

Johann-Essex, V., Keles, C. and Sarver, E. (2017) A Computer-Controlled SEM-EDX Routine for Characterizing Respirable Coal Mine Dust, *Minerals*. MDPI AG, 7(1), p. 15. doi: 10.3390/min7010015.

Johansson, M. (2008) Air Pollution and Climate: Standards for Particulate Matter, in *Standards and Thresholds for Impact Assessment*. Berlin, Heidelberg: Springer Berlin Heidelberg, pp. 291–299. doi: 10.1007/978-3-540-31141-6_23.

John, W. (2011) Size Distribution Characteristics of Aerosols, in Baron, P. . and Willeke, K. (eds) *Aerosol Measurement: Principles, Techniques and Applications*. Third. John Wiley & Sons, Inc., pp. 591–614. doi: 10.1002/9781118001684.ch4.

Johnson, G. (2010) *Thermogravimetric Analysis – GC Mass Spectrometry*. Shelton, CT 06484 USA. Available at: http://labsense.fi.

Johnston, J. (2000) Hazard Prevention and Control in the Work Environment: Airborne Dust. Protection of the Human Environment Occupational Health and Environmental Health Series, Geneva, 1999, World Health Organization WHO/SDE/OEH/99.14, *The Annals of Occupational Hygiene*. Elsevier BV, 44(5), p. 405. doi: 10.1016/s0003-4878(00)00023-5.

Joint Coal Board (1999) *Diesel Particulate in Coal Mines*. Joint Coal Board. Available at: https://www.coalservices.com.au/wp-content/uploads/2016/12/DieselParticulateBooklet1999.pdf.

Jones, A. M. and Harrison, R. M. (2005) Interpretation of particulate elemental and organic carbon concentrations at rural, urban and kerbside sites, *Atmospheric Environment*. Elsevier BV, 39(37), pp. 7114–7126. doi: 10.1016/j.atmosenv.2005.08.017.

Jones, M. L., Kalmanovitch, D. P., Steadman, E. N., Zygarlicke, C. J. and Benson, S. A. (1992) Application of SEM Techniques to the Characterization of Coal and Coal Ash Products, *Advances in Coal Spectroscopy*. Springer US, pp. 1–27. doi: 10.1007/978-1-4899-3671-4_1.

Jones, T., Blackmore, P., Leach, M., BéruBé, K., Sexton, K. and Richards, R. (2002) Characterisation of airborne particles collected within and proximal to an opencast coalmine: South Wales, UK, *Environmental Monitoring and Assessment*. Springer Nature, 75(3), pp. 293–312. doi: 10.1023/a:1014808419171.

Kantová, N, Holubčík, M., Jandačka, J. and Čaja, A. (2017) Comparison of particulate matter properties from combustion of wood biomass and brown coal, in *International Scientific Conference on Sustainable, Modern and Safe Transport*. Zillina.

Kantová, Nikola, Holubčík, M., Jandačka, J. and Čaja, A. (2017) Comparison of Particulate Matter Properties from Combustion of Wood Biomass and Brown Coal, *Procedia Engineering*. Elsevier BV, 192, pp. 416–420. doi: 10.1016/j.proeng.2017.06.072.

Karanasiou, A., Minguillón, M. C., Viana, M., Alastuey, A., Putaud, J.-P., Maenhaut, W., Panteliadis, P., Močnik, G., Favez, O. and Kuhlbusch, T. A. J. (2015) Thermal-optical analysis for the measurement of elemental carbon (EC) and organic carbon (OC) in ambient air. A literature review, *Atmospheric Measurement Techniques Discussions*. Copernicus GmbH, 8(9), pp. 9649–9712. doi: 10.5194/amtd-8-9649-2015.

Karnani, S., Edwards, R., Fisher, E. M., Johnson, M., Naeher, L., Smith, K. R. and Morawska, L. (2014) *Review 2: Emissions of Health-Damaging Pollutants from Household Stoves. WHO Indoor Air Quality Guidelines: Household Fuel Combustion*.

Kawamura, K., Kobayashi, M., Tsubonuma, N., Mochida, M., Watanabe, T. and Lee, M. (2004) Organic and inorganic compositions of marine aerosols from East Asia: Seasonal variations of water-soluble dicarboxylic acids, major ions, total carbon and nitrogen, and stable C and N isotopic composition, *The Geochemical Society Special Publications*. Elsevier, pp. 243–265. doi: 10.1016/s1873-9881(04)80019-1.

Kaygusuz, K. (2012) Energy for sustainable development: A case of developing countries, *Renewable and Sustainable Energy Reviews*. Elsevier BV, 16(2), pp. 1116–1126. doi: 10.1016/j.rser.2011.11.013.

Kelly, S., Brodie, C. and Hilkert, A. (2018) Isotopic-Spectroscopic Technique: Stable Isotope-Ratio Mass Spectrometry (IRMS), *Modern Techniques for Food Authentication*. Elsevier, pp. 349–413. doi: 10.1016/b978-0-12-814264-6.00011-6.

Kelly, S. D., Stein, C. and Jickells, T. D. (2005) Carbon and nitrogen isotopic analysis of atmospheric organic matter, *Atmospheric Environment*. Elsevier BV, 39(32), pp. 6007–6011. doi: 10.1016/j.atmosenv.2005.05.030.

Kesavachandran, C. N., Kamal, R., Bihari, V., Pathak, M. K. and Singh, A. (2015) Particulate matter in ambient air and its association with alterations in lung functions and respiratory health problems among outdoor exercisers in National Capital Region, India, *Atmospheric Pollution Research*. Elsevier BV, 6(4), pp. 618–625. doi: 10.5094/apr.2015.070.

Kgabi, N. A. (2010) An assessment of common atmospheric particulate matter sampling and toxic metal analysis method, *African Journal of Environmental Science and Technology*, 4(11), pp. 718–728. Available at: http://www.academicjournals.org/AJEST (Accessed: 25 July 2018).

Kim, K.-H., Kabir, E. and Kabir, S. (2015) A review on the human health impact of airborne particulate matter, *Environment International*. Elsevier BV, 74, pp. 136–143. doi: 10.1016/j.envint.2014.10.005.

Kissell, F. N. (2003) *Handbook for Dust Control in Mining. Information Circular #9465. DHHS (NIOSH) Pub #2003-147*. US Department of Health and Human Services.

Klejnowski, K., Janoszka, K. and Czaplicka, M. (2017) Characterization and Seasonal Variations of Organic and Elemental Carbon and Levoglucosan in PM10 in Krynica Zdroj, Poland, *Atmosphere*. MDPI AG, 8(12), p. 190. doi: 10.3390/atmos8100190.

Kohfeld, K. E. and Harrison, S. P. (2001) DIRTMAP: the geological record of dust, *Earth-Science Reviews*. Elsevier BV, 54(1–3), pp. 81–114. doi: 10.1016/s0012-8252(01)00042-3.

Kohfeld, K. E. and Tegen, I. (2007) Record of Mineral Aerosols and Their Role in the Earth System, *Treatise on Geochemistry*. Elsevier, pp. 1–26. doi: 10.1016/b978-008043751-4/00236-4.

Kohn,M.J. (2010) Carbon isotope compositions of terrestrial C3 plants as indicators of (paleo) ecology and (paleo) climate. PNAS November 16, 2010 107 (46) pp19691-19695. https://doi.org/10.1073/pnas.1004933107

Kothai, P., Saradhi, I. V, Pandit, G. G. and Puranik, V. D. (2009) Characterisation of Atmospheric Particulate Matter using PIXE Technique, *International Journal of Environmental and Ecological Engineering*, 3(3), pp. 39–42.

Koval, S., Krahenbuhl, G., Warren, K. and O'Brien, G. (2018) Optical microscopy as a new approach for characterising dust particulates in urban environment, *Journal of Environmental Management*. Elsevier BV, 223, pp. 196–202. doi: 10.1016/j.jenvman.2018.06.038.

Kruszewski, Ł. (2013) Supergene sulphate minerals from the burning coal mining dumps in the Upper Silesian Coal Basin, South Poland, *International Journal of Coal Geology*. Elsevier BV, 105, pp. 91–109. doi: 10.1016/j.coal.2012.12.007.

Kumar, P., Ketzel, M., Vardoulakis, S., Pirjola, L. and Britter, R. (2011) Dynamics and dispersion modelling of nanoparticles from road traffic in the urban atmospheric environment—A review, *Journal of Aerosol Science*. Elsevier BV, 42(9), pp. 580–603. doi: 10.1016/j.jaerosci.2011.06.001.

Kumar, P., Morawska, L., Birmili, W., Paasonen, P., Hu, M., Kulmala, M., Harrison, R. M., Norford, L. and Britter, R. (2014) Ultrafine particles in cities, *Environment International*. Elsevier BV, 66, pp. 1–10. doi: 10.1016/j.envint.2014.01.013.

Kundu, S., Kawamura, K. and Lee, M. (2010) Seasonal variation of the concentrations of nitrogenous species and their nitrogen isotopic ratios in aerosols at Gosan, Jeju Island: Implications for atmospheric processing and source changes of aerosols, *Journal of Geophysical Research*. American Geophysical Union (AGU), 115(D20). doi: 10.1029/2009jd013323.

Kunwar, B., Kawamura, K. and Zhu, C. (2016) Stable carbon and nitrogen isotopic compositions of ambient aerosols collected from Okinawa Island in the western North Pacific Rim, an outflow region of Asian dusts and pollutants, *Atmospheric Environment*. Elsevier BV, 131, pp. 243–253. doi: 10.1016/j.atmosenv.2016.01.035.

Kunzli, N. and Tager, I. B. (2000) Long-Term Health Effects of Particulate and Other Ambient Air Pollution: Research Can Progress Faster If We Want It to, *Environmental Health Perspectives*. JSTOR, 108(10), p. 915. doi: 10.2307/3435048.

Kwon, H. B. and Vastola, F. J. (1995) Thermal analysis of coal under conditions of rapid heating, *Fuel Processing Technology*. Elsevier BV, 44(1–3), pp. 13–24. doi: 10.1016/0378-3820(94)00120-i.

L, S. (2004) Introduction and overview, *International Journal of Coal Geology*. Elsevier BV, 58(3), pp. 131–132. doi: 10.1016/s0166-5162(03)00191-5.

Lagzi, I., Mészáros, R. and Leelőssy, G. G. . (2014) *Atmospheric Chemistry. Eotvos Lorand University*. First. Budapest, Hungary: Eotvos Lorand University.

Lal, B. and Tripathy, S. S. (2012) Prediction of dust concentration in opencast coal mine using artificial neural network, *Atmospheric Pollution Research*. Elsevier BV, 3(2), pp. 211–218. doi: 10.5094/APR.2012.023.

Language, B., Piketh, S. J., Wernecke, B. and Burger, R. (2016) Household air pollution in South African low-income settlements: a case study, *Air Pollution XXIV*. WIT Press. doi: 10.2495/air160211.

Laskin, A., Laskin, J. and Nizkorodov, S. A. (2012) Mass spectrometric approaches for chemical characterisation of atmospheric aerosols: critical review of the most recent advances, *Environmental Chemistry*. CSIRO Publishing, 9(3), p. 163. doi: 10.1071/en12052.

Lazzeri, P., Clauser, G., Iacob, E., Lui, A., Tonidandel, G. and Anderle, M. (2003) ToF-SIMS and XPS characterisation of urban aerosols for pollution studies, *Applied Surface Science*. Elsevier BV, 203–204, pp. 767–771. doi: 10.1016/s0169-4332(02)00813-9.

Lei, Y., Li, L. and Pan, D. (2014) Study on the Relationships Between Coal Consumption and Economic Growth of the Six Biggest Coal Consumption Countries: With Coal Price as a Third Variable, *Energy Procedia*. Elsevier BV, 61, pp. 624–634. doi: 10.1016/j.egypro.2014.11.1185.

Lewis, E. and Lewis, E. (2018) Paris Climate Agreement, in *Sustainaspeak*. New York : Routledge, 2018.: Routledge, pp. 198–199. doi: 10.4324/9781315270326-142.

Li, Q.-F., Wang-Li, L., Liu, Z. and Heber, A. J. (2012) Field evaluation of particulate matter measurements using tapered element oscillating microbalance in a layer house, *Journal of the Air & Waste Management Association*. Informa UK Limited, 62(3), pp. 322–335. doi: 10.1080/10473289.2011.650316.

Li, Q.-F., Wang-Li, L., Jayanty, R. K. M. and Shah, S. B. (2013) Organic and Elemental Carbon in Atmospheric Fine Particulate Matter in an Animal Agriculture Intensive Area in North Carolina: Estimation of Secondary Organic Carbon Concentrations, *Open Journal of Air Pollution*. Scientific Research Publishing, Inc, 02(01), pp. 7–18. doi: 10.4236/ojap.2013.21002.

Li, Q.-F., Wang-Li, L., Jayanty, R. K. M. and Shah, S. (2015) Elemental Compositions and Chemical Mass Closure of Fine Particulate in an Animal Feeding Operation Facility and Its Vicinity, *Journal of Environmental Protection*. Scientific Research Publishing, Inc, 06(05), pp. 409–425. doi: 10.4236/jep.2015.65040.

Li, Q., Zhao, C., Chen, X., Wu, W. and Li, Y. (2009) Comparison of pulverized coal combustion in air and in O2/CO2 mixtures by thermo-gravimetric analysis, *Journal of Analytical and Applied Pyrolysis*. Elsevier BV, 85(1–2), pp. 521–528. doi: 10.1016/j.jaap.2008.10.018.

Li, S., Whitely, N., Xu, W. and Pan, W.-P. (2005) Characterisation of Coal by Thermal Analysis Methods, in Diaz, A. (ed.) *In Thermal Analysis. Fundamentals and Applications to Material Characterisation*, pp. 111–120.

Liao, Y. (2018) *Practical Electron Microscopy and Database. An Online Book*. Second Edi. GlobalSino. Available at: http://www.globalsino.com.

Ličbinský, R., Frýbort, A., Huzlík, J., Adamec, V., Effenberger, K., Mikuška, P., Vojtěšek, M. and Křůmal, K. (2010) Usage of Scanning Electron Microscopy for Particulate Matter Sources Identification, *Transactions on Transport Sciences*. Palacky University Olomouc, 3(3), pp. 137–144. doi: 10.2478/v10158-010-0019-8.

Lim, S. S., Vos, T., Flaxman, A. D., Danaei, G., Shibuya, K., Ezzati, M., *et al.* (2012) A comparative risk assessment of burden of disease and injury attributable to 67 risk factors and risk factor clusters in 21 regions, 1990–2010: a systematic analysis for the Global Burden of Disease Study 2010, *The Lancet*. Elsevier BV, 380(9859), pp. 2224–2260. doi: 10.1016/s0140-6736(12)61766-8.

Lindon., J. C., Tranter, G. E. and Koppenaal, D. W. (2016) Infrared and Raman Spectroscopy of minerals and inorganic materials. In Encyclopedia of Spectroscopy and Spectrometry, in Lindon., J. ., Tranter, G. ., and Koppenaal, D. . (eds). Academic Press, p. 3584.

Liousse, C., Cachier, H. and Jennings, S. G. (1993) Optical and thermal measurements of black carbon aerosol content in different environments: Variation of the specific attenuation cross-section, sigma (σ), *Atmospheric Environment. Part A. General Topics*. Elsevier BV,

27(8), pp. 1203–1211. doi: 10.1016/0960-1686(93)90246-u.

Lipsky, E., Stanier, C. O., Pandis, S. N. and Robinson, A. L. (2002) Effects of Sampling Conditions on the Size Distribution of Fine Particulate Matter Emitted from a Pilot-Scale Pulverized-Coal Combustor, *Energy & Fuels*. American Chemical Society (ACS), 16(2), pp. 302–310. doi: 10.1021/ef0102014.

Liu, L.-J. S., Koutrakis, P., Leech, J. and Broder, I. (1995) Assessment of Ozone Exposures in the Greater Metropolitan Toronto Area, *Journal of the Air & Waste Management Association*. Informa UK Limited, 45(4), pp. 223–234. doi: 10.1080/10473289.1995.10467362.

Liu, X., X, M., Yu, D., Gao, X., Cao, Q. and Hao, W. (2007) Influence of mineral transformation on emission of particulate matters during coal combustion, *Frontiers of Energy and Power Engineering in China*, 1(2), pp. 213–217. Available at: https://link.springer.com/article/10.1007/s00000-007-0028-4 (Accessed: 15 May 2019).

Liu, Y. C. (2014) Coal Mine Land Reclamation Measures — Open-Pit Coal Mine of Baofa Coal Co., Ltd, *Advanced Materials Research*. Trans Tech Publications, 1006–1007, pp. 78–82. doi: 10.4028/www.scientific.net/amr.1006-1007.78.

Lloyd, P. (2002) Coal mining and the environment, in *International Bar Association (IBA)*. Durban, p. 7. Available at: http://www.erc.uct.ac.za.

Lord, R. C. (1965) Introduction to Infrared and Raman Spectroscopy, *Journal of the American Chemical Society*. American Chemical Society (ACS), 87(5), pp. 1155–1156. doi: 10.1021/ja01083a063.

Lu, W., Cao, Y.-J. and Tien, J. C. (2017) Method for prevention and control of spontaneous combustion of coal seam and its application in mining field, *International Journal of Mining Science and Technology*. Elsevier BV, 27(5), pp. 839–846. doi: 10.1016/j.ijmst.2017.07.018.

Major, I., Gyökös, B., Túri, M., Futó, I., Filep, Á., Hoffer, A., Furu, E., Timothy Jull, A. J. and Molnár, M. (2017) Evaluation of an automated EA-IRMS method for total carbon analysis of atmospheric aerosol at HEKAL, *Journal of Atmospheric Chemistry*. Springer Science and Business Media LLC, 75(1), pp. 85–96. doi: 10.1007/s10874-017-9363-y.

Makonese, T., Masekameni, D. M., Annegarn, H. J. and Forbes, P. B. C. (2017) Emission factors for domestic coal-burning braziers, *South African Journal of Science*, 113(3/4), pp. 1–11. Available at: http://dx.doi.org/10.17159/ (Accessed: 4 December 2019).

Mamani-Paco, R. M. and Helble, J. J. (2007) Particle size and time of the day influences on the morphology distributions of atmospheric fine particles at the Baltimore supersite, *Atmospheric Environment*. Elsevier BV, 41(37), pp. 8021–8029. doi: 10.1016/j.atmosenv.2007.07.007.

Mamurekli, D. (2010) Environmental impacts of coal mining and coal utilization in the UK, *Acta Montanistica Slovaca*, 15(2), pp. 134–144. Available at: https://actamont.tuke.sk/pdf/2010/n2/5makurekli.pdf.

Mannucci, P. and Franchini, M. (2017) Health Effects of Ambient Air Pollution in Developing Countries, *International Journal of Environmental Research and Public Health*. MDPI AG, 14(9), p. 1048. doi: 10.3390/ijerph14091048.

Manoj, B. and Kunjomana, A. G. (2010) FT-Raman Spectroscopic Study of Indian Bituminous and Sub-bitumionus Coal, *Asian Journal of Materials Science*. Science Alert, 2(4), pp. 204–210. doi: 10.3923/ajmskr.2010.204.210.

Marimon, R. M., Perona, J. and Teixidor, P. (2012) Isotope Ratio Mass Spectrometry, in Seoane, J. . and Llovet, X. (eds) *In Handbook of instrumental techniques for materials, chemical and biosciences research*. Universitat de Barcelona. Available at: https://www.academia.edu/18907298/Handbook_of_instrumental_techniques_for_materials_chemical_and_biosciences_research.

Mašalaitė, A., Garbaras, A. and Remeikis, V. (2012) Stable isotopes in environmental investigations, *Lithuanian Journal of Physics*. Lithuanian Academy of Sciences, 52(3), pp. 261–268. doi: 10.3952/lithjphys.52314.

Material Evaluation and Engineering (2018) *X-ray Photoelectron Spectroscopy-XPS*. Available at: https://www.mee-inc.com/hamm/x-ray-photoelectron-spectroscopy-xps (Accessed: 25 October 2018).

Mayoral, M. C., Izquierdo, M. T., Andrés, J. M. and Rubio, B. (2001) Different approaches to proximate analysis by thermogravimetry analysis, *Thermochimica Acta*. Elsevier BV, 370(1–2), pp. 91–97. doi: 10.1016/s0040-6031(00)00789-9.

McSween, H. Y., J., Richardson, S. M. and Uhle, M. E. (2003) Geochemistry: Pathways and Processes, *Geological Magazine*, pp. 141–142. doi: doi:10.1017/S0016756805370439.

Menon, S., Unger, N., Koch, D., Francis, J., Garrett, T., Sednev, I., Shindell, D. and Streets, D. (2008) Aerosol climate effects and air quality impacts from 1980 to 2030, *Environmental Research Letters*. IOP Publishing, 3(2), p. 24004. doi: 10.1088/1748-9326/3/2/024004.

Merefield, J., Stone, I., Jarman, P., Rees, G., Roberts, J., Jones, J. and Dean, A. (1995) Environmental dust analysis in opencast mining areas, *Geological Society, London, Special Publications*. Geological Society of London, 82(1), pp. 181–188. doi: 10.1144/gsl.sp.1995.082.01.11.

Mertes, S., Dippel, B. and Schwarzenböck, A. (2004) Quantification of graphitic carbon in atmospheric aerosol particles by Raman spectroscopy and first application for the determination of mass absorption efficiencies, *Journal of Aerosol Science*. Elsevier BV, 35(3), pp. 347–361. doi: 10.1016/j.jaerosci.2003.10.002.

Meuleman, E., Cottrell, A. and Ghayur, A. (2016) Treatment of flue-gas impurities for liquid absorbent-based post-combustion CO2 capture processes, *Absorption-Based Post-combustion Capture of Carbon Dioxide*. Elsevier, pp. 519–551. doi: 10.1016/b978-0-08-100514-9.00022-6.

Miller, B. G. and Tillman, D. A. (2008) Coal Characteristics, in *Combustion Engineering Issues for Solid Fuel Systems*. West Lafayette, IN: Indiana Center for Coal Technology Research, pp. 33–81. doi: 10.1016/B978-0-12-373611-6.00002-1.

Minerals Council South Africa (2018) *Coal*. Available at: http://www.mineralscouncil.org.za/sa-mining/coal (Accessed: 12 August 2018).

MineSurveyor (2016) *Coal stockpiling*, *Mine Surveyor.net*. Available at: https://www.minesurveyor.net (Accessed: 15 March 2018).

Mining Industrial Photographer (2017) *Drilling and Blasting*. Available at: https://miningindustrialphotographer.com (Accessed: 29 November 2019).

Mishra, A. ., Maiti, S. . and Pal, A. K. (2013) Status of PM10 bound heavy metals in ambient air in certain parts of Jharia coal field, Jharkhand, India, *International Journal of Environmental Sciences*, 4(2), pp. 142–150. doi: 10.6088/ijes.2013040200003.

Mishra, D. P. and Azam, S. (2018) Experimental investigation on effects of particle size, dust concentration and dust-dispersion-air pressure on minimum ignition temperature and combustion process of coal dust clouds in a G-G furnace, *Fuel*. Elsevier BV, 227, pp. 424–433. doi: 10.1016/j.fuel.2018.04.122.

Mohomed, K. (2016) *Thermogravimetric Analysis (TGA) Theory and Applications*. Available at: https://www.tainstruments.com (Accessed: 26 May 2018).

Moroeng O.M., Wagner, N.J., Hall, G. and Roberts, R.J. (2018) Using δ15N and δ13C and nitrogen functionalities to support a fire origin for certain inertinite macerals in a No. 4 Seam Upper Witbank coal, South Africa. *Org Geochem* 125 pp 23-32

Muccio, Z. and Jackson, G. P. (2009) Isotope ratio mass spectrometry, *The Analyst*. Royal Society of Chemistry (RSC), 134(2), pp. 213–222. doi: 10.1039/b808232d.

Muenstermann, I. (2012) Australia's climate change, wind farming, coal industry and the 'big carbon plan': Mine coal, sell coal, repeat until rich, *Rural Society*. Informa UK Limited, 21(3), pp. 231–249. doi: 10.5172/rsj.2012.21.3.231.

Mujuru, M., McCrindle, R. I. and Panichev, N. (2009) Characterisation of coal slurries for introduction into ICP OES for multi-element determinations, *Journal of Analytical Atomic Spectrometry*. Royal Society of Chemistry (RSC), 24(4), p. 494. doi: 10.1039/b819963a.

Mukota, T (2019) Local development and calibration of a passive sampler for monitoring of particulate matter. MEng thesis, EBIT faculty, University of Pretoria.

Mukota, T. and Kornelius, G. (2017) Local development of passive PM monitors, in *2018 Conference of the National Association for Clean Air*. Vanderbijlpark, South Africa: University of Pretoria, p. 8. Available at: http://www.naca.org.za.

Munawer, M. E. (2018) Human health and environmental impacts of coal combustion and post-combustion wastes, *Journal of Sustainable Mining*. Elsevier BV, 17(2), pp. 87–96. doi: 10.1016/j.jsm.2017.12.007.

Munnik, V., Hochmann, G. and Law, S. (2010) *The Social and Environmental Consequences of Coal Mining in South Africa: A Case Study*. Cape Town. Available at: https://www.bothends.org/uploaded_files/uploadlibraryitem/1case_study_South_Africa_updated.pdf (Accessed: 30 November 2019).

Myhre, G., Shindell, D., Bréon, F.-M., Collins, W. J., Fuglestvedt, J., Huang, D., Koch, J.-F., Lamarque, D., Lee, B., Mendoza, T., Nakajima, A., Robock, G., Stephens, T., Takemura and Zhang (2013) *Anthropogenic and Natural Radiative Forcing. In: Climate Change 2013: The Physical Science Basis. Contribution of Working Group I to the Fifth Assessment Report of the Intergovernmental Panel on Climate Change*, *Climate Change 2013 - The Physical Science Basis*. Edited by V. B. and P. M. M. Stocker, T.F., D. Qin, G.-K. Plattner, M. Tignor, S.K. Allen, J. Boschung, A. Nauels, Y. Xia. Cambridge University Press. doi: 10.1017/cbo9781107415324.019.

Nagar, J. K., Akolkar, A. B. and Raj, K. (2014) A review on airborne particulate matter and its sources, chemical composition and impact on human respiratory system, *International Journal of Environmental Sciences*, 5(2), pp. 447–463. doi: 10.6088/ijes.2014050100039.

Naidoo, S., Piketh, S. and Christoper, C. (2015) Domestic Fuel Combustion in Un-electrified Low-income Settlements in South Africa, in *United States Environmental Protection Agency (USEPA)*. North Carolina, p. 21. Available at: https://www3.epa.gov/ttn/chief/conference/ei21/session2/naidoo.pdf (Accessed: 13 February 2019).

Nanophoton (2018) *What is Raman Spectroscopy?* Available at: https://www.nanophoton.net (Accessed: 9 April 2019).

Nanoscience Instruments (2018) *Scanning Electron Microscopy*. Available at: https://www.nanoscience.com/techniques/scanning-electron-microscopy (Accessed: 16 July 2018).

National Aeronautics and Space Administration (NASA) (2006) *Visible Earth Observatory*. Available at: https://earthobservatory.nasa.gov (Accessed: 12 February 2019).

National Planning Commission (NPC) (2010) *National Development Plan (2030)*, *Department: The Presedency Republic of South Africa*. Available at: https://www.gov.za/issues/national-development-plan-2030 (Accessed: 4 September 2019).

National Pollution Inventory (NPi) (2012) *Emission estimation Technique Manaul for Mining, Version 3.1*. Available at: http://www.npi.gov.au/system/files/resources.

National Research Council (NRC) (2007) *Coal*. Washington, D.C.: National Academies Press. doi: 10.17226/11977.

Ngele, A. (2017) *Review of Australian diesel particulate matter standard for underground coal mines*. University of Queensland Library. doi: 10.14264/uql.2018.338.

Ngwenyama, P. L., de Graaf, W. W. and Preis, E. P. (2017) Factors and challenges affecting coal recovery by opencast pillar mining in the Witbank coalfield, *Journal of the Southern African Institute of Mining and Metallurgy*. Academy of Science of South Africa, 117(3), pp. 215–222. doi: 10.17159/2411-9717/2017/v117n3a2.

Norman, R., Bradshaw, D., Schneider, M., Joubert, J., Groenewald, P., Lewin, S., Steyn, K., Vos, T., Laubscher, R., Nannan, N., Nojilana, B. and Pieterse, D. (2007) A comparative risk assessment for South Africa in 2000: Towards promoting health and preventing disease, *South African Medical Journal*, 97(8), pp. 637–641. Available at: https://www.ncbi.nlm.nih.gov/pubmed.

Norman, R., Bradshaw, D., Steyn, K., Gaziano, T. and South African Comparative Risk Assessment Collaborating Group (2007) Estimating the burden of disease attributable to high cholesterol in South Africa in 2000, *South African Medical Journal*, 97(8), pp. 708–715. Available at: https://www.ncbi.nlm.nih.gov/pubmed.

Norman, R., Cairncross, E, Witi, J., Bradshaw, D. and South African Comparative Risk Assessment Collaborating Group (2007) Estimating the burden of disease attributable to outdoor air pollution in South Africa in 2000, *South African Medical Journal*, 97(7), pp. 782–790. Available at: http://www.samj.org.za/index.php/samj/article/view.

Norman, R., Matzopoulos, R, Groenewald, P. and Bradshaw, D. (2007) Norman, R Matzopoulos, R Groenewald, P Bradshaw, D, *Bulletin of the World Health Organization*, 85(9), pp. 695–702. doi: 10.2471/blt.06.037184.

Novakov, T. (1984) The role of soot and primary oxidants in atmospheric chemistry, *Science of The Total Environment*. Elsevier BV, 36, pp. 1–10. doi: 10.1016/0048-9697(84)90241-9.

O'Brien, G., Warren, K., Koval, S. and Hibberd, M. (2017) Quantifying coal dust in urban samples, in *Proceedings of the 40th Symposium on Advances in the Study of the Sydney Basin: Weathering change*. Pokolbin, New South Wales, p. 5.

Olson, E. (2011) Particle shape factors and their use in image analysis- Part 1 Theory, *Journal of GXP Compliance*, 15(3), pp. 85–96. Available at: https//pdfs.semanticsscholar.org.

Olson, N. (2018) Current Trends in Analytical Spectroscopy: Technique and Instrument Modifications for both New and Improved Measurements, *Spectroscopy*, 33(3), pp. 34–39. Available at: http://www.spectroscopyonline.com.

Ozdogan, M. V, Turan, G., Karakus, D. and Onur, A. H. (2018) Prevention of spontaneous combustion in coal drifts using a lining material: a case study of the Tuncbilek Omerler underground mine, Turkey, *Journal of the Southern African Institute of Mining and Metallurgy*. Academy of Science of South Africa, 118(2), pp. 149–156. doi: 10.17159/2411-9717/2018/v118n2a8.

Palmer, K. (2011) IARC Monographs on the Evaluation of Carcinogenic Risks to Humans. Volume 98: Painting, Firefighting and Shiftwork. International Agency for Research on Cancer, *Occupational Medicine*. Oxford University Press (OUP), 61(7), pp. 521–522. doi: 10.1093/occmed/kqr127.

Pandey, B., Agrawal, M. and Singh, S. (2014) Assessment of air pollution around a coal mining area: Emphasizing on spatial distributions, seasonal variations and heavy metals, using cluster and principal component analysis, *Atmospheric Pollution Research*. Elsevier BV, 5(1), pp. 79–86. doi: 10.5094/apr.2014.010.

Panyacosit, L. (2000) A Review of Particulate Matter and Health: Focus on Developing Countries, *SSRN Electronic Journal*. Elsevier BV. doi: 10.2139/ssrn.235099.

Patra, A. K., Gautam, S. and Kumar, P. (2016) Emissions and human health impact of particulate matter from surface mining operation—A review, *Environmental Technology & Innovation*. Elsevier BV, 5, pp. 233–249. doi: 10.1016/j.eti.2016.04.002.

Pavuluri, C. M., Kawamura, K., Tachibana, E. and Swaminathan, T. (2010) Elevated nitrogen isotope ratios of tropical Indian aerosols from Chennai: Implication for the origins of aerosol nitrogen in South and Southeast Asia, *Atmospheric Environment*. Elsevier BV, 44(29), pp. 3597–3604. doi: 10.1016/j.atmosenv.2010.05.039.

Pavuluri, C. M., Kawamura, K., Aggarwal, S. G. and Swaminathan, T. (2011) Characteristics, seasonality and sources of carbonaceous and ionic components in the tropical aerosols from Indian region, *Atmospheric Chemistry and Physics*. Copernicus GmbH, 11(15), pp. 8215–8230. doi: 10.5194/acp-11-8215-2011.

Penner, J. E., Eddleman, H. and Novakov, T. (1993) Towards the development of a global inventory for black carbon emissions, *Atmospheric Environment. Part A. General Topics*. Elsevier BV, 27(8), pp. 1277–1295. doi: 10.1016/0960-1686(93)90255-w.

Perkinelmaer (2018) *Thermogravimetric Analysis (TGA)*. Available at: https://www.perkinelmer.com (Accessed: 9 September 2018).

Perrino, C. (2010) Atmospheric Particulate Matter, in *Proceedings of a C.I.S.B. Minisymposium*. Rome, Italy: C.N..R. Institute of Atmospheric Pollution, pp. 35–43. Available at: https://www.cognitivephilology.uniroma1.

Petavratzi, E., Kingman, S. and Lowndes, I. (2005) Particulates from mining operations: A review of sources, effects and regulations, *Minerals Engineering*. Elsevier BV, 18(12), pp. 1183–1199. doi: 10.1016/j.mineng.2005.06.017.

Pevelen, D. D. Le and Tranter, G. E. (2017) FT-IR and Raman Spectroscopies, Polymorphism Applications, *Encyclopedia of Spectroscopy and Spectrometry*. Elsevier, pp. 750–761. doi: 10.1016/b978-0-12-409547-2.12161-4.

Pless-Mulloli, T. (2000) Living near opencast coal mining sites and children's respiratory health, *Occupational and Environmental Medicine*. BMJ, 57(3), pp. 145–151. doi: 10.1136/oem.57.3.145.

Pokorná, P., Hovorka, J. and Brejcha, J. (2016) Impact of mining activities on air quality in a village nearby a coal Strip Mine, *IOP Conference Series: Earth and Environmental Science*. IOP Publishing, 44, p. 32021. doi: 10.1088/1755-1315/44/3/032021.

Pone, J. D. N., Hein, K. A. A., Stracher, G. B., Annegarn, H. J., Finkleman, R. B., Blake, D. R., McCormack, J. K. and Schroeder, P. (2007) The spontaneous combustion of coal and its by-products in the Witbank and Sasolburg coalfields of South Africa, *International Journal of Coal Geology*. Elsevier BV, 72(2), pp. 124–140. doi: 10.1016/j.coal.2007.01.001.

Popescu, F. and Ionel, I. (2010) Anthropogenic air pollution sources, *Air Quality*. Sciyo. doi: 10.5772/9751.

Pöschl, U. (2003) Aerosol particle analysis: challenges and progress, *Analytical and Bioanalytical Chemistry*. Springer Science and Business Media LLC, 375(1), pp. 30–32. doi: 10.1007/s00216-002-1611-5.

Pöschl, U. (2005) Atmospheric Aerosols: Composition, Transformation, Climate and Health Effects, *Angewandte Chemie International Edition*. Wiley, 44(46), pp. 7520–7540. doi: 10.1002/anie.200501122.

Potgieter-Vermaak, S., Maledi, N., Wagner, N., Van Heerden, J. H. P., Van Grieken, R. and Potgieter, J. H. (2011) Raman spectroscopy for the analysis of coal: a review, *Journal of Raman Spectroscopy*. Wiley, 42(2), pp. 123–129. doi: 10.1002/jrs.2636.

Potgieter-Vermaak, S. S. and Van Grieken, R. (2006) Preliminary evaluation of micro-raman spectrometry for the characterization of individual aerosol particles, *Applied Spectroscopy*. SAGE Publications, 60(1), pp. 39–47. doi: 10.1366/000370206775382848.

Pratt, K. A. and Prather, K. A. (2011) Mass spectrometry of atmospheric aerosols-Recent developments and applications. Part I: Off-line mass spectrometry techniques, *Mass Spectrometry Reviews*. Wiley, 31(1), pp. 1–16. doi: 10.1002/mas.20322.

Pretty, M. M. and Odeku, K. O. (2017) Harmful mining activities, environmental impacts and effects in the mining communities in South Africa: A critical perspective, *Environmental Economics*. LLC CPC Business Perspectives, 8(4), pp. 14–24. doi: 10.21511/ee.08(4).2017.02.

Prevost, X. M. (2004) South African Reserves and the Minerals Act, in *Coaltrans*. Cape Town, p. 6.

Princeton Instruments (2018) *Raman Spectroscopy Basis*. Available at: http://web.pdx.edu/~larosaa/Applied_Optics_464-564/)Spectroscopy_Basics (Accessed: 18 March 2019).

Prusty, B. K. (2015) *Coal Genesis and Characterisation*. Kharagpur. Available at: www.saarcenergy.org.

Pulles, T. and Heslinga, D. (2007) *The Art of Emission Inventorying*. TNO-Environment and Geosciences. doi: 10.13140/RG.2.1.2082.8007.

Putman, W. and da Silva, A. (2013) *Simulating the Transport of Aerosols with GEOS-5*. Available at: https://gmao.gsfc.nasa.gov/research/aerosol/modeling/nr1_movie/ (Accessed: 7 January 2019).

Queensland Rail Management (QRM) (2008) *Environmental Evaluation of Fugitive Coal Dust Emissions from Coal Trains Goonyella, Blackwater and Moura Coal Rail Systems*. Available at: http://thegenerator.com.au.

Rai, P. K. (2015) Multifaceted health impacts of particulate matter (PM) and its management: An overview, *Environmental Skeptics and Critics*, 4(1), pp. 1–26. Available at: http://www.iaees.org/publications/journals/environsc/onlineversion.%0Aasp.

Rajasegar, R. and Kyritsis, D. C. (2015) Experimental Investigation of Coal Combustion in Coal-Laden Methane Jets, *Journal of Energy Engineering*. American Society of Civil Engineers (ASCE), 141(2). doi: 10.1061/(asce)ey.1943-7897.0000228.

Ramachandran, S. (2018) *Atmospheric Aerosols*. CRC Press. doi: 10.1201/9781315152400.

Ramani, R. V and Evans, A. (2017) Coal Mining, *Encyclopaedia Brittanica.* Available at: https://www.britannica.com/technology/coal-mining.

Ramirez-Leal, R., Esparza-Ponce, H., Varela-Sortillón, A., Astorga-Reyes, A. and Roman-B., A. (2009) Characterization of inhalable particulate matter in ambient air by scanning electron microscopy and energy-dispersive X-ray analysis, *Microscopy and Microanalysis*. Cambridge University Press (CUP), 15(SUPPL. 2), pp. 1320–1321. doi: 10.1017/S1431927609097335.

Ramirez-Leal, R., Valle-Martinez, M. and Cruz-Campas, M. (2014) Chemical and Morphological Study of PM10 Analysed by SEM-EDS, *Open Journal of Air Pollution*. Scientific Research Publishing, Inc, 03(04), pp. 121–129. doi: 10.4236/ojap.2014.34012.

Reddy, G. S. and Ruj, B. (2003) Ambient air quality status in Raniganj-Asansol area, India, *Environmental Monitoring and Assessment*. Springer Science and Business Media LLC, 89(2), pp. 153–163. doi: 10.1023/a:1026070506481.

Reimer, L. (1998) *Scanning Electron Microscopy: Physics of Image Formation and Microanalysis*. Second, *Image Formation in Low-Voltage Scanning Electron Microscopy*. Second. Springer Berlin Heidelberg. doi: 10.1117/3.2265074.ch6.

Roberts, O. C., Saghafi, A., Cheng, J., Perrier, C. and Carras, J. N. (2004) *Rehabilitation of spontaneous combustion prone spoil piles. Australian Coal Industry's Research Project (ACARP). Project C9031 Final Report, Australian Coal Association.* Brisbane. Available at: https://www.acarp.com.au/abstracts.aspx?repId=C9031.

Roy, D. and Singh, G. (2014) Source Apportionment of Particulate Matter (PM10) In an Integrated Coal Mining Complex of Jharia Coalfield, Eastern India, A Review., *Journal of Engineering Research and Applications*, 4(4 (Version 1)), pp. 97–113. Available at: www.ijera.com.

Sahu, S. P., Patra, A. K. and Kolluru, S. S. R. (2018) Spatial and temporal variation of respirable particles around a surface coal mine in India, *Atmospheric Pollution Research*. Elsevier BV, 9(4), pp. 662–679. doi: 10.1016/j.apr.2018.01.010.

Salma, I., Németh, Z., Weidinger, T., Maenhaut, W., Claeys, M., Molnár, M., Major, I., Ajtai, T., Utry, N., and Bozóki, Z. (2017) Source apportionment of carbonaceous chemical species to fossil fuel combustion, biomass burning and biogenic emissions by a coupled radiocarbon–levoglucosan marker method. *Atmos. Chem. Phys*., 17pp 13767–13781.

Savard, M. M., Cole, A., Smirnoff, A. and Vet, R. (2017) δ 15 N values of atmospheric N species simultaneously collected using sector-based samplers distant from sources – Isotopic inheritance and fractionation, *Atmospheric Environment*. Elsevier BV, 162, pp. 11–22. doi: 10.1016/j.atmosenv.2017.05.010.

Scaggs, M., Sarvera, E. and Keles, C. (2015) Considerations for TGA of Respirable Coal Mine Dust Samples, in Jong, E. et al. (eds) *15th North American Mine Ventilation Symposium*. Blacksburg, Viginia (USA): Virginia Tech Department of Mining and Minerals Engineering, pp. 1–11.

Schmid, H. (2001) Results of the 'Carbon Conference' International Aerosol Carbon Round Robin Test Stage I, *Atmospheric Environment*. Elsevier BV, 35(12), pp. 2111–2121. doi: 10.1016/s1352-2310(00)00493-3.

Schwarz, J., Chi, X., Maenhaut, W., Civiš, M., Hovorka, J. and Smolík, J. (2008) Elemental and organic carbon in atmospheric aerosols at downtown and suburban sites in Prague, *Atmospheric Research*. Elsevier BV, 90(2–4), pp. 287–302. doi: 10.1016/j.atmosres.2008.05.006.

Scorgie, Y., Annegarn, H. J. and Burger, L. W. (2004) *Fund for Research into Industrial Development Growth and Equity (FRIDGE). Study to examine the potential socio-economic impact of measures to reduce air pollution from combustion. Report no: PA 1970 Final Report Version 26.* Available at: https://nedlac.org.za/research-reports/.

Seinfeld, J. H., Pandis, S. N. and Noone, K. (1998) Atmospheric Chemistry and Physics: From Air Pollution to Climate Change, *Physics Today*. AIP Publishing, 51(10), pp. 88–90. doi: 10.1063/1.882420.

Sellaro, R. and Sarver, E. (2014) Preliminary investigation of SEM-EDX as a tool for characterization of coal mine dusts, *Environmental Engineering*, 66, pp. 16–40.

Sellaro, R., Sarver, E. and Baxter, D. (2015) A Standard Characterization Methodology for Respirable Coal Mine Dust Using SEM-EDX, *Resources*. MDPI AG, 4(4), pp. 939–957. doi: 10.3390/resources4040939.

Shenfeld, L. (1970) Meteorological aspects of air pollution control, *Atmosphere*. Informa UK Limited, 8(1), pp. 3–13. doi: 10.1080/00046973.1970.9676578.

Sheppard, S. M. F. (2004) *Experimental Measurement of Isotopic Fractionation Factors and Rates and Mechanisms of Reaction*. First Edit, *Handbook of Stable Isotope Analytical Techniques*. First Edit. Edited by P. . De Groot. doi: 10.1016/B978-044451114-0/50048-X.

Shukla, P. R. (2019) Justice, Equity and Efficiency in Climate Change: A Developing Country Perspective, *Fair Weather?* Routledge, pp. 145–159. doi: 10.4324/9781315071251-9.

Siegbahn, K. (1982) Electron Spectroscopy for Atoms, Molecules and Condensed Matter, *Science*. American Association for the Advancement of Science (AAAS), 217(4555), pp. 111–121. doi: 10.1126/science.217.4555.111.

Sielicki, P., Janik, H., Guzman, A. and Namieśnik, J. (2011) The progress in electron microscopy studies of particulate matters to be used as a standard monitoring method for air dust pollution, *Critical Reviews in Analytical Chemistry*. Informa UK Limited, 41(4), pp. 314–334. doi: 10.1080/10408347.2011.607076.

Silva Filho, C. G. da and Milioli, F. E. (2008) A thermogravimetric analysis of the combustion of a Brazilian mineral coal, *Química Nova*. FapUNIFESP (SciELO), 31(1), pp. 98–103. doi: 10.1590/S0100-40422008000100021.

Singh, A. K., Srivastava, M. K., Singh, M., Srivastava, A., Kumar, S., Tiwari, S., Singh, B. P., Bisht, D. S. and Tiwari, S. (2014) Characterisation of Atmospheric Aerosol by SEM-EDX and Ion-Chromatography Techniques for Eastern Indo-Gangetic Plain Location, Varanasi, India, *International Journal of Advances in Earth Sciences*, 3(2), pp. 41–51. Available at: https://www.researchgate.net/publication/264623418_Characterisation_of_Atmospheric_Aerosol_by_SEM-EDX_and_Ion-Chromatography_Techniques_for_Eastern_Indo-Gangetic_Plain_Location_Varanasi_India.

Singh, R. V. K. (2013) Spontaneous Heating and Fire in Coal Mines, *Procedia Engineering*. Elsevier BV, 62, pp. 78–90. doi: 10.1016/j.proeng.2013.08.046.

Singh, T. N. (1998) *Determination of Emission Factors for Various Opencast Mining Operations*. Dhanbad. Available at: http://envfor.nic.in/divisions/re/ta12p1.html.

Smit, B. and Pilifosova, O. (2003) Adaptation to climate change in the context of sustainable development and equity, *Sustainable Development*, 8(9), p. 9. Available at: https://www.researchgate.net/publication/281322507_Adaptation_to_Climate_Change_in_the_Context_of_Sustainable_Development_and_Equity.

Smith, B. (2016) *Latest Developments in Spectroscopy in Azo Materials*.

Smith, K. R. (1993) Fuel Combustion, Air Pollution Exposure, and Health: The Situation in Developing Countries, *Annual Review of Energy and the Environment*. Annual Reviews, 18(1), pp. 529–566. doi: 10.1146/annurev.eg.18.110193.002525.

Snyder, E. G., Watkins, T. H., Solomon, P. A., Thoma, E. D., Williams, R. W., Hagler, G. S. W., Shelow, D., Hindin, D. A., Kilaru, V. J. and Preuss, P. W. (2013) The Changing Paradigm of Air Pollution Monitoring, *Environmental Science & Technology*. American Chemical Society (ACS), 47(20), pp. 11369–11377. doi: 10.1021/es4022602.

Snyman, C. P. and Botha, W. J. (1993) Coal in South Africa, *Journal of African Earth Sciences (and the Middle East)*. Elsevier BV, 16(1–2), pp. 171–180. doi: 10.1016/0899-5362(93)90165-m.

Song, J. and Peng, P. (2009) Surface Characterization of Aerosol Particles in Guangzhou, China: A Study by XPS, *Aerosol Science and Technology*. Informa UK Limited, 43(12), pp. 1230–1242. doi: 10.1080/02786820903325394.

South African National Standards (SANS) 7404-1:2015 (ISO 7404-2:2009). Methods for the petrographic analysis of coals Part 2: Methods of preparing coal samples.

Spackman, W. (1958) Section of Geology and Mineralogy: The Maceral Concept and the Study of Modern Environments as a Means of Understanding the Nature of Coal, *Transactions of the New York Academy of Sciences*. Wiley, 20(5 Series II), pp. 411–423. doi: 10.1111/j.2164-0947.1958.tb00602.x.

Speight, J. (2012) *The Chemistry and Technology of Coal*. Third Edition, *Chemical Industries*. Third Edit. CRC Press (Chemical Industries). doi: 10.1201/b12497.

Speight, J. G. (2015) *Handbook of Coal Analysis*. Hoboken, NJ, USA: John Wiley & Sons, Inc. doi: 10.1002/9781119037699.

Spengler, J. D., Brauer, M. and Koutrakis, P. (1990) Acid air and health, *Environmental Science & Technology*. American Chemical Society (ACS), 24(7), pp. 946–956. doi: 10.1021/es00077a002.

Stern, A. C., Boubel, R. W. and Turner, D. B. (1984) *Fundamentals of Air Pollution*. Second Edi. Academic Press. doi: 13: 9780126665802.

Stevens, J. S., Newton, L. K., Jaye, C., Muryn, C. A., Fischer, D. A. and Schroeder, S. L. M. (2015) Proton Transfer, Hydrogen Bonding and Disorder: Nitrogen Near-Edge X-ray Absorption Fine Structure and X-ray Photoelectron Spectroscopy of Bipyridine–Acid Salts and Co-crystals, *Crystal Growth & Design*. American Chemical Society (ACS), 15(4), pp. 1776–1783. doi: 10.1021/cg5018278.

Suh, H. H., Spengler, J. D. and Koutrakis, P. (1992) Personal exposures to acid aerosols and ammonia, *Environmental Science & Technology*. American Chemical Society (ACS), 26(12), pp. 2507–2517. doi: 10.1021/es00036a026.

Sunset Laboratory Inc (2019) *Carbon Aerosol Particulate Analysis Instruments*. Available at: https://www.sunlab.com (Accessed: 20 May 2019).

Suto, N. and Kawashima, H. (2016) Global mapping of carbon isotope ratios in coal, *Journal of Geochemical Exploration*. Elsevier BV, 167, pp. 12–19. doi: 10.1016/j.gexplo.2016.05.001.

Swapp, S. (2018) *Geochemical Instrumentation and Analysis-Scanning Electron Microscopy (SEM)*. https://serc.carleton.edu/research_education/geochemsheets/techniques/SEM.html (Accessed: 11 September 2018).

Szmigielski, R. (2013) *Chemistry of Organic Sulfates and Nitrates in the Urban Atmosphere*, *Disposal of Dangerous Chemicals in Urban Areas and Mega Cities.* Warsaw, Poland: Springer Netherlands. doi: 10.1007/978-94-007-5034-0_17.

TA Instruments (2006) *TGA- Thermogravimetric Analyzer*. Available at: http://www.tainstruments.com/pdf/TGA Brochure.pdf (Accessed: 18 June 2019).

Tanaka, M., Takeguchi, M. and Furuya, K. (2008) X-ray analysis and mapping by wavelength dispersive X-ray spectroscopy in an electron microscope, *Ultramicroscopy*. Elsevier BV, 108(11), pp. 1427–1431. doi: 10.1016/j.ultramic.2008.05.011.

Task Force on Climate related Financial Disclosures (TCFD) (2017a) *Recommendations of the Task Force on Climate-related Financial Disclosures: Final Report*. Available at: https://www.fsb-tcfd.org/wp-content/uploads/2017/06/FINAL-2017-TCFD-Report-11052018.pdf.

Task Force on Climate related Financial Disclosures (TCFD) (2017b) *Technical Supplement: The Use of Scenario Analysis in Disclosure of Climate-related Risks and Opportunities*. Available at: https://www.fsb-tcfd.org/wp-content/uploads/2017/06/FINAL-TCFD-Technical-Supplement-062917.pdf.

Tegen, I., Harrison, S. P., Kohfeld, K., Prentice, I. C., Coe, M. and Heimann, M. (2002) Impact of vegetation and preferential source areas on global dust aerosol: Results from a model study, *Journal of Geophysical Research: Atmospheres*. American Geophysical Union (AGU), 107(D21), p. AAC 14-1-AAC 14-27. doi: 10.1029/2001jd000963.

Tegen, I. and Kohfeld, K. E. (2006) Atmospheric transport of silicon, in Ittekkot, V. et al. (eds) *The Silicon Cycle: Human Perturbations and Impacts on Aquatic Systems*. Washington: Island Press, Scope, 66, p. 81. Available at: https://books.google.co.za.

The United Kingdom (UK) Department of the Environment (1993) *Fine Particulate Matter (PM2.5) in the United Kingdom*. Available at: https://uk-air.defra.gov.uk/assets/documents/reports/cat11/1212141150_AQEG_Fine_Particulate_Matter_in_the_UK.pdf (Accessed: 12 March 2019).

Thompson, R. J. and Visser, A. T. (2003) Mine haul road fugitive dust emission and exposure characterisation, *Environmental Health Risk II*. WIT Press. doi: 10.2495/ehr030111.

Trivedi, R., Mondal, A., Chakraborty, M. K. and Tewary, B. K. (2010) A Statistical analysis of ambient air quality around opencast coal projects in Warda Valley Coalfields, Western Coalfields Limited, India, *Indian Journal of Environmental Protection*, 30(12), pp. 969–977. Available at: http://cimfr.csircentral.net/id/eprint/499.

Trivedi, R., Chakrabotry, M. K., Sangode, A. G. and Tewary, B. K. (2010) A Study of Air Pollution Load Assessment Around an Opencast Coal Project in India, *Indian Journal of Environmental Protection*, 30(3), pp. 198–206. Available at: http://cimfr.csircentral.net/35/1/S32.pdf.

Tsiouri, V., Kakosimos, K. E. and Kumar, P. (2014) Concentrations, sources and exposure risks associated with particulate matter in the Middle East Area—a review, *Air Quality, Atmosphere & Health*. Springer Science and Business Media LLC, 8(1), pp. 67–80. doi: 10.1007/s11869-014-0277-4.

Tuinstra, F. and Koenig, J. L. (1970) Raman Spectrum of Graphite, *The Journal of Chemical Physics*. AIP Publishing, 53(3), pp. 1126–1130. doi: 10.1063/1.1674108.

Turpin, B. J., Huntzicker, J. J. and Adams, K. M. (1990) Intercomparison of photoacoustic and thermal-optical methods for the measurement of atmospheric elemental carbon, *Atmospheric Environment. Part A. General Topics*. Elsevier BV, 24(7), pp. 1831–1835. doi: 10.1016/0960-1686(90)90515-o.

Turpin, B. J., Huntzicker, J. J. and Hering, S. V (1994) Investigation of organic aerosol sampling artifacts in the los angeles basin, *Atmospheric Environment*. Elsevier BV, 28(19), pp. 3061–3071. doi: 10.1016/1352-2310(94)00133-6.

Tyagi, S. (2018) What comes next: responding to recommendations from the task force on climate-related financial disclosures (TCFD), *The APPEA Journal*. CSIRO Publishing, 58(2), p. 633. doi: 10.1071/aj17179.

Tyson, P. D. and Preston-Whyte, R. A. (2002) The weather and climate of southern Africa by P. D. Tyson and R. A. Preston-Whyte. Oxford University Press Southern Africa, Cape Town, 2000. No. of pages: xii + 396. Price £32.50. ISBN 0-19-571806-2 (paperback)., *International Journal of Climatology*. Wiley, 22(7), pp. 883–884. doi: 10.1002/joc.725.

Ulrich, E., Beckmann, C. and Israël, G. (1990) The characterization of carbon species in particulate matter by successive thermal desorption, *Journal of Aerosol Science*. Elsevier BV, 21, pp. S609–S612. doi: 10.1016/0021-8502(90)90316-p.

United Nations (UN) (2018) *Climate change*. Available at: https://www.unenvironment.org/explore-topics/climate-change (Accessed: 6 June 2018).

United Nations Environment Programme (UNEP) (2015) *Adoption of the Paris Agreement*. Available at: https://unfccc.int/sites/default/files/english_paris_agreement.pdf (Accessed: 20 May 2018).

United Nations Environment Programme (UNEP) (2018) *Climate change*. Available at: https://www.unenvironment.org/explore-topics/climate-change (Accessed: 18 May 2018).

United States Energy Information Administration (EIA) (1978a) *Bituminous Coal and Lignite Production and Mine Operations*. Washington DC. Available at: http://emfi.mines.edu/emfi2011/Coal Mining Methods- EMFISummary.pdf.

United States Energy Information Administration (EIA) (1978b) *Total Energy*. Available at: https://www.eia.gov/totalenergy/data/monthly/previous.php (Accessed: 2 November 2019).

United States Environmental Protection Agency (USEPA) (1996) *Compilation of Air Pollution Emission Factors (AP-42), 6th Edition, Volume 1, as contained in the AirCHIEF (AIR Clearinghouse for Inventories and Emission Factors)*. North Carolina. Available at: http://www.epa.gov/ttn/chief/ap42.

United States Environmental Protection Agency (USEPA) (2002) *Health Assessment Document for Diesel Engine Exhaust. EPA-600/R-02-076, 2002.* North Carolina. Available at: http://www.epa.gov/ttn/atw/dieselfinal.pdf.

United States Environmental Protection Agency (USEPA) (2004) *AERMOD: Description of Model Formulation*. North Carolina. Available at: https://www3.epa.gov/scram001/7thconf/aermod/aermod_mfd.pdf.

United States Environmental Protection Agency (USEPA) (2009) *Particulate Matter National Ambient Air Quality Standards: Scope and Methods Plan for Urban Visibility Impact Assessment. Air Quality Planning and Standards, Research Triangle Park*. North Carolina.

United States Environmental Protection Agency (USEPA) (2011) *Emission Factor Documentation for AP-42, Section 13.2.1, Paved Roads*. North Carolina. Available at: https://www3.epa.gov/ttn/chief/ap42/ch13/bgdocs/b13s0201.pdf.

United States Environmental Protection Agency (USEPA) (2012) *Report to Congress on Black Carbon: Department of the Interior, Environment, and Related Agencies Appropriations Act, 2010*. Available at: www.epa.gov/blackcarbon.

United States Environmental Protection Agency (USEPA) (2018) *Managing Air Quality - Control Strategies to Achieve Air Pollution Reduction*. North Carolina.

United States Environmental Protection Agency (USEPA) (2019) *User's Guide for the AMS/EPA Regulatory Model (AERMOD)*. North Carolina.

Unsworth, J. F. and Gough, H. (1989) Characterization of coals by automated optical image analysis 2. Inertinite reflectance, *Journal of Microscopy*. Wiley, 156(3), pp. 327–342. doi: 10.1111/j.1365-2818.1989.tb02934.x.

Vallius, M. (2005) *Characteristics and sources of fine particulate matter in urban air*. Kuopio, Finland. Available at: https://www.researchgate.net/publication/242532060_Characteristics_and_sources_of_fine_particulate_matter_in_urban_air (Accessed: 4 August 2019).

Vleeskens, J. M., Bos, P., Kos, C. H. and Roos, M. (1985) Pyrite association and coal cleaning, *Fuel*. Elsevier BV, 64(3), pp. 342–347. doi: 10.1016/0016-2361(85)90421-1.

Wagner, J. and Leith, D. (2001a) Field tests of a passive aerosol sampler, *Journal of Aerosol Science*. Elsevier BV, 32(1), pp. 33–48. doi: 10.1016/s0021-8502(00)00055-0.

Wagner, J. and Leith, D. (2001b) Passive Aerosol Sampler. Part I: Principle of Operation, *Aerosol Science and Technology*. Informa UK Limited, 34(2), pp. 186–192. doi: 10.1080/027868201300034808.

Wagner, J. and Leith, D. (2001c) Passive Aerosol Sampler. Part II: Wind Tunnel Experiments, *Aerosol Science and Technology*. Informa UK Limited, 34(2), pp. 193–201. doi: 10.1080/027868201300034826.

Wallace, W. E., Harrison, J. C. and Keane, M. J. (1990) Clay occlusion of respirable quartz particles detected by low voltage scanning electron microscopy X-ray analysis, *The Annals of Occupational Hygiene*. Oxford University Press (OUP), 34, pp. 195–204. doi: 10.1093/annhyg/34.2.195.

Walters, W. W., Tharp, B. D., Fang, H., Kozak, B. J. and Michalski, G. (2015) Nitrogen Isotope Composition of Thermally Produced NOx from Various Fossil-Fuel Combustion Sources, *Environmental Science & Technology*. American Chemical Society (ACS), 49(19), pp. 11363–11371. doi: 10.1021/acs.est.5b02769.

Ward, C. R. and Suárez-Ruiz, I. (2008) Introduction to Applied Coal Petrology, in *Applied Coal Petrology*. Elsevier, pp. 1–18. doi: 10.1016/B978-0-08-045051-3.00001-4.

Warren, K, Krahenbuhl, G., Mahoney, M., O'Brien, G. and Hapugoda, P. (2015) Estimating the fusible content of individual coal grains and its application in coke making, *International Journal of Coal Geology*. Elsevier BV, 152, pp. 3–9. doi: 10.1016/j.coal.2015.09.012.

Warren, Karryn, Krahenbuhl, G., O'Brien, G. and Hapugoda, P. (2015) Quantifying Coal Dust in Urban Samples. CSIRO, Energy Flagship, in *2015 ICCS&T/ACSE*. Melbourne, Australia, p. 4.

Watson, J. G., Chow, J. C. and Chen, L.-W. A. (2005) Summary of Organic and Elemental Carbon/Black Carbon Analysis Methods and Intercomparisons, *Aerosol and Air Quality Research*. Taiwan Association for Aerosol Research, 5(1), pp. 65–102. doi: 10.4209/aaqr.2005.06.0006.

Wei, D., Cameron, E., Harris, S., Prattico, E., Scheerder and G Zhou, J. (2016) *The Paris Agreement: What it Means for Business*. Available at: 2019 Business for Social Responsibility (Accessed: 29 November 2019).

Weisenburger, S. and Sandoghdar, V. (2015) Light microscopy: an ongoing contemporary revolution, *Contemporary Physics*. Informa UK Limited, 56(2), pp. 123–143. doi: 10.1080/00107514.2015.1026557.

Wentzel, M. J. (2015) *Characterisation of airborne dust in South African underground and opencast coal mines: A pilot study*. North West University. Available at: https://repository.nwu.ac.za/handle/10394/15808 (Accessed: 29 November 2017).

Wetzel, R. G. (2001) The Inorganic Carbon Complex, in *Limnology*. Third Edit. Elsevier, pp. 187–204. doi: 10.1016/B978-0-08-057439-4.50015-0.

Wichmann, J. (2017) *Africa has an air pollution problem but lacks the data to tackle it*. Available at: https://www.up.ac.za/news/post_2417554-africa-has-an-air-pollution-problem-but-lacks-the-data-to-tackle-it (Accessed: 23 September 2017).

Widory, D. (2007) Nitrogen isotopes: Tracers of origin and processes affecting PM10 in the atmosphere of Paris. *Atm Env* 41 (2007) 2382–2390 doi:10.1016/j.atmosenv.2006.11.009.

Widory, D., Roy, S., Moullec, Y. Le, Goupil, G., Cocherie, A. and Guerrot, C. (2004) The origin of atmospheric particles in Paris: A view through carbon and lead isotopes, *Atmospheric Environment*. Elsevier BV, 38(7), pp. 953–961. doi: 10.1016/j.atmosenv.2003.11.001.

Wijaya, A. S. (2014) Climate Change, Global Warming and Global Inequity in Developed and Developing Countries (Analytical Perspective, Issue, Problem and Solution), *IOP Conference Series: Earth and Environmental Science*. IOP Publishing, 19, p. 12008. doi: 10.1088/1755-1315/19/1/012008.

Willis, R. D., Blanchard, F. T. and Conner, T. L. (2002) *Guidelines for the Application of SEM/EDX Analytical Techniques to Particulate Matter Samples*. North Carolina. Available at: https://nepis.epa.gov/Exe/ZyNET.exe (Accessed: 26 January 2019).

Windfinder (2018) *Wind forecasts, wind speed, live weather and wind map*. Available at: https://www.windfinder.com/#3/57.2942/12.7143 (Accessed: 3 April 2018).

Winey, M., Meehl, J. B., O'Toole, E. T. and Giddings, T. H. (2014) Conventional transmission electron microscopy, *Molecular Biology of the Cell*. American Society for Cell Biology (ASCB), 25(3), pp. 319–323. doi: 10.1091/mbc.e12-12-0863.

World Coal Association (2018) *Coal Mining*. Available at: https://www.worldcoal.org/coal/coal-mining (Accessed: 10 June 2019).

World Health Organisation (WHO) (1999) *Hazard Prevention and Control in the Work Environment: Airborne Dust*, *Occupational Health*. Geneva, Switzerland. Available at: https://www.who.int/occupational_health/publications/airdust/en/ (Accessed: 21 February 2017).

World Health Organisation (WHO) (2003) *Climate change and human health: Risks and responses*. Edited by A. McMichael *et al*. Geneva, Switzerland. Available at: https://apps.who.int/iris/handle/10665/42742.

World Health Organisation (WHO) (2006) *WHO Air quality guidelines for particulate matter, ozone, nitrogen dioxide and sulfur dioxide: Global update 2005-Summary of risk assessment*. Geneva, Switzerland. Available at: https://apps.who.int/iris/bitstream/handle/10665/69477/WHO_SDE_PHE_OEH_06.02_eng.pdf?sequence=1&isAllowed=y (Accessed: 5 March 2018).

World Health Organisation (WHO) (2016) *Public Health, Environmental and Social Determinants of Health (PHE)*. Geneva, Switzerland. Available at: https://www.who.int/phe/news/e-News-82.pdf?ua=1 (Accessed: 12 January 2019).

WorldWatch Institution (2018) *Global Security Brief #3: Climate Change Poses Greater Security Threat than Terrorism.* Washington DC. Available at: http://www.worldwatch.org/node/77. (Accessed: 6 June 2018).

Wozniak, A. S., Bauer, J. E., Dickhut, R. M., Xu, L. and McNichol, A. P. (2012) Isotopic characterization of aerosol organic carbon components over the eastern United States, *Journal of Geophysical Research: Atmospheres*. American Geophysical Union (AGU), 117(D13). doi: 10.1029/2011jd017153.

Wróblewski, R. and Ceran, B. (2016) Thermogravimetric analysis in the study of solid fuels, *E3S Web of Conferences*. EDP Sciences, 10, p. 109. doi: 10.1051/e3sconf/20161000109.

Wu, Y.-C., Shiledar, A., Li, Y.-C., Wong, J., Feng, S., Chen, X., Chen, C., Jin, K., Janamian, S., Yang, Z., Ballard, Z. S., Göröcs, Z., Feizi, A. and Ozcan, A. (2017) Air quality monitoring using mobile microscopy and machine learning, *Light: Science & Applications*. Springer Science and Business Media LLC, 6(9), pp. e17046–e17046. doi: 10.1038/lsa.2017.46.

Xie, K.-C. (2015) *Structure and Reactivity of Coal: A Survey of Selected Chinese Coals*. First. Springer-Verlag Berlin Heidelberg. doi: 10.1007/978-3-662-47337-5_2.

Yu, J. Z., Xu, J. and Yang, H. (2002) Charring Characteristics of Atmospheric Organic Particulate Matter in Thermal Analysis, *Environmental Science & Technology*. American Chemical Society (ACS), 36(4), pp. 754–761. doi: 10.1021/es015540q.

Zhang, J., Liu, S. M., Ren, J. L., Wu, Y. and Zhang, G. L. (2007) Nutrient gradients from the eutrophic Changjiang (Yangtze River) Estuary to the oligotrophic Kuroshio waters and re-evaluation of budgets for the East China Sea Shelf, *Progress in Oceanography*. Elsevier BV, 74(4), pp. 449–478. doi: 10.1016/j.pocean.2007.04.019.

Zhang, Q., Jimenez, J. L., Canagaratna, M. R., Allan, J. D., Coe, H., Ulbrich, I., Alfarra, M. R., Takami, A., Middlebrook, A. M., Sun, Y. L., Dzepina, K., Dunlea, E., Docherty, K., DeCarlo, P. F., Salcedo, D., Onasch, T., Jayne, J. T., Miyoshi, T., Shimono, A., Hatakeyama, S., Takegawa, N., Kondo, Y., Schneider, J., Drewnick, F., Borrmann, S., Weimer, S., Demerjian, K., Williams, P., Bower, K., Bahreini, R., Cottrell, L., Griffin, R. J., Rautiainen, J., Sun, J. Y., Zhang, Y. M. and Worsnop, D. R. (2007) Ubiquity and dominance of oxygenated species in organic aerosols in anthropogenically-influenced Northern Hemisphere midlatitudes, *Geophysical Research Letters*. American Geophysical Union (AGU), 34(13), p. n/a-n/a. doi: 10.1029/2007gl029979.

Zhang, R., Tao, J., Ho, K. F., Shen, Z., Wang, G., Cao, J., Liu, S., Zhang, L. and Lee, S. C. (2012) Characterization of Atmospheric Organic and Elemental Carbon of PM2.5 in a Typical Semi-Arid Area of Northeastern China, *Aerosol and Air Quality Research*. Taiwan Association for Aerosol Research, 12(5), pp. 792–802. doi: 10.4209/aaqr.2011.07.0110.

ZMSYY (2018) *Opencast Coal Mine*. Available at: www.zmsyy.com (Accessed: 6 June 2018).

APPENDIX A: MITIGATION MEASURES FOR COAL MINING OPERATIONS

The application of mitigation measures generally results in the reduction of fugitive dust and particulate emissions. In a typical opencast coal mining operation, mitigation measures include the following;

- Wet suppression to minimise fugitive dust emissions from unpaved haul roads, open areas and during topsoil stripping. Unpaved haul roads are generally the main contributing sources to fugitive dust emissions in opencast coal mining operations (Cowherd and Englehart, 1985). Therefore, mitigation measures which result in higher control efficiencies such as chemical suppression can be applied to primary haul roads within the mine (Cowherd and Englehart, 1985; Cecala *et al*., 2012). Chemical suppressants or dust control additives are affective as they bind fine particulates on the surface of the road and improve road compaction and stability (NPi, 2012, Cecala *et al*., 2012). However, the success rate or effectiveness of a chemical suppressant is determined by factors which include the unpaved road surface characteristics, rate of application and application method and frequency of re-application and the nature and type of the chemical suppressant (Kissell, 2003). In general, some chemical suppressants have been proven to achieve PM_{10} control efficiencies of between 80- 90% with regular application on the unpaved road surfaces (Kissell, 2003). Wet suppression results in control efficiencies of 50% or more and is largely affected by factors such as evaporation and type of source (Cowherd and Englehart, 1985).
- Wet drilling for the reduction of fugitive dust emissions;
- Optimum mine designing and planning to minimise the occurrence of large or exposed open areas.
- Planning or scheduling mining activities to coincide with atmospheric conditions associated with favorable weather conditions. These activities include material and product loading, material transfer or handling and blasting (Cecala *et al*., 2012).
- Rehabilitation and re-vegetation of mined out areas to reduce soil erosion and fugitive dust emissions;
- Fugitive dust reduction through the enclosure of crushing operations. According to the Australian National Pollution Inventory (NPi, 2012), wet suppression through water sprays can result in 75% control efficiency. Enclosure of stockpiles would reduce emissions by control efficiencies of up to 99% (NPi, 2012).

- The control of vehicle speeds and traffic volumes on unpaved roads are other mitigation measures that can be applied for fugitive dust emissions reduction. According to research study undertaken at the University of Nevada, an increase in vehicle speed of 16km per hour results in PM_{10} emissions increases of between 1.5 and 3 times. Similar studies also concluded that a reduction in speed from 40 km/hr to 24 km/hr resulted in a reduction of 35-42% in PM_{10} emissions (NPi, 2012).

As previously mentioned, spontaneous combustion is one of the significant sources of gases and particulate matter. Hence, the prevention of spontaneous combustion in coal mines should also be applied as a mitigation measure for the reduction of particulate emissions and other pollutants such as SO_2, NO_x and greenhouse gases which include CO_2 and CH_4. The most appropriate method for the prevention of spontaneous combustion is the understanding of the coal properties, the likelihood of the coal to self-heat and methods for monitoring self-heating. There are different techniques for predicting the coal self-heating properties and these include thermal analysis, a method which is based on thermogravimetric techniques and differential scanning calorimetry.

Methods for controlling spontaneous combustion include the following;

- The detection of the sources of spontaneous combustion;
- Extinguishing the fire directly through methods such as gel injection and mud grouting;
- Injection of form or inert gases such as carbon dioxide and nitrogen for fire extinguishing;
- The adjustment of pressure to obtain a positive pressure in the coal mining area can be implemented. However, safety considerations should be prioritised;
- Adopting a control strategy for the affected areas by sealing and stopping the fire. If the area affected by the fire is large, the effective approach is to divide the large area into small areas (Lu *et al*., 2017).

The prevention and control of spontaneous combustion in coal mining regions such as the Mpumalanga Highveld can result in significant reductions in particulate matter and other pollutants. Although the extent of emission reduction efforts cannot be accurately quantified due to challenges associated with the quantification of spontaneous combustion emissions, these efforts will nonetheless, contribute positively to air pollution mitigation in the region.